IMPACT OF PERIPHERAL IMMUNE CELLS AND SIGNALS ON BRAIN AND BEHAVIOUR OUTCOMES

IMPACT OF PERIPHERAL IMMUNE CELLS AND SIGNALS ON BRAIN AND BEHAVIOUR OUTCOMES

By SHAWNA LEE THOMPSON, BSc.H.

A Thesis

Submitted to the School of Graduate Studies

In Partial Fulfillment of the Requirements for the Degree

Doctor of Philosophy

DOCTOR OF PHILOSOPHY (2022) MCMASTER UNIVERSITY

(Health Science - Neuroscience) Hamilton, Ontario, Canada

TITLE: Impact of peripheral immune cells and signals on brain and behaviour outcomes

AUTHOR: Shawna Lee Thompson, BSc. H.

SUPERVISOR: Professor Jane A Foster

NUMBER OF PAGES: xxi, 152

LAY ABSTRACT

The immune system has been linked to mental health, therefore understanding how it interacts with the brain is critical. T cells do not normally enter brain tissue but affect brain structure. Examining microglia – the brain's immune cell – in mice without T cells revealed number and density differences in stress-associated brain areas. Research on gut bacteria-brain communication uses germ free (GF) mice, which live in sterile conditions. GF mice behave differently than controls, so neuroanatomy was mapped to identify regions most reactive to bacteria, and a timeline for microbe-associated neurodevelopmental changes was made. Mice without T cells seem less anxious than normal mice. Different immune cell varieties were collected from T cell deficient mice across puberty to identify immune-brain connections that might become compromised in neurodevelopmental disorders. Identifying changes in immune cells surrounding adolescence and linking to behaviour may reveal how immune-brain communication contributes to the onset of mental health disorders.

ABSTRACT

Immune-brain communication is a critical component of the microbiome-gut-brain axis, and an important topic for today's neuroscientists. Recent behavioural studies revealed that mice lacking the b and d chains of the T cell receptor (*TCRb-/-d-/-*) – which are functionally deficient in T cells – showed reduced anxiety-like behaviour on approach/avoidance tests. Therefore, in order to contribute to the knowledge of how the adaptive immune system participates in neurodevelopment, *this thesis examines adaptive immune influence on the brain and behaviour: the impact of T cell deletion on microglia, myeloid cells in the blood, and behaviour, and of microbiota manipulation on neuroanatomy*. The first study examined microglia number and density in adult *TCRb-/-d-/-* mice and showed increased numbers of microglia in the basolateral amygdala, and evidence of regional reductions in microglial density in *TCRb-/-d-/-* mice. Mice completely lacking microbiomes (Germ free - GF), are generally recognized to be deficient in mature lymphocytes. To determine how the microbiome impacts brain development, structural brain imaging was used to identify volume changes in neuroanatomy both globally, and regionally in stress circuitry. GF mice had smaller total brain volumes, and larger cortex but smaller hippocampus volumes, relative to total brain volume. Two models of recolonization indicate roles for the microbiome in postnatal brain volume development and contributed to identifying regional volumes that remain susceptible to postnatal microbiota influence. To understand how T cell deletion impacts peripheral immunophenotype, the final study investigated circulating myeloid cell numbers before and after puberty, alongside approach-avoidance behaviour tasks. Results indicate that *TCRb-/-d-/-* mice have higher monocyte and lower neutrophil

numbers compared to controls, and lack typical maturation of population heterogeneity and monocyte subtype observed in controls. Overall, this thesis demonstrates that the adaptive immune system is essential for typical neurodevelopment and contributes to efforts to identify the potential neuroimmune basis of neurodevelopmental disorders.

ACKNOWLEDGEMENTS

Above all, I would like to thank my supervisor Dr. Jane Foster. This work would not have been possible without her unwavering support, mentorship, and expertise. Every PhD journey is unique; however we have overcome more obstacles together than I could have ever foreseen. Through the years I have grown not only as a scientist but also as a person, and I owe a big part of that to you and your never-ending reassurance.

Thank you to my supervisory committee, Dr. Henry Szechtman, Dr. Michael Van Ameringen and Dr. Dawn Bowdish, my work is greatly improved thanks to the discussions and advice you provided throughout the research process. Partnerships with Dr. Jacob Ellegood and Dr. Jason Lerch in the POND project made this work possible.

The Foster Lab has evolved with my project, and I appreciate the input, friendship, and scholarly discussions I have shared with all members. Special thanks to Dr. Jon Lai and Dr. Karen-Anne McVey-Neufeld for your advice in the early days, Dr. Sarra Bahna for the edits and Starbucks runs, and Miranda, Sarah, Craig and April for the encouragement through the final stages of my thesis. An extra thank you to Shane Cleary for your sharp eye and excellent advice through the writing and defence preparation stages. Many undergraduate students have contributed to the projects presented here; thank you Bryce, Owen, Sureka, Cocoro, Gavin, Doug, Daiana, and

Angela. An extra thank you to Nima Karimi for the countless hours you have spent working with me – my hands appreciate your dedication!

Thank you to my cheering squad at home for all of their support and inspiration through this process – you have persevered through the long behaviour nights and endless hours of reading, writing, and meetings alongside me, I could not have finished without you. Thank you to my parents Heather and Kevin – to whom this thesis is dedicated – for teaching me persistence and work ethic, for your guidance, wisdom, and patience. To my sisters Carise and Rochelle: thank you for being my best friends and being excited to celebrate even the tiniest of milestones with me. I aspire to develop even a fraction of the dedication, kindness, compassion, and gumption that my family shows the world. Thank you, Grandpa and Grandpy, for giving me all the hugs I needed and never asking for an explanation. I am so honoured to represent you both with my name.

Thank you, Diana Shenwang, for being by my side to the very end, encouraging me to write, and for being my hands for hours of typing, making figures, and formatting animations on slide decks when my own hands would not. I will always be grateful for your constant support – you mean the world to me and to this dissertation.

Thanks to my forever friends – Lara Overmeyer, Max Sherry, Josh Si, Carmen Chan, Jake Roberts – and my family for your support and enthusiasm about my work, it makes all the difference to know that you have my back. I have met so many amazing people during my time at McMaster, thank you Ximena, Annia, Xiao, Zsu, Tinajero, Lety, Mark, Kumru, Carlos, Emma, Jenn, Melih, and all of my amazing soccer team and

Fairweather crew friends – no matter what goes down in the lab before, seeing you always has me smiling by the end of the day.

TABLE OF CONTENTS

LIST OF FIGURES

LIST OF TABLES

LIST OF ABBREVIATIONS

5HIAA	5-hydroxy indoleacetic acid
5HT	5-hydroxytryptamine
5HT2c	5-hydroxytryptamine 2c receptor
ACTH	adrenocorticotropic hormone
Ag	antigen
ANOVA	analysis of variance
ANTS	advanced normalization tools
ASD	autism spectrum disorder
ASF	Altered Shaedler Flora
B10.PL	B10.PL-H2u H2-T18a/(73NS)SnJ mouse strain
B6	C57Bl/6
BBB	blood brain barrier
BDNF	brain derived neurotrophic factor
BLA	basolateral amygdala
BrdU	bromodeoxyuridine
BST	bed nucleus of the stria terminalis
CA1	*Cornu Ammonis* 1
CA2	*Cornu Ammonis* 2
CA3	*Cornu Ammonis* 3
CCA	canonical correlation analysis
Ccl5-/-	C-C motif chemokine ligand 5 homozygous knockout
CCR2	C-chemokine receptor type 2
CD	cluster of differentiation
CD40L	cluster of differentiation 40 ligand
CD45	cluster of differentiation 45/lymphocyte common antigen
CeA	central amygdala
CNS	central nervous system
CSF	cerebrospinal fluid
Csf2-/-	colony stimulating factor 2 homozygous knockout
CTLA4	cytotoxic T lymphocyte-associated protein 4
Cx3cr1-/-	C-X3-C motif chemokine receptor 1 homozygous knockout
CXCL9	CXC motif chemokine ligand 9
DAMP	damage associated molecular pattern
DG	dentate gyrus
DR	dorsal raphe
dsRNA	double-stranded ribonucleic acid
EAE	experimental autoimmune encephalomyelitis
EDTA	ethylenediaminetetraacetic acid

EPM	elevated plus maze
FACS	fluorescence-activated cell sorting
FDR	false discovery rate
Foxn-/-	forkhead box n homozygous knockout
Foxp3	forkhead box P3
GF	germ free
GF/SPF	GF mice recolonized with SPF microbes
GFP	green fluorescent protein
GM-CSF	granulocyte monocyte colony stimulating factor
HIP	hippocampus
HPA	hypothalamic pituitary adrenal axis
HYP	hypothalamus
Iba1	ionized calcium binding adaptor molecule 1
ICAM-1	intercellular adhesion molecule 1
IFNb	interferon b
IFN_c	interferon c
Ifng-/-	interferon gamma homozygous knockout
IL	interleukin
Il12rb1-/-	interleukin 12 receptor subunit beta 1 homozygous knockout
Il17a-/-	interleukin 17a homozygous knockout
IRAK	IL1 receptor-associated kinase
IRF3	interferon regulatory factor 3
JNK	c-Jun N-terminal kinases
LD	light dark box test
LPS	lipopolysaccharide
Ly6C	lymphocyte antigen 6 complex, locus C
MAPK	mitogen-activated protein kinases
MBP	myelin basic protein
MD	Mahalanobis distance
MECP2	methyl CpG binding protein 2
MHCI	major histocompatibility complex 1
MHCII	major histocompatibility complex 2
microRNA	micro ribonucleic acid
MPTP	1-methyl-4-phenyl-1,2,3,6-tetrahydropyridine
MRI	magnetic resonance imaging
mSOD1-/-	mutant superoxide dismutase 1 homozygous knockout
MWM	Morris water maze
MyD88	myeloid differentiation primary response 88
N-α-syn	N-terminal region of alpha synuclein
NF-kB	nuclear factor kappa-light-chain-enhancer of activated B cells

NIH	National Institutes of Health
NK	natural killer
NK1.1	natural killer 1.1
NMDAR2B	N-methyl-D-aspartate receptor 2B
NO	novel object
NOD	non-obese diabetic
NLR	NOD-like receptor
NSERC	National Science and Engineering Research Council
nu/nu	homozygous nude
OBI	Ontario Brain Institute
OF	open field test
P	postnatal day
PAG	periaqueductal grey
PAMP	pathogen associated molecular pattern
pAPC	professional antigen presenting cell
PBS	phosphate buffered saline
PCA	principal component analysis
PFA	paraformaldehyde
PFC	prefrontal cortex
PRR	pattern recognition receptor
PSD95	postsynaptic density protein 95
PVN	paraventricular nucleus of the hypothalamus
RAG	V(D)J recombination activating gene
RNA	ribonucleic acid
Rorc-/-	RAR-related orphan receptor C
RS	Rett Syndrome
SCID	severe combined immunodeficiency
SEM	standard error of the mean
SJL/J	Swiss Jim Lambert
SLC6A4	solute carrier family 6 member 4
SPF	specific pathogen free
STAT	signal transducer and activator of transcription
TBS	tris buffered saline
TCR	T cell receptor
TCRβ-/-δ-/-	T cell receptor β and δ chain knockout
TCRγδ	gamma delta T cell receptor
TE	echo time
Th1 cells	type 1 helper T cells
TIR	Toll-IL1 receptor
TLR	Toll like receptor

TNF_a	tumour necrosis factor a
TNFR	tumor necrosis factor receptor
TR	repetition time
TRAF6	TNFR-associated factor 6
Treg	regulatory T cell
w	weeks (old)
WT	wild type
μMT-/-	B cell deficient mouse model

DECLARATION OF ACADEMIC ACHIEVEMENT

The author would like to gratefully acknowledge the following individuals for their experimental contributions and collaborations on this project. Sureka Pavalagantharajah for her help with animal husbandry and behavioural data collection for Paper 1; Cocoro Mori for her help with animal husbandry and behavioural data collection for Paper 1; Miranda Green for her help with PCA and density figure making and canonical correlation analysis in Paper 1; Bryce Kwiecien-Delaney for his help with animal husbandry for paper 1 and his help with the collection and analysis of densitometry data and collection of cell counts in paper 2; Owen Luo for his help with the collection and analysis of densitometry data in paper 2; Roksana Khalid for her help with taking photos of the BST in Paper 2 and collection of some tissue for Paper 3; Sarra Bahna for her help with collection of some tissue for Paper 3; Jacob Ellegood for his help with MRI scanning, analysis, and figure making in Paper 3. Nima Karimi for his help with typing, literature review and collection, and citation management for Papers 1-3.

All further data acquisition, analysis, and interpretation of the data from the above experiments was performed by the author as part of the thesis requirements. These contributions to the project are as follows: Paper 1. Data collection (behavioural testing, blood collection, tissue processing, flow cytometry), data analysis and interpretation, preparation and writing of manuscript. Paper 2. Data collection (tissue collection, image acquisition, optimization of image analysis software program), data analysis and interpretation, preparation and writing of manuscript. Paper 3. Data collection (perfusion, tissue collection), data analysis and interpretation, preparation and writing of manuscript.

In addition to the papers included in the thesis, during graduate studies the author was involved with the dissemination of the knowledge and findings associated with this project at local, national, and international conferences. The author also contributed to the field through already published work:

> Normandeau CP, Naumova D, Thompson SL**,** Ebrahimzadeh M, Liu YQ, Reynolds L, Ren HY, Hawken ER, Dumont ÉC. (2017). Advances in understanding and treating mental illness: proceedings of the 40th Canadian College of Neuropsychopharmacology Annual Meeting Symposia. J Psychiatry Neurosci. 42(5):353-358.

Each of the above achievements contributed to honours including the W. G. Dewhurst Travel Award (2015), Outstanding Poster Award (2016), H. G. Bertram Foundation Ontario Graduate Scholarship (2015-2016), Jock Cleghorn Prize (2017), Ontario Graduate Fellowship (2017-2018), Faculty of Health Science Program Excellence Award (2018), and the Rockton Lion's Club Scholarship (2018-2019).

Chapter 1

General Introduction

Neuroimmunology studies the connections and communications between the immune system and the brain. From a neuroscience perspective, the birth of "neuroimmunology" can be traced back to two seminal papers published in 1987 (Berkenbosch et al., 1987; Sapolsky et al., 1987). The following paradigm shift challenged the philosophies of both neuroscience and immunology. Until the early 2000s, the majority of research suggested that under healthy homeostatic conditions, the immune and nervous systems did not communicate due to the "immune privilege" of the central nervous system (CNS). It was hypothesized that immune impact on the brain and spinal cord was detrimental to neural function (Quan and Banks, 2007). Due to this predominant view, the majority of research surrounding immune-brain communication was dedicated to stroke conditions, spinal cord injury or multiple sclerosis. Conditions where immune cells access the CNS parenchyma cause some degree of injury to the CNS (Quan and Banks, 2007). However, molecules thought to be unique to the immune system are present and functional in the brain. In fact, the brain and immune system share neurotransmitters and their receptors, cytokines and chemokines and their receptors, integrins, and cell adhesion molecules.

Microglia, the innate immune cells of the brain and the spinal cord, were initially thought to be dormant in the healthy brain and activated only in response to insults such as infection or traumatic injury (Gehrmann et al., 1995; Kreutzberg, 1995; Soltys et al., 2001). In the past two decades, the importance of microglia to brain function has expanded with pivotal work demonstrating that microglia actively survey the entire parenchymal space every hour, even under unchallenged conditions (Davalos et al., 2005; Nimmerjahn et al., 2005; Paolicelli et al., 2011). Microglia are now known to have

highly motile processes even in their most ramified state, which contact all types of parenchymal cells and play critical roles in maintaining brain homeostasis as well as responding to illness and injury in the CNS.

The peripheral immune system is composed of two main branches: the innate and adaptive immune systems. The cells that make up the innate immune system include monocytes – the macrophage of the blood –, neutrophils, other granulocytes that release histamine particles in response to challenge, dendritic cells, and other tissue-specific macrophages, including microglia in the CNS. Primarily, the innate immune system's function is to respond quickly and non-specifically to pattern recognition receptors (PRRs) – primarily pathogen-associated molecular patterns (PAMPs) or damage-associated molecular patterns (DAMPs) – through recognition of surface toll-like receptors (TLRs), or NOD-like receptors (NLRs) in the cytoplasm (Janeway's Immunobiology 8th edition). In TLR signaling, recognition leads to dimer or oligomerization of TLR proteins, followed by interactions between Toll-IL1 receptor (TIR) domains in the cytoplasmic tail of each TLR chain (Janeway's Immunobiology 8th edition). The important universal adaptor, myeloid differentiation primary response 88 (MyD88), allows these receptor interactions to stimulate inflammatory responses, by either activating mitogen-activated protein kinases (MAPKs), or interacting with these TIR domains and recruiting the serine-threonine kinase IL1 receptor-associated kinase (IRAK) to the receptor tails, where it self-phosphorylates (Kawai and Akira, 2007, Takeda and Akira, 2004). Tumor necrosis factor receptor (TNFR)-associated factor 6 (TRAF6) then associates with the activated IRAK, which triggers one of many possible TLR-dependent cascades. These cascades either lead to c-Jun N-terminal kinase (JNK)

signaling or nuclear factor k-light-chain-enhancer of activated B cells (NF-kB), both of which end up in transcription regulation changes specific to the antigen which was initially recognized (Kawai and Akira, 2007, Takeda and Akira, 2004). NLR activation likewise activates NF-kB, causing transcriptional changes resulting in the same inflammatory outcomes as TLR activation, just originating by pattern recognition in the cytoplasm (Janeway's Immunobiology 8th edition). Alternatively, there is also a MyD88-independent pathway that can be induced when TLR4 is activated by lipopolysaccharide (LPS) or double-stranded ribonucleic acid (dsRNA) activation of TLR3. The transcription factor interferon regulatory factor 3 (IRF3) is activated, induces interferon b (IFNb), which then activates signal transducer and activator of transcription 1 (STAT1) and results in transcriptional changes (Takeda and Akira, 2004). Transcriptional changes resulting from PRR activation result in the upregulation of genes encoding pro-inflammatory cytokines, and co-stimulatory molecules on antigen presenting cells, allowing them to communicate with T cells (Kawai and Akira, 2007). The activation of these signaling cascades in response to an immune stimulus is referred to as the innate immune response. NLR signaling in the gut and brain has been associated with behaviour regulation (Pusceddu et al., 2019).

The adaptive immune system functions to recognize specific antigens and coordinate the most appropriate immune responses for each pathogen type. This response is accomplished through interactions with the professional antigen presenting cells (pAPCs) of the innate immune system and the production of antibodies and complement (Janeway's Immunobiology 8th edition). The other key roles of the adaptive immune system are in self-regulation of immune responses and creating immune

memory – where long-lived cells are prepared to respond quickly should the organism be re-exposed to an infectious agent (Janeway et al., 2005). T lymphocytes - widely known as T cells, B cells, and Natural Killer (NK) cells compose the adaptive immune system. T cells are an important part of the adaptive immune system, responding to epitopes presented by pAPCs to coordinate immune responses to specific pathogens, and also being critical holders of immune memory (Janeway's Immunobiology 8th edition). T cells produce and respond to many signaling molecules, including cytokines and chemokines, and express many different types of receptors and cellular adhesion molecules, allowing them to communicate with almost every cell type (Janeway *et al.*, 2005). B cells make antibodies critical for antigen-specific humoral immune responses, and NK cells, NK T cells and some CD8+ T cells, destroy host cells infected with viruses.

It is now widely accepted within the scientific community that the immune system communicates with the nervous system during healthy homeostatic conditions and in disease states. However, the immune system is specialized within the CNS and therefore it functions differently than it does in the periphery. The CNS is protected from many of the insults in the periphery by the blood brain barrier (BBB) (Kadry et al., 2020). The BBB primarily comprises endothelial cell tight junctions and astrocyte end feet, which prevent large and hydrophobic molecules from entering the CNS. This barrier also excludes the majority of immune cells from the circulation and lymphatic systems from entering the brain tissue, as well as some immune molecules. Within the brain parenchyma, microglia are the predominant immune cells. They constantly sample the extracellular fluid, phagocytose cellular debris, and interact with other parenchymal cells

to monitor for signs of infection. Under homeostatic conditions, microglia also play critical roles in synaptic pruning, developmental processes, neuroprotection, and metabolism (Tremblay, 2011; Tremblay et al., 2011). The ability of these dynamic cells to communicate with both neural and immune cells make them a good candidate to confer messages from the adaptive immune system necessary for the normal development of the brain.

Research indicating important roles for microglia in healthy homeostatic conditions has been growing. However, understanding how microglia confer messages from the periphery to the CNS is still in its infancy. To fill this gap, work in rats described regional differences in microglia number and morphology that changed over postnatal development, including sex differences across development persisting to adulthood in parts of the brain implicated in stress circuitry (Lenz et al., 2013; Schwarz and Bilbo, 2012). Microglia express several important surface receptors that allow them to respond to both neural and immune signaling (reviewed in Prinz and Priller 2014, Grabert 2016, Böttcher 2019). One important pathway described by which microglia may respond to T cell communication from the brain periphery is via interleukin 4 (IL4) signaling (reviewed in Gadani 2012). Microglia respond to IL4, a helper T cell cytokine, by adopting a more neuroprotective phenotype, upregulating expression of major histocompatibility complex 2 (MHCII) through activation of the STAT signaling cascade, and decreasing transcription of tumour necrosis factor a (TNF_a), a key pro-inflammatory cytokine (Butovsky 2005). These IL4-stimulated microglia support neurogenesis, promote neuron survival, and induce differentiation of neural stem cells (Butovsky 2006). IL4 knock out mice have impaired performance on the Morris Water Maze (MWM) task for spatial

learning and memory, a finding that has been associated with meningeal helper T cell production of IL4 and interferon c (IFN_c) (Derecki 2010). Indeed, evidence suggests that in the absence of these important signals from the peripheral immune system and gut microbiota, microglia fail to reach maturity in both morphology and gene expression (Erny et al., 2015; Thion and Garel, 2018; Thion et al., 2018a; Thion et al., 2018b).

Trillions of microbes, mainly bacteria, but also archaea, yeasts, helminth parasites, viruses, and protozoa are found in the gut (Eckburg et al., 2005; Gaci et al., 2014; Lankelma et al., 2015; Scarpellini et al., 2015; Williamson et al., 2016). Scholarly investigation across biomedical research areas has revealed that these microorganisms play an essential role in the functioning of our normal physiology. They are both commensal and symbiotic with the host, having a significant impact on health and disease. Evidence has shown that the relationship between the gut microbiome and its host influences the innate and adaptive immune system, the regulation of various metabolic pathways, and the physiology of the gut (Backhed et al., 2015; Erny *et al.*, 2015; Mayer et al., 2014; Murphy et al., 2010; Turnbaugh et al., 2007; Zhang et al., 2013). In the past decade, the role of the microbiome, and in particular, gut microbiota, in brain function has moved to the forefront of neuroscience research (Cryan et al., 2019). In 2004, a pivotal study by Sudo and colleagues demonstrated the importance of microbes in stress reactivity (Sudo et al., 2004). Germ-free (GF) mice, lacking all commensal bacteria, in comparison to conventionally housed mice, exhibited exaggerated levels of corticosterone and adrenocorticotropic hormone (ACTH) following restraint stress (Sudo *et al.*, 2004). These findings indicated that presence of microbiota is important for the proper functioning of the hypothalamic pituitary adrenal (HPA) axis

(Sudo *et al.*, 2004). Since then, the use of GF mice and other manipulations of gut microbiota have been used to explore the role of microbiota in brain function and behaviour (Cryan *et al.*, 2019; Luczynski et al., 2016). Signaling pathways between the gut microbiota and the brain include neural pathways such as the vagus nerve, immune, and humoral pathways. Gut microbiota influence host metabolism through local interactions, peripheral systems, and bidirectional communication with the liver (Cryan *et al.*, 2019; Foster, 2016; Foster and McVey Neufeld, 2013; Foster et al., 2017). In the absence of microbiota, as in GF conditions, the immune system is unable to develop completely; in particular, the adaptive immune system requires these microbe-based signals in order to allow for complete development of mature T and B cells (Zhao and Elson, 2018).

The immune system plays an important role in the communication between the brain and the gut (Bengmark, 2013). The HPA axis, the autonomic and enteric nervous systems interact with the immune system (Bateman et al., 1989; Genton and Kudsk, 2003; Hori et al., 1995; Leonard, 2005; Nance and Sanders, 2007). The gut itself is an important immune organ that provides a vital defensive barrier between externally derived pathogens and the internal biological environment. Gut-associated lymphoid tissues form the largest immune organ of the human body, comprising more than 70% of the total immune system (Vighi et al., 2008). The links between microbiota-immune communication are now a key consideration in efforts to understand mechanisms of immune-brain communication in animal studies and in clinical research.

In the early 2000s, a thorough investigation of sex differences in numbers of all major circulating immune cell types between 30 strains of mice commonly used in

biomedical research was reported, making a substantial contribution to immunophenotyping research (Petkova et al., 2008). In C57BL/6 mice, used in all three studies making up this thesis work as well as the majority of biomedical research using transgenic mice, there were no sex differences in numbers of granulocytes, eosinophils, monocytes, lymphocytes, or the major lymphocyte types: B cells, cluster of differentiation 4 (CD4)+ T cells, CD8+ T cells, or NK cells (Petkova *et al.*, 2008). Of note, C57BL/6 mice have among the highest lymphocyte numbers, lower than average monocyte numbers, and the lowest numbers of granulocytes out of all 30 strains immunophenotyped as part of the study (Petkova *et al.*, 2008). Among lymphocyte categories, C57BL/6 mice had average numbers of CD8+ T cells and NK cells, but more B cells and less CD4+ T cells than average (Petkova *et al.*, 2008). These strain differences in immunophenotype may contribute to some of the variation between behaviour studies in different laboratories and support the idea that peripheral immune cells may provide a temporal readout of environmental factors that could also affect immune signaling to the brain. Mouse models with broad immunodeficiencies, especially those with no adaptive immune cells, were reported to perform differently on major behavioural tests compared to wild type (WT) controls, suggesting a role for adaptive immune cells in behaviour (Rilett and Foster, 2014). Evidence from athymic nude mice that are T cell deficient suggests that T cells may be predominantly responsible for the changes observed in mice with broader adaptive immunodeficiencies due to both behaviour and brain structure changes (Diamond et al., 1986; Pan et al., 2018). In addition, mouse models of specific CD8+ and CD4+ T cell deficiencies show behaviour changes, but no gross neuroanatomical or cytokine

changes (Rattazzi et al., 2013). A seminal observation, in 2004, demonstrated that mice with adaptive immune system deficiencies performed worse than WT on spatial learning in the Morris Water Maze (MWM) (Kipnis et al., 2004). Based on these studies, it was concluded that T cells affect cognition, a surprising and impactful discovery. As a direct result, multiple laboratories investigated roles for T cells in neurogenesis, which led to the additional conclusion that while T cells are unlikely to enter the brain parenchyma under healthy conditions, they are able to influence brain function at the cellular level (Wolf et al., 2009; Ziv et al., 2006). This body of information collectively established the relationship between adaptive immune signals and the CNS, which is critical for healthy function.

Research using immunodeficient mouse models has provided evidence that the immune system is essential for brain development under homeostatic conditions. Further, research using models of adaptive immune deficiency, including V(D)J recombination activation gene (*RAG*) 1 and *RAG2* knock-out mice, and severe combined immunodeficiency (SCID) mice, has demonstrated that B and T cells impact behaviour. Behavioural tests where immunodeficient mice perform in an atypical manner include the Morris Water Maze, the light dark test, marble burying test, nestlet shredding test, predator odor exposure test, novel object recognition test, social interaction test, sucrose preference test, elevated plus maze, and open field (Clark et al., 2014; Clark et al., 2016; Clark et al., 2018; Cushman et al., 2003; Rattazzi *et al.*, 2013; Smith et al., 2014). In addition, targeted knockdown of *RAG1* in the amygdala impaired contextual fear memory on the classical fear conditioning task (Castro-Perez et al., 2016). A model of premature immunosenescence in mice, characterized by fewer

lymphocytes, demonstrated higher stress reactivity, increased anxiety-like behaviour, lower motor activity and neuromuscular coordination compared to controls (De la Fuente et al., 1998; Viveros et al., 2001). There is also a considerable body of research identifying neurobiological differences in mice with adaptive immune deficiencies including: increased microglia number in SCID mice (Lorke et al., 2008), decreased hippocampal neurogenesis and brain derived neurotrophic factor (BDNF) levels in *RAG2-/-* mice (Wolf *et al.*, 2009), increased hippocampal BDNF levels in *RAG2-/-* mice (Clark *et al.*, 2014), decreased expression of cFos, an immediate early gene suggesting neural activity, in the hippocampus and increased serum corticosterone (Smith *et al.*, 2014), less responsive microglia to immune challenge in *RAG2-/-* mice (Clark et al., 2015), and smaller brains in non-obese diabetic (NOD)/SCID mice compared to controls (Sajja et al., 2016). Studies have also shown that T cells specifically play important roles in brain development. For example, work using athymic nude mice, which have very small numbers of functional T cells (Ikehara et al., 1984), has shown some volume decreases in cortical thickness of the frontal lobe in female nude mice (Diamond *et al.*, 1986) and deficiencies in microglia surface receptor expression and function (Pan *et al.*, 2018). T cell receptor (TCR) double knock out (*TCRβ-/-δ-/-)* mice, deficient in all mature T cells by genetic deletion of the b and d chains of the TCR, also have behavioural differences on approach-avoidance tests (Mombaerts et al., 1992; Rilett et al., 2015). Interestingly, a rare human fetus found to have nude/SCID mutations was found to have the complete absence of a corpus callosum, but no other major CNS structural changes (Amorosi et al., 2010), while another individual with a mutation resulting in SCID had

global neurological abnormalities including microcephaly, specifically in the hippocampus and cortex (Woodbine et al., 2013).

Several studies have demonstrated the role of T cells and microglia in neurodevelopmental disorders such as Rett Syndrome (RS) and autism spectrum disorder (ASD) (Ashwood et al., 2011; Cronk et al., 2015; Estes and McAllister, 2015; Filiano et al., 2015; Li et al., 2014; Prinz and Priller, 2014; Vargas et al., 2005). Altered T cell phenotypes were observed in human patients with ASD, type 1 helper T cell (Th1) cytokines correlated with symptom severity, and Th2 cytokines correlated with cognitive function (Ashwood *et al.*, 2011). Furthermore, there is evidence that mutations in MECP2 (methyl CpG binding protein 2) lead to impaired T cell function in RS. Regulatory T cells express a signaling molecule that MECP2 regulates. Therefore mutations causing RS may cause dysregulation in the adaptive immune system (Li *et al.*, 2014). As in forkhead box P3 (Foxp3) in regulatory T cells, MECP2 is believed to regulate genes necessary for control of microglia and macrophage immune responses, leading to microglial dysfunction in RS (Cronk *et al.*, 2015). One study observed an increased area of immunostaining for microglial cell markers in the cerebellar grey and white matter in brain tissue of ASD patients compared to controls (Vargas *et al.*, 2005). They also found increased pro-inflammatory cytokine and chemokine levels in these patients (Vargas *et al.*, 2005).

The influences of peripheral immune cells on the healthy CNS have also been recognized. Mice with deficiencies in adaptive immune cells have altered behaviour, with deficits in learning and memory (Brynskikh et al., 2008) and reduced anxiety-like behaviours (Neufeld et al., 2011; Rilett *et al.*, 2015). While bidirectional communication

between the brain and periphery is now accepted, more investigation is required to determine the mechanisms involved. Our laboratory has considered the role of T cells in behaviour and brain structure (Rilett *et al.*, 2015; Sankar et al., 2012). Changes in anxiety-like behaviour and fear memory are observed in *TCRβ-/-δ-/-* mice (Rilett *et al.*, 2015). *Ex vivo* structural magnetic resonance imaging (MRI) revealed genotype and sex-by-genotype differences in the volume of several brain regions believed to be part of this circuitry in *TCRβ-/-δ-/-*mice compared to WT (Rilett *et al.*, 2015). Evidence suggests that T cell related neural effects may be mediated by microglia (Xie et al., 2015). Understanding the impact of T cell deficiency on the brain may allow us to make connections between peripheral immune dysfunction and brain function.

Hypothesis

Bidirectional and continuous communication between the immune system and the brain is essential to neuronal development, excitability, neuroplasticity, and neurotransmission. The *central hypothesis* that guides this thesis project is that a lack of peripheral immune regulation and alterations in peripheral immune function are underlying mechanisms contributing neurodevelopmental behavioural impairments.

Specific Aims

1. To determine the impact of T cell deficiency on microglia in stress circuitry in adult mice.
2. To determine the impact of T cell deficiency on peripheral myeloid cell populations from pre-puberty to adulthood.

3. To determine the neuroanatomical changes at the global level, and specifically in stress circuitry, associated with manipulations of the microbiota during postnatal development.

Chapter 2

Quantification of Microglia in Stress Circuitry of T-cell deficient Mice

Shawna L. Thompson, Bryce Kwiecien-Delaney, Owen Dan Luo, Sureka Pavalagantharajah, Roksana Khalid, and Jane A. Foster

Psychiatry and Behavioural Neuroscience, McMaster University, Hamilton, Ontario

CHAPTER LINK – Manuscript #1

There is ample evidence supporting that manipulations of the adaptive immune system result in changes to a number of different behaviour domains in healthy animals. Previous work identified a number of neuroanatomical changes in T cell deficient mice in regions that are part of the brain's stress circuitry – regions that are involved in many of the affected behaviours. Research suggests that T cells do not reside in the brain parenchyma under these homeostatic conditions, necessitating communication across the blood brain barrier to create behaviour changes. Previous work (reviewed in this chapter) observed sex differences in microglia number in the cortex, hippocampus, and amygdala of rats across postnatal development and into adulthood. Given that T cells signal via various cytokines and chemokines that microglia can receive and respond to (and vice versa), we decided to quantify microglia in the absence of T cells, to determine whether the loss of T cell signaling led to persistent changes in microglia number or density in regions with known volume changes and that are implicated in anxiety-like behaviour.

Abstract

The adaptive immune system affects risk of psychiatric illness, brain structure, and behaviour. Recent research suggests a role for microglia in communicating changes from T cells to neurons. Brain tissue from adult mice functionally deficient of T cells due to genetic knockout of the β and δ chains of the T cell receptor (*TCRβ-/-δ-/-)* and wild type (WT) mice was stained with the microglial marker Iba1, followed by densitometry analysis and cell counts. Genotype effects indicated increased Iba1+ microglia number in the basolateral amygdala in *TCRβ-/-δ-/-* mice. Male *TCRβ-/-δ-/-* mice showed reduced microglial density in the hippocampus and female *TCRβ-/-δ-/-* mice showed reduced microglial density in the prefrontal cortex in comparison to their sex-matched WT counterparts. This study provides evidence that T lymphocytes influence the number and density of resident microglia in central nervous system stress circuitry.

Introduction

Animal and clinical studies provide evidence that adaptive immunity may play an important role in modulating the risk of psychiatric illness, including anxiety disorders (Atanackovic et al., 2004; Guo et al., 2015; Masi et al., 2015; Neufeld et al., 2011; Rilett et al., 2015). In general, mice with adaptive immune deficits show behavioural differences in comparison to wild type (WT) mice in exploratory, anxiety-like, and activity measures (Brynskikh et al., 2008; Clark et al., 2016; Kipnis et al., 2004; Rattazzi et al., 2013; Rilett, et al., 2015; Sankar et al., 2012; Wolf et al., 2009; Ziv et al., 2006). Understanding the molecular changes underlying these behavioural differences is an important topic in neuroimmunology.

The importance of adaptive immunity to neuroanatomy is evident in the body of literature describing work on immunocompromised mice. For example, germ free (GF) mice do not develop complete adaptive immune systems due to their lack of bacteria in the gut and are typically considered to have reduced and immature T cell populations (Round and Mazmanian, 2009). GF mice have also been shown to have increased amygdala and hippocampus volumes, compared to conventionally housed mice, an observation that was associated with changes in dendritic morphology (Luczynski et al., 2016). Additional brain volume differences have been reported, especially in white matter regions, in GF mice prior to puberty (Lu et al., 2018). Brain volume differences in mice lacking all functional T cells due to knock out of T cell receptor β and δ chains (*TCRβ-/-δ-/-*) have been reported (Rilett, et al., 2015). Several stress-related brain regions including the prefrontal cortex (PFC), bed nucleus of the stria terminalis (BST), basolateral amygdala (BLA), paraventricular nucleus of the hypothalamus (PVN),

hippocampus (HIP), periaqueductal grey (PAG), and dorsal raphe nucleus (DR), showed genotype differences or genotype and sex interactions between *TCRβ-/-δ-/-* and WT mice (Rilett, et al., 2015). In addition, *TCRβ-/-δ-/-* mice have increased baseline plasma corticosterone and an exaggerated changes in gene expression in CNS stress circuitry in response to repeated restraint stress (Rilett et al., 2020). To date, it is not clear whether the long-term changes in brain structure and function are reflective of underlying changes in neuronal cells or glial cells.

Microglia play critical roles in brain development, structure, and behaviour in physiological conditions. Interestingly, T lymphocytes are known to regulate microglia function (Garber et al., 2019; Xie et al., 2015), and severe combined immunodeficiency mice that lack both mature T and B lymphocytes have been shown to have increased microglia density (Lorke et al., 2008), whereas athymic nude mice lacking mature T lymphocytes were shown to have no difference in microglia number in the brainstem (Pan et al., 2018). The current work utilized T cell deficient mice, lacking all functional T cells, as a result of double knock-out of the β and δ chains of the T-cell receptor (*TCR β-/-δ-/-)* to examine the impact of loss of T cells on microglia number and density in key stress brain regions in male and female T cell deficient mice and WT mice.

Experimental Procedues

Animals

Mice lacking T cells due to a genetic knockout of the T cell receptor β and δ chains (*TCRβ-/-δ-/-*) on a C57Bl/6 background (Mombaerts et al., 1994) and C57Bl/6 (WT) mice were obtained from Dr. Andrew MacPherson at McMaster University and were

bred in-house. Mice were housed in a specific pathogen free environment with a 12-hour light/dark cycle and access to food and water *ad libitum*. All experiments were completed in accordance with the guidelines set out by the Canadian Council on Animal Care and were approved by the McMaster Animal Research Ethics Board.

Tissue Preparation.

Male and female WT and *TCRβ-/-δ-/-* mice (n=6) were perfused transcardially at 11 weeks of age, beginning with a 30-minute flush with phosphate buffered saline (PBS), pH 7.4 (Bioshop, Burlington, ON) and heparin (Sandoz Canada Inc., Boucherville QC), followed by a 30-minute fixation with 4% paraformaldehyde (PFA) in PBS, pH 7.4 (Alfa Aesar, Ward Hill MA) at a rate of 1 ml/min. One male and one female mice from 6 litters were included in the experiment. Brains were removed, post-fixed in PFA overnight, and then transferred to PBS. Brains were sent to Neuroscience Associates (Knoxville, TN), where they were treated overnight with 20% glycerol and 2% dimethylsulfoxide. All 24 brains were embedded in a gelatin matrix using MultiBrain™ Technology (NeuroScience Associates, Knoxville, TN). The gelatin block was cryoprotected with sucrose and fixed with 4% PFA before being rapidly frozen in isopentane at -70°C. The block was coronally sectioned at 36 µm on an AO 860 sliding microtome, and sections were placed in Antigen Preserve solution (50% PBS pH 7.0, 50% Ethylene glycol, 1% Polyvinyl Pyrrolidone) and kept at -20°C until immunohistochemistry.

Immunohistochemistry.

Free-floating immunohistochemistry was performed on every 8th section using anti-Iba1 antibody (Rabbit anti-mouse Iba1, 1:15000, Wako Chemicals). Endogenous

peroxidases were quenched with 0.9% hydrogen peroxide in 0.02%Triton X in Tris-buffered saline (TBS) before the sections were blocked with serum and then washed in TBS containing Triton X100 (0.1%). Sections were incubated in primary antibody overnight at room temperature, then rinsed with TBS before incubation in biotinylated secondary antibody (Vecta Elite Goat anti-Rabbit concentration). Avidin-biotin-horseradish peroxidase complex (Vectastain elite ABC kit, Vector, Burlingame, CA) was then applied for 30 mins before rinsing and treatment with diaminobenzidine tetrahydrochloride and hydrogen peroxide. Sections were mounted on gelatin-subbed slides, air-dried, dehydrated in alcohol, cleared in xylene and cover slipped.

Image Analysis and Densitometry

Slide images were analyzed on a Macintosh computer using the NIH Image program (developed at the U.S. National Institutes of Health and available on the Internet at http://rsb.info.nih.gov/nih-image). Matched tissue sections across animals were selected at low magnification and images collected at higher magnification. One left and right image was collected for each brain region analysed, except for DR, where a single midline image was collected. Two blinded, independent observers defined the threshold for Iba1+ stained signal pixels by determining the optical density of cell-poor areas within the grey scale digitized images. The number of pixels and mean signal intensity above this determined background was then computed (Density Slice function; NIH image). A measure of % Iba1+ signal area in mm^2 was obtained by dividing the previously computed number of stained pixels by the total number of pixels on the image and multiplying by the total histological area of the image. An Iba1+ integrated density value was then calculated by multiplying the % Iba1+ signal area and the Iba1+

mean signal area intensity. For brain regions with bilateral symmetry, values from the left and right hemispheres of the mouse brain were averaged to obtain a single Iba1+ integrated density value per brain region of interest for each mouse.

Quantification of Iba1-positive cells

Brain regions examined included the prefrontal cortex (PFC, Bregma 2.10 mm), dorsal and ventral bed nucleus of stria terminalis (BST, Bregma 0.38 mm), paraventricular nucleus of the hypothalamus (PVN, Bregma -0.70 mm), basolateral amydgala (BLA, Bregma -1.22 mm), CA1 region of the hippocampus (HIP, Bregma -1.94 mm), periaqueductal gray (PAG, Bregma -4.36 mm), and dorsal raphe (DR, Bregma -4.48 mm) (Paxinos and Franklin, 2001). Immunostaining was observed with a 40x objective using a Zeiss Axioskop 2 Plus microscope and photographed using the AxioCam MRc microscope camera. One left and right image was collected for each brain region analysed, except for DR, where a single midline image was collected. Using AxioVision microscope automated software, microglia were quantified by threshold analysis. Thresholds were set to soma quantification, and all regions smaller than 21μm^2 were excluded. Artifacts were manually removed by the scorer, and the program was visually quality controlled by three blind observers, and microglia cell counts were averag

Data Analysis

GraphPad Prism 9.1.2 (La Jolla, CA) was used for statistical analysis and to create graphs. Microglia density data was analyzed by ANOVA with region, genotype, and sex as factors. Microglia cell count data was analyzed by ANOVA with sex and genotype as factors. Posthoc analysis was conducted using Bonferroni's multiple

comparisons test. A p-value of <0.05 was considered significant.

Results

Densitometry Analysis of Iba1+ Staining

To assess the impact of loss of functional T cells on microglial density, the expression of the microglia marker, Iba1, was quantified across several stress-related brain regions (Fig. 2-1A). Omnibus analysis of Iba1+ integrated density revealed main effects of region ($F[6, 112] = 19.13$, $p < 0.05$), genotype ($F(1, 112) = 9.23$, $p<0.05$), interaction between genotype and region ($F[6, 112] = 3.04$, $p<0.05$), and interaction between genotype and sex ($F[6, 112] = 4.87$, $p<0.05$). Post-hoc analysis showed reduced Iba1+ integrated density in the PFC in female *TCRβ-/-δ-/-* mice compared to female WT mice ($p=0.045$; Fig 2-1B) and there was also a reduction in Iba1+ integrated density of male *TCRβ-/-δ-/-* mice relative to sex-matched WT mice in the HIP ($p=0.013$; Fig 2-1B).

TCRβ-/-δ-/- mice have more Iba1+ microglial cells in the BLA

Representative images of Iba1+ immunostaining for each brain region and the number of Iba1+ microglia cells are shown in Fig. 2-22. No sex differences in microglial number were observed; however, a significant difference in microglia number was found in the BLA ($p=0.046$, 95% CI [0.5142-57.073]), where more microglia were found in *TCRβ-/-δ-/-* mice. No differences in microglia number or morphology related to the impact of *TCRβ-/-δ-/-* genotype and sex were found in other brain regions (Fig 2). Additionaly, all microglia observed in this study had a ramified morphology. No amoeboid microglia were observed.

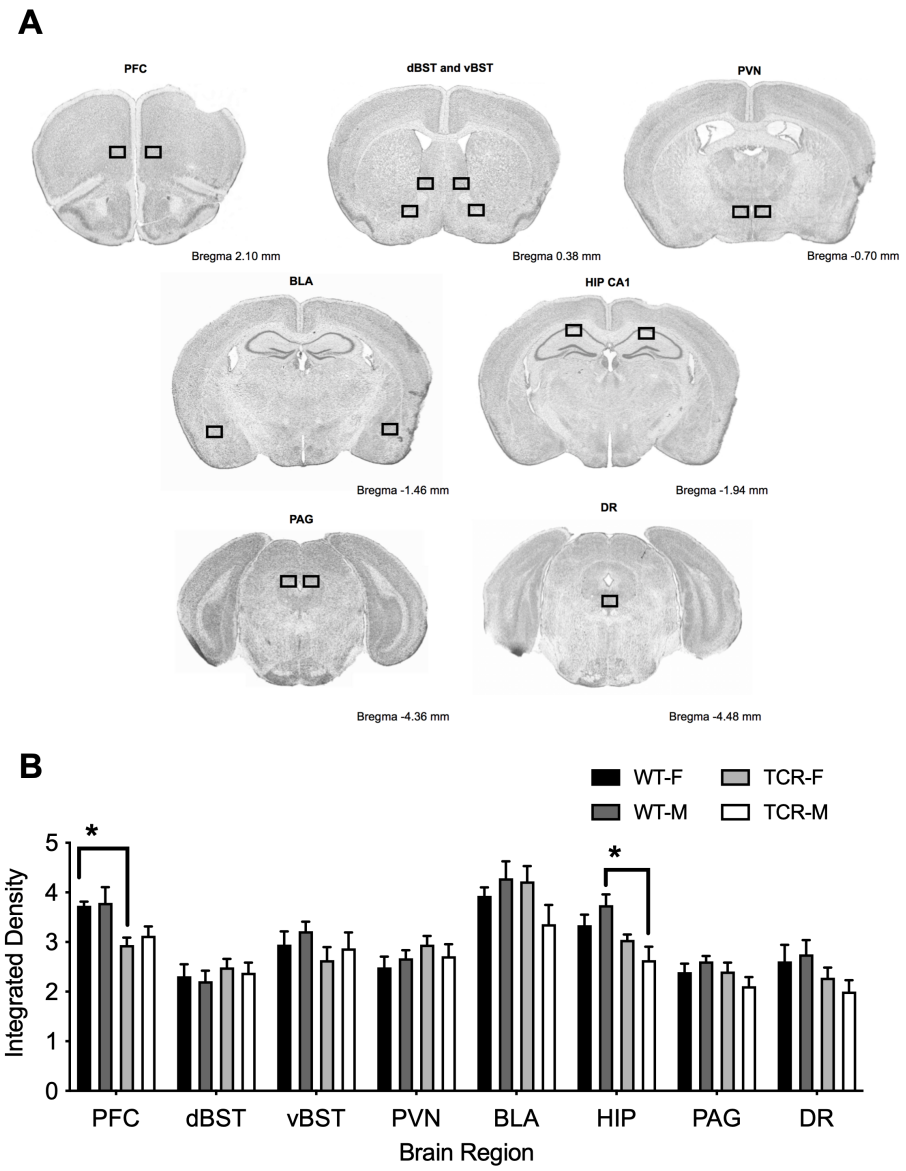

Fig. 2-1. Immunohistochemical analysis of microglia density in WT and *TCRβ-/-δ-/-* mice. To assess the impact of loss of functional T cells on microglial density, the expression of the microglia marker, Iba1, was quantified across several stress-related brain regions (A). Reduced Iba1 density in the PFC was observed in female *TCRβ-/-δ-/-* mice compared to female WT mice and male *TCRβ-/-δ-/-* mice showed reduced Iba1 density relative to sex-matched WT mice in the HIP (B). Data shown are mean +/- SEM, statistically significant differences are indicated by *p<0.05.

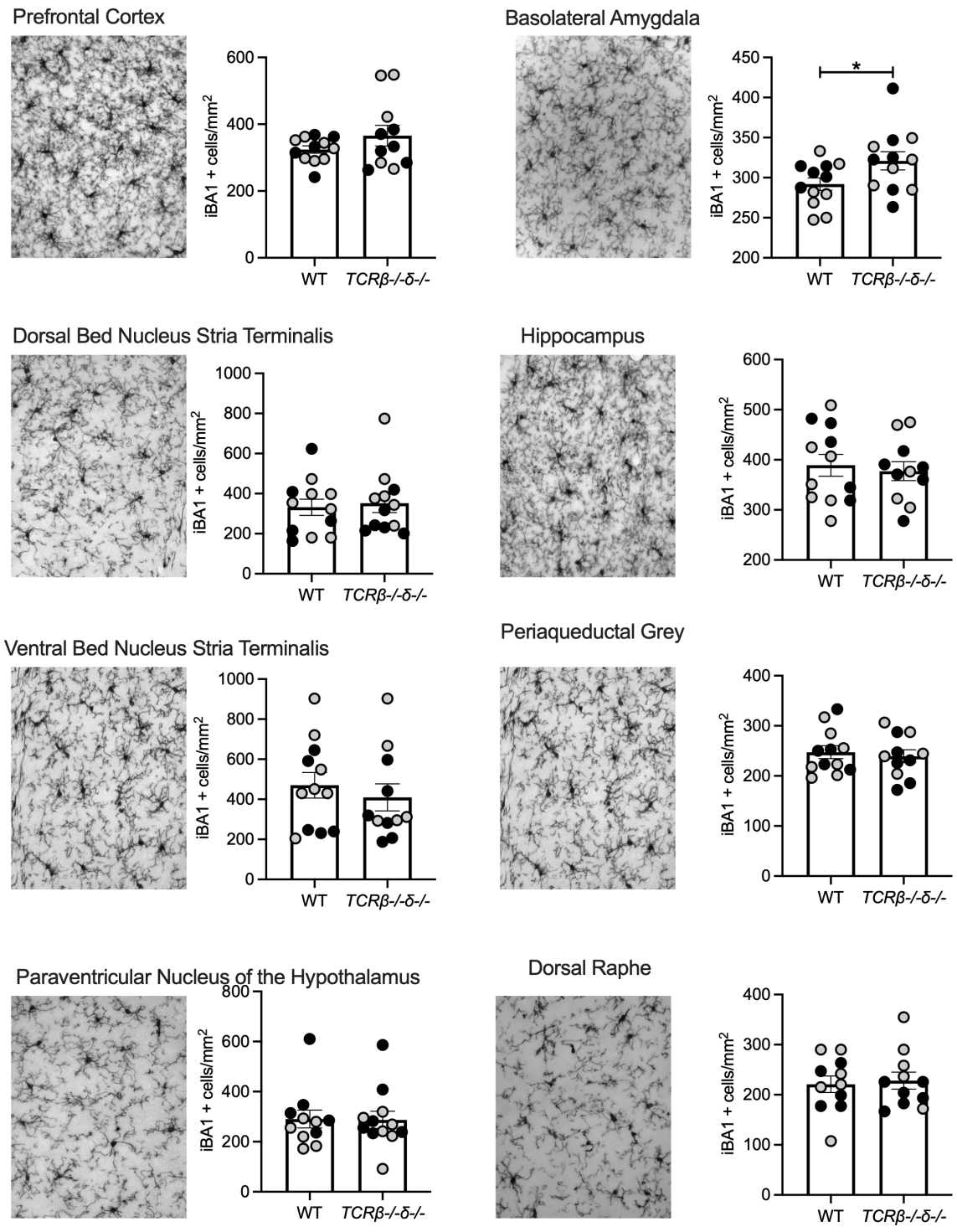

Fig. 2-2. Immunohistochemical analysis of microglia cell count in WT and *TCRβ-/-δ-/-* mice. Quantification of Iba1+ cells/mm^2 was performed on 20x images of regions of

interest: prefrontal cortex, dorsal bed nucleus stria terminalis, ventral bed nucleus stria terminalis, paraventricular nucleus of the hypothalams, basolateral amygdala, hippocampus, periaqueductal grey, and dorsal raphe. A significant genotype difference was observed in the basolateral amygdalat, where more Iba1+ microglial cells were found in T cell deficient mice. No significant sex differences were observed in any of the regions investigated (Male ●, Female ○). Data shown are mean +/- SEM, statistically significant differences are indicated by *p<0.05

Discussion

Microglia, the immune cell of the brain and spinal cord, have been shown to have necessary homeostatic functions, as well as roles to mitigate responses to injury and infection in the central nervous system (CNS) (Belfiore et al., 2019; Bernier et al., 2020; Thion and Garel, 2018). Regardless of the location of T cells in respect to the CNS, be it in the parenchyma or surrounding tissues, substantial evidence supports T cell communication to microglial cells (Table 1). Admittedly there is some controversy over whether T cells from the periphery enter the brain parenchyma in homeostatic conditions, with some of the more recent publications indicating that small numbers exist in the parenchyma very transiently (Pasciuto et al., 2020; Song et al., 2016). Still, it has been well established that these adaptive immune cells are in close proximity to microglia and other parenchymal cells that express the necessary receptors for bidirectional communication with the adaptive immune system, in the CNS lymphatic vessels, the choroid plexus, blood vessels and perivascular spaces, and in circumventricular organs. The discovery of CNS lymphatic vessels in 2015 has led to

Table 2-1. Key studies examining T cell impact on microglia

Conditions	Strain	Model	Design	Communication Type	Outcome	Reference
Homeostatic	Human		Co-culture	Cell to cell contact	T cells induce microglia to secrete Il-10 in a contact-dependent manner (CD40-CD40L, CD28-CTLA4-B7, and CD23-CD11b/c)	(Chabot et al., 1999)
	C57Bl/6, B10.PL	*CD40-/-*	Experimental Autoimmune Encephalomye-litis (EAE)	Cell to cell contact (CD40/CD40L interaction)	Cell contact between T cells and microglia is essential for microglia to reach their maximally activated state.	(Ponomarev et al., 2007)
	BALB/c	DO11.10 TCR transgenic mice	Neurantigen stimulation	Cell to cell contact (MHCII/Ag - TCR interaction), cytokine (IFNγ, GM-CSF)	Th1 cells induced microglia expression of costimulatory markers (MHCII, CD40, and CD54) GM-CSF from T cells stimulate microglia to induce T cell proliferation	(Aloisi et al., 2000)
	C57Bl/6, SJL/J	OTII *RAG/-TCRα-/-, MHCII-/-*, anti-CD4	Culture, cultured brain slice seeded	Cell to cell contact, cytokines	In the absence of T cells, microglia are unable to differentiate from an immature embryonic	(Pasciuto, et al., 2020)

	depleting antibodies	with CD4+ T cells		state to a mature adult phenotype. This was reversible with T cell transfer to deficient animals.	
C57Bl/6	*Foxn-/- Cx3cr1-/- Ccr2-/- Ccr2-/-, Ccl5-/-*	Athymic (nude) mice (T cell deficient)	Cytokine	No difference was observed in microglia number in the brain stem of nude mice. An increased percentage of amoeboid microglia was observed compared to control. A functional deficit was determined including altered gene expression profile, decreased cytokine release and decreased phagocytosis.	(Pan, et al., 2018)
C57Bl/6	Control	Aged (18-22 month) compared to adult (8-12 week old)	Cytokine (TNF-α)	Increased CD8+ T cell numbers correlate with increased microglia number and decreased microglia size	(Ritzel et al., 2016)
SJL/J, C57Bl/6	*Il12rb1-/-, Il12rb2-/-, Ifng-/-,*	*GM-CSF-/-* T cell transfer	Cytokines	T cells induce microglia to adopt an activated phenotype upon release of GM-CSF	(Codarri et al., 2011)

	Csf2-/-, Csf2rb-/-, Rorc$^{GFP/GFP}$, Il17a-/-				
BALB/c	nu/nu (Athymic)	Athymic mice (T cell deficient)	Soluble factors	Neonatal and adult athymic mice have large decreases in microglia number. Microglia in T cell deficient mice did not show any major morphological changes.	(Htain et al., 1995)
C57Bl/6	Control	Exercise enrichment	Soluble factors	No difference in number or morphology of microglia in exercise enriched mice was determined, even though increases in T cell-induced neurogenesis have been described in this model.	(Olah et al., 2009)
C57Bl/6	Control	Culture	Soluble factors	Gene expression profiles in microglia were affected by exposure to Th1 cell-conditioned medium. Microglia were induced to adopt a more activated phenotype, while Th17 cells were	(Prajeeth et al., 2014)

					unable to induce a notable change.	
	C57Bl/6	Control	Culture	Soluble factors	Microglia exposed to Th1 cell- conditioned medium express an entirely different transcriptional profile. Many of the pathways most affected are associated with T cell activation or signaling cascades.	(Prajeeth et al., 2018)
Pathology	C57Bl/6	Bone marrow transfer	MPTP challenge	Cell to cell contact	Infiltrating T cells contacted phagocytic, MHCII expressing microglia	(Depboylu et al., 2012)
	SJL/J	Control	Neurantigen-primed T cell transfer	Cell to cell contact	T cells from female, but not male, mice are able to activate microglia to produce reactive oxygen species. Castrated male T cells behaved like T cells from females, and either of these were able to activate microglia from male mice.	(Dasgupta et al., 2005)

C57Bl/6	*IFNg-/-*	T cell immunotherapy	Cell to cell contact, chemokine	T cells induce microglia to express CD11c, MHCI, MHCII, CXCL9, and CCL5.	(Herz et al., 2015)
C57Bl/6	N-α-syn stimulation	Culture	Cell to cell contact, cytokine	Regulatory T cells induce microglia to express an altered gene expression profile, largely influencing microglia to adopt an anti-inflammatory phenotype. Phagocytosis was increased after Treg exposure, suggesting a functional change in microglia.	(Reynolds et al., 2009)
B10.PL	Transgenic mice carrying a TCR for MBP peptide Ac1-11	Organotypic brain slices exposed to T cells	Cell to cell contact, cytokine (TNF-α)	T cells induce microglia to become activated and adopt a more amoeboid morphology.	(Gimsa et al., 2000)
SJL/J	Control	Adoptive T cell transfer	Cytokine	Lesion-associated T cells induce microglia to release cytokines	(Grebing et al., 2016)
C57Bl/6, B10.PL	*GM-CSF-/-*	EAE	Cytokine (GM-CSF)	T cells use GM-CSF to activate to microglia to attract more T cells and induce their proliferation	(Ponomarev, et al., 2007)

	C57Bl/6	*mSOD1-/-*	Culture	Cytokine (IL4)	T-reg cells increased microglia release of reactive oxygen species	(Zhao et al., 2012)

the current understanding that T cells, among other circulating immune cells, reside in a space adjacent to brain tissue (Louveau et al., 2015). Recently, it was shown that meningeal TCRγδ cells mediate behaviour through signaling to the CNS (Alves De Lima et al., 2020).

Peripheral T cells contribute to synaptic pruning via their action on microglial maturation in the postnatal mouse brain (Pasciuto et al., 2020). This report shows that *TCR β-/-δ-/-* mice have reduced microglia density in the prefrontal cortex and hippocampus, as well as increased number of microglia in the basolateral amygdala, in adult mice. Studies evaluating microglial number have reported no differences in brain stems of T cell deficient nude mice (Pan, et al., 2018) or in the hippocampus (Olah, et al., 2009). Notably, an increased percentage of amoeboid microglia was recently reported in nude mice compared to controls, and functional deficit in cytokine response to lipopolysaccaride and phagocytosis (Pan, et al., 2018). Changes in microglial morphology do not directly relate to functional changes that may be mediated by T cells. A finding lending an explanation to the contradictions in the reports are partially explained by studies showing transcriptional profiles of microglia could be influenced by T cells, regardless of their effect on microglia number or morphology. Cultured microglia exposed to conditioned medium from Th1 cells expressed a large number of differentially expressed genes, often associated with microglia activation, inflammation,

phagocytosis, and cell to cell communication (Prajeeth, et al., 2018; Prajeeth, et al., 2014). Microglia were found to down-regulate genes associated with cholesterol biosynthesis, which may be associated with cytoskeleton modifications, thereby resulting in morphological changes. T cells were also found to be differentially able to induce these microglia phenotypic changes, demonstrating that exposure to Th1, but not Th17, conditioned medium is able to activate microglia to express inflammatory transcripts and increased phagocytosis (Prajeeth, et al., 2014). Regulatory T cells were similarly found to affect microglia transcriptional, inducing microglia to adopt an anti-inflammatory phenotype in diseased conditions (Reynolds, et al., 2009). Furthermore, a large study recently profiled microglia transcription across the life span in T cell deficient and control mice, and found that in the absence of T cells, microglia were unable to differentiate to adopt a mature phenotype (Pasciuto, et al., 2020). This robust finding was rescued by transfer of T cells to deficient animals, and replicated by anti-CD4 antibodies delivered to WT mice (Pasciuto, et al., 2020). Further investigation into the potential for functional changes to microglia based on this compelling transcriptomic evidence is needed in T cell deficient mice, with special attention paid to the differences between current models of T cell deficiency and their impact on the findings.

Substantial research that demonstrates the ability of helper T cells to stimulate microglia to upregulate surface marker expression and cytokine secretion under specific conditions *in vitro,* demonstrating mechanisms for T cells to cause functional changes in microglia without necessarily affecting cell number. A number of studies have investigated the mechanisms of T cell-microglia communication *in vitro,* which can be a

helpful tool with the caveat that microglia respond to culture conditions, so morphology and functional findings especially require confirmation in *in vivo* conditions. IFNγ, a major Th1 cytokine, causes microglia to upregulate the expression of MHC II, CD40, and ICAM-1, secrete IL-2, IL-4, IFNγ, and induce T cell proliferation (Aloisi et al., 1998) Neither TNF- α or IL-1 β were able to induce microglia with the same result (Aloisi, et al., 1998). Likewise, Th1 cells can induce microglia to express MHC II, CD40, and CD54 upon MHC II/Ag - TCR interaction; consequently affecting their ability to communicate with other immune cells (Aloisi, et al., 2000). A number of immune cells residing in the meningeal space are capable of secreting GM-CSF, which is also able to stimulate microglia to activate Th1 cells, but without upregulating MHC II and CD40 on their surface, contrary to IFNγ (Aloisi, et al., 2000; Codarri, et al., 2011; Ponomarev, et al., 2007).

One possible reason for the limited observed differences in microglial number or density in the target brain regions is that brain volume changes previously observed in this mouse model resulted from structural modifications to neurons, resulting from functional changes in microglia to prune synapses and secrete trophic factors (Rilett, et al., 2015). Brain region volume differences in GF mice have been measured by immunohistochemistry that were largely due to axonal and dendritic arborization rather than cell number in either neuron or glial populations (Luczynski, et al., 2016). Additionally, brain volume measured by MRI, as is typical in human neuroscience research, has been demonstrated to be affected by a number of factors including hydration, time of day of measurement, medications, hypertension and type 2 diabetes (Reviewed in Dieleman et al. , 2017). This, in combination with research indicating

synaptic pruning deficits in immature microglia from T cell deficient mice, and impaired phagocytic capacity identified in many studies of T cell manipulation, increases the likelihood that we might observe structural change in neurons resulting from microglia impairment in the absence of T cell signals (Pan, et al., 2018; Pasciuto, et al., 2020; Reynolds, et al., 2009). Future studies investigating neuronal morphology and number are merited to determine the underlying cause of MRI volume differences in T cell deficient mice in the absence of changes in microglial number.

In this study, we observed increases in microglia cell number in the BLA of T cell deficient mice. Likewise, mice deficient in B and T cells were found to have more microglia than control animals, with increased microglial cell density reported in the motor cortex, hippocampus, fimbria of the hippocampus, facial nucleus, and cerebellum (Lorke, et al., 2008). No differences were reported in the number of Iba1+ cells between *TLR4-/-* or *TLR4+/-* mice compared to controls, suggesting that TLR4 signaling to T cells is not necessarily part of the mechanism for increased microglia number in the BLA of *TCRβ-/-δ-/-* mice (Bolton et al., 2017). Research in T cell deficient nude mice showed a significant decrease in microglia number, comparable to this study's observation of reduced Iba1+ staining density in the PFC of female *TCRβ-/-δ-/-* mice and the hippocampus of male *TCRβ-/-δ-/-* mice, which may represent some concordance with the nude mouse model (Htain, et al., 1995). Similarly, mice lacking all B and T cells were found to have reduced numbers of Iba1+ microglia in the hypothalamus (Clark et al., 2015).

Notably, the microglial density differences observed in this study were sex-specific. Dasgupta *et al* observed a functional difference in the ability of T cells from female and male animals to activate microglia (Dasgupta, et al., 2005), suggesting that sex-by-genotype effects on microglia might arise from T cell deficiency. One limitation to the findings of the study concerns the species of model organism employed. In the seminal work by Schwartz et al., a sex difference in microglia number and morphology in the CA1 region of the hippocampus in rats (Schwarz et al., 2012), has been replicated in both rats (Lenz et al., 2013) and mice (Guneykaya et al., 2018; Mouton et al., 2002). While an increased number of microglial cells was found in the brains of adult female rats, no difference was observed in mice in the present study and several other recent publications (Bolton, et al., 2017; Doyle et al., 2017; Hanamsagar et al., 2017; Nelson et al., 2017; Perez-Pouchoulen et al., 2015; Posillico et al., 2015). In addition, this study examined adult mice and alterations in immune-brain interactions earlier in postnatal development could impact microglial density and function.

Conclusion

In conclusion, we quantified microglia and Iba1 staining density in 8 brain regions and identified genotype effects in microglia number in the BLA. *TCRβ-/-δ-/-* mice have more microglia in the BLA compared to WT controls, however no genotype- or sex-by-genotype effects in microglial cell count were observed elsewhere. T cell deficient females were found to have reduced Iba1+ density in the PFC; similarly, *TCRβ-/-δ-/-* males had reduced Iba1+ density in the CA1 region of the hippocampus. We present here a systematic evaluation of microglia number and density by two unbiased methods

in 8 brain regions often investigated in neuroimmunology research due to their roles in stress circuitry. By using *TCRβ-/-δ-/-* mice, a model of selective T cell-mediated immunodeficiency, we differentiate T cell- specific effects on microglia from the cumulative effects of the depletion of all adaptive immune cells, adding to the body of immune-brain research. Future studies should investigate T cell-microglia communication, specifically in the BLA, PFC, and HIP, to identify the effects of microglial density on their function, and investigate functional and neuronal features in the stress circuitry of immunodeficient mice.

References

Aloisi F, De Simone R, Columba-Cabezas S, Penna G, Adorini L (2000), Functional maturation of adult mouse resting microglia into an APC is promoted by granulocyte-macrophage colony-stimulating factor and interaction with Th1 cells. J Immunol 164:1705-1712.

Aloisi F, Ria F, Penna G, Adorini L (1998), Microglia Are More Efficient Than Astrocytes in Antigen Processing and in Th1 But Not Th2 Cell Activation. The Journal of Immunology 160:4671-4680.

Alves de Lima K, Rustenhoven J, Da Mesquita S, Wall M, Salvador AF, Smirnov I, Martelossi Cebinelli G, Mamuladze T, et al. (2020), Meningeal γδ T cells regulate anxiety-like behavior via IL-17a signaling in neurons. Nat Immunol 21:1421-1429.

Atanackovic D, Kroger H, Serke S, Deter HC (2004), Immune parameters in patients with anxiety or depression during psychotherapy. J Affect Disord 81:201-209.

Belfiore R, Rodin A, Ferreira E, Velazquez R, Branca C, Caccamo A, Oddo S (2019), Temporal and regional progression of Alzheimer's disease-like pathology in 3xTg-AD mice. Aging Cell 18:e12873.

Bernier LP, York EM, Kamyabi A, Choi HB, Weilinger NL, MacVicar BA (2020), Microglial metabolic flexibility supports immune surveillance of the brain parenchyma. Nat Commun 11:1559.

Bolton JL, Marinero S, Hassanzadeh T, Natesan D, Le D, Belliveau C, Mason SN, Auten RL, et al. (2017), Gestational Exposure to Air Pollution Alters Cortical Volume,

Microglial Morphology, and Microglia-Neuron Interactions in a Sex-Specific Manner. Front Synaptic Neurosci 9:10.

Brynskikh A, Warren T, Zhu J, Kipnis J (2008), Adaptive immunity affects learning behavior in mice. Brain Behav Immun 22:861-869.

Chabot S, Williams G, Hamilton M, Sutherland G, Yong VW (1999), Mechanisms of IL-10 Production in Human Microglia-T Cell Interaction. The Journal of Immunology 162:6819-6828.

Clark SM, Michael KC, Klaus J, Mert A, Romano-Verthelyi A, Sand J, Tonelli LH (2015), Dissociation between sickness behavior and emotionality during lipopolysaccharide challenge in lymphocyte deficient Rag2(-/-) mice. Behav Brain Res 278:74-82.

Clark SM, Soroka JA, Song C, Li X, Tonelli LH (2016), CD4(+) T cells confer anxiolytic and antidepressant-like effects, but enhance fear memory processes in Rag2(-/-) mice. Stress 19:303-311.

Codarri L, Gyülvészi G, Tosevski V, Hesske L, Fontana A, Magnenat L, Suter T, Becher B (2011), RORγt drives production of the cytokine GM-CSF in helper T cells, which is essential for the effector phase of autoimmune neuroinflammation. Nature Immunology 12:560-567.

Dasgupta S, Jana M, Liu X, Pahan K (2005), Myelin basic protein-primed T cells of female but not male mice induce nitric-oxide synthase and proinflammatory cytokines in microglia: implications for gender bias in multiple sclerosis. J Biol Chem 280:32609-32617.

Depboylu C, Stricker S, Ghobril JP, Oertel WH, Priller J, Höglinger GU (2012), Brain-resident microglia predominate over infiltrating myeloid cells in activation, phagocytosis and interaction with T-lymphocytes in the MPTP mouse model of Parkinson disease. Exp Neurol 238:183-191.

Dieleman N, Koek HL, Hendrikse J (2017), Short-term mechanisms influencing volumetric brain dynamics. NeuroImage: Clinical 16:507-513.

Doyle HH, Eidson LN, Sinkiewicz DM, Murphy AZ (2017), Sex Differences in Microglia Activity within the Periaqueductal Gray of the Rat: A Potential Mechanism Driving the Dimorphic Effects of Morphine. J Neurosci 37:3202-3214.

Garber C, Soung A, Vollmer LL, Kanmogne M, Last A, Brown J, Klein RS (2019), T cells promote microglia-mediated synaptic elimination and cognitive dysfunction during recovery from neuropathogenic flaviviruses. Nature Neuroscience 22:1276-1288.

Gimsa U, Peter SV, Lehmann K, Bechmann I, Nitsch R (2000), Axonal damage induced by invading T cells in organotypic central nervous system tissue in vitro: involvement of microglial cells. Brain Pathol 10:365-377.

Grebing M, Nielsen HH, Fenger CD, K TJ, von Linstow CU, Clausen BH, Söderman M, Lambertsen KL, et al. (2016), Myelin-specific T cells induce interleukin-1beta expression in lesion-reactive microglial-like cells in zones of axonal degeneration. Glia 64:407-424.

Guneykaya D, Ivanov A, Hernandez DP, Haage V, Wojtas B, Meyer N, Maricos M, Jordan P, et al. (2018), Transcriptional and Translational Differences of Microglia from Male and Female Brains. Cell Rep 24:2773-2783.e2776.

Guo J, Liu C, Wang Y, Feng B, Zhang X (2015), Role of T helper lymphokines in the immune-inflammatory pathophysiology of schizophrenia: Systematic review and meta-analysis. Nordic Journal of Psychiatry 69:364-372.

Hanamsagar R, Alter MD, Block CS, Sullivan H, Bolton JL, Bilbo SD (2017), Generation of a microglial developmental index in mice and in humans reveals a sex difference in maturation and immune reactivity. Glia 65:1504-1520.

Herz J, Johnson KR, McGavern DB (2015), Therapeutic antiviral T cells noncytopathically clear persistently infected microglia after conversion into antigen-presenting cells. J Exp Med 212:1153-1169.

Htain WW, Leong SK, Ling EA (1995), A qualitative and quantitative study of the glial cells in normal and athymic mice. Glia 15:11-21.

Kipnis J, Cohen H, Cardon M, Ziv Y, Schwartz M (2004), T cell deficiency leads to cognitive dysfunction: implications for therapeutic vaccination for schizophrenia and other psychiatric conditions. Proc Natl Acad Sci U S A 101:8180-8185.

Lenz KM, Nugent BM, Haliyur R, McCarthy MM (2013), Microglia are essential to masculinization of brain and behavior. J Neurosci 33:2761-2772.

Lorke DE, Ip CW, Schumacher U (2008), Increased number of microglia in the brain of severe combined immunodeficient (SCID) mice. Histochem Cell Biol 130:693-697.

Louveau A, Smirnov I, Keyes TJ, Eccles JD, Rouhani SJ, Peske JD, Derecki NC, Castle D, et al. (2015), Structural and functional features of central nervous system lymphatic vessels. Nature 523:337-341.

Lu J, Synowiec S, Lu L, Yu Y, Bretherick T, Takada S, Yarnykh V, Caplan J, et al. (2018), Microbiota influence the development of the brain and behaviors in C57BL/6J mice. PLOS ONE 13:e0201829.

Luczynski P, Whelan SO, O'Sullivan C, Clarke G, Shanahan F, Dinan TG, Cryan JF (2016), Adult microbiota-deficient mice have distinct dendritic morphological changes: differential effects in the amygdala and hippocampus. Eur J Neurosci 44:2654-2666.

Masi A, Quintana DS, Glozier N, Lloyd AR, Hickie IB, Guastella AJ (2015), Cytokine aberrations in autism spectrum disorder: a systematic review and meta-analysis. Molecular Psychiatry 20:440-446.

Mombaerts P, Mizoguchi E, Ljunggren HG, Iacomini J, Ishikawa H, Wang L, Grusby MJ, Glimcher LH, et al. (1994), Peripheral lymphoid development and function in TCR mutant mice. Int Immunol 6:1061-1070.

Mouton PR, Long JM, Lei DL, Howard V, Jucker M, Calhoun ME, Ingram DK (2002), Age and gender effects on microglia and astrocyte numbers in brains of mice. Brain Res 956:30-35.

Nelson LH, Warden S, Lenz KM (2017), Sex differences in microglial phagocytosis in the neonatal hippocampus. Brain Behav Immun 64:11-22.

Neufeld KA, Kang N, Bienenstock J, Foster JA (2011), Effects of intestinal microbiota on anxiety-like behavior. Commun Integr Biol 4:492-494.

Olah M, Ping G, De Haas AH, Brouwer N, Meerlo P, Van Der Zee EA, Biber K, Boddeke HW (2009), Enhanced hippocampal neurogenesis in the absence of microglia T cell interaction and microglia activation in the murine running wheel model. Glia 57:1046-1061.

Pan Y, Xiong M, Chen R, Ma Y, Corman C, Maricos M, Kindler U, Semtner M, et al. (2018), Athymic mice reveal a requirement for T-cell-microglia interactions in establishing a microenvironment supportive of. Genes Dev 32:491-496.

Pasciuto E, Burton OT, Roca CP, Lagou V, Rajan WD, Theys T, Mancuso R, Tito RY, et al. (2020), Microglia Require CD4 T Cells to Complete the Fetal-to-Adult Transition. Cell 182:625-640.e624.

Paxinos G, Franklin KBJ (2001) The Mouse Brain in Stereotaxic Coordinates. New York: Academic Press.

Perez-Pouchoulen M, VanRyzin JW, McCarthy MM (2015), Morphological and Phagocytic Profile of Microglia in the Developing Rat Cerebellum. eNeuro 2.

Ponomarev ED, Shriver LP, Maresz K, Pedras-Vasconcelos J, Verthelyi D, Dittel BN (2007), GM-CSF production by autoreactive T cells is required for the activation of microglial cells and the onset of experimental autoimmune encephalomyelitis. J Immunol 178:39-48.

Posillico CK, Terasaki LS, Bilbo SD, Schwarz JM (2015), Examination of sex and minocycline treatment on acute morphine-induced analgesia and inflammatory gene expression along the pain pathway in Sprague-Dawley rats. Biol Sex Differ 6:33.

Prajeeth CK, Dittrich-Breiholz O, Talbot SR, Robert PA, Huehn J, Stangel M (2018), IFN-γ Producing Th1 Cells Induce Different Transcriptional Profiles in Microglia and Astrocytes. Frontiers in Cellular Neuroscience 12.

Prajeeth CK, Löhr K, Floess S, Zimmermann J, Ulrich R, Gudi V, Beineke A, Baumgärtner W, et al. (2014), Effector molecules released by Th1 but not Th17 cells drive an M1 response in microglia. Brain Behav Immun 37:248-259.

Rattazzi L, Piras G, Ono M, Deacon R, Pariante CM, D'Acquisto F (2013), $CD4^+$ but not $CD8^+$ T cells revert the impaired emotional behavior of immunocompromised RAG-1-deficient mice. Transl Psychiatry 3:e280.

Reynolds AD, Stone DK, Mosley RL, Gendelman HE (2009), Proteomic studies of nitrated alpha-synuclein microglia regulation by CD4+CD25+ T cells. J Proteome Res 8:3497-3511.

Rilett KC, Friedel M, Ellegood J, MacKenzie RN, Lerch JP, Foster JA (2015), Loss of T cells influences sex differences in behavior and brain structure. Brain Behav Immun 46:249-260.

Rilett KC, Luo OD, McVey-Neufeld KA, MacKenzie RN, Foster JA (2020), Loss of T cells influences sex differences in stress-related gene expression. J Neuroimmunol 343:577213.

Ritzel RM, Crapser J, Patel AR, Verma R, Grenier JM, Chauhan A, Jellison ER, McCullough LD (2016), Age-Associated Resident Memory CD8 T Cells in the Central Nervous System Are Primed To Potentiate Inflammation after Ischemic Brain Injury. J Immunol 196:3318-3330.

Round JL, Mazmanian SK (2009), The gut microbiota shapes intestinal immune responses during health and disease. Nature Reviews Immunology 9:313-323.

Sankar A, Mackenzie RN, Foster JA (2012), Loss of class I MHC function alters behavior and stress reactivity. J Neuroimmunol 244:8-15.

Schwarz JM, Sholar PW, Bilbo SD (2012), Sex differences in microglial colonization of the developing rat brain. J Neurochem 120:948-963.

Song C, Nicholson JD, Clark SM, Li X, Keegan AD, Tonelli LH (2016), Expansion of brain T cells in homeostatic conditions in lymphopenic Rag2(-/-) mice. Brain Behav Immun 57:161-172.

Thion MS, Garel S (2018), Microglia Under the Spotlight: Activity and Complement-Dependent Engulfment of Synapses. Trends Neurosci 41:332-334.

Wolf SA, Steiner B, Akpinarli A, Kammertoens T, Nassenstein C, Braun A, Blankenstein T, Kempermann G (2009), CD4-positive T lymphocytes provide a neuroimmunological link in the control of adult hippocampal neurogenesis. J Immunol 182:3979-3984.

Xie L, Choudhury GR, Winters A, Yang SH, Jin K (2015), Cerebral regulatory T cells restrain microglia/macrophage-mediated inflammatory responses via IL-10. Eur J Immunol 45:180-191.

Zhao W, Beers DR, Liao B, Henkel JS, Appel SH (2012), Regulatory T lymphocytes from ALS mice suppress microglia and effector T lymphocytes through different cytokine-mediated mechanisms. Neurobiol Dis 48:418-428.

Ziv Y, Ron N, Butovsky O, Landa G, Sudai E, Greenberg N, Cohen H, Kipnis J, et al. (2006), Immune cells contribute to the maintenance of neurogenesis and spatial learning abilities in adulthood. Nat Neurosci 9:268-275.

Chapter 3

Sex- and brain region-specific alterations in brain volume in germ-free mice

Shawna L. Thompson[1], Jacob Ellegood[2], Dawn M. E. Bowdish[3], Jason P. Lerch[2,4], and Jane A. Foster[1,5]

[1]Psychiatry and Behavioural Neuroscience, McMaster University, Hamilton, ON, Canada

[2] Mouse Imaging Centre, The Hospital for Sick Children, Toronto, ON, Canada

[3] Department of Medicine and McMaster Immunology Research Centre, McMaster University, Hamilton, ON, Canada

[4] Wellcome Centre for Integrative Neuroimaging, FMRIB, Nuffield Department of Clinical Neurosciences, University of Oxford, Oxford UK

[5]Research Institute at St. Joe's Hamilton, Hamilton, ON Canada

CHAPTER LINK – Manuscript #2

In the previous chapter, it was demonstrated that the loss of T cells results in an increased number of microglia in the basolateral amygdala of adult mice, and that there were sex-by-genotype effects in microglial staining density in multiple brain regions. Earlier findings from the ongoing collaboration of Dr. Jane Foster with Dr. Jacob Ellegood and Dr. Jason Lerch at the Mouse Imaging Centre at the Hospital for Sick Children identified a number of neuroanatomical changes in T cell deficient mice in regions that are part of the brain's stress circuitry. GF mice completely lack microbiota, and as a result have underdeveloped adaptive immune systems and deficits in mature T and B cells. A substantial body of research has identified that GF mice perform unusually on a wide variety of behavioural tasks, including anxiety-like, exploratory, locomotor, cognitive, and social behaviours (reviewed in this chapter). This study investigates the neuroanatomy of GF compared to conventionally housed SPF mice. Past work from a number of laboratories has suggested that conventionalization of GF mice in adulthood with microbes from control animals does not correct the observed behaviour abnormalities, therefore the neuroanatomy of GF mice recolonized at weaning (5w) was also examined in adulthood.

Abstract

Several lines of evidence demonstrate that microbiota influence brain development. Using high resolution *ex vivo* MRI, this study examined the impact of microbiota status on brain volume and revealed microbiota-related differences that sex- and brain region-dependent. Cortical and hippocampal regions demonstrate increased sensitivity to microbiota status during the first 5 weeks of postnatal life, effects that were greater in male GF mice. Conventionalization of GF mice at puberty did not normalize brain volume changes. These data add to the existing literature and highlight the need to focus more attention on early life microbiota-brain axis mechanisms in order to understand the regulatory role of the microbiome in brain development.

Introduction

Studies linking the microbiome to behaviour and brain function utilize germ-free (GF) mice. GF mice lack all commensal microbes and were first generated by cesarean section delivery under sterile conditions (Gustafsson et al., 1957). GF mice have since provided a useful animal model for researchers to identify systems that are influenced by commensal microbiota (Luczynski et al., 2016). In a seminal paper in 2004, GF mice were shown to have an exaggerated response to immobilization stress (Sudo et al., 2004). Since then, research has shown that GF mice have reduced anxiety-like behaviour, measured by various approach-avoidance tasks (Chen et al., 2017; Clarke et al., 2013; Diaz Heijtz, 2016; Diaz Heijtz et al., 2011; Huo et al., 2017; Neufeld et al., 2011a; Neufeld et al., 2011b). Additional microbiota-related behaviours include learning and memory (Gareau et al., 2011; Hoban et al., 2017b), activity (Campos et al., 2016; Diaz Heijtz *et al.*, 2011; Huo *et al.*, 2017), grooming behaviour (Desbonnet et al., 2014), and social behaviour (Arentsen et al., 2015; Buffington et al., 2016; Desbonnet *et al.*, 2014). Notably, conventionalization of GF mice during early postnatal life has been shown to restore the behavioural phenotype to varying degrees, depending on the timing of reconstitution of the microbiome, and the behaviour outcome considered (Clarke *et al.*, 2013; Diaz Heijtz *et al.*, 2011; Foster and McVey Neufeld, 2013; Neufeld *et al.*, 2011a; Neufeld *et al.*, 2011b)

In parallel with behavioural studies, accumulating evidence of molecular differences in GF mice compared to conventionally housed mice including monoamines, neurotrophic factors, orexigenic and anorexigenic peptides, amino acids, and metabolites. Targeted analysis of expression of RNA and microRNAs as well as

examination of microglia, myelination, and neurogenesis show that many CNS systems are influenced by microbiota-brain communication (Arentsen et al., 2017; Chen *et al.*, 2017; Diaz Heijtz *et al.*, 2011; Erny et al., 2015; Hoban et al., 2017a; Hoban *et al.*, 2017b; Hoban et al., 2016; Kawase et al., 2017; Moloney et al., 2017; Neufeld *et al.*, 2011b; Ogbonnaya et al., 2015; Schele et al., 2013; Stilling et al., 2015; Swann et al., 2017; Thion et al., 2017). Both neuronal and glial changes have been reported in GF mice. Neuroanatomical differences in GF mice include increased amygdala and hippocampus volumes that were associated with increased dendritic arborization and spine density in the same regions (Luczynski *et al.*, 2016). An increased number of cortical microglia was observered in GF mice in parallel with an immature morphological microglial phenotype, including longer processes with more branch points, compared to control mice (Erny *et al.*, 2015). Using magnetic resonance imaging (MRI) in GF mice compared to controls, widespread regional volume differences were observed, including decreased myelination in white matter regions and fiber tracts of these GF mice, suggesting less mature myelination patterns in the absence of microbiota (Lu et al., 2018).

The current study examined the impact of microbiota colonization status on brain volume using *ex vivo* high resolution structural MRI (7 Tesla) in C57Bl/6 mice. Brain volume was studied in specific pathogen-free (SPF), germ-free (GF), and altered Schaedler flora (ASF) colonized gnotobiotic C57Bl/6 female and male adult mice. Conventionalization of germ-free mice at 5 weeks of age (GF/SPF) was used to test the hypothesis that microbiota-host communication in the pre-pubertal period is critical to neuroanatomical development. The resulting *ex vivo* imaging data collected in young

adulthood revealed long-term changes in brain volume in GF and GF/SPF mice that were more pronounced in male mice compared to female mice. These data complement previous findings that suggest early postnatal life is a critical period for microbiota-host interactions on neurodevelopment.

Experimental Procedures

Animals. SPF, GF, and ASF C57Bl/6 mice were bred in-house. All animals were exposed to a 12-hour light/dark cycle and were given access to food and water *ad libitum*. ASF colonized offspring were derived from GF females, who were introduced to an ASF environment prior to conception. ASF colonized mice were housed in ultraclean conditions using ventilated racks. GF mice were conventionalized at 5 weeks of age, to generate GF/SPF mice, by exposure to fresh SPF bedding material, and housed in the same room as SPF mice. All experiments were completed in accordance with the guidelines set out by the Canadian Council on Animal Care and were approved by the McMaster Animal Research Ethics Board.

Tissue Preparation. Female and male mice were perfused transcardially at 9 weeks of age, beginning with a 30-minute flush with phosphate buffered saline (PBS) and heparin (1U/mL, Sandoz Canada Inc., Boucherville QC), followed by a 30-minute fixation with 4% paraformaldehyde (PFA) (Alfa Aesar, Ward Hill MA) and 2 mM Prohance (Gadolinum contrast agent required for the MRI imaging, Bracco Diagnostics, NJ, USA) in PBS at a rate of 1 ml/min. After perfusion skulls were removed and stored overnight at 4°C in 4% paraformaldehyde containing 2 mM Prohance before being transferred to a

0.1M phosphate buffered solution containing 0.02% sodium azide and 2mM Prohance for storage at 4°C until imaging.

MRI Imaging. A multi-channel 7.0 Tesla MRI scanner (Agilent Inc., Palo Alto, CA) was used to image the brains within their skulls. Sixteen custom-built solenoid coils were used to image the brains in parallel (Bock et al., 2005; Lerch et al., 2011).

Anatomical Scan. In order to detect volumetric changes, a T2- weighted, 3-D fast spin-echo MRI sequence was used with the following parameters: a cylindrical acquisition of k-space, a TR of 350 ms, and TEs of 12 ms per echo for 6 echoes, field-of-view equaled to 20 x 20 x 25 mm^3 and matrix size equaled to 504 x 504 x 630. Our parameters output an image with 0.040 mm isotropic voxels. The total imaging time was ~14 hours (Spencer Noakes et al., 2017).

MRI Registration and Analysis. To visualize and compare any changes in the mouse brains the images are linearly (6 followed by 12 parameter) and non-linearly registered together. Registrations were performed with a combination of mni_autoreg tools (Collins et al., 1994) and ANTS (advanced normalization tools) (Avants et al., 2008; Avants et al., 2011). After registration, all scans are resampled with the appropriate transform and averaged to create a population atlas representing the average anatomy of the study sample. The registration creates deformation fields that are required to bring the images into alignment with each other in an unbiased fashion. To calculate volumes, the deformations needed to take each individual mouse's anatomy into this final atlas space are analyzed (Lerch et al., 2008; Nieman et al., 2006). The Jacobian determinants of the deformation fields are then calculated as measures of volume at each voxel. Significant regional volume differences can then be calculated by warping a pre-existing classified MRI atlas onto the population atlas, which allows for the volume of 182 different segmented structures encompassing cortical lobes, large white matter structures (i.e. corpus callosum), ventricles, cerebellum, brain stem, and olfactory bulbs

(Dorr et al., 2008; Richards et al., 2011; Steadman et al., 2013; Ullmann et al., 2013) to be assessed in all brains. Further, these measurements can be examined on a voxel-wise basis in order to localize the differences found within regions or across the brain. Multiple comparisons in this study were controlled for using the False Discovery Rate (FDR) (Genovese et al., 2002).

Results

Absolute and relative volume differences were observed in GF mice

Brain volume differences between GF and SPF adult male and female mice, were assessed by absolute volume, measured in mm^3, and relative volume, measured as a percentage of the total brain volume. The coronal view of both absolute differences and relative differences is shown in Figure 3-1. Brain regions that were larger in SPF mice are visualized in shades of pink and brain regions that were smaller in SPF mice are visualized in shades of blue. The total brain volume of GF mice was significantly reduced in comparison to SPF mice as visualized by the extensive shaded pink regions in Figure 3-1A left panel and graphically in Figure 3-1B. Absolute volume difference for all brain regions are listed in Supplemental Table 3-1. In male GF mice, 174 of 182 segmented regions were significantly smaller compared to male SPF mice (FDR<0.05). In female GF mice, 146 of 182 segmented regions were significantly smaller compared to female SPF mice (FDR<0.05). Relative differences in brain volume are visualized in the right panel of Figure 3-1A. Several brain regions showed significant differences between GF and SPF mice including isocortex, hippocampus, and cerebellum (Figure 3-1, Supplemental Table 3-1).

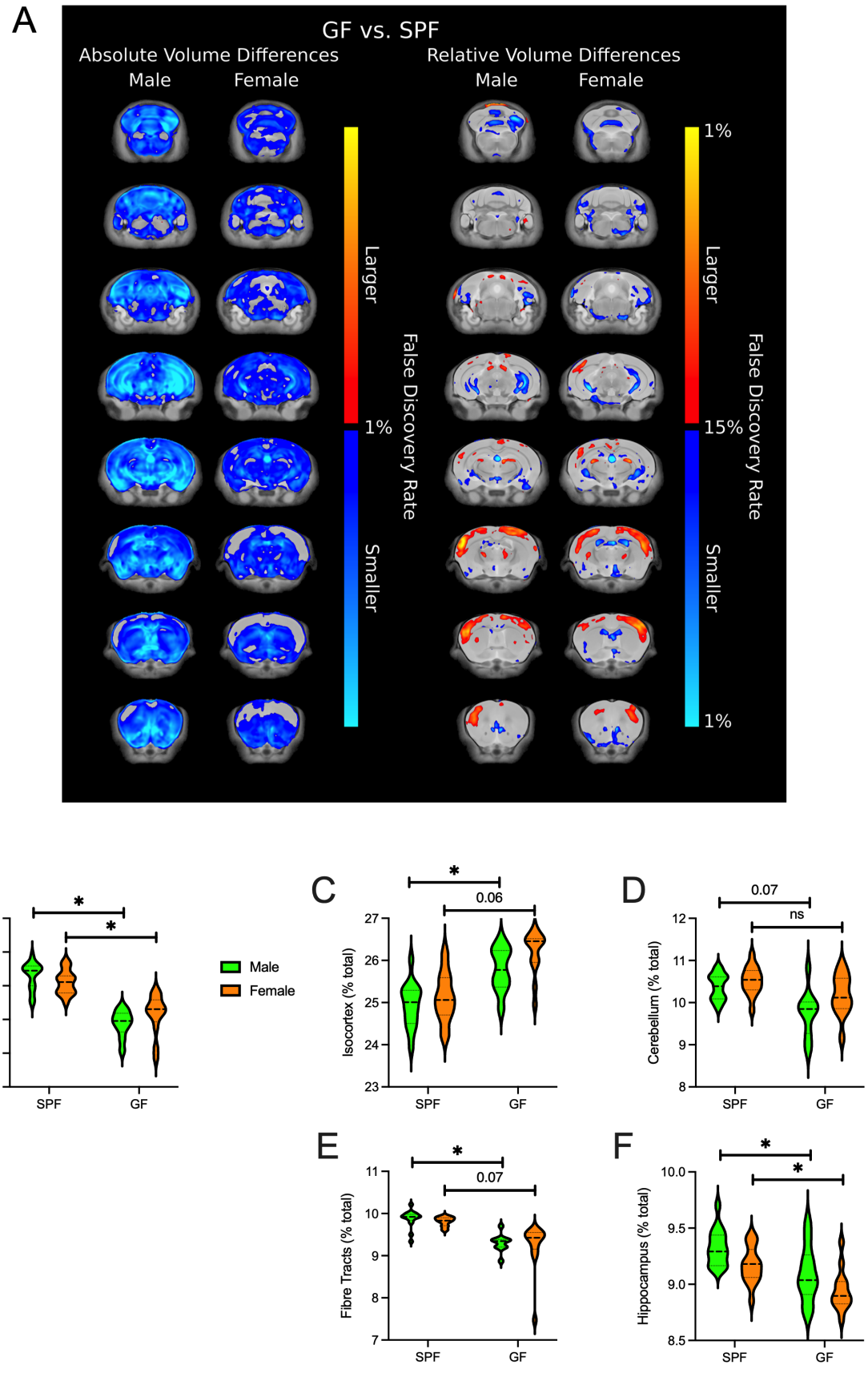
A
GF vs. SPF
Absolute Volume Differences
Male
Female
Relative Volume Differences
Male
Female
Larger
1%
False Discovery Rate
Smaller
1%
Larger
1%
15%
False Discovery Rate
Smaller
1%
B
Total Brain Volume (mm3)
500
450
400
350
300
250
SPF
GF
*
*
Male
Female
C
Isocortex (% total)
27
26
25
24
23
SPF
GF
*
0.06
D
Cerebellum (% total)
12
11
10
9
8
SPF
GF
0.07
ns
E
Fibre Tracts (% total)
11
10
9
8
7
SPF
GF
*
0.07
F
Hippocampus (% total)
10.0
9.5
9.0
8.5
SPF
GF
*
*

Figure 3-1. Fly through of coronal slices in the brain highlighting the voxel-wise significant absolute volume (left panel-A) and relative volume (right panel-A) differences between male and female germ-free (GF) and specific pathogen free (SPF) mice. Orange/red highlighted regions were significantly larger in SPF mice compared to GF mice and blue highlighted regions were significantly smaller in SPF mice. All changes highlighted were significant at an FDR value of <5%. Total brain volume in GF mice was significantly reduced compared to SPF mice (B). Relative volume differences were observed in isocortex (C), hippocampus (D), cerebellum (E), and fibre tracts (F). * shows FDR values <5%.

Increased relative volume of isocortex was observed in both male (FDR <0.05) and female (FDR=0.06) GF mice compared to SPF mice. More specifically, cingulate cortex: area 24b', retrospenial area, dorsal part, ectorhinal area, secondary somatomotor area, posterior parietal association areas, somatosensoary areas, as well as some visual areas were significantly increased in male GF mice compared to male SPF mice (Supplemental Table 3-1). While 4 subregions of isocortex showed increase brain volume with FDR<10% in female GF mice, no differences reached FDR<5% (Supplemental Table 3-1). Relative hippocampal volume was reduced in both male and female GF mice (FDR<0.05; Figure 3-1C, 3-1D). Similar to the observations noted above for isocortex, hippocampal subregions including CA1, CA2, CA3, and dentate gyrus showed significantly reduced volume (FDR<0.05 in male GF mice compared to male SPF mice, whereas only the dentate gyrus, granule layer was significant (FDR<0.05) in female GF mice compared to female SPF mice (Supplemental Table 3-

1). The cerebellum was smaller in male GF mice compared to male SPF mice (FDR=0.07), but not significantly different between female GF and SPF mice (Figure 3-1E). Fibre tract volume was also reduced in male (FDR<0.05) and female GF (FDR=0.07) mice compared to SPF mice. Overall, in addition to the differences noted above, a greater number of brain regions showed relative volume differences in male GF mice compared to female GF mice (Supplemental Table 3-1), revealing a microbiota-brain sex difference in adult GF mice.

Colonization of GF mice at 5 weeks of age did not normalize brain volume

A visual flythrough of absolute and relative differences between SPF and other housing conditions is provided in Figure 3-2. ASF conventionalized gnotobiotic mice had no total brain volume differences observed between both female and male SPF and ASF mice (Figure 3-3). GF conventionalization at 5 weeks of age (GF/SPF) with SPF microbiota did not normalize total brain volume. Total brain volume remained significantly reduced in GF/SPF mice compared to SPF mice for both female and male mice (Figure 3-3). To note, male GF/SPF mice showed a reduced total brain volume compared to SPF male mice, however it was significantly larger than male GF mice. Similar to GF mice, the relative brain volume of isocortex was significantly increased in GF/SPF male mice compared to SPF mice (Figure 3-3). A significant increase was also observed in female GF/SPF female mice compared to female SPF mice. Fibre tract volume was significantly reduced in both female and male GF/SPF mice (Figure 3). These data demonstrate that normal brain development requires gut microbiota prior to 5 weeks of age. Further, introduction of gut microbiota, and related host immune and

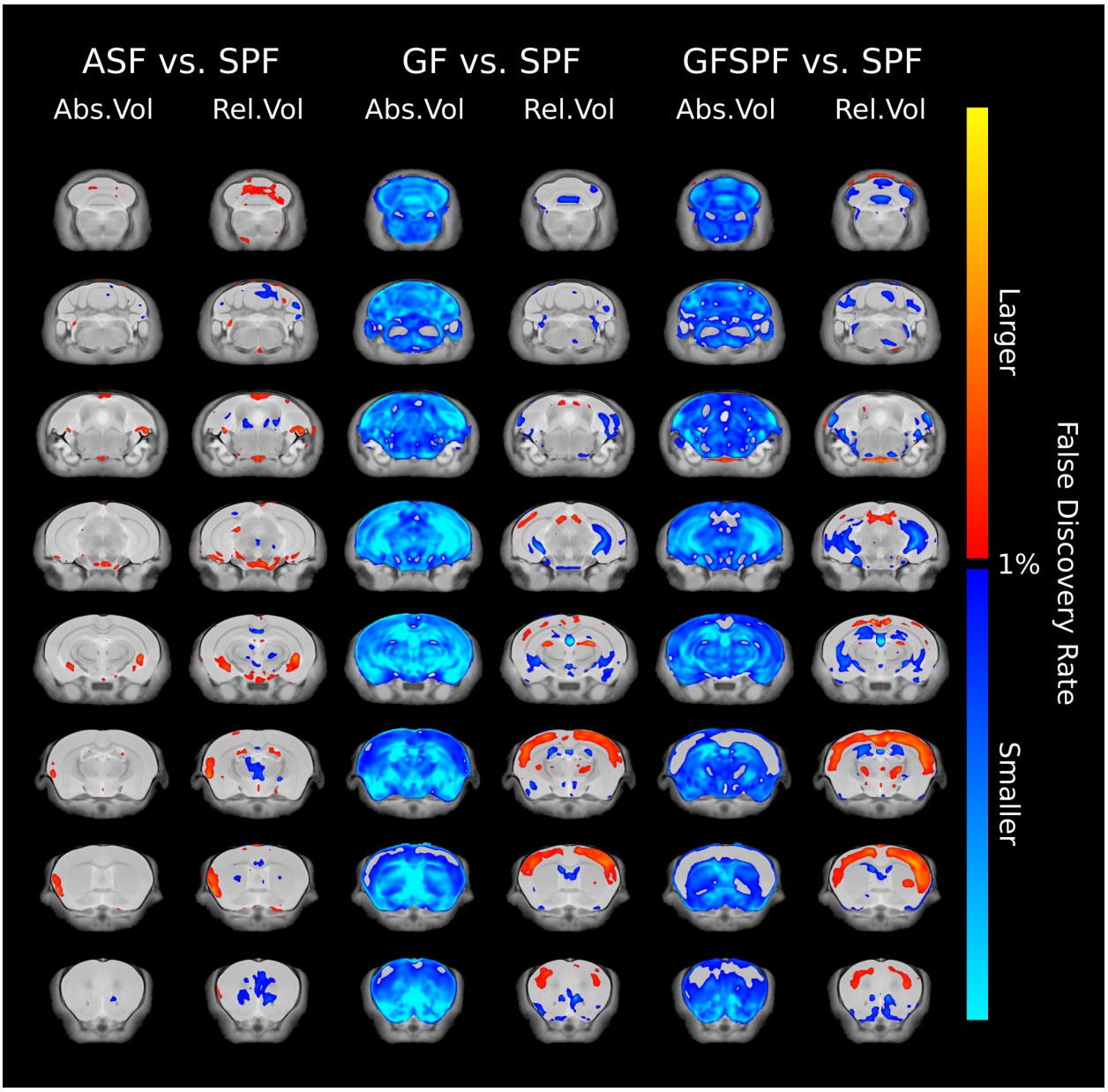

Figure 3-2. Fly through of coronal slices in the brain highlighting the voxel-wise significant differences in absolute and relative volume between housing conditions. Left panel - differences between altered Schaedler flora (ASF) and specific pathogen free (SPF) mice, middle panel – differences between germ-free (GF) and SPF mice, right panel – differences between conventionalized GF (GFSPF) and SPF mice. Orange/red highlighted regions were significantly larger in SPF mice compared to GF

mice and blue highlighted regions were significantly smaller in SPF mice. All changes highlighted were significant at an FDR value of <5%.

metabolic changes are not sufficient to normalize brain volume differences observed in GF mice.

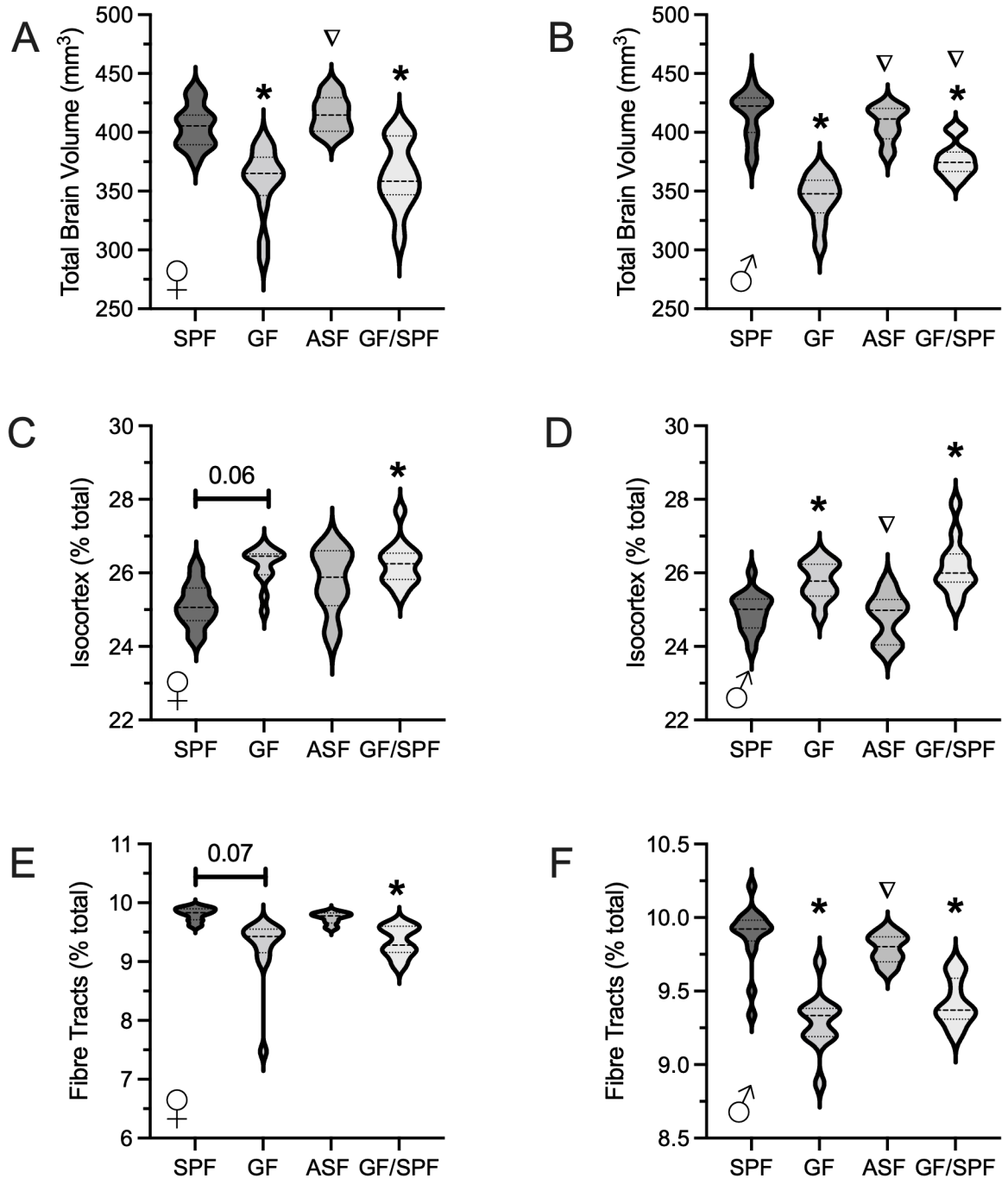

Figure 3-3. Brain volume differences based on microbiota status.

Conventionalization of GF mice at birth with Altered Schaedler's Flora (ASF) normalized total brain volume in female (A) and male (B) mice. Similarly, no relative brain volume differences were observed in isocortex or fibre tracts between SPF and ASF female (C,E) and male (D, F) mice. Total brain volume of female and male mice conventionalized at 5 weeks of age (GF/SPF) was reduced compared to SPF mice (A, B). In addition, GF/SPF showed reduced isocortex and fibre tract relative brain volume (C-F). * shows FDR values <5% compared to sex-matched SPF mice; ∇ shows FDR values <5% compared to sex-matched GF mice.

Absence of microbiota affected hippocampal volume to a greater extent in male GF mice

Sex differences in the impact of microbiota status was further investigated in subregions of the hippocampus (Figure 4). Microbiota status had a greater impact on male mice than female mice. No sigificant differences in relative volume were observed across groups (SPF, GF, ASF, GF/SPF) in hippocampal CA1, CA2, or CA3 regions. A reduced hippocampal volume was observed in female GF (FDR=0.08) and GF/SPF female mice (FDR<0.05) (Figure 4). Reduced relative volume in all hippocampal subregions were observed in male GF/SPF mice compared to male SPF mice, similar to male GF mice. No differences were observed in hypothalamic volume across groups for either male or female mice (Figure 4). These data further demonstrate an increased sensitivity of male mice to microbiota status compared to female mice.

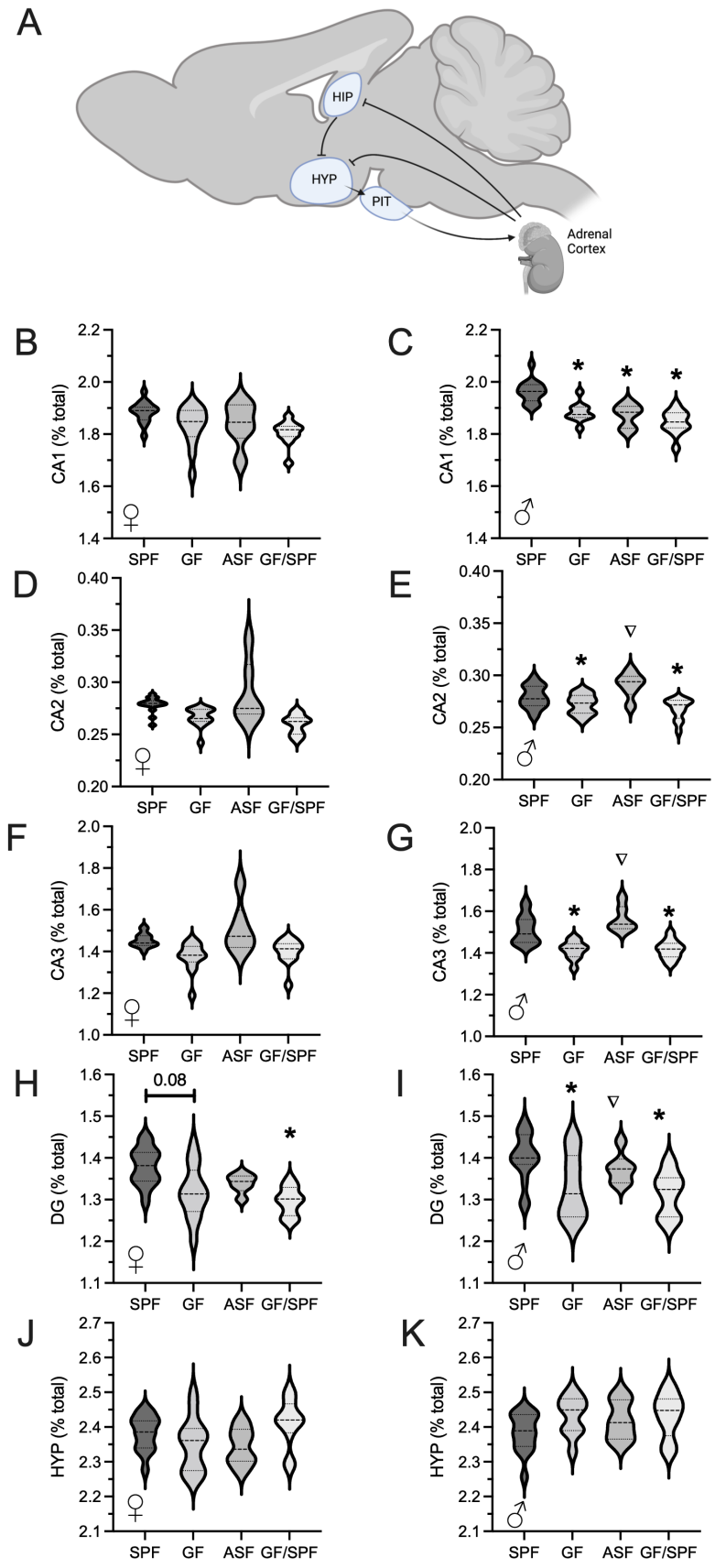
A
HIP
HYP
PIT
Adrenal Cortex
B
C
D
E
F
G
H
I
J
K
CA1 (% total)
CA2 (% total)
CA3 (% total)
DG (% total)
HYP (% total)
SPF GF ASF GF/SPF
0.08
♀
♂

Figure 3-4. Hippocampal regional differences based on microbiota status. Female mice showed no significant differences in relative volume of CA1 (A), CA2 (D), and CA3 (F) subregions. Smaller volume in the dentate gyrus was observed in GF and GF/SPF female mice compared to SPF female mice (H). Conventionalization of GF mice at birth with Altered Schaedler's Flora (ASF) normalized hippocampal subregions volumes in male mice (B, E, G). Significant smaller volumes were observed in GF and GF/SPF male mice compared to SPF male mice in CA1 (B), CA2 (E), CA3 (G), and DG (I) subregions. No differences in hypothalamus were observed (J,K). * shows FDR values <5% compared to sex-matched SPF mice; ∇ shows FDR values <5% compared to sex-matched GF mice.

Discussion

In healthy mice, gut microbiota composition and diversity increases during the first 4 weeks of postnatal life and several lines of evidence demonstrate that microbiota are essential to normal brain development. The maturation and diversification of the gut microbiota during postnatal life is coincident with a critical window during which microbiota-brain communication may impact the developmental trajectory of the brain. Here we show that microbiota are important for normal brain development as GF mice had significant differences in brain volume that were both brain region- and sex-dependent. GF status had a greater impact on male mice compared to female mice, in particular, all hippocampal subregions were reduced in volume in male GF mice, where as only the dentate granuale region was reduced in female GF mice. Not surprisingly, conventionalization of GF mice at 5 weeks of age was not able to normalize brain

volume measured at 9 weeks of age, confirming that microbe-host communication in the first few weeks of life are critical to neurodevelopment and that investigations aimed at understanding microbe-host mechanisms pre-puberty are needed.

A myriad of brain-related differences in GF mice have been reported (Cryan et al., 2019), however, only a small group of studies have included both male and female mice. A couple recent studies that included male and female mice have revealed sex-dependent microbiota-related differences in microglia and in neurogenesis (Scott et al., 2020; Thion et al., 2018). Increased microglial density and immature microglial morphology have been reported in adult GF mice (Erny *et al.*, 2015). Developmentally regulated sex differences in microglial gene expression have also been reported, such that male GF mice were more susceptible to the absence of microbiota early in brain development with higher numbers of differentially expressed genes (embryonically), whereas adult female GF mice showed more differentially expressed genes, compared to adult female SPF mice (Thion *et al.*, 2018). Interestingly, a significant decrease in expression of immune-related genes in female GF mice was noted, suggesting that microbiota may influence sex differences in immune activation (Thion *et al.*, 2018). The current anatomical work also demonstrated an increased sensitivity of male mice to the absence of microbiota during the first 5 weeks of life, however, functional changes in gene expression in the current study were not considered.

Using doublecortin labelling to examine immature neurons and BrdU staining to examine cell proliferation in the dentate gyrus of the hippocampus, a disrupted trajectory of hippocampal neurogenesis was revealed in GF mice compared to SPF mice (Scott *et al.*, 2020). In normally housed male mice, the total number of proliferating

and immature cells decreased over postnatal development (4, 8, 12 weeks), whereas GF male mice had reduced neurogenesis at 4 weeks of age compared to SPF male mice. In contrast, female GF mice showed increased neurogenesis at 8 weeks of age compared to female SPF mice, suggesting that microbiota influence the trajectory of hippocampal maturation in a sex-dependent manner (Scott *et al.*, 2020). Further, in male mice, reduced neurogenesis was associated with reduced hippocampal functional connectivity in GF mice compared to SPF mice, demonstrating that microbiota-related changes can influence brain function (Scott *et al.*, 2020). This observation is further supported by recent findings using resting-state functional MRI to examine functional connectivity in GF and normally colonized male mice (Aswendt et al., 2021). Specifically, a higher and more variable functional connectivity was observed in adult male GF mice compared to SPF mice (Aswendt *et al.*, 2021). These data and the current results highlight key microbiota-sensitive regions including the hippocampus and cortical regions.

The hypothalamic-pituitary-adrenal (HPA) stress axis undergoes significant postnatal development and refinement throughout early life. During this period, environmental factors play a key role in shaping the trajectory of development and thus ultimate long-term function of the stress axis. GF mice show marked HPA axis hyperreactivity following exposure to stress in adulthood (Sudo *et al.*, 2004). While no brain volume differences were observed for the hypothalamus in GF male or female mice compared to SPF mice, reduced volumes observed in the hippocampal regions in GF mice could impact HPA negative feedback circuits and contribute to the observed exaggerated stress reactivity. Moreover, it is possible that alterations in the functional

aspects of stress circuitry could underlie behavioural differences observed in GF mice. Notably, corticosterone levels in GF mice were recently shown to influence social activity in adult GF mice, via microbiota regulation of glucocorticoid receptors and central stress circuitry (Wu et al., 2021).

The observation that conventionalization of GF mice (GF/SPF) at 5 weeks of age did not normalize brain structure differences observed in GF mice demonstrates the importance of the role of microbiota-brain signaling in brain development pre-puberty. This is consistent with the observation that conventionalization of GF mice at 5 weeks of age did not normalize hippocampal differential expression or the related reduced anxiety and depressive-like behaviour in male and female BALB/c mice (Pan et al., 2019; Zhou et al., 2020). In contrast, analysis of differential hippocampal proteins between SPF and GF mice revealed that approximately 50% of protein levels normalized in GF mice conventionalized at 5 weeks of age (Rao et al., 2021). The mosaic picture that is emerging across studies is that microbiota-brain interactions are influenced by age, sex, and brain system. For example, conventionalization of GF mice at birth was also reported to normalize deficits in fear-related extinction learning, however, normalization of the molecular changes were not observed in that study, suggesting that the *in utero* period is an important developmental window during which maternal microbiota may influence outcomes in the offspring (Chu et al., 2019; Jasarevic and Bale, 2019). Further, it is established that serotonergic systems differ between GF and SPF mice (Clarke *et al.*, 2013; Neufeld *et al.*, 2011b; van de Wouw et al., 2019) and in response to acute stress microbiota modulate serotonergic responses in both gastrointestinal and CNS systems in a sex-dependent manner (Lyte et al.,

2020). Interestingly, GF mice showed increased prevalence of post-translationally edited isoforms of the serotonergic 5HT2c receptor in the amygdala, hypothalamus, prefrontal cortex, and striatum, which was partially corrected when GF mice were conventionalized at weaning (postnatal day 21) (van de Wouw *et al.*, 2019). Notably, antibiotic depletion of microbiota in adult mice did not alter the 5HT2c isoforms reiterating the importance of microbiota regulation of brain systems earlier in development (van de Wouw *et al.*, 2019).

Overall, an extended body of evidence is accumulating that demonstrates that microbiota are important to brain development. Using high resolution *ex vivo* MRI, this study revealed microbiota-related differences that sex- and brain region-dependent. As in previous studies, cortical and hippocampal regions demonstrate increased sensitivity to microbiota status during the first 5 weeks of postnatal life. Conventionalization of GF mice at puberty was not able to normalize the majority of brain volume changes, comparable to findings in other behavioural and brain systems previously reported. Focusing more attention on early life microbiota-brain axis mechanisms is an important next step in understanding the regulatory role of the microbiome in brain development.

References

Arentsen, T., Qian, Y., Gkotzis, S., Femenia, T., Wang, T., Udekwu, K., Forssberg, H., and Diaz Heijtz, R. (2017). The bacterial peptidoglycan-sensing molecule Pglyrp2 modulates brain development and behavior. Mol Psychiatry *22*, 257-266. 10.1038/mp.2016.182.

Arentsen, T., Raith, H., Qian, Y., Forssberg, H., and Diaz Heijtz, R. (2015). Host microbiota modulates development of social preference in mice. Microb Ecol Health Dis *26*, 29719. 10.3402/mehd.v26.29719.

Aswendt, M., Green, C., Sadler, R., Llovera, G., Dzikowski, L., Heindl, S., Gomez de Aguero, M., Diedenhofen, M., Vogel, S., Wieters, F., et al. (2021). The gut microbiota modulates brain network connectivity under physiological conditions and after acute brain ischemia. iScience *24*, 103095. 10.1016/j.isci.2021.103095.

Avants, B.B., Epstein, C.L., Grossman, M., and Gee, J.C. (2008). Symmetric diffeomorphic image registration with cross-correlation: evaluating automated labeling of elderly and neurodegenerative brain. Medical image analysis *12*, 26-41. 10.1016/j.media.2007.06.004.

Avants, B.B., Tustison, N.J., Song, G., Cook, P.A., Klein, A., and Gee, J.C. (2011). A reproducible evaluation of ANTs similarity metric performance in brain image registration. Neuroimage *54*, 2033-2044. 10.1016/j.neuroimage.2010.09.025.

Bock, N.A., Nieman, B.J., Bishop, J.B., and Mark Henkelman, R. (2005). In vivo multiple-mouse MRI at 7 Tesla. Magnetic resonance in medicine : official journal of the

Society of Magnetic Resonance in Medicine / Society of Magnetic Resonance in Medicine *54*, 1311-1316. 10.1002/mrm.20683.

Buffington, S.A., Di Prisco, G.V., Auchtung, T.A., Ajami, N.J., Petrosino, J.F., and Costa-Mattioli, M. (2016). Microbial Reconstitution Reverses Maternal Diet-Induced Social and Synaptic Deficits in Offspring. Cell *165*, 1762-1775. 10.1016/j.cell.2016.06.001.

Campos, A.C., Rocha, N.P., Nicoli, J.R., Vieira, L.Q., Teixeira, M.M., and Teixeira, A.L. (2016). Absence of gut microbiota influences lipopolysaccharide-induced behavioral changes in mice. Behav Brain Res *312*, 186-194. 10.1016/j.bbr.2016.06.027.

Chen, J.J., Zeng, B.H., Li, W.W., Zhou, C.J., Fan, S.H., Cheng, K., Zeng, L., Zheng, P., Fang, L., Wei, H., and Xie, P. (2017). Effects of gut microbiota on the microRNA and mRNA expression in the hippocampus of mice. Behav Brain Res *322*, 34-41. 10.1016/j.bbr.2017.01.021.

Chu, C., Murdock, M.H., Jing, D., Won, T.H., Chung, H., Kressel, A.M., Tsaava, T., Addorisio, M.E., Putzel, G.G., Zhou, L., et al. (2019). The microbiota regulate neuronal function and fear extinction learning. Nature *574*, 543-548. 10.1038/s41586-019-1644-y.

Clarke, G., Grenham, S., Scully, P., Fitzgerald, P., Moloney, R.D., Shanahan, F., Dinan, T.G., and Cryan, J.F. (2013). The microbiome-gut-brain axis during early life regulates the hippocampal serotonergic system in a sex-dependent manner. Mol Psychiatry *18*, 666-673. 10.1038/mp.2012.77.

Collins, D.L., Neelin, P., Peters, T.M., and Evans, A.C. (1994). Automatic 3D intersubject registration of MR volumetric data in standardized Talairach space. Journal of computer assisted tomography *18*, 192-205.

Cryan, J.F., O'Riordan, K.J., Cowan, C.S.M., Sandhu, K.V., Bastiaanssen, T.F.S., Boehme, M., Codagnone, M.G., Cussotto, S., Fulling, C., Golubeva, A.V., et al. (2019). The Microbiota-Gut-Brain Axis. Physiol Rev *99*, 1877-2013. 10.1152/physrev.00018.2018.

Desbonnet, L., Clarke, G., Shanahan, F., Dinan, T.G., and Cryan, J.F. (2014). Microbiota is essential for social development in the mouse. Mol Psychiatry *19*, 146-148. 10.1038/mp.2013.65.

Diaz Heijtz, R. (2016). Fetal, neonatal, and infant microbiome: Perturbations and subsequent effects on brain development and behavior. Semin Fetal Neonatal Med *21*, 410-417. 10.1016/j.siny.2016.04.012.

Diaz Heijtz, R., Wang, S., Anuar, F., Qian, Y., Bjorkholm, B., Samuelsson, A., Hibberd, M.L., Forssberg, H., and Pettersson, S. (2011). Normal gut microbiota modulates brain development and behavior. Proc Natl Acad Sci U S A *108*, 3047-3052. 10.1073/pnas.1010529108.

Dorr, A.E., Lerch, J.P., Spring, S., Kabani, N., and Henkelman, R.M. (2008). High resolution three-dimensional brain atlas using an average magnetic resonance image of 40 adult C57Bl/6J mice. Neuroimage *42*, 60-69. 10.1016/j.neuroimage.2008.03.037.

Erny, D., Hrabe de Angelis, A.L., Jaitin, D., Wieghofer, P., Staszewski, O., David, E., Keren-Shaul, H., Mahlakoiv, T., Jakobshagen, K., Buch, T., et al. (2015). Host microbiota constantly control maturation and function of microglia in the CNS. Nat Neurosci *18*, 965-977. 10.1038/nn.4030.

Foster, J.A., and McVey Neufeld, K.A. (2013). Gut-brain axis: how the microbiome influences anxiety and depression. Trends Neurosci *36*, 305-312. 10.1016/j.tins.2013.01.005.

Gareau, M.G., Wine, E., Rodrigues, D.M., Cho, J.H., Whary, M.T., Philpott, D.J., Macqueen, G., and Sherman, P.M. (2011). Bacterial infection causes stress-induced memory dysfunction in mice. Gut *60*, 307-317. 10.1136/gut.2009.202515.

Genovese, C.R., Lazar, N.A., and Nichols, T. (2002). Thresholding of statistical maps in functional neuroimaging using the false discovery rate. Neuroimage *15*, 870-878. 10.1006/nimg.2001.1037.

Hoban, A.E., Stilling, R.M., G, M.M., Moloney, R.D., Shanahan, F., Dinan, T.G., Cryan, J.F., and Clarke, G. (2017a). Microbial regulation of microRNA expression in the amygdala and prefrontal cortex. Microbiome *5*, 102. 10.1186/s40168-017-0321-3.

Hoban, A.E., Stilling, R.M., Moloney, G., Shanahan, F., Dinan, T.G., Clarke, G., and Cryan, J.F. (2017b). The microbiome regulates amygdala-dependent fear recall. Mol Psychiatry. 10.1038/mp.2017.100.

Hoban, A.E., Stilling, R.M., Ryan, F.J., Shanahan, F., Dinan, T.G., Claesson, M.J., Clarke, G., and Cryan, J.F. (2016). Regulation of prefrontal cortex myelination by the microbiota. Transl Psychiatry *6*, e774. 10.1038/tp.2016.42.

Huo, R., Zeng, B., Zeng, L., Cheng, K., Li, B., Luo, Y., Wang, H., Zhou, C., Fang, L., Li, W., et al. (2017). Microbiota Modulate Anxiety-Like Behavior and Endocrine Abnormalities in Hypothalamic-Pituitary-Adrenal Axis. Front Cell Infect Microbiol *7*, 489. 10.3389/fcimb.2017.00489.

Jasarevic, E., and Bale, T.L. (2019). Prenatal and postnatal contributions of the maternal microbiome on offspring programming. Frontiers in neuroendocrinology *55*, 100797. 10.1016/j.yfrne.2019.100797.

Kawase, T., Nagasawa, M., Ikeda, H., Yasuo, S., Koga, Y., and Furuse, M. (2017). Gut microbiota of mice putatively modifies amino acid metabolism in the host brain. The British journal of nutrition *117*, 775-783. 10.1017/S0007114517000678.

Lerch, J.P., Carroll, J.B., Spring, S., Bertram, L.N., Schwab, C., Hayden, M.R., and Henkelman, R.M. (2008). Automated deformation analysis in the YAC128 Huntington disease mouse model. Neuroimage *39*, 32-39. 10.1016/j.neuroimage.2007.08.033.

Lerch, J.P., Sled, J.G., and Henkelman, R.M. (2011). MRI phenotyping of genetically altered mice. Methods in molecular biology (Clifton, N.J *711*, 349-361. 10.1007/978-1-61737-992-5_17.

Lu, J., Lu, L., Yu, Y., Cluette-Brown, J., Martin, C.R., and Claud, E.C. (2018). Effects of Intestinal Microbiota on Brain Development in Humanized Gnotobiotic Mice. Sci Rep *8*, 5443. 10.1038/s41598-018-23692-w.

Luczynski, P., McVey Neufeld, K.A., Oriach, C.S., Clarke, G., Dinan, T.G., and Cryan, J.F. (2016). Growing up in a Bubble: Using Germ-Free Animals to Assess the Influence of the Gut Microbiota on Brain and Behavior. Int J Neuropsychopharmacol *19*. 10.1093/ijnp/pyw020.

Lyte, J.M., Gheorghe, C.E., Goodson, M.S., Kelley-Loughnane, N., Dinan, T.G., Cryan, J.F., and Clarke, G. (2020). Gut-brain axis serotonergic responses to acute stress exposure are microbiome-dependent. Neurogastroenterol Motil *32*, e13881. 10.1111/nmo.13881.

Moloney, G.M., O'Leary, O.F., Salvo-Romero, E., Desbonnet, L., Shanahan, F., Dinan, T.G., Clarke, G., and Cryan, J.F. (2017). Microbial regulation of hippocampal miRNA expression: Implications for transcription of kynurenine pathway enzymes. Behav Brain Res *334*, 50-54. 10.1016/j.bbr.2017.07.026.

Neufeld, K.A., Kang, N., Bienenstock, J., and Foster, J.A. (2011a). Effects of intestinal microbiota on anxiety-like behavior. Commun Integr Biol *4*, 492-494. 10.4161/cib.4.4.15702.

Neufeld, K.M., Kang, N., Bienenstock, J., and Foster, J.A. (2011b). Reduced anxiety-like behavior and central neurochemical change in germ-free mice. Neurogastroenterol Motil *23*, 255-264, e119. 10.1111/j.1365-2982.2010.01620.x.

Nieman, B.J., Flenniken, A.M., Adamson, S.L., Henkelman, R.M., and Sled, J.G. (2006). Anatomical phenotyping in the brain and skull of a mutant mouse by magnetic resonance imaging and computed tomography. Physiol Genomics *24*, 154-162. 10.1152/physiolgenomics.00217.2005.

Ogbonnaya, E.S., Clarke, G., Shanahan, F., Dinan, T.G., Cryan, J.F., and O'Leary, O.F. (2015). Adult Hippocampal Neurogenesis Is Regulated by the Microbiome. Biol Psychiatry *78*, e7-9. 10.1016/j.biopsych.2014.12.023.

Pan, J.X., Deng, F.L., Zeng, B.H., Zheng, P., Liang, W.W., Yin, B.M., Wu, J., Dong, M.X., Luo, Y.Y., Wang, H.Y., et al. (2019). Absence of gut microbiota during early life affects anxiolytic Behaviors and monoamine neurotransmitters system in the hippocampal of mice. J Neurol Sci *400*, 160-168. 10.1016/j.jns.2019.03.027.

Rao, X., Liu, L., Wang, H., Yu, Y., Li, W., Chai, T., Zhou, W., Ji, P., Song, J., Wei, H., and Xie, P. (2021). Regulation of Gut Microbiota Disrupts the Glucocorticoid Receptor Pathway and Inflammation-related Pathways in the Mouse Hippocampus. Exp Neurobiol *30*, 59-72. 10.5607/en20055.

Richards, K., Watson, C., Buckley, R.F., Kurniawan, N.D., Yang, Z., Keller, M.D., Beare, R., Bartlett, P.F., Egan, G.F., Galloway, G.J., et al. (2011). Segmentation of the mouse hippocampal formation in magnetic resonance images. Neuroimage *58*, 732-740. 10.1016/j.neuroimage.2011.06.025.

Schele, E., Grahnemo, L., Anesten, F., Hallen, A., Backhed, F., and Jansson, J.O. (2013). The gut microbiota reduces leptin sensitivity and the expression of the obesity-

suppressing neuropeptides proglucagon (Gcg) and brain-derived neurotrophic factor (Bdnf) in the central nervous system. Endocrinology *154*, 3643-3651. 10.1210/en.2012-2151.

Scott, G.A., Terstege, D.J., Vu, A.P., Law, S., Evans, A., and Epp, J.R. (2020). Disrupted Neurogenesis in Germ-Free Mice: Effects of Age and Sex. Front Cell Dev Biol *8*, 407. 10.3389/fcell.2020.00407.

Spencer Noakes, T.L., Henkelman, R.M., and Nieman, B.J. (2017). Partitioning k-space for cylindrical three-dimensional rapid acquisition with relaxation enhancement imaging in the mouse brain. NMR in biomedicine *30*. 10.1002/nbm.3802.

Steadman, P.E., Ellegood, J., Szulc, K.U., Turnbull, D.H., Joyner, A.L., Henkelman, R.M., and Lerch, J.P. (2013). Genetic Effects on Cerebellar Structure Across Mouse Models of Autism Using a Magnetic Resonance Imaging Atlas. Autism Res. 10.1002/aur.1344.

Stilling, R.M., Ryan, F.J., Hoban, A.E., Shanahan, F., Clarke, G., Claesson, M.J., Dinan, T.G., and Cryan, J.F. (2015). Microbes & neurodevelopment--Absence of microbiota during early life increases activity-related transcriptional pathways in the amygdala. Brain Behav Immun *50*, 209-220. 10.1016/j.bbi.2015.07.009.

Sudo, N., Chida, Y., Aiba, Y., Sonoda, J., Oyama, N., Yu, X.N., Kubo, C., and Koga, Y. (2004). Postnatal microbial colonization programs the hypothalamic-pituitary-adrenal system for stress response in mice. J Physiol *558*, 263-275. 10.1113/jphysiol.2004.063388.

Swann, J.R., Garcia-Perez, I., Braniste, V., Wilson, I.D., Sidaway, J.E., Nicholson, J.K., Pettersson, S., and Holmes, E. (2017). Application of (1)H NMR spectroscopy to the metabolic phenotyping of rodent brain extracts: A metabonomic study of gut microbial influence on host brain metabolism. J Pharm Biomed Anal *143*, 141-146. 10.1016/j.jpba.2017.05.040.

Thion, M.S., Low, D., Silvin, A., Chen, J., Grisel, P., Schulte-Schrepping, J., Blecher, R., Ulas, T., Squarzoni, P., Hoeffel, G., et al. (2017). Microbiome Influences Prenatal and Adult Microglia in a Sex-Specific Manner. Cell. 10.1016/j.cell.2017.11.042.

Thion, M.S., Low, D., Silvin, A., Chen, J., Grisel, P., Schulte-Schrepping, J., Blecher, R., Ulas, T., Squarzoni, P., Hoeffel, G., et al. (2018). Microbiome Influences Prenatal and Adult Microglia in a Sex-Specific Manner. Cell *172*, 500-516 e516. 10.1016/j.cell.2017.11.042.

Ullmann, J.F., Watson, C., Janke, A.L., Kurniawan, N.D., and Reutens, D.C. (2013). A segmentation protocol and MRI atlas of the C57BL/6J mouse neocortex. Neuroimage *78*, 196-203. 10.1016/j.neuroimage.2013.04.008.

van de Wouw, M., Stilling, R.M., Peterson, V.L., Ryan, F.J., Hoban, A.E., Shanahan, F., Clarke, G., Claesson, M.J., Dinan, T.G., Cryan, J.F., and Schellekens, H. (2019). Host Microbiota Regulates Central Nervous System Serotonin Receptor 2C Editing in Rodents. ACS Chem Neurosci *10*, 3953-3960. 10.1021/acschemneuro.9b00414.

Wu, W.L., Adame, M.D., Liou, C.W., Barlow, J.T., Lai, T.T., Sharon, G., Schretter, C.E., Needham, B.D., Wang, M.I., Tang, W., et al. (2021). Microbiota regulate social

behaviour via stress response neurons in the brain. Nature *595*, 409-414. 10.1038/s41586-021-03669-y.

Zhou, C., Rao, X., Wang, H., Zeng, B., Yu, Y., Chen, J., Zhong, J., Qi, X., Zeng, L., Zheng, P., et al. (2020). Hippocampus-specific regulation of long non-coding RNA and mRNA expression in germ-free mice. Funct Integr Genomics *20*, 355-365. 10.1007/s10142-019-00716-w.

	Absolute Volumes Male									Absolute Volumes Female			
	GF		SPF						Relative Volun	GF			
	Mean	SD	Mean	SD	%Diff	Effect	P-Value	FDR		FDR	Mean	SD	
Total Brain Volume	343.89	19.74	415.13	20.16	-17.16	-3.53	0.00	0.00	**	1.00	357.61	29.36	
¦--Basic cell groups and regions	307.67	16.97	368.12	17.94	-16.42	-3.37	0.00	0.00	**	0.00	**	320.14	24.71
¦ ¦--Cerebrum	194.18	9.88	230.36	11.92	-15.71	-3.03	0.00	0.00	**	0.03	*	201.01	17.19
¦ ¦ ¦--Cerebral cortex	162.07	8.11	191.37	9.66	-15.31	-3.03	0.00	0.00	**	0.02	*	168.44	14.37
¦ ¦ ¦ ¦--Cortical subplate	10.38	0.51	12.38	0.54	-16.15	-3.67	0.00	0.00	**	1.00		10.39	0.77
¦ ¦ ¦ ¦ ¦--Cortical subplate-other	7.52	0.42	9.03	0.37	-16.74	-4.12	0.00	0.00	**	1.00		7.47	0.55
¦ ¦ ¦ ¦ ¦--Claustrum	0.85	0.07	0.99	0.09	-13.79	-1.60	0.00	0.00	**	1.00		0.87	0.12
¦ ¦ ¦ ¦ ¦ ¦--Claustrum-other	0.27	0.02	0.31	0.02	-10.92	-1.52	0.00	0.01	*	1.00		0.27	0.04
¦ ¦ ¦ ¦ ¦ ¦--Claustrum: dorsal part	0.17	0.02	0.21	0.03	-15.77	-1.27	0.00	0.03	*	1.00		0.18	0.03
¦ ¦ ¦ ¦ ¦ °--Claustrum: ventral part	0.41	0.04	0.48	0.04	-14.77	-1.58	0.00	0.00	**	1.00		0.41	0.05
¦ ¦ ¦ ¦ °--Endopiriform nucleus	2.01	0.08	2.36	0.13	-14.87	-2.76	0.00	0.00	**	1.00		2.04	0.14
¦ ¦ ¦ ¦ ¦--Endopiriform nucleus, dorsal part	1.55	0.06	1.84	0.11	-15.53	-2.54	0.00	0.00	**	1.00		1.57	0.12
¦ ¦ ¦ ¦ ¦ ¦--Dorsal nucleus of the endopiriform	1.13	0.04	1.34	0.09	-16.13	-2.45	0.00	0.00	**	1.00		1.13	0.09
¦ ¦ ¦ ¦ ¦ °--Intermediate nucleus of the endopiriform claustrum	0.43	0.02	0.50	0.03	-13.91	-2.10	0.00	0.00	**	1.00		0.44	0.03
¦ ¦ ¦ ¦ °--Endopiriform nucleus, ventral part	0.45	0.03	0.52	0.04	-12.50	-1.80	0.00	0.00	**	1.00		0.47	0.04
¦ ¦ ¦ °--Cortical plate	151.70	7.69	179.00	9.26	-15.25	-2.95	0.00	0.00	**	0.02	*	158.06	13.64
¦ ¦ ¦ ¦--Olfactory areas	31.79	1.70	36.66	1.78	-13.30	-2.74	0.00	0.00	**	1.00		32.35	2.54
¦ ¦ ¦ ¦ ¦--Olfactory areas-other	1.97	0.10	2.29	0.11	-14.03	-3.04	0.00	0.00	**	1.00		1.99	0.16
¦ ¦ ¦ ¦ ¦--Postpiriform transition area	0.84	0.06	1.01	0.04	-16.86	-3.88	0.00	0.00	**	1.00		0.88	0.07
¦ ¦ ¦ ¦ ¦--Piriform area	8.89	0.56	10.73	0.35	-17.09	-5.28	0.00	0.00	**	1.00		9.43	0.66
¦ ¦ ¦ ¦ ¦ ¦--Cortex-amygdala transition zones	0.66	0.11	0.76	0.04	-12.68	-2.24	0.00	0.01	**	1.00		0.70	0.07
¦ ¦ ¦ ¦ ¦ °--Piriform cortex	8.23	0.47	9.97	0.32	-17.43	-5.47	0.00	0.00	**	1.00		8.73	0.61
¦ ¦ ¦ ¦ ¦--Taenia tecta	0.98	0.03	1.12	0.07	-12.27	-1.84	0.00	0.00	**	1.00		1.02	0.09
¦ ¦ ¦ ¦ ¦ ¦--Taenia tecta, dorsal part	0.87	0.03	1.00	0.07	-13.18	-1.96	0.00	0.00	**	1.00		0.90	0.09
¦ ¦ ¦ ¦ ¦ °--Taenia tecta, ventral part	0.11	0.01	0.12	0.01	-4.57	-0.46	0.24	1.00		0.46		0.11	0.01
¦ ¦ ¦ ¦ ¦--Cortical amygdalar area	1.64	0.10	1.90	0.11	-13.39	-2.32	0.00	0.00	**	1.00		1.67	0.08
¦ ¦ ¦ ¦ ¦ °--Cortical amygdalar area, posterior part	1.64	0.10	1.90	0.11	-13.39	-2.32	0.00	0.00	**	1.00		1.67	0.08
¦ ¦ ¦ ¦ ¦ ¦--Cortical amygdalar area, posterior part, lateral zone	0.70	0.05	0.81	0.05	-13.30	-2.11	0.00	0.00	**	1.00		0.71	0.05
¦ ¦ ¦ ¦ ¦ °--Cortical amygdalar area, posterior part, medial zone	0.94	0.07	1.09	0.07	-13.46	-2.06	0.00	0.00	**	1.00		0.96	0.06
¦ ¦ ¦ ¦ ¦--Piriform-amygdalar area	0.33	0.02	0.40	0.02	-17.39	-3.26	0.00	0.00	**	0.34		0.36	0.03
¦ ¦ ¦ ¦ ¦--Main olfactory bulb	14.52	0.98	16.42	1.20	-11.56	-1.58	0.00	0.00	**	1.00		14.43	1.63
¦ ¦ ¦ ¦ ¦ ¦--Main olfactory bulb, glomerular layer	3.64	0.29	4.18	0.33	-12.79	-1.61	0.00	0.00	**	1.00		3.63	0.52
¦ ¦ ¦ ¦ ¦ ¦--Main olfactory bulb, outer plexiform layer	5.39	0.36	6.06	0.41	-11.02	-1.61	0.00	0.01	**	0.71		5.45	0.49
¦ ¦ ¦ ¦ ¦ ¦--Main olfactory bulb, mitral layer	0.82	0.06	0.89	0.11	-8.64	-0.72	0.05	0.61		1.00		0.77	0.16
¦ ¦ ¦ ¦ ¦ ¦--Main olfactory bulb, inner plexiform layer	0.72	0.06	0.82	0.10	-11.92	-0.96	0.01	0.13		1.00		0.69	0.15
¦ ¦ ¦ ¦ ¦ °--Main olfactory bulb, granule layer	3.94	0.26	4.46	0.30	-11.66	-1.73	0.00	0.00	**	1.00		3.89	0.41
¦ ¦ ¦ ¦ ¦--Accessory olfactory bulb	0.70	0.04	0.74	0.05	-4.88	-0.71	0.06	0.51		1.00		0.66	0.07
¦ ¦ ¦ ¦ ¦ ¦--Accessory olfactory bulb, glomerular layer	0.49	0.02	0.50	0.03	-0.68	-0.10	0.79	1.00		0.27		0.47	0.04
¦ ¦ ¦ ¦ ¦ °--Accessory olfactory bulb, granular layer	0.21	0.01	0.24	0.02	-13.56	-1.76	0.00	0.00	**	1.00		0.20	0.03
¦ ¦ ¦ ¦ °--Anterior olfactory nucleus	1.92	0.08	2.07	0.12	-7.50	-1.35	0.00	0.00	**	0.86		1.92	0.17
¦ ¦ ¦ ¦--Hippocampal formation	31.27	1.97	38.71	1.69	-19.22	-4.41	0.00	0.00	**	0.00	**	31.99	2.64
¦ ¦ ¦ ¦ ¦--Retrohippocampal region	14.39	0.88	17.31	0.77	-16.90	-3.79	0.00	0.00	**	0.85		14.83	0.97
¦ ¦ ¦ ¦ ¦ ¦--Subiculum	4.53	0.30	5.41	0.34	-16.19	-2.55	0.00	0.00	**	1.00		4.63	0.47
¦ ¦ ¦ ¦ ¦ ¦ ¦--pre-para subiculum	1.88	0.15	2.19	0.20	-14.30	-1.58	0.00	0.00	**	1.00		1.95	0.22
¦ ¦ ¦ ¦ ¦ ¦ °--subiculum	2.65	0.15	3.22	0.17	-17.47	-3.34	0.00	0.00	**	0.80		2.68	0.26
¦ ¦ ¦ ¦ ¦ °--Entorhinal area	9.86	0.61	11.91	0.50	-17.22	-4.10	0.00	0.00	**	0.75		10.20	0.59
¦ ¦ ¦ ¦ ¦ ¦--Entorhinal area, medial part, dorsal zone	4.77	0.33	5.85	0.34	-18.51	-3.19	0.00	0.00	**	0.18		5.03	0.33
¦ ¦ ¦ ¦ ¦ ¦--Entorhinal area, lateral part	4.51	0.29	5.37	0.17	-16.06	-5.07	0.00	0.00	**	1.00		4.57	0.38
¦ ¦ ¦ ¦ ¦ ¦ ¦--Dorsal intermediate entorhinal cortex	1.46	0.09	1.73	0.06	-15.81	-4.98	0.00	0.00	**	1.00		1.47	0.12
¦ ¦ ¦ ¦ ¦ ¦ ¦--Dorsolateral entorhinal cortex	2.09	0.15	2.53	0.12	-17.23	-3.76	0.00	0.00	**	1.00		2.11	0.21
¦ ¦ ¦ ¦ ¦ ¦ °--Ventral intermediate entorhinal cortex	0.95	0.06	1.11	0.04	-13.76	-3.39	0.00	0.00	**	1.00		0.98	0.07
¦ ¦ ¦ ¦ ¦ °--Entorhinal area, medial part, ventral zone	0.58	0.04	0.69	0.03	-15.39	-3.39	0.00	0.00	**	1.00		0.61	0.05
¦ ¦ ¦ ¦ °--Hippocampal region	16.88	1.12	21.40	1.06	-21.10	-4.26	0.00	0.00	**	0.00	**	17.16	1.78
¦ ¦ ¦ ¦ ¦--Ammon's horn	12.30	0.77	15.58	0.75	-21.05	-4.40	0.00	0.00	**	0.00	**	12.44	1.31
¦ ¦ ¦ ¦ ¦ ¦--Field CA1	6.48	0.40	8.15	0.45	-20.51	-3.75	0.00	0.00	**	0.00	**	6.56	0.67
¦ ¦ ¦ ¦ ¦ ¦ ¦--Field CA1, stratum oriens	1.68	0.15	2.14	0.15	-21.39	-2.96	0.00	0.00	**	0.46		1.68	0.22
¦ ¦ ¦ ¦ ¦ ¦ ¦--Field CA1, stratum lacunosum-moleculare	1.89	0.11	2.38	0.13	-20.36	-3.62	0.00	0.00	**	0.00	**	1.93	0.18
¦ ¦ ¦ ¦ ¦ ¦ ¦--Field CA1, stratum radiatum	2.05	0.11	2.57	0.15	-19.95	-3.40	0.00	0.00	**	0.00	**	2.09	0.19
¦ ¦ ¦ ¦ ¦ ¦ °--Field CA1, pyramidal layer	0.85	0.06	1.06	0.06	-20.44	-3.49	0.00	0.00	**	0.01	*	0.85	0.09
¦ ¦ ¦ ¦ ¦ ¦--Field CA2	0.94	0.06	1.16	0.06	-19.27	-3.49	0.00	0.00	**	0.01	**	0.95	0.10
¦ ¦ ¦ ¦ ¦ ¦ ¦--Field CA2, pyramidal layer	0.16	0.01	0.20	0.01	-19.75	-3.30	0.00	0.00	**	0.01	**	0.17	0.02
¦ ¦ ¦ ¦ ¦ ¦ ¦--Field CA2, stratum oriens	0.41	0.03	0.50	0.02	-18.23	-4.03	0.00	0.00	**	0.04	*	0.41	0.05
¦ ¦ ¦ ¦ ¦ ¦ °--Field CA2, stratum radiatum	0.36	0.02	0.46	0.04	-20.20	-2.35	0.00	0.00	**	0.18		0.38	0.04
¦ ¦ ¦ ¦ ¦ °--Field CA3	4.89	0.34	6.27	0.32	-22.09	-4.39	0.00	0.00	**	0.00	**	4.93	0.55
¦ ¦ ¦ ¦ ¦ ¦--Field CA3, pyramidal layer	0.87	0.06	1.11	0.05	-21.66	-4.37	0.00	0.00	**	0.01	**	0.87	0.10
¦ ¦ ¦ ¦ ¦ ¦ ¦--CA3Py Inner	0.11	0.01	0.14	0.01	-22.73	-4.18	0.00	0.00	**	0.00	**	0.11	0.01
¦ ¦ ¦ ¦ ¦ ¦ °--CA3Py Outer	0.76	0.06	0.96	0.05	-21.50	-4.12	0.00	0.00	**	0.02	*	0.75	0.09
¦ ¦ ¦ ¦ ¦ ¦--Field CA3, stratum oriens	2.07	0.15	2.74	0.18	-24.32	-3.74	0.00	0.00	**	0.00	**	2.08	0.24
¦ ¦ ¦ ¦ ¦ ¦--Field CA3, stratum radiatum	1.44	0.09	1.80	0.09	-20.02	-3.85	0.00	0.00	**	0.44		1.47	0.16
¦ ¦ ¦ ¦ ¦ ¦ °--Field CA3, stratum lucidum	0.51	0.03	0.63	0.03	-19.05	-3.67	0.00	0.00	**	1.00		0.51	0.06
¦ ¦ ¦ ¦ ¦ °--Dentate gyrus	4.58	0.39	5.81	0.41	-21.24	-3.02	0.00	0.00	**	0.01	**	4.72	0.50
¦ ¦ ¦ ¦ ¦ ¦--Dentate gyrus, molecular layer	3.18	0.26	4.01	0.28	-20.53	-2.95	0.00	0.00	**	0.02	*	3.29	0.35
¦ ¦ ¦ ¦ ¦ °--Dentate gyrus, granule cell layer	1.40	0.13	1.81	0.13	-22.82	-3.15	0.00	0.00	**	0.00	**	1.43	0.16
¦ ¦ ¦ ¦ ¦ ¦--GrDG	0.96	0.09	1.23	0.09	-22.43	-3.08	0.00	0.00	**	0.00	**	0.98	0.11
¦ ¦ ¦ ¦ ¦ °--PoDG	0.44	0.04	0.58	0.04	-23.64	-3.25	0.00	0.00	**	0.00	**	0.45	0.05
¦ ¦ ¦ ¦ °--Isocortex	88.64	4.53	103.62	6.34	-14.46	-2.36	0.00	0.00	**	0.00	**	93.72	8.63
¦ ¦ ¦ ¦ ¦--Anterior cingulate area	4.02	0.28	4.72	0.33	-14.98	-2.12	0.00	0.00	**	1.00		4.21	0.45
¦ ¦ ¦ ¦ ¦ ¦--Anterior cingulate area, ventral part	2.38	0.16	2.76	0.21	-13.75	-1.80	0.00	0.00	**	1.00		2.46	0.27
¦ ¦ ¦ ¦ ¦ ¦ ¦--Cingulate cortex: area 24a	1.65	0.13	1.97	0.17	-16.36	-1.87	0.00	0.00	**	1.00		1.72	0.21
¦ ¦ ¦ ¦ ¦ ¦ °--Cingulate cortex: area 24a'	0.73	0.05	0.79	0.06	-7.25	-1.02	0.02	0.10	-	1.00		0.74	0.07
¦ ¦ ¦ ¦ ¦ °--Anterior cingulate area, dorsal part	1.64	0.14	1.96	0.16	-16.71	-2.10	0.00	0.00	**	0.67		1.75	0.20
¦ ¦ ¦ ¦ ¦ ¦--Cingulate cortex: area 24b	1.16	0.12	1.41	0.13	-17.62	-1.93	0.00	0.00	**	1.00		1.24	0.16
¦ ¦ ¦ ¦ ¦ °--Cingulate cortex: area 24b'	0.48	0.03	0.56	0.04	-14.40	-1.85	0.00	0.00	**	0.01	*	0.52	0.06
¦ ¦ ¦ ¦ ¦--Infralimbic area	0.43	0.04	0.57	0.08	-24.16	-1.80	0.00	0.00	**	0.78		0.44	0.05
¦ ¦ ¦ ¦ ¦--Retrosplenial area	4.86	0.36	5.62	0.52	-13.50	-1.46	0.00	0.00	**	0.06	-	5.08	0.52
¦ ¦ ¦ ¦ ¦ ¦--Retrosplenial area, ventral part	2.60	0.21	2.94	0.28	-11.51	-1.23	0.00	0.00	**	0.46		2.69	0.28
¦ ¦ ¦ ¦ ¦ ¦ ¦--Cingulate cortex: area 29a	0.58	0.05	0.68	0.08	-14.96	-1.30	0.00	0.00	**	1.00		0.59	0.07
¦ ¦ ¦ ¦ ¦ ¦ ¦--Cingulate cortex: area 29b	0.35	0.04	0.39	0.05	-8.49	-0.62	0.11	0.48		0.96		0.35	0.05
¦ ¦ ¦ ¦ ¦ ¦ °--Cingulate cortex: area 29c	1.67	0.12	1.88	0.16	-10.89	-1.27	0.00	0.00	**	0.52		1.74	0.18
¦ ¦ ¦ ¦ ¦ °--Retrosplenial area, dorsal part	2.26	0.17	2.68	0.27	-15.67	-1.57	0.00	0.00	**	0.02	*	2.40	0.26
¦ ¦ ¦ ¦ ¦--Prelimbic area	2.22	0.16	2.46	0.17	-9.76	-1.42	0.00	0.02	*	0.38		2.30	0.25
¦ ¦ ¦ ¦ ¦--Auditory areas	3.86	0.25	4.67	0.32	-17.53	-2.55	0.00	0.00	**	0.99		4.03	0.40

¦ ¦ ¦ ¦ ¦--Primary auditory area	1.24	0.08	1.51	0.12	-17.63	-2.30	0.00	0.00 **	1.00	1.30	0.12
¦ ¦ ¦ ¦ ¦--Dorsal auditory area	1.17	0.08	1.40	0.10	-16.58	-2.26	0.00	0.00 **	0.12	1.23	0.11
¦ ¦ ¦ ¦ °--Ventral auditory area	1.44	0.10	1.77	0.12	-18.21	-2.59	0.00	0.00 **	1.00	1.50	0.17
¦ ¦ ¦ ¦--Agranular insular area	0.85	0.03	0.89	0.05	-3.65	-0.67	0.08	1.00	0.07 -	0.91	0.11
¦ ¦ ¦ ¦ °--Agranular insular area, dorsal part	0.85	0.03	0.89	0.05	-3.65	-0.67	0.08	1.00	0.07 -	0.91	0.11
¦ ¦ ¦ ¦--Ectorhinal area	8.24	0.64	9.71	0.61	-15.20	-2.43	0.00	0.00 **	0.01 **	8.59	1.00
¦ ¦ ¦ ¦ ¦--Ectorhinal cortex	2.08	0.16	2.54	0.19	-17.93	-2.37	0.00	0.00 **	0.01 **	2.18	0.32
¦ ¦ ¦ ¦ °--Insular region: not subdivided	6.16	0.50	7.18	0.46	-14.23	-2.21	0.00	0.00 **	0.03 *	6.41	0.68
¦ ¦ ¦ ¦--Somatomotor areas	11.43	0.59	13.45	0.65	-15.02	-3.09	0.00	0.00 **	0.22	11.98	1.10
¦ ¦ ¦ ¦ ¦--Primary motor area	6.23	0.31	7.50	0.36	-16.91	-3.52	0.00	0.00 **	1.00	6.61	0.57
¦ ¦ ¦ ¦ ¦ ¦--Frontal cortex: area 3	0.54	0.03	0.63	0.04	-13.55	-2.39	0.00	0.00 **	1.00	0.58	0.06
¦ ¦ ¦ ¦ ¦ °--Primary motor cortex	5.69	0.29	6.87	0.34	-17.22	-3.51	0.00	0.00 **	1.00	6.04	0.52
¦ ¦ ¦ ¦ °--Secondary motor area	5.20	0.29	5.95	0.33	-12.64	-2.26	0.00	0.00 **	0.01 *	5.36	0.56
¦ ¦ ¦ ¦--Frontal pole, cerebral cortex	6.39	0.21	6.75	0.39	-5.29	-0.92	0.01	0.15	0.08 -	6.76	0.41
¦ ¦ ¦ ¦--Orbital area	5.76	0.33	6.60	0.38	-12.74	-2.19	0.00	0.00 **	1.00	5.98	0.59
¦ ¦ ¦ ¦ ¦--Orbital area, lateral part	3.07	0.16	3.36	0.21	-8.66	-1.37	0.00	0.01 **	0.54	3.12	0.29
¦ ¦ ¦ ¦ ¦--Orbital area, medial part	1.47	0.09	1.77	0.11	-16.98	-2.64	0.00	0.00 **	1.00	1.58	0.16
¦ ¦ ¦ ¦ °--Orbital area, ventrolateral part	1.22	0.10	1.47	0.09	-16.97	-2.81	0.00	0.00 **	1.00	1.28	0.16
¦ ¦ ¦ ¦--Posterior parietal association areas	1.90	0.12	2.24	0.19	-14.86	-1.75	0.00	0.00 **	0.01 **	2.01	0.21
¦ ¦ ¦ ¦ ¦--Lateral parietal association cortex	0.17	0.02	0.21	0.02	-19.85	-2.11	0.00	0.00 **	0.73	0.19	0.02
¦ ¦ ¦ ¦ ¦--Medial parietal association cortex	0.30	0.04	0.38	0.04	-19.64	-1.91	0.00	0.00 **	0.52	0.32	0.04
¦ ¦ ¦ ¦ ¦--Parietal cortex: posterior area: rostral part	0.08	0.01	0.10	0.01	-20.62	-2.54	0.00	0.00 **	1.00	0.08	0.02
¦ ¦ ¦ ¦ °--Secondary visual cortex: mediomedial area	1.35	0.07	1.54	0.14	-12.62	-1.36	0.00	0.00 **	0.01 *	1.41	0.14
¦ ¦ ¦ ¦--Perirhinal area	1.97	0.15	2.41	0.12	-18.55	-3.76	0.00	0.00 **	1.00	2.06	0.30
¦ ¦ ¦ ¦--Somatosensory areas	26.43	1.51	31.21	2.19	-15.30	-2.18	0.00	0.00 **	0.01 **	28.52	2.82
¦ ¦ ¦ ¦ ¦--Primary somatosensory area	21.35	1.16	25.33	1.73	-15.70	-2.29	0.00	0.00 **	0.06 -	23.11	2.14
¦ ¦ ¦ ¦ ¦ ¦--Primary somatosensory area-other	3.44	0.17	4.06	0.24	-15.15	-2.51	0.00	0.00 **	0.07 -	3.64	0.37
¦ ¦ ¦ ¦ ¦ ¦--Primary somatosensory area, barrel field	7.63	0.41	8.76	0.70	-12.94	-1.62	0.00	0.00 **	0.07 -	8.23	0.68
¦ ¦ ¦ ¦ ¦ ¦--Primary somatosensory area, trunk	0.78	0.07	0.97	0.07	-19.74	-2.57	0.00	0.00 **	1.00	0.86	0.09
¦ ¦ ¦ ¦ ¦ ¦ ¦--Primary somatosensory cortex: dysgranular zone	0.25	0.03	0.32	0.02	-22.32	-2.97	0.00	0.00 **	1.00	0.28	0.04
¦ ¦ ¦ ¦ ¦ ¦ ¦--Primary somatosensory cortex: shoulder region	0.13	0.01	0.16	0.02	-18.69	-1.72	0.00	0.00 **	1.00	0.15	0.02
¦ ¦ ¦ ¦ ¦ ¦ °--Primary somatosensory cortex: trunk region	0.39	0.04	0.48	0.04	-18.36	-2.45	0.00	0.00 **	1.00	0.44	0.04
¦ ¦ ¦ ¦ ¦ ¦--Primary somatosensory area, upper limb	2.85	0.25	3.63	0.27	-21.39	-2.84	0.00	0.00 **	1.00	3.18	0.33
¦ ¦ ¦ ¦ ¦ ¦--Primary somatosensory area, lower limb	1.91	0.19	2.42	0.22	-21.26	-2.35	0.00	0.00 **	0.46	2.13	0.23
¦ ¦ ¦ ¦ ¦ ¦--Primary somatosensory area, mouth	0.46	0.03	0.58	0.04	-21.66	-3.28	0.00	0.00 **	1.00	0.50	0.06
¦ ¦ ¦ ¦ ¦ °--Primary somatosensory area, nose	4.29	0.23	4.91	0.30	-12.64	-2.05	0.00	0.00 **	0.01 *	4.56	0.50
¦ ¦ ¦ ¦ °--Supplemental somatosensory area	5.08	0.49	5.88	0.55	-13.57	-1.46	0.00	0.01 *	0.00 **	5.41	0.77
¦ ¦ ¦ ¦--Temporal association areas	2.32	0.19	2.84	0.20	-18.48	-2.64	0.00	0.00 **	0.04 *	2.42	0.29
¦ ¦ ¦ ¦ °--Visual areas	7.95	0.39	9.47	0.97	-15.99	-1.56	0.00	0.00 **	0.07 -	8.44	0.71
¦ ¦ ¦ ¦ ¦--Primary visual area	1.76	0.10	2.16	0.23	-18.46	-1.69	0.00	0.00 **	0.86	1.92	0.15
¦ ¦ ¦ ¦ ¦--Lateral visual area	1.62	0.10	1.93	0.21	-15.97	-1.49	0.00	0.00 **	0.50	1.71	0.13
¦ ¦ ¦ ¦ ¦--posteromedial visual area	1.60	0.08	1.79	0.20	-10.78	-0.98	0.01	0.01 *	0.04 *	1.69	0.17
¦ ¦ ¦ ¦ ¦--Anterolateral visual area	2.18	0.13	2.68	0.27	-18.75	-1.85	0.00	0.00 **	0.44	2.29	0.22
¦ ¦ ¦ ¦ °--Anteromedial visual area	0.80	0.05	0.91	0.10	-12.30	-1.16	0.00	0.01 **	0.01 **	0.83	0.11
¦ ¦ °--Cerebral nuclei	32.11	1.86	38.99	2.37	-17.64	-2.90	0.00	0.00 **	1.00	32.57	2.93
¦ ¦ ¦--Pallidum	8.14	0.49	9.73	0.57	-16.36	-2.80	0.00	0.00 **	1.00	8.12	0.73
¦ ¦ ¦ ¦--Pallidum, ventral region	3.93	0.23	4.56	0.28	-13.80	-2.24	0.00	0.00 **	1.00	3.93	0.31
¦ ¦ ¦ ¦--Pallidum, caudal region	0.99	0.08	1.24	0.09	-20.37	-2.85	0.00	0.00 **	1.00	0.94	0.10
¦ ¦ ¦ ¦ °--Bed nuclei of the stria terminalis	0.99	0.08	1.24	0.09	-20.37	-2.85	0.00	0.00 **	1.00	0.94	0.10
¦ ¦ ¦ ¦--Pallidum, dorsal region	2.23	0.16	2.80	0.20	-20.42	-2.91	0.00	0.00 **	1.00	2.27	0.26
¦ ¦ ¦ °--Pallidum, medial region	0.99	0.07	1.13	0.06	-12.26	-2.43	0.00	0.00 **	1.00	0.99	0.08
¦ ¦ ¦ °--Medial septal complex	0.99	0.07	1.13	0.06	-12.26	-2.43	0.00	0.00 **	1.00	0.99	0.08
¦ ¦ °--Striatum	23.97	1.38	29.26	1.83	-18.07	-2.89	0.00	0.00 **	1.00	24.44	2.20
¦ ¦ ¦--Striatum ventral region	5.68	0.36	6.63	0.37	-14.26	-2.54	0.00	0.00 **	1.00	5.82	0.40
¦ ¦ ¦ ¦--Fundus of striatum	0.11	0.01	0.13	0.01	-11.32	-1.64	0.00	0.00 **	0.27	0.11	0.01
¦ ¦ ¦ ¦--Nucleus accumbens	3.00	0.17	3.59	0.21	-16.50	-2.88	0.00	0.00 **	1.00	3.01	0.28
¦ ¦ ¦ ¦ °--Olfactory tubercle	2.57	0.31	2.91	0.29	-11.60	-1.18	0.01	0.01 *	1.00	2.70	0.32
¦ ¦ ¦ ¦--Lateral septal complex	2.24	0.17	2.86	0.19	-21.73	-3.28	0.00	0.00 **	0.38	2.24	0.27
¦ ¦ ¦ ¦--Striatum dorsal region	15.21	0.95	18.81	1.43	-19.18	-2.52	0.00	0.00 **	1.00	15.59	1.59
¦ ¦ ¦ ¦ °--Caudoputamen	15.21	0.95	18.81	1.43	-19.18	-2.52	0.00	0.00 **	1.00	15.59	1.59
¦ ¦ ¦ °--Striatum-like amygdalar nuclei	0.84	0.06	0.96	0.05	-11.76	-2.24	0.00	0.00 **	1.00	0.80	0.06
¦ ¦ ¦ °--Medial amygdalar nucleus	0.84	0.06	0.96	0.05	-11.76	-2.24	0.00	0.00 **	1.00	0.80	0.06
¦--Brain stem	79.91	4.60	94.68	4.88	-15.61	-3.03	0.00	0.00 **	1.00	82.65	4.83
¦ ¦--Midbrain	23.38	1.48	27.88	1.88	-16.14	-2.39	0.00	0.00 **	1.00	23.77	2.05
¦ ¦ ¦--Midbrain, sensory related	10.39	0.65	12.28	0.92	-15.43	-2.07	0.00	0.00 **	0.27	10.68	0.80
¦ ¦ ¦ ¦--Inferior colliculus	4.04	0.26	4.85	0.36	-16.71	-2.27	0.00	0.00 **	0.76	4.31	0.37
¦ ¦ ¦ °--Superior colliculus, sensory related	6.35	0.42	7.44	0.59	-14.60	-1.85	0.00	0.00 **	0.38	6.37	0.67
¦ ¦ ¦--Midbrain, behavioral state related	0.21	0.02	0.25	0.02	-16.28	-2.65	0.00	0.00 **	1.00	0.21	0.02
¦ ¦ ¦ °--Midbrain raphe nuclei	0.21	0.02	0.25	0.02	-16.28	-2.65	0.00	0.00 **	1.00	0.21	0.02
¦ ¦ ¦ °--Interpeduncular nucleus	0.21	0.02	0.25	0.02	-16.28	-2.65	0.00	0.00 **	1.00	0.21	0.02
¦ ¦ ¦--Midbrain-other	9.88	0.66	11.79	0.78	-16.22	-2.45	0.00	0.00 **	1.00	9.93	1.05
¦ ¦ °--Midbrain, motor related	2.90	0.19	3.55	0.21	-18.34	-3.16	0.00	0.00 **	1.00	2.94	0.26
¦ ¦ °--Periaqueductal gray	2.90	0.19	3.55	0.21	-18.34	-3.16	0.00	0.00 **	1.00	2.94	0.26
¦ ¦--Hindbrain	35.08	1.98	41.18	2.01	-14.82	-3.03	0.00	0.00 **	1.00	36.99	2.56
¦ ¦ ¦--Medulla	21.32	1.26	24.76	1.37	-13.88	-2.51	0.00	0.00 **	1.00	22.78	2.39
¦ ¦ ¦ ¦--Medulla, sensory related	0.21	0.03	0.24	0.04	-12.48	-0.78	0.04	0.05 *	1.00	0.23	0.06
¦ ¦ ¦ ¦ °--Dorsal column nuclei	0.21	0.03	0.24	0.04	-12.48	-0.78	0.04	0.05 *	1.00	0.23	0.06
¦ ¦ ¦ ¦ °--Cuneate nucleus	0.21	0.03	0.24	0.04	-12.48	-0.78	0.04	0.05 *	1.00	0.23	0.06
¦ ¦ ¦ ¦--Medulla, motor related	0.30	0.04	0.32	0.03	-5.63	-0.59	0.19	0.69	1.00	0.27	0.09
¦ ¦ ¦ ¦ °--Inferior olivary complex	0.30	0.04	0.32	0.03	-5.63	-0.59	0.19	0.69	1.00	0.27	0.09
¦ ¦ ¦ °--Medulla-other	20.81	1.22	24.20	1.33	-14.00	-2.54	0.00	0.00 **	1.00	22.28	2.47
¦ ¦ °--Pons	13.76	0.76	16.42	0.76	-16.25	-3.53	0.00	0.00 **	1.00	14.20	0.83
¦ ¦ ¦--Pons-other	12.60	0.69	15.08	0.69	-16.49	-3.61	0.00	0.00 **	1.00	12.97	0.73
¦ ¦ ¦--Pons, behavioral state related	0.59	0.06	0.70	0.06	-15.82	-1.91	0.00	0.00 **	1.00	0.64	0.08
¦ ¦ ¦ °--Pontine reticular nucleus	0.59	0.06	0.70	0.06	-15.82	-1.91	0.00	0.00 **	1.00	0.64	0.08
¦ ¦ °--Pons, sensory related	0.57	0.04	0.64	0.05	-10.93	-1.30	0.00	0.00 **	0.86	0.59	0.05
¦ ¦ °--Superior olivary complex	0.57	0.04	0.64	0.05	-10.93	-1.30	0.00	0.00 **	0.86	0.59	0.05
¦ °--Interbrain	21.45	1.32	25.62	1.46	-16.29	-2.85	0.00	0.00 **	1.00	21.89	2.32
¦ ¦--Hypothalamus	8.37	0.47	9.90	0.48	-15.48	-3.21	0.00	0.00 **	1.00	8.40	0.71
¦ ¦ ¦--Hypothalamus-other	7.86	0.45	9.32	0.46	-15.57	-3.18	0.00	0.00 **	1.00	7.88	0.67
¦ ¦ °--Hypothalamic medial zone	0.50	0.04	0.58	0.04	-14.10	-2.33	0.00	0.00 **	1.00	0.52	0.05
¦ ¦ ¦--Mammillary body	0.37	0.04	0.43	0.03	-13.90	-1.75	0.00	0.00 **	1.00	0.40	0.05
¦ ¦ °--Medial preoptic nucleus	0.13	0.01	0.15	0.01	-14.67	-1.74	0.00	0.00 **	1.00	0.12	0.02
¦ °--Thalamus	13.08	0.92	15.72	1.07	-16.80	-2.47	0.00	0.00 **	1.00	13.49	1.69
°--Cerebellum	33.58	3.26	43.07	1.66	-22.03	-5.71	0.00	0.00 **	0.07 -	36.47	3.84
¦--Cerebellar cortex	32.69	3.19	41.92	1.63	-22.03	-5.66	0.00	0.00 **	0.08 -	35.57	3.75

¦ ¦ ¦–Vermal regions	14.09	1.31	18.40	0.79	-23.41	-5.44	0.00	0.00 **	0.01 *	15.53	1.57
¦ ¦ ¦ ¦–Lingula (I)	1.34	0.09	1.78	0.19	-24.58	-2.31	0.00	0.00 **	1.00	1.49	0.15
¦ ¦ ¦ ¦–Central lobule	1.45	0.15	2.11	0.17	-31.23	-4.00	0.00	0.00 **	0.23	1.65	0.39
¦ ¦ ¦ ¦–Culmen	4.31	0.36	5.65	0.26	-23.77	-5.24	0.00	0.00 **	0.00 **	4.64	0.44
¦ ¦ ¦ ¦ ¦–Culmen-other	3.09	0.27	4.03	0.18	-23.43	-5.23	0.00	0.00 **	0.00 **	3.33	0.31
¦ ¦ ¦ ¦ °–Lobules IV-V	1.22	0.10	1.62	0.10	-24.63	-3.92	0.00	0.00 **	0.32	1.31	0.14
¦ ¦ ¦ ¦–Declive (VI)	1.93	0.24	2.37	0.16	-18.83	-2.73	0.00	0.00 **	1.00	2.12	0.49
¦ ¦ ¦ ¦–Folium-tuber vermis (VII)	0.69	0.10	0.90	0.11	-22.99	-1.96	0.00	0.00 **	1.00	0.78	0.25
¦ ¦ ¦ ¦–Pyramus (VIII)	1.09	0.16	1.54	0.12	-29.16	-3.61	0.00	0.00 **	0.26	1.22	0.29
¦ ¦ ¦ ¦–Uvula (IX)	2.20	0.24	2.72	0.15	-19.27	-3.46	0.00	0.00 **	0.71	2.42	0.23
¦ ¦ ¦ °–Nodulus (X)	1.08	0.12	1.32	0.06	-18.12	-3.72	0.00	0.00 **	1.00	1.22	0.14
¦ ¦ °–Hemispheric regions	18.60	1.95	23.52	0.87	-20.94	-5.64	0.00	0.00 **	0.53	20.03	2.22
¦ ¦ ¦–Simple lobule	3.74	0.39	4.64	0.20	-19.43	-4.56	0.00	0.00 **	1.00	4.17	0.46
¦ ¦ ¦–Ansiform lobule	6.25	0.73	8.11	0.39	-22.94	-4.80	0.00	0.00 **	0.07 -	6.68	0.91
¦ ¦ ¦ ¦–Crus 1	3.21	0.37	4.29	0.21	-25.21	-5.20	0.00	0.00 **	0.01 *	3.48	0.35
¦ ¦ ¦ °–Crus 2	3.04	0.36	3.82	0.19	-20.40	-4.04	0.00	0.00 **	0.62	3.20	0.62
¦ ¦ ¦–Paramedian lobule	3.13	0.40	3.97	0.22	-21.16	-3.83	0.00	0.00 **	0.07 -	3.47	0.52
¦ ¦ ¦–Copula pyramidis	1.84	0.19	2.33	0.14	-21.16	-3.42	0.00	0.00 **	1.00	2.00	0.28
¦ ¦ ¦–Flocculus	0.75	0.08	0.96	0.06	-21.77	-3.50	0.00	0.00 **	0.99	0.80	0.08
¦ ¦ °–Paraflocculus	2.88	0.34	3.50	0.31	-17.70	-1.99	0.00	0.00 **	1.00	2.90	0.49
¦ °–Cerebellar nuclei	0.89	0.09	1.15	0.05	-22.03	-4.67	0.00	0.00 **	1.00	0.91	0.12
¦ ¦–Dentate nucleus	0.25	0.02	0.32	0.02	-21.23	-4.31	0.00	0.00 **	1.00	0.25	0.04
¦ ¦–Interposed nucleus	0.32	0.03	0.41	0.02	-21.82	-4.17	0.00	0.00 **	1.00	0.32	0.04
¦ °–Fastigial nucleus	0.32	0.03	0.42	0.02	-22.83	-4.72	0.00	0.00 **	1.00	0.33	0.04
°–fiber tracts	32.02	2.43	41.01	2.26	-21.93	-3.98	0.00	0.00 **	0.00 **	33.18	4.27
¦–cranial nerves	5.27	0.34	6.33	0.31	-16.70	-3.42	0.00	0.00 **	0.87	5.28	0.67
¦ ¦–olfactory nerve	1.97	0.13	2.34	0.13	-15.73	-2.87	0.00	0.00 **	1.00	1.96	0.23
¦ ¦ ¦–anterior commissure, olfactory limb	0.78	0.06	0.97	0.06	-19.67	-3.28	0.00	0.00 **	0.03 *	0.79	0.11
¦ ¦ °–lateral olfactory tract, general	1.19	0.08	1.36	0.08	-12.92	-2.27	0.00	0.00 **	1.00	1.17	0.13
¦ ¦–facial nerve	0.16	0.01	0.20	0.01	-19.61	-3.74	0.00	0.00 **	0.06 -	0.16	0.02
¦ ¦–dorsal roots	1.91	0.13	2.30	0.12	-17.02	-3.24	0.00	0.00 **	1.00	1.93	0.32
¦ ¦ °–cervicothalamic tract	1.91	0.13	2.30	0.12	-17.02	-3.24	0.00	0.00 **	1.00	1.93	0.32
¦ ¦ °–medial lemniscus	1.91	0.13	2.30	0.12	-17.02	-3.24	0.00	0.00 **	1.00	1.93	0.32
¦ ¦–optic nerve	1.13	0.09	1.36	0.08	-16.64	-2.90	0.00	0.00 **	1.00	1.13	0.11
¦ ¦ °–optic tract	1.13	0.09	1.36	0.08	-16.64	-2.90	0.00	0.00 **	1.00	1.13	0.11
¦ °–oculomotor nerve	0.09	0.01	0.13	0.01	-24.90	-3.04	0.00	0.00 **	0.13	0.10	0.01
¦ °–posterior commissure	0.09	0.01	0.13	0.01	-24.90	-3.04	0.00	0.00 **	0.13	0.10	0.01
¦–medial forebrain bundle system	4.92	0.42	6.53	0.46	-24.74	-3.51	0.00	0.00 **	0.04 *	5.05	0.67
¦ ¦–cerebrum related	4.03	0.36	5.44	0.40	-25.82	-3.51	0.00	0.00 **	0.04 *	4.15	0.58
¦ ¦ ¦–anterior commissure, temporal limb	0.29	0.03	0.37	0.02	-20.89	-3.69	0.00	0.00 **	0.19	0.29	0.04
¦ ¦ ¦–fornix system	2.53	0.25	3.47	0.29	-26.94	-3.27	0.00	0.00 **	0.08 -	2.61	0.38
¦ ¦ ¦ ¦–fimbria	2.08	0.22	2.87	0.26	-27.58	-3.04	0.00	0.00 **	0.14	2.15	0.33
¦ ¦ ¦ °–dorsal fornix	0.46	0.04	0.60	0.04	-23.90	-3.67	0.00	0.00 **	0.03 *	0.46	0.06
¦ ¦ ¦–stria terminalis	0.61	0.04	0.78	0.06	-22.15	-3.13	0.00	0.00 **	1.00	0.62	0.08
¦ ¦ °–cingulum bundle	0.60	0.06	0.82	0.08	-26.76	-2.63	0.00	0.00 **	0.03 *	0.63	0.09
¦ ¦ °–hypothalamus related	0.88	0.06	1.09	0.07	-19.35	-3.07	0.00	0.00 **	0.34	0.90	0.10
¦ ¦ ¦–epithalamus related	0.70	0.05	0.86	0.05	-18.31	-3.13	0.00	0.00 **	0.29	0.71	0.08
¦ ¦ ¦ ¦–fasciculus retroflexus	0.18	0.01	0.22	0.01	-17.57	-2.76	0.00	0.00 **	0.71	0.18	0.02
¦ ¦ ¦ ¦–habenular commissure	0.02	0.00	0.03	0.00	-33.06	-3.23	0.00	0.00 **	0.00 **	0.02	0.00
¦ ¦ ¦ °–stria medullaris	0.50	0.03	0.61	0.04	-17.91	-2.87	0.00	0.00 **	1.00	0.51	0.06
¦ ¦ °–mammillary related	0.18	0.02	0.24	0.02	-23.09	-2.72	0.00	0.00 **	1.00	0.19	0.02
¦ ¦ °–mammilothalmic tract	0.18	0.02	0.24	0.02	-23.09	-2.72	0.00	0.00 **	1.00	0.19	0.02
¦–cerebellum related fiber tracts	8.09	0.72	10.49	0.46	-22.84	-5.16	0.00	0.00 **	0.01 *	8.59	1.18
¦ ¦–cerebellar peduncles	2.15	0.17	2.74	0.15	-21.39	-4.00	0.00	0.00 **	0.02 *	2.27	0.29
¦ ¦ ¦–inferior cerebellar peduncle	0.58	0.05	0.74	0.04	-22.47	-3.81	0.00	0.00 **	0.04 *	0.61	0.09
¦ ¦ ¦–middle cerebellar peduncle	0.83	0.08	1.08	0.07	-22.74	-3.29	0.00	0.00 **	0.07 -	0.90	0.13
¦ ¦ °–superior cerebelar peduncles	0.75	0.06	0.92	0.07	-18.93	-2.67	0.00	0.00 **	1.00	0.76	0.09
¦ °–arbor vitae	5.94	0.56	7.75	0.33	-23.35	-5.43	0.00	0.00 **	0.03 *	6.32	0.90
¦ ¦–trunk of arbor vita	2.88	0.26	3.64	0.16	-20.70	-4.61	0.00	0.00 **	1.00	3.07	0.25
¦ ¦–lobule 1-2 white matter	0.06	0.01	0.08	0.01	-30.13	-1.91	0.00	0.00 **	1.00	0.06	0.01
¦ ¦–lobule 3 white matter	0.13	0.02	0.19	0.02	-33.38	-3.94	0.00	0.00 **	1.00	0.13	0.03
¦ ¦–trunk of lobules 1-3 white matter	0.10	0.01	0.13	0.01	-26.04	-2.87	0.00	0.00 **	0.80	0.10	0.02
¦ ¦–lobules 4-5 white matter	0.36	0.04	0.50	0.03	-27.20	-4.82	0.00	0.00 **	0.00 **	0.37	0.09
¦ ¦–lobules 6-7 white matter	0.47	0.05	0.60	0.04	-22.08	-3.29	0.00	0.00 **	0.75	0.51	0.16
¦ ¦–lobule 8 white matter	0.09	0.03	0.14	0.01	-34.11	-4.94	0.00	0.00 **	0.39	0.11	0.03
¦ ¦–trunk of lobules 6-8 white matter	0.07	0.01	0.10	0.01	-32.59	-4.53	0.00	0.00 **	0.00 **	0.08	0.02
¦ ¦–lobule 9 white matter	0.20	0.02	0.27	0.01	-25.92	-5.54	0.00	0.00 **	0.07 -	0.22	0.05
¦ ¦–lobule 10 white matter	0.06	0.01	0.08	0.01	-26.20	-2.45	0.00	0.00 **	1.00	0.06	0.02
¦ ¦–anterior lobule white matter	0.06	0.01	0.09	0.01	-31.60	-4.00	0.00	0.00 **	0.07 -	0.06	0.02
¦ ¦–simple lobule white matter	0.25	0.04	0.34	0.02	-25.53	-4.27	0.00	0.00 **	1.00	0.27	0.06
¦ ¦–crus 1 white matter	0.24	0.04	0.35	0.02	-31.36	-6.55	0.00	0.00 **	0.00 **	0.26	0.07
¦ ¦–trunk of simple and crus 1 white matter	0.11	0.02	0.13	0.01	-18.10	-2.56	0.00	0.00 **	1.00	0.11	0.03
¦ ¦–crus 2 white matter	0.19	0.03	0.26	0.01	-26.92	-5.10	0.00	0.00 **	0.00 **	0.20	0.06
¦ ¦–paramedian lobule	0.09	0.02	0.13	0.01	-29.39	-3.00	0.00	0.00 **	0.01 **	0.11	0.03
¦ ¦–trunk of crus 2 and paramedian white matter	0.25	0.03	0.30	0.02	-16.91	-2.75	0.00	0.00 **	1.00	0.26	0.06
¦ ¦–copula white matter	0.05	0.01	0.07	0.00	-23.66	-3.79	0.00	0.00 **	1.00	0.06	0.01
¦ ¦–paraflocculus white matter	0.23	0.03	0.29	0.03	-19.61	-2.25	0.00	0.00 **	1.00	0.23	0.06
¦ °–flocculus white matter	0.04	0.01	0.06	0.01	-24.01	-2.00	0.00	0.00 **	1.00	0.05	0.01
¦–lateral forebrain bundle system	13.64	1.02	17.55	1.16	-22.27	-3.37	0.00	0.00 **	0.01 *	14.16	1.78
¦ ¦–corticospinal tract	4.94	0.35	6.11	0.35	-19.13	-3.31	0.00	0.00 **	1.00	5.06	0.69
¦ ¦ ¦–cerebal peduncle	1.48	0.13	1.89	0.11	-21.50	-3.71	0.00	0.00 **	0.01 **	1.52	0.19
¦ ¦ ¦–corticospinal tract-other	1.36	0.10	1.57	0.10	-13.45	-2.17	0.00	0.00 **	0.08 -	1.39	0.25
¦ ¦ °–internal capsule	2.10	0.14	2.65	0.19	-20.82	-2.91	0.00	0.00 **	1.00	2.15	0.28
¦ °–corpus callosum	8.70	0.67	11.44	0.84	-23.94	-3.27	0.00	0.00 **	0.00 **	9.09	1.11
°–extrapyramidal fiber systems	0.10	0.01	0.12	0.01	-14.87	-2.49	0.00	0.00 **	1.00	0.10	0.01
°–rubrospinal tract	0.10	0.01	0.12	0.01	-14.87	-2.49	0.00	0.00 **	1.00	0.10	0.01
°–ventral tegmental decussation	0.10	0.01	0.12	0.01	-14.87	-2.49	0.00	0.00 **	1.00	0.10	0.01
°–ventricular systems	4.20	0.47	5.99	0.50	-29.95	-3.57	0.00	0.00 **	0.27	4.28	0.55
¦–cerebral aqueduct	0.33	0.03	0.43	0.04	-23.26	-2.70	0.00	0.00 **	1.00	0.34	0.05
¦–fourth ventricle	0.65	0.04	0.78	0.04	-16.21	-3.33	0.00	0.00 **	1.00	0.72	0.11
¦–lateral ventricle	2.26	0.38	3.58	0.52	-37.02	-2.54	0.00	0.00 **	0.32	2.25	0.42
¦ ¦–lateral ventricle-other	2.22	0.38	3.53	0.52	-37.27	-2.53	0.00	0.00 **	0.32	2.20	0.41
¦ °–subependymal zone	0.04	0.00	0.05	0.00	-19.80	-2.49	0.00	0.00 **	1.00	0.04	0.01
°–third ventricle	0.95	0.08	1.19	0.05	-20.12	-4.52	0.00	0.00 **	1.00	0.98	0.14

								Absolute Volumes Male									
SPF							Relative Volu	GFSPF		SPF							Relative Volumes
Mean	SD	%Diff	Effect	P-Value	FDR		FDR	Mean	SD	Mean	SD	%Diff	Effect	P-Value	FDR		FDR
404.98	17.82	-11.70	-2.66	0.00	0.00	**	1.00	376.87	14.31	415.13	20.16	-9.22	-1.90	0.00	0.00	**	1.00
359.40	15.78	-10.92	-2.49	0.00	0.00	**	0.08 -	336.45	12.11	368.12	17.94	-8.60	-1.77	0.00	0.00	**	0.00 **
224.62	10.58	-10.51	-2.23	0.00	0.00	**	0.77	212.11	6.98	230.36	11.92	-7.92	-1.53	0.00	0.00	**	0.03 *
186.47	8.77	-9.67	-2.05	0.00	0.00	**	0.30	177.40	5.17	191.37	9.66	-7.30	-1.45	0.00	0.00	**	0.02 *
11.85	0.57	-12.35	-2.55	0.00	0.00	**	1.00	11.26	0.65	12.38	0.54	-9.00	-2.05	0.00	0.00	**	1.00
8.60	0.36	-13.07	-3.16	0.00	0.00	**	1.00	8.15	0.47	9.03	0.37	-9.75	-2.40	0.00	0.00	**	1.00
0.93	0.12	-6.21	-0.50	0.20	0.83		0.29	0.93	0.10	0.99	0.09	-6.16	-0.72	0.10	0.64		1.00
0.30	0.03	-9.08	-0.97	0.03	0.12		1.00	0.29	0.03	0.31	0.02	-6.50	-0.90	0.04	0.37		1.00
0.18	0.03	-1.58	-0.09	0.81	1.00		0.17	0.19	0.03	0.21	0.03	-6.47	-0.52	0.23	1.00		1.00
0.44	0.06	-6.18	-0.48	0.20	0.82		0.33	0.45	0.05	0.48	0.04	-5.80	-0.62	0.13	0.87		1.00
2.33	0.15	-12.12	-1.94	0.00	0.00	**	1.00	2.18	0.14	2.36	0.13	-7.31	-1.36	0.00	0.01	*	1.00
1.79	0.12	-12.52	-1.80	0.00	0.00	**	1.00	1.69	0.12	1.84	0.11	-8.35	-1.37	0.00	0.01	**	1.00
1.30	0.11	-13.48	-1.66	0.00	0.00	**	1.00	1.23	0.10	1.34	0.09	-8.54	-1.30	0.00	0.01	*	1.00
0.49	0.03	-9.97	-1.82	0.00	0.00	**	1.00	0.46	0.03	0.50	0.03	-7.82	-1.18	0.00	0.03	*	1.00
0.53	0.05	-10.79	-1.12	0.00	0.01	*	1.00	0.50	0.03	0.52	0.04	-3.62	-0.52	0.16	0.84		1.00
174.62	8.28	-9.48	-2.00	0.00	0.00	**	0.20	166.14	4.67	179.00	9.26	-7.18	-1.39	0.00	0.01	**	0.02 *
35.68	1.46	-9.33	-2.28	0.00	0.00	**	1.00	33.85	1.03	36.66	1.78	-7.67	-1.58	0.00	0.01	**	1.00
2.19	0.12	-9.21	-1.64	0.00	0.00	**	1.00	2.06	0.11	2.29	0.11	-9.83	-2.13	0.00	0.00	**	1.00
1.00	0.06	-11.94	-2.13	0.00	0.00	**	1.00	0.92	0.05	1.01	0.04	-8.98	-2.07	0.00	0.00	**	1.00
10.67	0.78	-11.65	-1.60	0.00	0.00	**	1.00	9.82	0.42	10.73	0.35	-8.51	-2.63	0.00	0.00	**	1.00
0.77	0.06	-9.42	-1.26	0.00	0.07	-	1.00	0.72	0.05	0.76	0.04	-5.83	-1.03	0.03	0.73		1.00
9.90	0.73	-11.82	-1.61	0.00	0.00	**	1.00	9.10	0.40	9.97	0.32	-8.71	-2.73	0.00	0.00	**	1.00
1.08	0.04	-6.21	-1.75	0.02	0.22		1.00	1.04	0.06	1.12	0.07	-7.23	-1.09	0.01	0.04	*	1.00
0.97	0.04	-6.46	-1.58	0.03	0.23		1.00	0.92	0.06	1.00	0.07	-8.28	-1.23	0.00	0.01	*	1.00
0.12	0.01	-4.17	-0.78	0.09	1.00		1.00	0.12	0.01	0.12	0.01	1.62	0.16	0.64	1.00		0.46
1.80	0.08	-7.33	-1.59	0.00	0.02	*	1.00	1.76	0.08	1.90	0.11	-7.28	-1.26	0.00	0.04	*	1.00
1.80	0.08	-7.33	-1.59	0.00	0.02	*	1.00	1.76	0.08	1.90	0.11	-7.28	-1.26	0.00	0.04	*	1.00
0.77	0.04	-7.32	-1.48	0.00	0.04	*	1.00	0.75	0.04	0.81	0.05	-7.22	-1.14	0.00	0.11		1.00
1.03	0.06	-7.34	-1.35	0.00	0.04	*	1.00	1.01	0.06	1.09	0.07	-7.32	-1.12	0.00	0.05	*	1.00
0.39	0.02	-8.91	-1.79	0.00	0.01	*	1.00	0.39	0.03	0.40	0.02	-2.62	-0.49	0.30	1.00		0.34
15.80	0.48	-8.67	-2.85	0.00	0.02	*	0.63	15.17	0.46	16.42	1.20	-7.61	-1.04	0.00	0.12		1.00
3.97	0.14	-8.60	-2.46	0.02	0.10	-	1.00	3.80	0.13	4.18	0.33	-9.09	-1.15	0.00	0.07	-	1.00
5.86	0.24	-7.02	-1.68	0.01	0.07	-	0.08 -	5.66	0.17	6.06	0.41	-6.55	-0.96	0.00	0.27		0.71
0.86	0.04	-9.83	-2.07	0.06	0.30		1.00	0.83	0.06	0.89	0.11	-7.30	-0.60	0.07	0.97		1.00
0.79	0.04	-12.16	-2.21	0.03	0.11		1.00	0.75	0.06	0.82	0.10	-8.59	-0.69	0.04	0.56		1.00
4.33	0.14	-10.09	-3.23	0.00	0.00	**	1.00	4.13	0.20	4.46	0.30	-7.54	-1.12	0.00	0.10	-	1.00
0.72	0.04	-8.22	-1.42	0.01	0.04	*	1.00	0.70	0.03	0.74	0.05	-4.70	-0.68	0.05	0.58		1.00
0.49	0.03	-3.79	-0.63	0.20	1.00		0.77	0.49	0.02	0.50	0.03	-1.39	-0.21	0.54	1.00		0.27
0.24	0.01	-17.29	-2.80	0.00	0.00	**	0.77	0.21	0.01	0.24	0.02	-11.54	-1.50	0.00	0.00	**	1.00
2.02	0.09	-4.97	-1.06	0.06	0.44		1.00	2.00	0.09	2.07	0.12	-3.48	-0.63	0.09	0.44		0.86
37.12	1.19	-13.82	-4.30	0.00	0.00	**	0.01 *	33.73	1.07	38.71	1.69	-12.88	-2.96	0.00	0.00	**	0.00 **
16.89	0.55	-12.18	-3.71	0.00	0.00	**	0.87	15.50	0.53	17.31	0.77	-10.49	-2.35	0.00	0.00	**	0.85
5.18	0.19	-10.60	-2.87	0.00	0.00	**	1.00	4.86	0.16	5.41	0.34	-10.09	-1.59	0.00	0.00	**	1.00
2.12	0.08	-8.11	-2.08	0.01	0.03	*	1.00	2.02	0.11	2.19	0.20	-7.67	-0.85	0.01	0.04	*	1.00
3.06	0.15	-12.33	-2.50	0.00	0.00	**	1.00	2.84	0.13	3.22	0.17	-11.75	-2.24	0.00	0.00	**	0.80
11.71	0.45	-12.88	-3.32	0.00	0.00	**	0.32	10.64	0.46	11.91	0.50	-10.67	-2.54	0.00	0.00	**	0.75
5.77	0.24	-12.86	-3.10	0.00	0.00	**	0.17	5.14	0.26	5.85	0.34	-12.06	-2.08	0.00	0.00	**	0.18
5.27	0.27	-13.32	-2.63	0.00	0.00	**	1.00	4.86	0.24	5.37	0.17	-9.52	-3.01	0.00	0.00	**	1.00
1.71	0.09	-14.10	-2.64	0.00	0.00	**	1.00	1.53	0.09	1.73	0.06	-11.57	-3.65	0.00	0.00	**	1.00
2.45	0.13	-13.67	-2.56	0.00	0.00	**	1.00	2.29	0.10	2.53	0.12	-9.48	-2.07	0.00	0.00	**	1.00
1.11	0.06	-11.32	-1.97	0.00	0.00	**	1.00	1.04	0.05	1.11	0.04	-6.42	-1.58	0.00	0.06	-	1.00
0.67	0.03	-9.58	-1.88	0.00	0.01	**	1.00	0.63	0.03	0.69	0.03	-7.72	-1.70	0.00	0.01	**	1.00
20.23	0.77	-15.20	-3.99	0.00	0.00	**	0.10 -	18.23	0.77	21.40	1.06	-14.81	-2.99	0.00	0.00	**	0.00 **
14.65	0.63	-15.10	-3.49	0.00	0.00	**	0.34	13.28	0.68	15.58	0.75	-14.77	-3.08	0.00	0.00	**	0.00 **
7.64	0.36	-14.14	-3.00	0.00	0.00	**	1.00	6.96	0.35	8.15	0.45	-14.64	-2.68	0.00	0.00	**	0.00 **
1.96	0.16	-14.39	-1.73	0.00	0.00	**	1.00	1.79	0.15	2.14	0.15	-16.42	-2.28	0.00	0.00	**	0.46
2.24	0.09	-13.80	-3.29	0.00	0.00	**	0.41	2.04	0.09	2.38	0.13	-14.03	-2.49	0.00	0.00	**	0.00 **
2.43	0.09	-14.13	-3.70	0.00	0.00	**	0.36	2.21	0.08	2.57	0.15	-13.74	-2.34	0.00	0.00	**	0.00 **
1.00	0.05	-14.41	-3.14	0.00	0.00	**	1.00	0.91	0.05	1.06	0.06	-14.60	-2.50	0.00	0.00	**	0.01 *
1.13	0.03	-15.31	-4.96	0.00	0.00	**	0.77	1.01	0.05	1.16	0.06	-13.01	-2.36	0.00	0.00	**	0.01 **
0.19	0.01	-14.96	-4.23	0.00	0.00	**	1.00	0.17	0.01	0.20	0.01	-13.33	-2.23	0.00	0.00	**	0.01 **
0.48	0.02	-14.57	-2.83	0.00	0.00	**	1.00	0.43	0.03	0.50	0.02	-13.80	-3.06	0.00	0.00	**	0.04 *
0.45	0.02	-16.25	-3.34	0.00	0.00	**	0.24	0.40	0.02	0.46	0.04	-11.98	-1.40	0.00	0.00	**	0.18
5.89	0.27	-16.31	-3.60	0.00	0.00	**	0.37	5.32	0.33	6.27	0.32	-15.27	-3.04	0.00	0.00	**	0.00 **
1.03	0.06	-16.14	-2.98	0.00	0.00	**	1.00	0.93	0.06	1.11	0.05	-15.67	-3.16	0.00	0.00	**	0.01 **
0.14	0.00	-17.41	-5.22	0.00	0.00	**	0.07 -	0.12	0.01	0.14	0.01	-15.46	-2.84	0.00	0.00	**	0.00 **
0.90	0.05	-15.94	-2.67	0.00	0.00	**	1.00	0.81	0.05	0.96	0.05	-15.70	-3.01	0.00	0.00	**	0.02 *
2.56	0.12	-18.71	-4.13	0.00	0.00	**	0.17	2.25	0.15	2.74	0.18	-17.82	-2.74	0.00	0.00	**	0.00 **
1.70	0.08	-13.53	-2.96	0.00	0.00	**	1.00	1.58	0.11	1.80	0.09	-12.10	-2.33	0.00	0.00	**	0.44
0.59	0.04	-14.16	-2.31	0.00	0.00	**	1.00	0.55	0.03	0.63	0.03	-12.54	-2.42	0.00	0.00	**	1.00
5.58	0.19	-15.45	-4.59	0.00	0.00	**	0.08 -	4.95	0.17	5.81	0.41	-14.90	-2.12	0.00	0.00	**	0.01 **
3.84	0.13	-14.48	-4.32	0.00	0.00	**	0.26	3.43	0.12	4.01	0.28	-14.24	-2.04	0.00	0.00	**	0.02 *
1.74	0.06	-17.61	-4.92	0.00	0.00	**	0.03 *	1.51	0.05	1.81	0.13	-16.37	-2.26	0.00	0.00	**	0.00 **
1.18	0.04	-17.12	-4.91	0.00	0.00	**	0.03 *	1.03	0.03	1.23	0.09	-16.07	-2.20	0.00	0.00	**	0.00 **
0.56	0.02	-18.65	-4.75	0.00	0.00	**	0.03 *	0.48	0.02	0.58	0.04	-17.00	-2.34	0.00	0.00	**	0.00 **
101.82	6.17	-7.96	-1.31	0.01	0.02	*	0.06 -	98.56	3.38	103.62	6.34	-4.88	-0.80	0.02	0.26		0.00 **
4.59	0.33	-8.25	-1.16	0.02	0.06	-	1.00	4.46	0.28	4.72	0.33	-5.63	-0.80	0.04	0.12		1.00
2.71	0.17	-9.17	-1.44	0.01	0.04	*	1.00	2.57	0.19	2.76	0.21	-6.76	-0.88	0.02	0.04	*	1.00
1.91	0.14	-10.30	-1.39	0.01	0.04	*	1.00	1.77	0.15	1.97	0.17	-10.14	-1.16	0.00	0.00	**	1.00
0.79	0.06	-6.45	-0.87	0.04	0.18		1.00	0.80	0.06	0.79	0.06	1.68	0.24	0.57	1.00		1.00
1.89	0.19	-6.93	-0.69	0.09	0.38		0.77	1.88	0.15	1.96	0.16	-4.03	-0.51	0.20	1.00		0.67
1.34	0.15	-7.78	-0.68	0.09	0.37		1.00	1.31	0.14	1.41	0.13	-6.65	-0.73	0.08	0.30		1.00
0.55	0.05	-4.84	-0.52	0.21	1.00		0.33	0.57	0.04	0.56	0.04	2.59	0.33	0.36	1.00		0.01 *
0.55	0.04	-20.17	-2.60	0.00	0.00	**	0.10	0.48	0.05	0.57	0.08	-16.61	-1.24	0.00	0.00	**	0.78
5.59	0.22	-9.05	-2.30	0.00	0.01	**	1.00	5.45	0.15	5.62	0.52	-3.12	-0.34	0.27	1.00		0.06 -
2.90	0.11	-7.31	-1.97	0.01	0.06	-	1.00	2.86	0.13	2.94	0.28	-2.65	-0.28	0.38	1.00		0.46
0.67	0.04	-10.76	-1.69	0.00	0.01	**	1.00	0.64	0.04	0.68	0.08	-5.09	-0.44	0.18	0.79		1.00
0.39	0.02	-9.61	-2.18	0.01	0.23		1.00	0.37	0.04	0.39	0.05	-3.27	-0.24	0.48	1.00		0.96
1.84	0.08	-5.58	-1.31	0.05	0.26		1.00	1.85	0.08	1.88	0.16	-1.64	-0.19	0.55	1.00		0.52
2.69	0.14	-10.92	-2.06	0.00	0.01	**	1.00	2.58	0.07	2.68	0.27	-3.63	-0.36	0.23	1.00		0.02 *
2.44	0.20	-5.86	-0.70	0.11	0.64		1.00	2.42	0.21	2.46	0.17	-1.71	-0.25	0.57	1.00		0.38
4.53	0.35	-11.14	-1.44	0.00	0.00	**	1.00	4.28	0.25	4.67	0.32	-8.38	-1.22	0.00	0.02	*	0.99

1.46	0.11	-11.11	-1.42	0.00	0.00 **	1.00	1.36	0.08	1.51	0.12	-9.49	-1.24	0.00	0.01 **	1.00
1.38	0.09	-10.88	-1.67	0.00	0.00 **	1.00	1.30	0.07	1.40	0.10	-7.55	-1.03	0.01	0.03 *	0.12
1.70	0.16	-11.37	-1.23	0.00	0.01 **	1.00	1.62	0.11	1.77	0.12	-8.10	-1.15	0.00	0.05 *	1.00
0.90	0.11	1.13	0.09	0.81	1.00	0.33	0.91	0.03	0.89	0.05	2.38	0.44	0.21	1.00	0.07 -
0.90	0.11	1.13	0.09	0.81	1.00	0.33	0.91	0.03	0.89	0.05	2.38	0.44	0.21	1.00	0.07 -
9.34	0.83	-8.04	-0.91	0.04	0.14	0.20	9.24	0.74	9.71	0.61	-4.90	-0.79	0.08	0.76	0.01 **
2.46	0.15	-11.25	-1.80	0.01	0.01 *	1.00	2.39	0.13	2.54	0.19	-5.79	-0.76	0.03	0.37	0.01 **
6.89	0.69	-6.90	-0.69	0.08	0.35	0.17	6.85	0.65	7.18	0.46	-4.59	-0.71	0.13	1.00	0.03 *
13.11	0.89	-8.64	-1.28	0.01	0.02 *	1.00	12.99	0.52	13.45	0.65	-3.47	-0.71	0.05	0.72	0.22
7.32	0.45	-9.73	-1.58	0.00	0.00 **	1.00	7.08	0.30	7.50	0.36	-5.57	-1.16	0.00	0.04 *	1.00
0.63	0.06	-8.97	-0.88	0.02	0.04 *	1.00	0.61	0.02	0.63	0.04	-3.63	-0.64	0.06	1.00	1.00
6.69	0.40	-9.80	-1.65	0.00	0.01 **	1.00	6.47	0.30	6.87	0.34	-5.75	-1.17	0.00	0.04 *	1.00
5.78	0.46	-7.25	-0.91	0.04	0.15	0.40	5.91	0.27	5.95	0.33	-0.81	-0.14	0.69	1.00	0.01 *
6.71	0.39	0.86	0.15	0.70	1.00	0.06 -	6.66	0.20	6.75	0.39	-1.36	-0.24	0.47	1.00	0.08 -
6.45	0.47	-7.32	-1.00	0.03	0.05 -	0.53	6.01	0.36	6.60	0.38	-8.92	-1.54	0.00	0.00 **	1.00
3.30	0.27	-5.44	-0.68	0.10	0.38	0.12	3.16	0.19	3.36	0.21	-6.03	-0.96	0.02	0.14	0.54
1.72	0.14	-8.01	-0.99	0.02	0.06 -	1.00	1.56	0.09	1.77	0.11	-11.88	-1.84	0.00	0.00 **	1.00
1.43	0.08	-10.84	-1.95	0.00	0.00 **	1.00	1.30	0.09	1.47	0.09	-11.99	-1.98	0.00	0.00 **	1.00
2.25	0.11	-10.80	-2.12	0.00	0.00 **	1.00	2.15	0.07	2.24	0.19	-3.82	-0.45	0.15	1.00	0.01 **
0.21	0.02	-9.96	-1.19	0.01	0.04 *	1.00	0.20	0.02	0.21	0.02	-5.59	-0.59	0.13	0.83	0.73
0.36	0.04	-11.75	-1.06	0.01	0.03 *	1.00	0.35	0.03	0.38	0.04	-6.51	-0.63	0.07	0.47	0.52
0.10	0.01	-17.44	-2.19	0.00	0.00 **	1.00	0.09	0.01	0.10	0.01	-7.06	-0.87	0.03	0.18	1.00
1.57	0.07	-10.27	-2.21	0.00	0.01 **	1.00	1.50	0.05	1.54	0.14	-2.71	-0.29	0.34	1.00	0.01 *
2.43	0.19	-15.00	-1.87	0.00	0.00 **	1.00	2.23	0.08	2.41	0.12	-7.43	-1.51	0.00	0.04 *	1.00
30.83	2.23	-7.51	-1.04	0.02	0.08 -	0.08 -	29.74	1.42	31.21	2.19	-4.72	-0.67	0.05	0.63	0.01 **
25.10	1.68	-7.92	-1.18	0.01	0.04 *	0.42	23.99	1.08	25.33	1.73	-5.30	-0.77	0.03	0.32	0.06 -
4.04	0.34	-9.85	-1.16	0.01	0.01 **	1.00	3.87	0.16	4.06	0.24	-4.64	-0.77	0.03	0.44	0.07 -
8.67	0.59	-5.09	-0.75	0.08	0.40	0.35	8.41	0.39	8.76	0.70	-3.94	-0.49	0.14	1.00	0.07 -
0.97	0.08	-10.52	-1.35	0.00	0.01 *	1.00	0.91	0.06	0.97	0.07	-6.22	-0.81	0.03	0.16	1.00
0.32	0.03	-13.49	-1.47	0.00	0.01 **	1.00	0.29	0.02	0.32	0.02	-9.92	-1.32	0.00	0.01 **	1.00
0.16	0.01	-11.59	-1.45	0.01	0.03 *	1.00	0.16	0.01	0.16	0.02	-3.48	-0.32	0.36	1.00	1.00
0.48	0.04	-8.13	-0.96	0.01	0.08 -	1.00	0.46	0.04	0.48	0.04	-4.65	-0.62	0.14	0.80	1.00
3.58	0.27	-11.04	-1.47	0.00	0.01 *	1.00	3.33	0.23	3.63	0.27	-8.21	-1.09	0.01	0.03 *	1.00
2.38	0.20	-10.20	-1.22	0.01	0.04 *	1.00	2.25	0.21	2.42	0.22	-7.06	-0.78	0.05	0.31	0.46
0.57	0.05	-12.19	-1.38	0.00	0.01 *	1.00	0.52	0.04	0.58	0.04	-11.24	-1.70	0.00	0.00 **	1.00
4.90	0.32	-6.95	-1.06	0.04	0.20	0.08 -	4.69	0.22	4.91	0.30	-4.38	-0.71	0.05	1.00	0.01 *
5.73	0.72	-5.72	-0.46	0.25	1.00	0.08 -	5.75	0.55	5.88	0.55	-2.19	-0.24	0.55	1.00	0.00 **
2.76	0.17	-12.42	-1.96	0.00	0.00 **	1.00	2.65	0.15	2.84	0.20	-6.69	-0.96	0.01	0.11	0.04 *
9.35	0.51	-9.70	-1.77	0.00	0.01 **	1.00	8.90	0.17	9.47	0.97	-5.92	-0.58	0.06	0.33	0.07 -
2.16	0.14	-11.41	-1.80	0.00	0.00 **	1.00	2.00	0.10	2.16	0.23	-7.10	-0.65	0.05	0.31	0.86
1.88	0.13	-9.00	-1.31	0.00	0.01 *	1.00	1.80	0.05	1.93	0.21	-6.55	-0.61	0.05	0.21	0.50
1.78	0.12	-5.26	-0.76	0.11	0.81	0.77	1.77	0.06	1.79	0.20	-1.33	-0.12	0.69	1.00	0.04 *
2.61	0.15	-12.42	-2.21	0.00	0.00 **	1.00	2.43	0.08	2.68	0.27	-9.20	-0.91	0.01	0.02 *	0.44
0.91	0.06	-7.90	-1.24	0.03	0.24	0.77	0.90	0.06	0.91	0.10	-1.23	-0.12	0.73	1.00	0.01 **
38.15	2.01	-14.63	-2.78	0.00	0.00 **	0.54	34.71	1.99	38.99	2.37	-10.99	-1.81	0.00	0.00 **	1.00
9.45	0.46	-14.04	-2.90	0.00	0.00 **	1.00	8.78	0.48	9.73	0.57	-9.77	-1.67	0.00	0.00 **	1.00
4.45	0.20	-11.66	-2.63	0.00	0.00 **	1.00	4.21	0.21	4.56	0.28	-7.81	-1.27	0.00	0.01 **	1.00
1.12	0.09	-16.07	-2.11	0.00	0.00 **	1.00	1.10	0.10	1.24	0.09	-11.39	-1.59	0.00	0.00 **	1.00
1.12	0.09	-16.07	-2.11	0.00	0.00 **	1.00	1.10	0.10	1.24	0.09	-11.39	-1.59	0.00	0.00 **	1.00
2.76	0.19	-17.74	-2.62	0.00	0.00 **	1.00	2.43	0.17	2.80	0.20	-13.18	-1.88	0.00	0.00 **	1.00
1.13	0.05	-12.39	-2.67	0.00	0.00 **	1.00	1.04	0.04	1.13	0.06	-7.41	-1.47	0.00	0.00 **	1.00
1.13	0.05	-12.39	-2.67	0.00	0.00 **	1.00	1.04	0.04	1.13	0.06	-7.41	-1.47	0.00	0.00 **	1.00
28.70	1.57	-14.82	-2.70	0.00	0.00 **	0.52	25.93	1.56	29.26	1.83	-11.39	-1.82	0.00	0.00 **	1.00
6.58	0.30	-11.60	-2.52	0.00	0.00 **	1.00	6.05	0.24	6.63	0.37	-8.74	-1.56	0.00	0.00 **	1.00
0.12	0.01	-8.36	-1.01	0.02	0.09 -	0.42	0.12	0.01	0.13	0.01	-5.52	-0.80	0.04	0.47	0.27
3.52	0.18	-14.41	-2.79	0.00	0.00 **	1.00	3.16	0.21	3.59	0.21	-11.99	-2.09	0.00	0.00 **	1.00
2.94	0.30	-8.37	-0.83	0.04	0.15	1.00	2.77	0.25	2.91	0.29	-4.85	-0.50	0.19	1.00	1.00
2.75	0.17	-18.73	-2.96	0.00	0.00 **	0.08 -	2.48	0.20	2.86	0.19	-13.49	-2.04	0.00	0.00 **	0.38
18.46	1.27	-15.57	-2.25	0.00	0.00 **	1.00	16.49	1.27	18.81	1.43	-12.36	-1.62	0.00	0.00 **	1.00
18.46	1.27	-15.57	-2.25	0.00	0.00 **	1.00	16.49	1.27	18.81	1.43	-12.36	-1.62	0.00	0.00 **	1.00
0.90	0.05	-11.03	-2.09	0.00	0.00 **	1.00	0.91	0.07	0.96	0.05	-4.51	-0.86	0.08	0.58	1.00
0.90	0.05	-11.03	-2.09	0.00	0.00 **	1.00	0.91	0.07	0.96	0.05	-4.51	-0.86	0.08	0.58	1.00
92.17	4.05	-10.33	-2.35	0.00	0.00 **	1.00	86.64	4.56	94.68	4.88	-8.49	-1.65	0.00	0.00 **	1.00
26.53	1.66	-10.41	-1.66	0.00	0.00 **	1.00	25.36	1.73	27.88	1.88	-9.04	-1.34	0.00	0.00 **	1.00
11.70	0.69	-8.70	-1.48	0.00	0.01 *	0.45	11.25	0.73	12.28	0.92	-8.44	-1.13	0.00	0.01 *	0.27
4.71	0.22	-8.47	-1.81	0.00	0.01 *	1.00	4.44	0.20	4.85	0.36	-8.35	-1.14	0.00	0.01 **	0.76
6.98	0.50	-8.86	-1.23	0.01	0.04 *	0.17	6.80	0.55	7.44	0.59	-8.49	-1.08	0.01	0.03 *	0.38
0.24	0.01	-10.49	-1.71	0.00	0.00 **	1.00	0.23	0.02	0.25	0.02	-8.14	-1.33	0.00	0.01 **	1.00
0.24	0.01	-10.49	-1.71	0.00	0.00 **	1.00	0.23	0.02	0.25	0.02	-8.14	-1.33	0.00	0.01 **	1.00
0.24	0.01	-10.49	-1.71	0.00	0.00 **	1.00	0.23	0.02	0.25	0.02	-8.14	-1.33	0.00	0.01 **	1.00
11.27	0.78	-11.83	-1.71	0.00	0.00 **	1.00	10.70	0.78	11.79	0.78	-9.25	-1.40	0.00	0.00 **	1.00
3.33	0.20	-11.57	-1.88	0.00	0.00 **	1.00	3.18	0.24	3.55	0.21	-10.49	-1.81	0.00	0.00 **	1.00
3.33	0.20	-11.57	-1.88	0.00	0.00 **	1.00	3.18	0.24	3.55	0.21	-10.49	-1.81	0.00	0.00 **	1.00
40.79	1.57	-9.33	-2.42	0.00	0.00 **	1.00	37.82	1.77	41.18	2.01	-8.16	-1.67	0.00	0.00 **	1.00
24.58	1.05	-7.32	-1.71	0.01	0.04 *	1.00	22.83	1.07	24.76	1.37	-7.80	-1.41	0.00	0.00 **	1.00
0.26	0.05	-13.30	-0.76	0.08	0.16	1.00	0.22	0.03	0.24	0.04	-7.41	-0.46	0.19	0.65	1.00
0.26	0.05	-13.30	-0.76	0.08	0.16	1.00	0.22	0.03	0.24	0.04	-7.41	-0.46	0.19	0.65	1.00
0.26	0.05	-13.30	-0.76	0.08	0.16	1.00	0.22	0.03	0.24	0.04	-7.41	-0.46	0.19	0.65	1.00
0.31	0.03	-13.30	-1.59	0.09	0.14	1.00	0.32	0.03	0.32	0.03	-0.66	-0.07	0.85	1.00	1.00
0.31	0.03	-13.30	-1.59	0.09	0.14	1.00	0.32	0.03	0.32	0.03	-0.66	-0.07	0.85	1.00	1.00
24.01	1.01	-7.18	-1.71	0.02	0.06 -	1.00	22.29	1.04	24.20	1.33	-7.89	-1.43	0.00	0.00 **	1.00
16.21	0.65	-12.37	-3.08	0.00	0.00 **	1.00	14.99	0.80	16.42	0.76	-8.71	-1.90	0.00	0.00 **	1.00
14.81	0.62	-12.40	-2.94	0.00	0.00 **	1.00	13.72	0.76	15.08	0.69	-9.02	-1.97	0.00	0.00 **	1.00
0.73	0.05	-12.61	-1.72	0.00	0.00 **	1.00	0.65	0.04	0.70	0.06	-7.00	-0.85	0.02	0.15	1.00
0.73	0.05	-12.61	-1.72	0.00	0.00 **	1.00	0.65	0.04	0.70	0.06	-7.00	-0.85	0.02	0.15	1.00
0.67	0.04	-11.41	-1.76	0.00	0.00 **	1.00	0.62	0.03	0.64	0.05	-3.34	-0.40	0.24	1.00	0.86
0.67	0.04	-11.41	-1.76	0.00	0.00 **	1.00	0.62	0.03	0.64	0.05	-3.34	-0.40	0.24	1.00	0.86
24.85	1.57	-11.90	-1.89	0.00	0.00 **	1.00	23.46	1.49	25.62	1.46	-8.42	-1.47	0.00	0.00 **	1.00
9.65	0.46	-12.96	-2.72	0.00	0.00 **	1.00	9.17	0.47	9.90	0.48	-7.36	-1.52	0.00	0.00 **	1.00
9.06	0.44	-13.00	-2.66	0.00	0.00 **	1.00	8.61	0.45	9.32	0.46	-7.55	-1.54	0.00	0.00 **	1.00
0.60	0.04	-12.40	-1.96	0.00	0.00 **	1.00	0.56	0.04	0.58	0.04	-4.22	-0.70	0.09	0.62	1.00
0.45	0.03	-12.27	-1.67	0.00	0.01 *	1.00	0.42	0.03	0.43	0.03	-4.14	-0.52	0.18	1.00	1.00
0.14	0.01	-12.82	-1.93	0.00	0.00 **	1.00	0.14	0.01	0.15	0.01	-4.43	-0.53	0.15	0.89	1.00
15.20	1.18	-11.22	-1.45	0.00	0.01 **	1.00	14.29	1.12	15.72	1.07	-9.10	-1.34	0.00	0.00 **	1.00
42.61	2.10	-14.40	-2.92	0.00	0.00 **	1.00	37.69	1.70	43.07	1.66	-12.49	-3.24	0.00	0.00 **	0.07 -
41.50	2.06	-14.30	-2.88	0.00	0.00 **	1.00	36.68	1.65	41.92	1.63	-12.51	-3.22	0.00	0.00 **	0.08 -

18.11	0.86	-14.20	-3.01	0.00	0.00 **	1.00	15.95	0.67	18.40	0.79	-13.34	-3.10	0.00	0.00 **	0.01 *
1.71	0.17	-13.01	-1.32	0.00	0.01 **	1.00	1.58	0.15	1.78	0.19	-11.23	-1.06	0.01	0.05 *	1.00
1.95	0.14	-15.06	-2.09	0.01	0.03 *	1.00	1.74	0.20	2.11	0.17	-17.53	-2.24	0.00	0.00 **	0.23
5.39	0.26	-14.00	-2.89	0.00	0.00 **	1.00	4.75	0.20	5.65	0.26	-15.97	-3.52	0.00	0.00 **	0.00 **
3.88	0.23	-14.25	-2.42	0.00	0.00 **	1.00	3.35	0.13	4.03	0.18	-16.93	-3.78	0.00	0.00 **	0.00 **
1.52	0.07	-13.35	-2.94	0.00	0.00 **	1.00	1.40	0.09	1.62	0.10	-13.58	-2.16	0.00	0.00 **	0.32
2.45	0.22	-13.72	-1.55	0.02	0.02 *	1.00	2.15	0.16	2.37	0.16	-9.42	-1.37	0.00	0.01 **	1.00
0.95	0.14	-18.07	-1.23	0.03	0.04 *	1.00	0.80	0.11	0.90	0.11	-11.11	-0.95	0.02	0.06 -	1.00
1.58	0.11	-22.90	-3.37	0.00	0.00 **	1.00	1.30	0.11	1.54	0.12	-15.95	-1.97	0.00	0.00 **	0.26
2.76	0.14	-12.37	-2.40	0.00	0.00 **	1.00	2.40	0.17	2.72	0.15	-11.71	-2.11	0.00	0.00 **	0.71
1.31	0.08	-6.76	-1.13	0.04	0.16	1.00	1.23	0.07	1.32	0.06	-7.04	-1.44	0.00	0.04 *	1.00
23.40	1.26	-14.38	-2.67	0.00	0.00 **	1.00	20.73	1.05	23.52	0.87	-11.86	-3.19	0.00	0.00 **	0.53
4.63	0.29	-9.77	-1.57	0.00	0.03 *	1.00	4.32	0.21	4.64	0.20	-6.90	-1.62	0.00	0.04 *	1.00
8.09	0.48	-17.46	-2.94	0.00	0.00 **	0.99	6.88	0.37	8.11	0.39	-15.19	-3.18	0.00	0.00 **	0.07 -
4.27	0.25	-18.47	-3.18	0.00	0.00 **	0.08 -	3.62	0.19	4.29	0.21	-15.68	-3.23	0.00	0.00 **	0.01 *
3.82	0.25	-16.34	-2.52	0.00	0.00 **	1.00	3.26	0.20	3.82	0.19	-14.64	-2.90	0.00	0.00 **	0.62
3.98	0.31	-12.90	-1.67	0.00	0.00 **	1.00	3.47	0.13	3.97	0.22	-12.69	-2.30	0.00	0.00 **	0.07 -
2.40	0.17	-16.61	-2.31	0.00	0.00 **	1.00	2.12	0.15	2.33	0.14	-9.07	-1.47	0.00	0.01 **	1.00
0.94	0.06	-14.12	-2.31	0.00	0.00 **	1.00	0.84	0.06	0.96	0.06	-13.29	-2.14	0.00	0.00 **	0.99
3.36	0.34	-13.53	-1.33	0.01	0.01 *	1.00	3.11	0.33	3.50	0.31	-11.27	-1.27	0.00	0.03 *	1.00
1.11	0.07	-18.02	-2.73	0.00	0.00 **	1.00	1.01	0.08	1.15	0.05	-11.82	-2.50	0.00	0.00 **	1.00
0.31	0.02	-18.00	-2.47	0.00	0.00 **	1.00	0.28	0.02	0.32	0.02	-11.57	-2.35	0.00	0.00 **	1.00
0.39	0.03	-17.52	-2.55	0.00	0.00 **	1.00	0.36	0.03	0.41	0.02	-12.26	-2.34	0.00	0.00 **	1.00
0.40	0.03	-18.52	-2.93	0.00	0.00 **	0.91	0.37	0.03	0.42	0.02	-11.57	-2.39	0.00	0.00 **	1.00
39.75	1.93	-16.51	-3.40	0.00	0.00 **	0.78	35.52	1.85	41.01	2.26	-13.40	-2.43	0.00	0.00 **	0.00 **
6.11	0.25	-13.49	-3.24	0.00	0.00 **	1.00	5.70	0.26	6.33	0.31	-9.91	-2.03	0.00	0.00 **	0.87
2.23	0.10	-11.83	-2.62	0.00	0.00 **	1.00	2.10	0.10	2.34	0.13	-10.22	-1.86	0.00	0.00 **	1.00
0.93	0.06	-15.05	-2.22	0.00	0.00 **	1.00	0.84	0.05	0.97	0.06	-13.78	-2.29	0.00	0.00 **	0.03 *
1.30	0.04	-9.54	-2.83	0.00	0.01 **	1.00	1.26	0.06	1.36	0.08	-7.68	-1.35	0.00	0.03 *	1.00
0.20	0.01	-19.03	-4.10	0.00	0.00 **	0.33	0.18	0.01	0.20	0.01	-11.66	-2.23	0.00	0.00 **	0.06 -
2.27	0.10	-14.98	-3.39	0.00	0.00 **	1.00	2.10	0.10	2.30	0.12	-8.82	-1.68	0.00	0.00 **	1.00
2.27	0.10	-14.98	-3.39	0.00	0.00 **	1.00	2.10	0.10	2.30	0.12	-8.82	-1.68	0.00	0.00 **	1.00
2.27	0.10	-14.98	-3.39	0.00	0.00 **	1.00	2.10	0.10	2.30	0.12	-8.82	-1.68	0.00	0.00 **	1.00
1.29	0.07	-12.45	-2.29	0.00	0.00 **	1.00	1.22	0.08	1.36	0.08	-10.28	-1.79	0.00	0.00 **	1.00
1.29	0.07	-12.45	-2.29	0.00	0.00 **	1.00	1.22	0.08	1.36	0.08	-10.28	-1.79	0.00	0.00 **	1.00
0.12	0.01	-18.04	-1.84	0.00	0.00 **	1.00	0.10	0.01	0.13	0.01	-17.36	-2.12	0.00	0.00 **	0.13
0.12	0.01	-18.04	-1.84	0.00	0.00 **	1.00	0.10	0.01	0.13	0.01	-17.36	-2.12	0.00	0.00 **	0.13
6.24	0.41	-19.05	-2.87	0.00	0.00 **	0.20	5.53	0.40	6.53	0.46	-15.34	-2.18	0.00	0.00 **	0.04 *
5.18	0.35	-19.94	-2.98	0.00	0.00 **	0.16	4.56	0.34	5.44	0.40	-16.08	-2.19	0.00	0.00 **	0.04 *
0.35	0.02	-16.83	-3.03	0.00	0.00 **	1.00	0.32	0.02	0.37	0.02	-13.51	-2.39	0.00	0.00 **	0.19
3.30	0.24	-20.94	-2.83	0.00	0.00 **	0.17	2.89	0.25	3.47	0.29	-16.71	-2.03	0.00	0.00 **	0.08 -
2.73	0.20	-21.22	-2.85	0.00	0.00 **	0.26	2.38	0.21	2.87	0.26	-17.04	-1.88	0.00	0.00 **	0.14
0.57	0.05	-19.60	-2.43	0.00	0.00 **	0.12	0.51	0.04	0.60	0.04	-15.17	-2.33	0.00	0.00 **	0.03 *
0.75	0.05	-16.49	-2.43	0.00	0.00 **	1.00	0.68	0.05	0.78	0.06	-12.65	-1.79	0.00	0.00 **	1.00
0.79	0.05	-20.45	-3.22	0.00	0.00 **	0.36	0.68	0.04	0.82	0.08	-17.79	-1.75	0.00	0.00 **	0.03 *
1.05	0.07	-14.65	-2.17	0.00	0.00 **	1.00	0.97	0.06	1.09	0.07	-11.65	-1.85	0.00	0.00 **	0.34
0.83	0.05	-14.17	-2.27	0.00	0.00 **	1.00	0.76	0.04	0.86	0.05	-11.15	-1.91	0.00	0.00 **	0.29
0.21	0.02	-13.01	-1.56	0.00	0.00 **	1.00	0.19	0.01	0.22	0.01	-11.82	-1.86	0.00	0.00 **	0.71
0.03	0.00	-32.93	-2.13	0.00	0.00 **	0.01 *	0.02	0.00	0.03	0.00	-23.14	-2.26	0.00	0.00 **	0.00 **
0.59	0.04	-13.66	-2.06	0.00	0.00 **	1.00	0.55	0.03	0.61	0.04	-10.37	-1.66	0.00	0.00 **	1.00
0.23	0.02	-16.40	-1.70	0.00	0.00 **	1.00	0.21	0.02	0.24	0.02	-13.47	-1.59	0.00	0.00 **	1.00
0.23	0.02	-16.40	-1.70	0.00	0.00 **	1.00	0.21	0.02	0.24	0.02	-13.47	-1.59	0.00	0.00 **	1.00
10.33	0.46	-16.80	-3.76	0.00	0.00 **	1.00	9.12	0.45	10.49	0.46	-13.02	-2.94	0.00	0.00 **	0.01 *
2.72	0.12	-16.48	-3.70	0.00	0.00 **	0.60	2.40	0.11	2.74	0.15	-12.26	-2.30	0.00	0.00 **	0.02 *
0.74	0.04	-17.79	-3.23	0.00	0.00 **	0.59	0.65	0.04	0.74	0.04	-13.37	-2.27	0.00	0.00 **	0.04 *
1.09	0.06	-17.49	-3.08	0.00	0.00 **	0.97	0.94	0.06	1.08	0.07	-13.00	-1.88	0.00	0.00 **	0.07 -
0.89	0.06	-14.13	-2.06	0.00	0.00 **	1.00	0.82	0.06	0.92	0.07	-10.50	-1.48	0.00	0.00 **	1.00
7.61	0.36	-16.92	-3.57	0.00	0.00 **	1.00	6.72	0.35	7.75	0.33	-13.29	-3.09	0.00	0.00 **	0.03 *
3.54	0.19	-13.39	-2.51	0.00	0.00 **	1.00	3.25	0.20	3.64	0.16	-10.54	-2.35	0.00	0.00 **	1.00
0.08	0.01	-19.05	-1.52	0.00	0.02 *	1.00	0.07	0.01	0.08	0.01	-16.28	-1.03	0.01	0.08 -	1.00
0.18	0.02	-27.62	-2.88	0.00	0.00 **	1.00	0.15	0.02	0.19	0.02	-20.65	-2.43	0.00	0.00 **	1.00
0.13	0.01	-19.19	-2.72	0.00	0.00 **	1.00	0.11	0.01	0.13	0.01	-14.11	-1.55	0.00	0.00 **	0.80
0.48	0.03	-22.88	-3.99	0.00	0.00 **	1.00	0.40	0.02	0.50	0.03	-19.58	-3.47	0.00	0.00 **	0.00 **
0.62	0.05	-18.08	-2.21	0.02	0.01 **	1.00	0.53	0.05	0.60	0.04	-12.12	-1.81	0.00	0.00 **	0.75
0.14	0.01	-24.00	-4.12	0.00	0.00 **	1.00	0.11	0.01	0.14	0.01	-18.06	-2.62	0.00	0.00 **	0.39
0.10	0.01	-24.54	-3.40	0.00	0.00 **	0.36	0.08	0.01	0.10	0.01	-25.14	-3.50	0.00	0.00 **	0.00 **
0.27	0.01	-19.11	-5.58	0.00	0.00 **	1.00	0.23	0.02	0.27	0.01	-15.44	-3.30	0.00	0.00 **	0.07 -
0.07	0.01	-16.04	-2.32	0.01	0.03 *	1.00	0.07	0.01	0.08	0.01	-8.20	-0.77	0.03	0.32	1.00
0.08	0.01	-20.70	-3.15	0.00	0.00 **	1.00	0.07	0.01	0.09	0.01	-19.79	-2.51	0.00	0.00 **	0.07 -
0.34	0.02	-21.75	-3.57	0.00	0.00 **	1.00	0.30	0.02	0.34	0.02	-11.63	-1.94	0.00	0.00 **	1.00
0.35	0.02	-24.70	-4.11	0.00	0.00 **	1.00	0.28	0.02	0.35	0.02	-20.24	-4.23	0.00	0.00 **	0.00 **
0.13	0.01	-18.13	-2.72	0.00	0.00 **	1.00	0.12	0.01	0.13	0.01	-9.98	-1.41	0.00	0.01 **	1.00
0.25	0.02	-19.21	-2.35	0.01	0.00 **	1.00	0.20	0.01	0.26	0.01	-23.52	-4.46	0.00	0.00 **	0.00 **
0.13	0.01	-17.55	-1.54	0.02	0.03 *	1.00	0.10	0.01	0.13	0.01	-21.95	-2.24	0.00	0.00 **	0.01 **
0.30	0.02	-13.85	-2.12	0.01	0.02 *	1.00	0.28	0.02	0.30	0.02	-7.09	-1.15	0.00	0.08 -	1.00
0.07	0.00	-15.96	-2.57	0.01	0.02 *	1.00	0.06	0.00	0.07	0.00	-11.21	-1.80	0.00	0.00 **	1.00
0.28	0.02	-16.42	-1.91	0.01	0.02 *	1.00	0.25	0.03	0.29	0.03	-13.92	-1.60	0.00	0.00 **	1.00
0.06	0.00	-15.69	-2.15	0.00	0.02 *	1.00	0.05	0.00	0.06	0.01	-11.09	-0.93	0.01	0.03 *	1.00
16.96	0.93	-16.52	-3.01	0.00	0.00 **	1.00	15.06	0.84	17.55	1.16	-14.19	-2.15	0.00	0.00 **	0.01 *
6.03	0.33	-15.96	-2.94	0.00	0.00 **	1.00	5.48	0.30	6.11	0.35	-10.31	-1.78	0.00	0.00 **	1.00
1.86	0.10	-18.10	-3.32	0.00	0.00 **	0.06 -	1.63	0.08	1.89	0.11	-13.73	-2.37	0.00	0.00 **	0.01 **
1.58	0.08	-11.84	-2.42	0.01	0.02 *	1.00	1.53	0.08	1.57	0.10	-2.86	-0.46	0.21	1.00	0.08 -
2.58	0.19	-16.95	-2.31	0.00	0.00 **	1.00	2.33	0.17	2.65	0.19	-12.30	-1.72	0.00	0.00 **	1.00
10.93	0.64	-16.83	-2.88	0.00	0.00 **	1.00	9.58	0.57	11.44	0.84	-16.27	-2.22	0.00	0.00 **	0.00 **
0.11	0.01	-12.74	-1.59	0.00	0.00 **	1.00	0.11	0.01	0.12	0.01	-8.62	-1.45	0.00	0.02 *	1.00
0.11	0.01	-12.74	-1.59	0.00	0.00 **	1.00	0.11	0.01	0.12	0.01	-8.62	-1.45	0.00	0.02 *	1.00
0.11	0.01	-12.74	-1.59	0.00	0.00 **	1.00	0.11	0.01	0.12	0.01	-8.62	-1.45	0.00	0.02 *	1.00
5.83	0.35	-26.51	-4.36	0.00	0.00 **	0.08 -	4.91	0.46	5.99	0.50	-18.10	-2.16	0.00	0.00 **	0.27
0.43	0.03	-20.02	-2.52	0.00	0.00 **	1.00	0.41	0.04	0.43	0.04	-5.91	-0.69	0.11	0.80	1.00
0.76	0.04	-5.77	-1.18	0.16	0.54	1.00	0.74	0.04	0.78	0.04	-4.89	-1.00	0.02	0.36	1.00
3.43	0.33	-34.44	-3.61	0.00	0.00 **	0.10	2.68	0.45	3.58	0.52	-25.15	-1.72	0.00	0.00 **	0.32
3.38	0.33	-34.74	-3.61	0.00	0.00 **	0.10	2.64	0.45	3.53	0.52	-25.35	-1.72	0.00	0.00 **	0.32
0.05	0.00	-12.69	-1.42	0.01	0.01 **	1.00	0.05	0.00	0.05	0.00	-11.36	-1.43	0.00	0.01 *	1.00
1.21	0.10	-19.48	-2.41	0.00	0.00 **	0.47	1.07	0.06	1.19	0.05	-9.99	-2.24	0.00	0.00 **	1.00

Absolute Volumes Female									Relative Volume	Absolute Volumes Male								
GFSPF		SPF								GFSPF		GF						
Mean	SD	Mean	SD	%Diff	Effect	P-Value	FDR		FDR	Mean	SD	Mean	SD	%Diff	Effect	P-Value	FDR	
363.18	28.46	404.98	17.82	-10.32	-2.35	0.00	0.00	**	1.00	376.87	14.31	343.89	19.74	9.59	1.67	0.00	0.01	**
324.55	24.53	359.40	15.78	-9.70	-2.21	0.00	0.00	**	0.29	336.45	12.11	307.67	16.97	9.35	1.70	0.00	0.01	**
204.94	14.23	224.62	10.58	-8.76	-1.86	0.00	0.00	**	0.28	212.11	6.98	194.18	9.88	9.23	1.81	0.00	0.01	*
171.37	11.78	186.47	8.77	-8.10	-1.72	0.00	0.01	*	0.19	177.40	5.17	162.07	8.11	9.46	1.89	0.00	0.01	*
10.87	0.82	11.85	0.57	-8.28	-1.71	0.00	0.01	**	1.00	11.26	0.65	10.38	0.51	8.53	1.74	0.00	0.02	*
7.81	0.63	8.60	0.36	-9.10	-2.20	0.00	0.00	**	1.00	8.15	0.47	7.52	0.42	8.40	1.49	0.00	0.02	*
0.90	0.06	0.93	0.12	-2.99	-0.24	0.48	1.00		0.15	0.93	0.10	0.85	0.07	8.85	1.05	0.06	0.40	
0.28	0.02	0.30	0.03	-6.22	-0.67	0.07	0.78		0.88	0.29	0.03	0.27	0.02	4.96	0.76	0.18	1.00	
0.19	0.02	0.18	0.03	0.76	0.04	0.90	1.00		0.18	0.19	0.03	0.17	0.02	11.04	0.79	0.13	0.66	
0.43	0.03	0.44	0.06	-2.35	-0.18	0.59	1.00		0.13	0.45	0.05	0.41	0.04	10.53	1.20	0.03	0.25	
2.15	0.17	2.33	0.15	-7.36	-1.18	0.01	0.05	*	1.00	2.18	0.14	2.01	0.08	8.87	2.36	0.00	0.03	*
1.65	0.12	1.79	0.12	-7.95	-1.14	0.01	0.04	*	1.00	1.69	0.12	1.55	0.06	8.50	2.33	0.01	0.08	-
1.20	0.09	1.30	0.11	-7.74	-0.95	0.02	0.09	-	1.00	1.23	0.10	1.13	0.04	9.05	2.28	0.01	0.08	-
0.45	0.04	0.49	0.03	-8.49	-1.55	0.01	0.04	*	1.00	0.46	0.03	0.43	0.02	7.07	1.91	0.01	0.28	
0.50	0.06	0.53	0.05	-5.39	-0.56	0.20	0.85		1.00	0.50	0.03	0.45	0.03	10.15	1.37	0.00	0.02	*
160.50	11.04	174.62	8.28	-8.09	-1.71	0.00	0.01	*	0.19	166.14	4.67	151.70	7.69	9.52	1.88	0.00	0.01	*
33.04	2.50	35.68	1.46	-7.39	-1.81	0.00	0.03	*	1.00	33.85	1.03	31.79	1.70	6.48	1.21	0.00	0.16	
2.00	0.12	2.19	0.12	-8.88	-1.58	0.00	0.01	**	1.00	2.06	0.11	1.97	0.10	4.88	0.95	0.04	0.37	
0.91	0.08	1.00	0.06	-9.09	-1.62	0.00	0.01	*	1.00	0.92	0.05	0.84	0.06	9.47	1.40	0.00	0.02	*
9.65	1.09	10.67	0.78	-9.59	-1.31	0.01	0.01	*	1.00	9.82	0.42	8.89	0.56	10.36	1.66	0.00	0.01	**
0.69	0.11	0.77	0.06	-10.63	-1.42	0.02	0.05	*	1.00	0.72	0.05	0.66	0.11	7.85	0.49	0.15	0.55	
8.96	0.98	9.90	0.73	-9.51	-1.30	0.01	0.01	*	1.00	9.10	0.40	8.23	0.47	10.56	1.85	0.00	0.01	**
1.02	0.08	1.08	0.04	-6.02	-1.70	0.01	0.35		1.00	1.04	0.06	0.98	0.03	5.75	1.64	0.02	0.44	
0.90	0.07	0.97	0.04	-6.59	-1.61	0.01	0.30		1.00	0.92	0.06	0.87	0.03	5.65	1.70	0.03	0.50	
0.12	0.01	0.12	0.01	-1.41	-0.27	0.66	1.00		1.00	0.12	0.01	0.11	0.01	6.49	0.79	0.07	0.79	
1.63	0.13	1.80	0.08	-9.51	-2.06	0.00	0.00	**	1.00	1.76	0.08	1.64	0.10	7.06	1.20	0.01	0.22	
1.63	0.13	1.80	0.08	-9.51	-2.06	0.00	0.00	**	1.00	1.76	0.08	1.64	0.10	7.06	1.20	0.01	0.22	
0.70	0.06	0.77	0.04	-8.81	-1.78	0.00	0.01	*	1.00	0.75	0.04	0.70	0.05	7.02	0.98	0.02	0.41	
0.93	0.08	1.03	0.06	-10.02	-1.85	0.00	0.00	**	1.00	1.01	0.06	0.94	0.07	7.09	0.92	0.02	0.25	
0.38	0.03	0.39	0.02	-3.78	-0.76	0.13	1.00		1.00	0.39	0.03	0.33	0.02	17.88	2.53	0.00	0.00	**
14.79	1.06	15.80	0.48	-6.34	-2.08	0.00	0.25		0.29	15.17	0.46	14.52	0.98	4.47	0.66	0.05	1.00	
3.69	0.30	3.97	0.14	-6.99	-2.00	0.00	0.39		1.00	3.80	0.13	3.64	0.29	4.24	0.53	0.11	1.00	
5.58	0.41	5.86	0.24	-4.68	-1.12	0.04	0.67		0.02 *	5.66	0.17	5.39	0.36	5.03	0.76	0.03	1.00	
0.80	0.07	0.86	0.04	-6.41	-1.35	0.01	1.00		1.00	0.83	0.06	0.82	0.06	1.47	0.18	0.65	1.00	
0.72	0.07	0.79	0.04	-7.74	-1.41	0.01	0.93		1.00	0.75	0.06	0.72	0.06	3.78	0.49	0.26	1.00	
3.99	0.28	4.33	0.14	-7.73	-2.48	0.00	0.07	-	1.00	4.13	0.20	3.94	0.26	4.66	0.71	0.07	1.00	
0.68	0.05	0.72	0.04	-6.63	-1.14	0.01	0.21		1.00	0.70	0.03	0.70	0.04	0.19	0.04	0.93	1.00	
0.47	0.03	0.49	0.03	-2.75	-0.46	0.27	1.00		0.78	0.49	0.02	0.49	0.02	-0.72	-0.14	0.72	1.00	
0.20	0.02	0.24	0.01	-14.58	-2.36	0.00	0.00	**	1.00	0.21	0.01	0.21	0.01	2.34	0.39	0.37	1.00	
1.99	0.19	2.02	0.09	-1.24	-0.26	0.66	1.00		0.19	2.00	0.09	1.92	0.08	4.35	1.02	0.04	0.34	
32.23	2.51	37.12	1.19	-13.18	-4.10	0.00	0.00	**	0.00 **	33.73	1.07	31.27	1.97	7.86	1.25	0.00	0.02	*
14.93	1.15	16.89	0.55	-11.57	-3.52	0.00	0.00	**	0.45	15.50	0.53	14.39	0.88	7.72	1.26	0.00	0.04	*
4.61	0.40	5.18	0.19	-10.97	-2.97	0.00	0.00	**	1.00	4.86	0.16	4.53	0.30	7.27	1.10	0.00	0.09	-
1.91	0.18	2.12	0.08	-9.94	-2.55	0.00	0.01	**	1.00	2.02	0.11	1.88	0.15	7.74	0.94	0.02	0.20	
2.70	0.24	3.06	0.15	-11.69	-2.37	0.00	0.00	**	1.00	2.84	0.13	2.65	0.15	6.93	1.19	0.01	0.13	
10.32	0.77	11.71	0.45	-11.84	-3.05	0.00	0.00	**	0.31	10.64	0.46	9.86	0.61	7.92	1.29	0.00	0.04	*
4.97	0.42	5.77	0.24	-13.93	-3.36	0.00	0.00	**	0.04 *	5.14	0.26	4.77	0.33	7.91	1.15	0.01	0.08	-
4.75	0.33	5.27	0.27	-9.85	-1.94	0.00	0.00	**	1.00	4.86	0.24	4.51	0.29	7.79	1.21	0.01	0.08	-
1.53	0.11	1.71	0.09	-10.48	-1.96	0.00	0.00	**	1.00	1.53	0.09	1.46	0.09	5.04	0.78	0.09	0.66	
2.20	0.17	2.45	0.13	-9.94	-1.86	0.00	0.00	**	1.00	2.29	0.10	2.09	0.15	9.37	1.29	0.00	0.05	*
1.01	0.08	1.11	0.06	-8.69	-1.51	0.00	0.03	*	1.00	1.04	0.05	0.95	0.06	8.51	1.37	0.00	0.05	-
0.61	0.05	0.67	0.03	-9.46	-1.86	0.00	0.02	*	1.00	0.63	0.03	0.58	0.04	9.06	1.49	0.00	0.03	*
17.29	1.49	20.23	0.77	-14.53	-3.82	0.00	0.00	**	0.03 *	18.23	0.77	16.88	1.12	7.98	1.20	0.00	0.03	*
12.59	1.13	14.65	0.63	-14.08	-3.25	0.00	0.00	**	0.20	13.28	0.68	12.30	0.77	7.96	1.27	0.00	0.03	*
6.56	0.58	7.64	0.36	-14.06	-2.98	0.00	0.00	**	0.38	6.96	0.35	6.48	0.40	7.39	1.19	0.01	0.07	-
1.67	0.19	1.96	0.16	-15.22	-1.83	0.00	0.00	**	1.00	1.79	0.15	1.68	0.15	6.32	0.73	0.10	0.79	
1.94	0.15	2.24	0.09	-13.37	-3.19	0.00	0.00	**	0.19	2.04	0.09	1.89	0.11	7.95	1.36	0.00	0.03	*
2.10	0.17	2.43	0.09	-13.49	-3.53	0.00	0.00	**	0.19	2.21	0.08	2.05	0.11	7.76	1.48	0.00	0.03	*
0.85	0.08	1.00	0.05	-14.71	-3.21	0.00	0.00	**	1.00	0.91	0.05	0.85	0.06	7.34	1.08	0.01	0.15	
0.95	0.10	1.13	0.03	-16.10	-5.21	0.00	0.00	**	0.17	1.01	0.05	0.94	0.06	7.75	1.19	0.00	0.04	*
0.16	0.02	0.19	0.01	-16.07	-4.54	0.00	0.00	**	0.20	0.17	0.01	0.16	0.01	7.99	1.40	0.00	0.04	*
0.40	0.05	0.48	0.02	-17.26	-3.35	0.00	0.00	**	0.84	0.43	0.03	0.41	0.03	5.41	0.64	0.10	0.46	
0.38	0.04	0.45	0.02	-14.86	-3.05	0.00	0.00	**	0.30	0.40	0.02	0.36	0.02	10.30	1.55	0.00	0.05	*
5.08	0.47	5.89	0.27	-13.71	-3.03	0.00	0.00	**	1.00	5.32	0.33	4.89	0.34	8.75	1.27	0.01	0.04	*
0.89	0.08	1.03	0.06	-14.07	-2.60	0.00	0.00	**	1.00	0.93	0.06	0.87	0.06	7.64	1.03	0.02	0.14	
0.12	0.01	0.14	0.00	-15.29	-4.58	0.00	0.00	**	0.13	0.12	0.01	0.11	0.01	9.41	1.04	0.01	0.03	*
0.77	0.07	0.90	0.05	-13.88	-2.32	0.00	0.00	**	1.00	0.81	0.05	0.76	0.06	7.38	0.98	0.03	0.20	
2.15	0.22	2.56	0.12	-15.95	-3.52	0.00	0.00	**	0.42	2.25	0.15	2.07	0.15	8.59	1.18	0.01	0.16	
1.51	0.14	1.70	0.08	-11.02	-2.41	0.00	0.00	**	1.00	1.58	0.11	1.44	0.09	9.90	1.53	0.00	0.02	*
0.53	0.05	0.59	0.04	-11.07	-1.81	0.00	0.05	-	1.00	0.55	0.03	0.51	0.03	8.04	1.19	0.01	0.41	
4.71	0.38	5.58	0.19	-15.72	-4.67	0.00	0.00	**	0.01 **	4.95	0.17	4.58	0.39	8.04	0.94	0.01	0.08	-
3.27	0.26	3.84	0.13	-14.97	-4.47	0.00	0.00	**	0.02 *	3.43	0.12	3.18	0.26	7.90	0.96	0.01	0.08	-
1.44	0.12	1.74	0.06	-17.36	-4.86	0.00	0.00	**	0.00 **	1.51	0.05	1.40	0.13	8.36	0.88	0.01	0.09	-
0.98	0.08	1.18	0.04	-17.17	-4.92	0.00	0.00	**	0.00 **	1.03	0.03	0.96	0.09	8.20	0.86	0.01	0.10	-
0.46	0.04	0.56	0.02	-17.76	-4.53	0.00	0.00	**	0.01 *	0.48	0.02	0.44	0.04	8.69	0.92	0.01	0.08	-
95.24	6.51	101.82	6.17	-6.47	-1.07	0.01	0.14		0.03 *	98.56	3.38	88.64	4.53	11.20	2.19	0.00	0.01	**
4.29	0.34	4.59	0.33	-6.67	-0.94	0.03	0.30		1.00	4.46	0.28	4.02	0.28	11.01	1.58	0.00	0.01	*
2.46	0.20	2.71	0.17	-9.03	-1.41	0.00	0.07	-	1.00	2.57	0.19	2.38	0.16	8.11	1.23	0.02	0.08	-
1.70	0.17	1.91	0.14	-11.42	-1.54	0.00	0.03	*	1.00	1.77	0.15	1.65	0.13	7.44	0.92	0.05	0.25	
0.77	0.05	0.79	0.06	-3.25	-0.44	0.25	1.00		1.00	0.80	0.06	0.73	0.05	9.63	1.37	0.01	0.05	-
1.82	0.16	1.89	0.19	-3.29	-0.33	0.39	1.00		0.27	1.88	0.15	1.64	0.14	15.22	1.74	0.00	0.01	**
1.27	0.13	1.34	0.15	-5.00	-0.44	0.25	1.00		1.00	1.31	0.14	1.16	0.12	13.32	1.29	0.01	0.03	*
0.55	0.05	0.55	0.05	0.91	0.10	0.81	1.00		0.03 *	0.57	0.04	0.48	0.03	19.85	3.17	0.00	0.00	**
0.46	0.04	0.55	0.04	-15.58	-2.01	0.00	0.00	**	0.84	0.48	0.05	0.43	0.04	9.96	1.13	0.03	0.38	
5.24	0.42	5.59	0.22	-6.14	-1.56	0.01	0.20		0.51	5.45	0.15	4.86	0.36	12.00	1.61	0.00	0.02	*
2.76	0.20	2.90	0.11	-4.74	-1.28	0.04	0.67		0.68	2.86	0.13	2.60	0.21	10.02	1.26	0.00	0.05	*
0.61	0.05	0.67	0.04	-8.54	-1.34	0.00	0.07	-	1.00	0.64	0.04	0.58	0.05	11.61	1.23	0.00	0.06	-
0.36	0.06	0.39	0.02	-7.55	-1.72	0.07	0.78		1.00	0.37	0.04	0.35	0.04	5.70	0.51	0.22	1.00	
1.79	0.11	1.84	0.08	-2.78	-0.66	0.18	1.00		0.45	1.85	0.08	1.67	0.12	10.38	1.44	0.00	0.03	*
2.48	0.24	2.69	0.14	-7.65	-1.44	0.01	0.15		1.00	2.58	0.07	2.26	0.17	14.29	1.89	0.00	0.01	*
2.30	0.17	2.44	0.20	-5.69	-0.68	0.08	0.87		1.00	2.42	0.21	2.22	0.16	8.93	1.25	0.02	0.14	
4.17	0.30	4.53	0.35	-7.95	-1.02	0.01	0.07	-	1.00	4.28	0.25	3.86	0.25	11.10	1.72	0.00	0.03	*

1.32	0.12	1.46	0.11	-9.34	-1.19	0.01	0.03 *	1.00	1.36	0.08	1.24	0.08	9.88	1.53	0.00	0.07 -
1.27	0.10	1.38	0.09	-7.70	-1.18	0.01	0.05 *	1.00	1.30	0.07	1.17	0.08	10.82	1.66	0.00	0.03 *
1.58	0.10	1.70	0.16	-6.97	-0.75	0.04	0.30	0.58	1.62	0.11	1.44	0.10	12.36	1.73	0.00	0.03 *
0.94	0.10	0.90	0.11	3.70	0.30	0.45	1.00	0.19	0.91	0.03	0.85	0.03	6.26	1.60	0.00	0.25
0.94	0.10	0.90	0.11	3.70	0.30	0.45	1.00	0.19	0.91	0.03	0.85	0.03	6.26	1.60	0.00	0.25
8.91	0.61	9.34	0.83	-4.61	-0.52	0.16	1.00	0.05 *	9.24	0.74	8.24	0.64	12.14	1.57	0.00	0.03 *
2.26	0.21	2.46	0.15	-7.76	-1.24	0.01	0.23	0.63	2.39	0.13	2.08	0.16	14.80	1.95	0.00	0.01 **
6.65	0.46	6.89	0.69	-3.49	-0.35	0.32	1.00	0.05 *	6.85	0.65	6.16	0.50	11.24	1.37	0.01	0.08 -
12.48	1.00	13.11	0.89	-4.75	-0.70	0.11	0.69	0.18	12.99	0.52	11.43	0.59	13.60	2.63	0.00	0.00 **
6.83	0.64	7.32	0.45	-6.79	-1.10	0.03	0.14	1.00	7.08	0.30	6.23	0.31	13.64	2.78	0.00	0.00 **
0.60	0.05	0.63	0.06	-5.16	-0.51	0.18	0.85	0.77	0.61	0.02	0.54	0.03	11.48	2.06	0.00	0.01 *
6.23	0.59	6.69	0.40	-6.94	-1.17	0.02	0.14	1.00	6.47	0.30	5.69	0.29	13.85	2.73	0.00	0.00 **
5.66	0.43	5.78	0.46	-2.17	-0.27	0.49	1.00	0.03 *	5.91	0.27	5.20	0.29	13.54	2.39	0.00	0.01 **
6.66	0.35	6.71	0.39	-0.74	-0.13	0.74	1.00	0.29	6.66	0.20	6.39	0.21	4.15	1.28	0.01	0.71
5.87	0.35	6.45	0.47	-8.98	-1.23	0.00	0.02 *	1.00	6.01	0.36	5.76	0.33	4.37	0.76	0.11	0.83
3.11	0.21	3.30	0.27	-5.71	-0.71	0.06	0.41	0.45	3.16	0.19	3.07	0.16	2.88	0.55	0.27	1.00
1.52	0.10	1.72	0.14	-11.83	-1.46	0.00	0.00 **	1.00	1.56	0.09	1.47	0.09	6.15	1.04	0.03	0.41
1.25	0.08	1.43	0.08	-13.06	-2.35	0.00	0.00 **	1.00	1.30	0.09	1.22	0.10	5.99	0.75	0.08	0.40
2.05	0.19	2.25	0.11	-8.77	-1.72	0.00	0.05 *	1.00	2.15	0.07	1.90	0.12	12.96	2.07	0.00	0.01 *
0.19	0.02	0.21	0.02	-8.54	-1.02	0.03	0.17	1.00	0.20	0.02	0.17	0.02	17.79	1.63	0.00	0.01 *
0.33	0.04	0.36	0.04	-8.95	-0.81	0.05	0.24	1.00	0.35	0.03	0.30	0.04	16.34	1.30	0.00	0.02 *
0.09	0.01	0.10	0.01	-8.02	-1.01	0.04	0.65	0.77	0.09	0.01	0.08	0.01	17.08	1.73	0.00	0.01 **
1.44	0.13	1.57	0.07	-8.80	-1.89	0.00	0.05 -	1.00	1.50	0.05	1.35	0.07	11.34	2.32	0.00	0.04 *
2.17	0.16	2.43	0.19	-10.39	-1.30	0.00	0.02 *	1.00	2.23	0.08	1.97	0.15	13.66	1.80	0.00	0.01 **
28.57	2.18	30.83	2.23	-7.33	-1.01	0.02	0.15	0.27	29.74	1.42	26.43	1.51	12.50	2.19	0.00	0.02 *
22.98	1.82	25.10	1.68	-8.45	-1.26	0.01	0.04 *	1.00	23.99	1.08	21.35	1.16	12.34	2.27	0.00	0.01 *
3.71	0.22	4.04	0.34	-8.03	-0.94	0.01	0.06 -	1.00	3.87	0.16	3.44	0.17	12.38	2.49	0.00	0.01 **
8.07	0.59	8.67	0.59	-7.00	-1.03	0.02	0.13	1.00	8.41	0.39	7.63	0.41	10.34	1.90	0.00	0.04 *
0.88	0.09	0.97	0.08	-8.98	-1.15	0.01	0.07 -	1.00	0.91	0.06	0.78	0.07	16.85	1.88	0.00	0.00 **
0.28	0.03	0.32	0.03	-14.24	-1.55	0.00	0.01 **	1.00	0.29	0.02	0.25	0.03	15.97	1.48	0.00	0.01 **
0.15	0.02	0.16	0.01	-7.37	-0.92	0.04	0.53	1.00	0.16	0.01	0.13	0.01	18.70	2.11	0.00	0.01 **
0.45	0.05	0.48	0.04	-5.96	-0.71	0.11	0.51	1.00	0.46	0.04	0.39	0.04	16.79	1.88	0.00	0.01 **
3.16	0.35	3.58	0.27	-11.70	-1.56	0.00	0.01 *	1.00	3.33	0.23	2.85	0.25	16.76	1.88	0.00	0.00 **
2.13	0.24	2.38	0.20	-10.54	-1.26	0.01	0.06 -	1.00	2.25	0.21	1.91	0.19	18.04	1.79	0.00	0.01 **
0.50	0.04	0.57	0.05	-12.09	-1.37	0.00	0.02 *	1.00	0.52	0.04	0.46	0.03	13.31	2.16	0.00	0.01 *
4.54	0.38	4.90	0.32	-7.42	-1.13	0.01	0.21	0.45	4.69	0.22	4.29	0.23	9.46	1.74	0.00	0.17
5.59	0.52	5.73	0.72	-2.45	-0.20	0.59	1.00	0.03 *	5.75	0.55	5.08	0.49	13.16	1.36	0.01	0.11
2.55	0.24	2.76	0.17	-7.62	-1.20	0.02	0.14	1.00	2.65	0.15	2.32	0.19	14.46	1.80	0.00	0.01 **
8.56	0.73	9.35	0.51	-8.40	-1.53	0.00	0.04 *	1.00	8.90	0.17	7.95	0.39	11.98	2.46	0.00	0.03 *
1.92	0.21	2.16	0.14	-11.22	-1.77	0.00	0.01 *	1.00	2.00	0.10	1.76	0.10	13.94	2.39	0.00	0.04 *
1.75	0.14	1.88	0.13	-6.74	-0.98	0.02	0.18	1.00	1.80	0.05	1.62	0.10	11.21	1.75	0.00	0.05 *
1.69	0.14	1.78	0.12	-4.92	-0.71	0.10	1.00	1.00	1.77	0.06	1.60	0.08	10.59	2.17	0.00	0.08 -
2.35	0.21	2.61	0.15	-10.02	-1.78	0.00	0.01 **	1.00	2.43	0.08	2.18	0.13	11.75	1.92	0.00	0.04 *
0.84	0.09	0.91	0.06	-7.34	-1.16	0.03	0.44	1.00	0.90	0.06	0.80	0.05	12.62	1.89	0.00	0.05 -
33.57	2.64	38.15	2.01	-12.00	-2.28	0.00	0.00 **	1.00	34.71	1.99	32.11	1.86	8.09	1.40	0.01	0.06 -
8.35	0.67	9.45	0.46	-11.65	-2.40	0.00	0.00 **	1.00	8.78	0.48	8.14	0.49	7.89	1.31	0.01	0.05 -
4.02	0.31	4.45	0.20	-9.65	-2.18	0.00	0.00 **	1.00	4.21	0.21	3.93	0.23	6.95	1.18	0.01	0.14
0.98	0.10	1.12	0.09	-12.49	-1.64	0.00	0.00 **	1.00	1.10	0.10	0.99	0.08	11.27	1.38	0.01	0.03 *
0.98	0.10	1.12	0.09	-12.49	-1.64	0.00	0.00 **	1.00	1.10	0.10	0.99	0.08	11.27	1.38	0.01	0.03 *
2.34	0.25	2.76	0.19	-15.25	-2.25	0.00	0.00 **	1.00	2.43	0.17	2.23	0.16	9.09	1.29	0.01	0.08 -
1.02	0.06	1.13	0.05	-9.94	-2.14	0.00	0.00 **	1.00	1.04	0.04	0.99	0.07	5.52	0.84	0.03	0.20
1.02	0.06	1.13	0.05	-9.94	-2.14	0.00	0.00 **	1.00	1.04	0.04	0.99	0.07	5.52	0.84	0.03	0.20
25.22	1.98	28.70	1.57	-12.11	-2.21	0.00	0.00 **	1.00	25.93	1.56	23.97	1.38	8.15	1.42	0.01	0.07 -
5.84	0.33	6.58	0.30	-11.34	-2.46	0.00	0.00 **	1.00	6.05	0.24	5.68	0.36	6.43	1.03	0.01	0.17
0.11	0.01	0.12	0.01	-6.85	-0.83	0.04	0.35	0.45	0.12	0.01	0.11	0.01	6.54	1.20	0.02	0.52
3.05	0.19	3.52	0.18	-13.22	-2.56	0.00	0.00 **	0.99	3.16	0.21	3.00	0.17	5.40	0.95	0.06	0.53
2.67	0.26	2.94	0.30	-9.28	-0.92	0.02	0.13	1.00	2.77	0.25	2.57	0.31	7.64	0.63	0.11	0.51
2.35	0.20	2.75	0.17	-14.58	-2.31	0.00	0.00 **	0.84	2.48	0.20	2.24	0.17	10.52	1.40	0.01	0.03 *
16.20	1.54	18.46	1.27	-12.23	-1.77	0.00	0.00 **	1.00	16.49	1.27	15.21	0.95	8.45	1.35	0.02	0.14
16.20	1.54	18.46	1.27	-12.23	-1.77	0.00	0.00 **	1.00	16.49	1.27	15.21	0.95	8.45	1.35	0.02	0.14
0.83	0.10	0.90	0.05	-7.78	-1.47	0.02	0.07 -	1.00	0.91	0.07	0.84	0.06	8.21	1.24	0.02	0.10
0.83	0.10	0.90	0.05	-7.78	-1.47	0.02	0.07 -	1.00	0.91	0.07	0.84	0.06	8.21	1.24	0.02	0.10
82.95	7.65	92.17	4.05	-10.00	-2.28	0.00	0.00 **	1.00	86.64	4.56	79.91	4.60	8.43	1.46	0.00	0.02 *
24.05	2.33	26.53	1.66	-9.36	-1.49	0.00	0.01 *	1.00	25.36	1.73	23.38	1.48	8.47	1.34	0.01	0.07 -
10.71	1.06	11.70	0.69	-8.42	-1.43	0.01	0.03 *	1.00	11.25	0.73	10.39	0.65	8.27	1.32	0.01	0.12
4.29	0.40	4.71	0.22	-8.92	-1.91	0.00	0.02 *	1.00	4.44	0.20	4.04	0.26	10.03	1.55	0.00	0.03 *
6.42	0.67	6.98	0.50	-8.09	-1.12	0.02	0.13	0.38	6.80	0.55	6.35	0.42	7.15	1.07	0.05	0.35
0.21	0.02	0.24	0.01	-11.88	-1.93	0.00	0.00 **	1.00	0.23	0.02	0.21	0.02	9.72	1.27	0.01	0.03 *
0.21	0.02	0.24	0.01	-11.88	-1.93	0.00	0.00 **	1.00	0.23	0.02	0.21	0.02	9.72	1.27	0.01	0.03 *
0.21	0.02	0.24	0.01	-11.88	-1.93	0.00	0.00 **	1.00	0.23	0.02	0.21	0.02	9.72	1.27	0.01	0.03 *
10.08	0.98	11.27	0.78	-10.49	-1.51	0.00	0.01 **	1.00	10.70	0.78	9.88	0.66	8.32	1.25	0.02	0.07 -
3.04	0.29	3.33	0.20	-8.63	-1.40	0.01	0.02 *	1.00	3.18	0.24	2.90	0.19	9.61	1.46	0.01	0.03 *
3.04	0.29	3.33	0.20	-8.63	-1.40	0.01	0.02 *	1.00	3.18	0.24	2.90	0.19	9.61	1.46	0.01	0.03 *
36.48	3.41	40.79	1.57	-10.57	-2.75	0.00	0.00 **	0.84	37.82	1.77	35.08	1.98	7.82	1.38	0.00	0.02 *
22.15	2.15	24.58	1.05	-9.91	-2.32	0.00	0.01 **	1.00	22.83	1.07	21.32	1.26	7.06	1.19	0.01	0.04 *
0.23	0.03	0.26	0.05	-13.59	-0.78	0.03	0.20	1.00	0.22	0.03	0.21	0.03	5.79	0.49	0.30	1.00
0.23	0.03	0.26	0.05	-13.59	-0.78	0.03	0.20	1.00	0.22	0.03	0.21	0.03	5.79	0.49	0.30	1.00
0.23	0.03	0.26	0.05	-13.59	-0.78	0.03	0.20	1.00	0.22	0.03	0.21	0.03	5.79	0.49	0.30	1.00
0.30	0.02	0.31	0.03	-5.15	-0.61	0.13	1.00	1.00	0.32	0.03	0.30	0.04	5.26	0.43	0.25	1.00
0.30	0.02	0.31	0.03	-5.15	-0.61	0.13	1.00	1.00	0.32	0.03	0.30	0.04	5.26	0.43	0.25	1.00
21.62	2.11	24.01	1.01	-9.93	-2.36	0.00	0.01 **	1.00	22.29	1.04	20.81	1.22	7.10	1.21	0.01	0.04 *
14.33	1.29	16.21	0.65	-11.59	-2.89	0.00	0.00 **	0.82	14.99	0.80	13.76	0.76	8.99	1.62	0.00	0.01 **
13.09	1.19	14.81	0.62	-11.60	-2.75	0.00	0.00 **	0.84	13.72	0.76	12.60	0.69	8.95	1.63	0.00	0.01 **
0.64	0.08	0.73	0.05	-12.10	-1.65	0.00	0.01 **	1.00	0.65	0.04	0.59	0.06	10.48	0.98	0.01	0.08 -
0.64	0.08	0.73	0.05	-12.10	-1.65	0.00	0.01 **	1.00	0.65	0.04	0.59	0.06	10.48	0.98	0.01	0.08 -
0.59	0.04	0.67	0.04	-10.75	-1.66	0.00	0.00 **	1.00	0.62	0.03	0.57	0.04	8.52	1.29	0.00	0.07 -
0.59	0.04	0.67	0.04	-10.75	-1.66	0.00	0.00 **	1.00	0.62	0.03	0.57	0.04	8.52	1.29	0.00	0.07 -
22.42	2.03	24.85	1.57	-9.76	-1.55	0.00	0.01 *	1.00	23.46	1.49	21.45	1.32	9.40	1.53	0.00	0.02 *
8.76	0.64	9.65	0.46	-9.31	-1.96	0.00	0.00 **	1.00	9.17	0.47	8.37	0.47	9.62	1.69	0.00	0.01 **
8.21	0.59	9.06	0.44	-9.35	-1.92	0.00	0.00 **	1.00	8.61	0.45	7.86	0.45	9.50	1.66	0.00	0.01 **
0.54	0.06	0.60	0.04	-8.75	-1.38	0.01	0.05 *	1.00	0.56	0.04	0.50	0.04	11.50	1.62	0.00	0.01 *
0.42	0.06	0.45	0.03	-8.52	-1.16	0.04	0.23	1.00	0.42	0.03	0.37	0.04	11.33	1.04	0.01	0.08 -
0.13	0.01	0.14	0.01	-9.47	-1.43	0.01	0.07 -	1.00	0.14	0.01	0.13	0.01	12.00	1.31	0.00	0.03 *
13.67	1.46	15.20	1.18	-10.04	-1.29	0.01	0.03 *	1.00	14.29	1.12	13.08	0.92	9.26	1.32	0.01	0.06 -
36.66	3.50	42.61	2.10	-13.96	-2.84	0.00	0.00 **	0.88	37.69	1.70	33.58	3.26	12.23	1.26	0.00	0.00 **
35.71	3.42	41.50	2.06	-13.96	-2.81	0.00	0.00 **	0.88	36.68	1.65	32.69	3.19	12.21	1.25	0.00	0.01 **

15.47	1.54	18.11	0.86	-14.58	-3.09	0.00	0.00 **	0.33	15.95	0.67	14.09	1.31	13.16	1.42	0.00	0.00 **
1.56	0.20	1.71	0.17	-8.90	-0.90	0.05	0.18	1.00	1.58	0.15	1.34	0.09	17.71	2.61	0.00	0.04 *
1.57	0.27	1.95	0.14	-19.26	-2.67	0.00	0.01 **	0.78	1.74	0.20	1.45	0.15	19.93	1.94	0.00	0.01 **
4.59	0.46	5.39	0.26	-14.97	-3.09	0.00	0.00 **	0.25	4.75	0.20	4.31	0.36	10.23	1.23	0.00	0.01 *
3.24	0.33	3.88	0.23	-16.40	-2.79	0.00	0.00 **	0.08 -	3.35	0.13	3.09	0.27	8.49	0.98	0.01	0.05 *
1.34	0.16	1.52	0.07	-11.32	-2.50	0.00	0.01 **	1.00	1.40	0.09	1.22	0.10	14.66	1.81	0.00	0.01 **
2.18	0.27	2.45	0.22	-11.04	-1.25	0.01	0.14	1.00	2.15	0.16	1.93	0.24	11.60	0.93	0.02	0.03 *
0.79	0.14	0.95	0.14	-17.61	-1.20	0.01	0.07 -	1.00	0.80	0.11	0.69	0.10	15.42	1.07	0.03	0.08 -
1.24	0.20	1.58	0.11	-21.51	-3.17	0.00	0.00 **	1.00	1.30	0.11	1.09	0.16	18.65	1.28	0.00	0.01 **
2.36	0.29	2.76	0.14	-14.33	-2.79	0.00	0.00 **	1.00	2.40	0.17	2.20	0.24	9.36	0.85	0.03	0.11
1.17	0.10	1.31	0.08	-10.08	-1.68	0.00	0.02 *	1.00	1.23	0.07	1.08	0.12	13.53	1.26	0.00	0.01 **
20.24	1.90	23.40	1.26	-13.48	-2.50	0.00	0.00 **	1.00	20.73	1.05	18.60	1.95	11.49	1.09	0.00	0.01 **
4.12	0.46	4.63	0.29	-10.88	-1.75	0.00	0.02 *	1.00	4.32	0.21	3.74	0.39	15.56	1.49	0.00	0.00 **
6.84	0.58	8.09	0.48	-15.50	-2.61	0.00	0.00 **	1.00	6.88	0.37	6.25	0.73	10.06	0.86	0.02	0.05 -
3.55	0.31	4.27	0.25	-16.77	-2.89	0.00	0.00 **	0.11	3.62	0.19	3.21	0.37	12.74	1.10	0.00	0.01 **
3.29	0.29	3.82	0.25	-14.08	-2.18	0.00	0.01 **	1.00	3.26	0.20	3.04	0.36	7.24	0.61	0.09	0.43
3.50	0.42	3.98	0.31	-12.03	-1.56	0.00	0.02 *	1.00	3.47	0.13	3.13	0.40	10.74	0.84	0.01	0.02 *
2.12	0.25	2.40	0.17	-11.45	-1.59	0.00	0.02 *	1.00	2.12	0.15	1.84	0.19	15.34	1.49	0.00	0.01 **
0.80	0.09	0.94	0.06	-14.32	-2.34	0.00	0.00 **	1.00	0.84	0.06	0.75	0.08	10.84	1.00	0.02	0.04 *
2.85	0.33	3.36	0.34	-15.17	-1.49	0.00	0.01 **	1.00	3.11	0.33	2.88	0.34	7.81	0.66	0.13	0.79
0.95	0.10	1.11	0.07	-13.84	-2.10	0.00	0.00 **	1.00	1.01	0.08	0.89	0.09	13.10	1.32	0.00	0.01 **
0.27	0.03	0.31	0.02	-13.62	-1.87	0.00	0.00 **	1.00	0.28	0.02	0.25	0.02	12.26	1.24	0.00	0.01 **
0.34	0.04	0.39	0.03	-13.54	-1.97	0.00	0.00 **	1.00	0.36	0.03	0.32	0.03	12.23	1.21	0.01	0.02 *
0.35	0.04	0.40	0.03	-14.30	-2.26	0.00	0.00 **	1.00	0.37	0.03	0.32	0.03	14.60	1.47	0.00	0.01 **
33.96	3.43	39.75	1.93	-14.56	-3.00	0.00	0.00 **	1.00	35.52	1.85	32.02	2.43	10.92	1.44	0.00	0.01 **
5.45	0.47	6.11	0.25	-10.66	-2.56	0.00	0.00 **	1.00	5.70	0.26	5.27	0.34	8.15	1.25	0.00	0.02 *
2.02	0.16	2.23	0.10	-9.20	-2.04	0.00	0.03 *	1.00	2.10	0.10	1.97	0.13	6.53	0.96	0.02	0.18
0.81	0.08	0.93	0.06	-13.11	-1.93	0.00	0.00 **	1.00	0.84	0.05	0.78	0.06	7.33	0.98	0.02	0.11
1.22	0.08	1.30	0.04	-6.41	-1.90	0.00	0.24	1.00	1.26	0.06	1.19	0.08	6.01	0.87	0.03	0.43
0.17	0.02	0.20	0.01	-15.49	-3.34	0.00	0.00 **	1.00	0.18	0.01	0.16	0.01	9.89	1.41	0.00	0.01 *
2.02	0.20	2.27	0.10	-11.05	-2.50	0.00	0.02 *	1.00	2.10	0.10	1.91	0.13	9.87	1.49	0.00	0.01 **
2.02	0.20	2.27	0.10	-11.05	-2.50	0.00	0.02 *	1.00	2.10	0.10	1.91	0.13	9.87	1.49	0.00	0.01 **
2.02	0.20	2.27	0.10	-11.05	-2.50	0.00	0.02 *	1.00	2.10	0.10	1.91	0.13	9.87	1.49	0.00	0.01 **
1.14	0.11	1.29	0.07	-11.28	-2.07	0.00	0.00 **	1.00	1.22	0.08	1.13	0.09	7.63	0.95	0.03	0.09 -
1.14	0.11	1.29	0.07	-11.28	-2.07	0.00	0.00 **	1.00	1.22	0.08	1.13	0.09	7.63	0.95	0.03	0.09 -
0.10	0.01	0.12	0.01	-16.02	-1.63	0.00	0.00 **	1.00	0.10	0.01	0.09	0.01	10.05	0.94	0.05	0.18
0.10	0.01	0.12	0.01	-16.02	-1.63	0.00	0.00 **	1.00	0.10	0.01	0.09	0.01	10.05	0.94	0.05	0.18
5.20	0.58	6.24	0.41	-16.61	-2.51	0.00	0.00 **	0.41	5.53	0.40	4.92	0.42	12.49	1.46	0.00	0.01 *
4.28	0.50	5.18	0.35	-17.43	-2.60	0.00	0.00 **	0.31	4.56	0.34	4.03	0.36	13.13	1.47	0.00	0.01 *
0.30	0.04	0.35	0.02	-14.67	-2.64	0.00	0.00 **	1.00	0.32	0.02	0.29	0.03	9.33	0.95	0.02	0.05 *
2.69	0.33	3.30	0.24	-18.56	-2.51	0.00	0.00 **	0.29	2.89	0.25	2.53	0.25	14.00	1.41	0.00	0.02 *
2.21	0.28	2.73	0.20	-18.98	-2.55	0.00	0.00 **	0.33	2.38	0.21	2.08	0.22	14.56	1.39	0.00	0.03 *
0.48	0.05	0.57	0.05	-16.53	-2.05	0.00	0.00 **	0.45	0.51	0.04	0.46	0.04	11.47	1.45	0.01	0.02 *
0.64	0.07	0.75	0.05	-13.63	-2.01	0.00	0.00 **	1.00	0.68	0.05	0.61	0.04	12.20	1.88	0.00	0.02 *
0.65	0.07	0.79	0.05	-17.51	-2.76	0.00	0.00 **	0.84	0.68	0.04	0.60	0.06	12.24	1.23	0.00	0.05 *
0.92	0.09	1.05	0.07	-12.61	-1.87	0.00	0.00 **	1.00	0.97	0.06	0.88	0.06	9.54	1.35	0.00	0.02 *
0.73	0.07	0.83	0.05	-12.23	-1.96	0.00	0.00 **	1.00	0.76	0.04	0.70	0.05	8.77	1.30	0.01	0.02 *
0.19	0.02	0.21	0.02	-10.01	-1.20	0.00	0.01 *	1.00	0.19	0.01	0.18	0.01	6.99	0.90	0.05	0.18
0.02	0.00	0.03	0.00	-26.62	-1.72	0.00	0.00 **	0.03 *	0.02	0.00	0.02	0.00	14.81	0.87	0.03	0.14
0.52	0.05	0.59	0.04	-12.31	-1.86	0.00	0.00 **	1.00	0.55	0.03	0.50	0.03	9.19	1.38	0.00	0.02 *
0.20	0.02	0.23	0.02	-14.00	-1.45	0.00	0.00 **	1.00	0.21	0.02	0.18	0.02	12.51	1.41	0.01	0.02 *
0.20	0.02	0.23	0.02	-14.00	-1.45	0.00	0.00 **	1.00	0.21	0.02	0.18	0.02	12.51	1.41	0.01	0.02 *
8.80	0.82	10.33	0.46	-14.76	-3.30	0.00	0.00 **	1.00	9.12	0.45	8.09	0.72	12.72	1.42	0.00	0.00 **
2.32	0.21	2.72	0.12	-14.58	-3.27	0.00	0.00 **	0.84	2.40	0.11	2.15	0.17	11.61	1.44	0.00	0.00 **
0.62	0.05	0.74	0.04	-15.64	-2.84	0.00	0.00 **	0.88	0.65	0.04	0.58	0.05	11.73	1.31	0.00	0.01 **
0.92	0.10	1.09	0.06	-15.36	-2.70	0.00	0.00 **	1.00	0.94	0.06	0.83	0.08	12.61	1.26	0.00	0.01 **
0.77	0.08	0.89	0.06	-12.73	-1.85	0.00	0.00 **	1.00	0.82	0.06	0.75	0.06	10.41	1.32	0.01	0.03 *
6.48	0.61	7.61	0.36	-14.82	-3.13	0.00	0.00 **	1.00	6.72	0.35	5.94	0.56	13.12	1.39	0.00	0.00 **
3.12	0.30	3.54	0.19	-12.10	-2.27	0.00	0.00 **	1.00	3.25	0.20	2.88	0.26	12.81	1.42	0.00	0.00 **
0.07	0.01	0.08	0.01	-13.00	-1.04	0.02	0.30	1.00	0.07	0.01	0.06	0.01	19.84	1.75	0.00	0.30
0.13	0.03	0.18	0.02	-26.11	-2.73	0.00	0.01 **	1.00	0.15	0.02	0.13	0.02	19.12	1.55	0.01	0.25
0.11	0.01	0.13	0.01	-15.74	-2.23	0.00	0.00 **	1.00	0.11	0.01	0.10	0.01	16.14	1.84	0.00	0.01 *
0.38	0.05	0.48	0.03	-21.35	-3.73	0.00	0.00 **	1.00	0.40	0.02	0.36	0.04	10.47	1.02	0.01	0.08 -
0.54	0.06	0.62	0.05	-13.08	-1.60	0.00	0.15	1.00	0.53	0.05	0.47	0.05	12.77	1.13	0.01	0.03 *
0.11	0.02	0.14	0.01	-25.66	-4.41	0.00	0.00 **	1.00	0.11	0.01	0.09	0.03	24.36	0.83	0.02	0.02 *
0.08	0.01	0.10	0.01	-25.62	-3.55	0.00	0.00 **	0.14	0.08	0.01	0.07	0.01	11.05	0.72	0.05	0.26
0.22	0.03	0.27	0.01	-18.61	-5.43	0.00	0.00 **	1.00	0.23	0.02	0.20	0.02	14.15	1.24	0.01	0.01 *
0.07	0.01	0.07	0.01	-11.06	-1.60	0.01	0.38	0.88	0.07	0.01	0.06	0.01	24.39	1.87	0.00	0.01 **
0.07	0.01	0.08	0.01	-15.36	-2.34	0.00	0.03 *	1.00	0.07	0.01	0.06	0.01	17.27	1.61	0.00	0.02 *
0.28	0.04	0.34	0.02	-18.69	-3.07	0.00	0.00 **	1.00	0.30	0.02	0.25	0.04	18.66	1.28	0.00	0.01 **
0.27	0.04	0.35	0.02	-22.71	-3.78	0.00	0.00 **	1.00	0.28	0.02	0.24	0.04	16.20	1.10	0.00	0.01 **
0.13	0.01	0.13	0.01	-3.87	-0.58	0.23	1.00	1.00	0.12	0.01	0.11	0.02	9.92	0.64	0.05	0.10
0.20	0.02	0.25	0.02	-21.48	-2.62	0.00	0.00 **	1.00	0.20	0.01	0.19	0.03	4.66	0.27	0.39	1.00
0.10	0.02	0.13	0.01	-20.36	-1.78	0.00	0.01 *	1.00	0.10	0.01	0.09	0.02	10.54	0.52	0.10	0.41
0.29	0.03	0.30	0.02	-5.21	-0.80	0.15	1.00	0.68	0.28	0.02	0.25	0.03	11.83	0.86	0.01	0.02 *
0.06	0.01	0.07	0.00	-11.17	-1.80	0.00	0.25	1.00	0.06	0.00	0.05	0.01	16.31	1.29	0.00	0.01 **
0.23	0.03	0.28	0.02	-16.10	-1.88	0.00	0.03 *	1.00	0.25	0.03	0.23	0.03	7.07	0.54	0.18	1.00
0.05	0.01	0.06	0.00	-13.91	-1.90	0.00	0.07 -	1.00	0.05	0.00	0.04	0.01	17.01	0.94	0.01	0.03 *
14.40	1.59	16.96	0.93	-15.11	-2.76	0.00	0.00 **	1.00	15.06	0.84	13.64	1.02	10.39	1.39	0.00	0.02 *
5.28	0.57	6.03	0.33	-12.31	-2.26	0.00	0.00 **	1.00	5.48	0.30	4.94	0.35	10.91	1.53	0.00	0.01 **
1.57	0.15	1.86	0.10	-15.84	-2.91	0.00	0.00 **	0.12	1.63	0.08	1.48	0.13	9.90	1.17	0.00	0.01 *
1.50	0.18	1.58	0.08	-5.40	-1.10	0.11	1.00	0.35	1.53	0.08	1.36	0.10	12.24	1.66	0.00	0.00 **
2.22	0.26	2.58	0.19	-14.01	-1.91	0.00	0.00 **	1.00	2.33	0.17	2.10	0.14	10.76	1.60	0.00	0.03 *
9.11	1.02	10.93	0.64	-16.65	-2.85	0.00	0.00 **	0.31	9.58	0.57	8.70	0.67	10.09	1.30	0.00	0.04 *
0.10	0.01	0.11	0.01	-12.15	-1.52	0.00	0.01 *	1.00	0.11	0.01	0.10	0.01	7.34	0.89	0.07	0.29
0.10	0.01	0.11	0.01	-12.15	-1.52	0.00	0.01 *	1.00	0.11	0.01	0.10	0.01	7.34	0.89	0.07	0.29
0.10	0.01	0.11	0.01	-12.15	-1.52	0.00	0.01 *	1.00	0.11	0.01	0.10	0.01	7.34	0.89	0.07	0.29
4.67	0.80	5.83	0.35	-19.98	-3.28	0.00	0.00 **	0.50	4.91	0.46	4.20	0.47	16.91	1.50	0.00	0.04 *
0.42	0.08	0.43	0.03	-3.02	-0.38	0.56	1.00	0.88 *	0.41	0.04	0.33	0.03	22.60	2.44	0.00	0.01 **
0.75	0.05	0.76	0.04	-1.29	-0.26	0.57	1.00	1.00	0.74	0.04	0.65	0.04	13.51	2.07	0.00	0.01 **
2.46	0.59	3.43	0.33	-28.27	-2.97	0.00	0.00 **	0.31	2.68	0.45	2.26	0.38	18.84	1.12	0.03	0.36
2.41	0.59	3.38	0.33	-28.52	-2.96	0.00	0.00 **	0.31	2.64	0.45	2.22	0.38	18.99	1.11	0.03	0.37
0.04	0.00	0.05	0.00	-10.84	-1.21	0.00	0.05 -	1.00	0.05	0.00	0.04	0.00	10.52	1.16	0.02	0.20
1.04	0.12	1.21	0.10	-14.35	-1.77	0.00	0.00 **	1.00	1.07	0.06	0.95	0.08	12.69	1.48	0.00	0.00 **

	Absolute Volumes Female									Relative Volumes	Absolute Volumes Male					
Relative Volume	GFSPF		GF								ASF		GF			
FDR	Mean	SD	Mean	SD	%Diff	Effect	P-Value	FDR	FDR		Mean	SD	Mean	SD	%Diff	Effect
0.79	363.18	28.46	357.61	29.36	1.56	0.19	0.64	1.00	1.00	1.00	407.57	15.09	343.89	19.74	18.52	3.23
1.00	324.55	24.53	320.14	24.71	1.38	0.18	0.67	1.00	1.00	1.00	360.43	13.42	307.67	16.97	17.15	3.11
1.00	204.94	14.23	201.01	17.19	1.95	0.23	0.55	1.00	1.00	1.00	225.66	9.83	194.18	9.88	16.21	3.19
1.00	171.37	11.78	168.44	14.37	1.74	0.20	0.60	1.00	1.00	1.00	188.00	9.06	162.07	8.11	16.00	3.20
1.00	10.87	0.82	10.39	0.77	4.64	0.63	0.15	1.00	1.00	1.00	12.24	0.49	10.38	0.51	17.92	3.65
1.00	7.81	0.63	7.47	0.55	4.56	0.62	0.17	1.00	1.00	1.00	9.02	0.43	7.52	0.42	19.94	3.54
1.00	0.90	0.06	0.87	0.12	3.43	0.26	0.45	1.00	1.00	1.00	0.90	0.07	0.85	0.07	5.97	0.71
1.00	0.28	0.02	0.27	0.04	3.14	0.25	0.48	1.00	1.00	1.00	0.28	0.02	0.27	0.02	3.42	0.53
1.00	0.19	0.02	0.18	0.03	2.39	0.15	0.68	1.00	1.00	1.00	0.18	0.02	0.17	0.02	3.97	0.28
1.00	0.43	0.03	0.41	0.05	4.09	0.32	0.36	1.00	1.00	1.00	0.44	0.04	0.41	0.04	8.54	0.97
1.00	2.15	0.17	2.04	0.14	5.42	0.81	0.09	1.00	1.00	1.00	2.32	0.07	2.01	0.08	15.45	4.11
1.00	1.65	0.12	1.57	0.12	5.23	0.67	0.11	1.00	1.00	1.00	1.80	0.07	1.55	0.06	15.97	4.37
1.00	1.20	0.09	1.13	0.09	6.63	0.79	0.06	1.00	1.00	1.00	1.32	0.05	1.13	0.04	17.15	4.32
1.00	0.45	0.04	0.44	0.03	1.64	0.21	0.65	1.00	1.00	1.00	0.48	0.02	0.43	0.02	12.87	3.47
1.00	0.50	0.06	0.47	0.04	6.06	0.78	0.16	1.00	1.00	1.00	0.51	0.02	0.45	0.03	13.62	1.84
1.00	160.50	11.04	158.06	13.64	1.55	0.18	0.64	1.00	1.00	1.00	175.76	8.71	151.70	7.69	15.87	3.13
1.00	33.04	2.50	32.35	2.54	2.14	0.27	0.51	1.00	1.00	1.00	36.65	2.27	31.79	1.70	15.29	2.86
1.00	2.00	0.12	1.99	0.16	0.37	0.05	0.90	1.00	1.00	1.00	2.27	0.06	1.97	0.10	15.46	3.00
1.00	0.91	0.08	0.88	0.07	3.24	0.43	0.34	1.00	1.00	1.00	0.96	0.07	0.84	0.06	14.70	2.18
1.00	9.65	1.09	9.43	0.66	2.32	0.33	0.55	1.00	1.00	1.00	10.70	0.74	8.89	0.56	20.28	3.24
1.00	0.69	0.11	0.70	0.07	-1.33	-0.14	0.80	1.00	1.00	1.00	0.81	0.09	0.66	0.11	21.67	1.37
1.00	8.96	0.98	8.73	0.61	2.62	0.37	0.50	1.00	1.00	1.00	9.89	0.65	8.23	0.47	20.17	3.53
1.00	1.02	0.08	1.02	0.09	0.20	0.02	0.96	1.00	1.00	1.00	1.12	0.03	0.98	0.03	14.52	4.13
1.00	0.90	0.07	0.90	0.09	-0.14	-0.01	0.97	1.00	1.00	1.00	0.99	0.02	0.87	0.03	13.73	4.12
1.00	0.12	0.01	0.11	0.01	2.87	0.38	0.47	1.00	1.00	1.00	0.14	0.01	0.11	0.01	20.62	2.52
1.00	1.63	0.13	1.67	0.08	-2.35	-0.49	0.39	1.00	1.00	1.00	1.95	0.24	1.64	0.10	18.57	3.15
1.00	1.63	0.13	1.67	0.08	-2.35	-0.49	0.39	1.00	1.00	1.00	1.95	0.24	1.64	0.10	18.57	3.15
1.00	0.70	0.06	0.71	0.05	-1.61	-0.25	0.60	1.00	1.00	1.00	0.81	0.11	0.70	0.05	15.81	2.20
1.00	0.93	0.08	0.96	0.06	-2.90	-0.49	0.35	1.00	1.00	1.00	1.14	0.14	0.94	0.07	20.63	2.66
1.00	0.38	0.03	0.36	0.03	5.64	0.63	0.12	1.00	1.00	1.00	0.39	0.04	0.33	0.02	18.96	2.68
1.00	14.79	1.06	14.43	1.63	2.54	0.23	0.53	1.00	1.00	1.00	16.42	1.56	14.52	0.98	13.09	1.95
1.00	3.69	0.30	3.63	0.52	1.76	0.12	0.72	1.00	1.00	1.00	4.32	0.33	3.64	0.29	18.71	2.35
1.00	5.58	0.41	5.45	0.49	2.51	0.28	0.47	1.00	1.00	1.00	6.02	0.61	5.39	0.36	11.63	1.76
1.00	0.80	0.07	0.77	0.16	3.80	0.18	0.58	1.00	1.00	1.00	0.91	0.14	0.82	0.06	10.73	1.35
1.00	0.72	0.07	0.69	0.15	5.03	0.23	0.49	1.00	1.00	1.00	0.79	0.12	0.72	0.06	9.66	1.25
1.00	3.99	0.28	3.89	0.41	2.62	0.25	0.49	1.00	1.00	1.00	4.38	0.42	3.94	0.26	11.04	1.69
1.00	0.68	0.05	0.66	0.07	1.73	0.17	0.64	1.00	1.00	1.00	0.74	0.07	0.70	0.04	6.25	1.23
1.00	0.47	0.03	0.47	0.04	1.09	0.11	0.75	1.00	1.00	1.00	0.52	0.05	0.49	0.02	4.96	0.98
1.00	0.20	0.02	0.20	0.03	3.27	0.26	0.50	1.00	1.00	1.00	0.23	0.02	0.21	0.01	9.31	1.56
1.00	1.99	0.19	1.92	0.17	3.93	0.45	0.31	1.00	1.00	1.00	2.09	0.08	1.92	0.08	9.16	2.15
1.00	32.23	2.51	31.99	2.64	0.74	0.09	0.82	1.00	1.00	1.00	37.96	1.06	31.27	1.97	21.39	3.39
1.00	14.93	1.15	14.83	0.97	0.69	0.11	0.81	1.00	1.00	1.00	17.19	0.69	14.39	0.88	19.45	3.18
1.00	4.61	0.40	4.63	0.47	-0.41	-0.04	0.92	1.00	1.00	1.00	5.32	0.18	4.53	0.30	17.36	2.63
1.00	1.91	0.18	1.95	0.22	-1.99	-0.18	0.64	1.00	1.00	1.00	2.22	0.06	1.88	0.15	18.26	2.22
1.00	2.70	0.24	2.68	0.26	0.73	0.07	0.85	1.00	1.00	1.00	3.10	0.16	2.65	0.15	16.72	2.88
1.00	10.32	0.77	10.20	0.59	1.19	0.21	0.67	1.00	1.00	1.00	11.87	0.64	9.86	0.61	20.42	3.32
1.00	4.97	0.42	5.03	0.33	-1.23	-0.19	0.69	1.00	1.00	1.00	5.96	0.26	4.77	0.33	24.98	3.62
1.00	4.75	0.33	4.57	0.38	4.00	0.47	0.23	1.00	1.00	1.00	5.23	0.35	4.51	0.29	16.01	2.49
1.00	1.53	0.11	1.47	0.12	4.22	0.51	0.20	1.00	1.00	1.00	1.66	0.13	1.46	0.09	13.69	2.11
1.00	2.20	0.17	2.11	0.21	4.32	0.44	0.25	1.00	1.00	1.00	2.52	0.16	2.09	0.15	20.34	2.80
1.00	1.01	0.08	0.98	0.07	2.97	0.41	0.36	1.00	1.00	1.00	1.05	0.07	0.95	0.06	10.03	1.61
1.00	0.61	0.05	0.61	0.05	0.13	0.01	0.97	1.00	1.00	1.00	0.68	0.03	0.58	0.04	17.26	2.84
1.00	17.29	1.49	17.16	1.78	0.79	0.08	0.84	1.00	1.00	1.00	20.77	0.49	16.88	1.12	23.04	3.48
1.00	12.59	1.13	12.44	1.31	1.21	0.11	0.77	1.00	1.00	1.00	15.17	0.35	12.30	0.77	23.32	3.71
1.00	6.56	0.58	6.56	0.67	0.09	0.01	0.98	1.00	1.00	1.00	7.62	0.27	6.48	0.40	17.69	2.86
1.00	1.67	0.19	1.68	0.22	-0.97	-0.07	0.85	1.00	1.00	1.00	1.94	0.10	1.68	0.15	15.17	1.74
1.00	1.94	0.15	1.93	0.18	0.49	0.05	0.89	1.00	1.00	1.00	2.22	0.07	1.89	0.11	17.44	2.98
1.00	2.10	0.17	2.09	0.19	0.74	0.08	0.84	1.00	1.00	1.00	2.46	0.08	2.05	0.11	19.83	3.77
1.00	0.85	0.08	0.85	0.09	-0.35	-0.03	0.94	1.00	1.00	1.00	1.00	0.04	0.85	0.06	18.11	2.67
1.00	0.95	0.10	0.95	0.10	-0.93	-0.09	0.83	1.00	1.00	1.00	1.19	0.05	0.94	0.06	26.64	4.08
1.00	0.16	0.02	0.17	0.02	-1.31	-0.13	0.75	1.00	1.00	1.00	0.20	0.01	0.16	0.01	24.95	4.38
1.00	0.40	0.05	0.41	0.05	-3.14	-0.27	0.54	1.00	1.00	1.00	0.50	0.03	0.41	0.03	20.68	2.46
1.00	0.38	0.04	0.38	0.04	1.65	0.16	0.69	1.00	1.00	1.00	0.49	0.03	0.36	0.02	34.14	5.13
1.00	5.08	0.47	4.93	0.55	3.11	0.28	0.48	1.00	1.00	1.00	6.36	0.11	4.89	0.34	30.13	4.37
1.00	0.89	0.08	0.87	0.10	2.47	0.22	0.57	1.00	1.00	1.00	1.10	0.02	0.87	0.06	26.64	3.60
1.00	0.12	0.01	0.11	0.01	2.56	0.25	0.54	1.00	1.00	1.00	0.15	0.00	0.11	0.01	32.92	3.63
1.00	0.77	0.07	0.75	0.09	2.46	0.21	0.59	1.00	1.00	1.00	0.95	0.02	0.76	0.06	25.71	3.43
1.00	2.15	0.22	2.08	0.24	3.39	0.29	0.46	1.00	1.00	1.00	2.95	0.14	2.07	0.15	42.15	5.81
1.00	1.51	0.14	1.47	0.16	2.91	0.27	0.49	1.00	1.00	1.00	1.76	0.05	1.44	0.09	22.20	3.43
1.00	0.53	0.05	0.51	0.06	3.61	0.29	0.44	1.00	1.00	1.00	0.55	0.05	0.51	0.03	9.47	1.40
1.00	4.71	0.38	4.72	0.50	-0.32	-0.03	0.94	1.00	1.00	1.00	5.60	0.16	4.58	0.39	22.29	2.60
1.00	3.27	0.26	3.29	0.35	-0.58	-0.06	0.88	1.00	1.00	1.00	3.86	0.12	3.18	0.26	21.27	2.57
1.00	1.44	0.12	1.43	0.16	0.30	0.03	0.94	1.00	1.00	1.00	1.74	0.04	1.40	0.13	24.63	2.60
1.00	0.98	0.08	0.98	0.11	-0.07	-0.01	0.99	1.00	1.00	1.00	1.18	0.03	0.96	0.09	23.83	2.50
1.00	0.46	0.04	0.45	0.05	1.09	0.10	0.80	1.00	1.00	1.00	0.56	0.01	0.44	0.04	26.35	2.79
1.00	95.24	6.51	93.72	8.63	1.61	0.18	0.64	1.00	1.00	1.00	101.15	5.77	88.64	4.53	14.12	2.76
1.00	4.29	0.34	4.21	0.45	1.72	0.16	0.66	1.00	1.00	1.00	4.43	0.18	4.02	0.28	10.26	1.48
1.00	2.46	0.20	2.46	0.27	0.16	0.01	0.97	1.00	1.00	1.00	2.61	0.12	2.38	0.16	9.66	1.46
1.00	1.70	0.17	1.72	0.21	-1.25	-0.10	0.79	1.00	1.00	1.00	1.85	0.06	1.65	0.13	12.14	1.51
1.00	0.77	0.05	0.74	0.07	3.42	0.37	0.32	1.00	1.00	1.00	0.76	0.08	0.73	0.05	4.08	0.58
1.00	1.82	0.16	1.75	0.20	3.91	0.34	0.38	1.00	1.00	1.00	1.82	0.09	1.64	0.14	11.13	1.27
1.00	1.27	0.13	1.24	0.16	3.01	0.24	0.54	1.00	1.00	1.00	1.27	0.06	1.16	0.12	9.42	0.91
0.79	0.55	0.05	0.52	0.06	6.04	0.55	0.18	1.00	1.00	1.00	0.55	0.04	0.48	0.03	15.32	2.45
1.00	0.46	0.04	0.44	0.05	5.75	0.51	0.20	1.00	1.00	1.00	0.52	0.03	0.43	0.04	18.86	2.13
1.00	5.24	0.42	5.08	0.52	3.20	0.31	0.42	1.00	1.00	1.00	5.55	0.34	4.86	0.36	14.16	1.91
1.00	2.76	0.20	2.69	0.28	2.77	0.27	0.47	1.00	1.00	1.00	2.88	0.22	2.60	0.21	10.72	1.35
1.00	0.61	0.05	0.59	0.07	2.49	0.22	0.55	1.00	1.00	1.00	0.65	0.04	0.58	0.05	12.71	1.34
1.00	0.36	0.06	0.35	0.05	2.28	0.17	0.71	1.00	1.00	1.00	0.40	0.03	0.35	0.04	11.90	1.06
1.00	1.79	0.11	1.74	0.18	2.97	0.29	0.42	1.00	1.00	1.00	1.84	0.17	1.67	0.12	9.79	1.36
1.00	2.48	0.24	2.40	0.26	3.67	0.33	0.41	1.00	1.00	1.00	2.67	0.13	2.26	0.17	18.12	2.40
1.00	2.30	0.17	2.30	0.25	0.18	0.02	0.96	1.00	1.00	1.00	2.34	0.15	2.22	0.16	5.25	0.74
1.00	4.17	0.30	4.03	0.40	3.58	0.36	0.34	1.00	1.00	1.00	4.51	0.34	3.86	0.25	17.04	2.64

1.00	1.32	0.12	1.30	0.12	2.00	0.21	0.60	1.00	1.00	1.46	0.11	1.24	0.08	17.91	2.77
1.00	1.27	0.10	1.23	0.11	3.56	0.38	0.32	1.00	1.00	1.36	0.08	1.17	0.08	16.10	2.48
1.00	1.58	0.10	1.50	0.17	4.96	0.43	0.23	1.00	1.00	1.69	0.16	1.44	0.10	17.04	2.39
1.00	0.94	0.10	0.91	0.11	2.54	0.22	0.60	1.00	1.00	0.94	0.11	0.85	0.03	10.07	2.57
1.00	0.94	0.10	0.91	0.11	2.54	0.22	0.60	1.00	1.00	0.94	0.11	0.85	0.03	10.07	2.57
1.00	8.91	0.61	8.59	1.00	3.73	0.32	0.36	1.00	1.00	9.76	0.60	8.24	0.64	18.44	2.38
1.00	2.26	0.21	2.18	0.32	3.93	0.27	0.46	1.00	1.00	2.54	0.15	2.08	0.16	21.93	2.89
1.00	6.65	0.46	6.41	0.68	3.66	0.34	0.34	1.00	1.00	7.22	0.46	6.16	0.50	17.26	2.11
1.00	12.48	1.00	11.98	1.10	4.25	0.46	0.25	1.00	1.00	13.18	0.79	11.43	0.59	15.29	2.96
0.79	6.83	0.64	6.61	0.57	3.26	0.38	0.39	1.00	1.00	7.35	0.46	6.23	0.31	18.00	3.66
1.00	0.60	0.05	0.58	0.06	4.18	0.42	0.30	1.00	1.00	0.66	0.05	0.54	0.03	20.90	3.75
0.79	6.23	0.59	6.04	0.52	3.17	0.37	0.41	1.00	1.00	6.69	0.42	5.69	0.29	17.72	3.50
1.00	5.66	0.43	5.36	0.56	5.48	0.53	0.17	1.00	1.00	5.83	0.37	5.20	0.29	12.05	2.13
1.00	6.66	0.35	6.76	0.41	-1.59	-0.26	0.50	1.00	1.00	6.96	0.40	6.39	0.21	8.88	2.74
1.00	5.87	0.35	5.98	0.59	-1.78	-0.18	0.61	1.00	1.00	6.24	0.28	5.76	0.33	8.41	1.45
0.79	3.11	0.21	3.12	0.29	-0.29	-0.03	0.93	1.00	1.00	3.23	0.22	3.07	0.16	5.28	1.00
1.00	1.52	0.10	1.58	0.16	-4.15	-0.41	0.25	1.00	1.00	1.61	0.06	1.47	0.09	9.89	1.68
1.00	1.25	0.08	1.28	0.16	-2.50	-0.20	0.56	1.00	1.00	1.40	0.04	1.22	0.10	14.47	1.80
1.00	2.05	0.19	2.01	0.21	2.28	0.22	0.59	1.00	1.00	2.19	0.15	1.90	0.12	15.08	2.41
1.00	0.19	0.02	0.19	0.02	1.58	0.14	0.74	1.00	1.00	0.20	0.02	0.17	0.02	18.51	1.70
1.00	0.33	0.04	0.32	0.04	3.17	0.27	0.51	1.00	1.00	0.34	0.04	0.30	0.04	13.85	1.10
1.00	0.09	0.01	0.08	0.02	11.40	0.49	0.16	1.00	1.00	0.09	0.01	0.08	0.01	14.68	1.49
1.00	1.44	0.13	1.41	0.14	1.64	0.16	0.69	1.00	1.00	1.55	0.09	1.35	0.07	14.94	3.05
1.00	2.17	0.16	2.06	0.30	5.43	0.37	0.28	1.00	1.00	2.50	0.22	1.97	0.15	27.08	3.57
1.00	28.57	2.18	28.52	2.82	0.19	0.02	0.96	1.00	1.00	30.13	2.44	26.43	1.51	13.98	2.45
1.00	22.98	1.82	23.11	2.14	-0.57	-0.06	0.87	1.00	1.00	24.49	1.94	21.35	1.16	14.72	2.71
1.00	3.71	0.22	3.64	0.37	2.02	0.20	0.57	1.00	1.00	4.04	0.30	3.44	0.17	17.43	3.50
1.00	8.07	0.59	8.23	0.68	-2.02	-0.24	0.53	1.00	1.00	8.47	0.64	7.63	0.41	11.13	2.05
1.00	0.88	0.09	0.86	0.09	1.72	0.16	0.69	1.00	1.00	0.88	0.06	0.78	0.07	13.45	1.50
1.00	0.28	0.03	0.28	0.04	-0.87	-0.06	0.87	1.00	1.00	0.28	0.02	0.25	0.03	12.58	1.17
1.00	0.15	0.02	0.15	0.02	4.77	0.30	0.41	1.00	1.00	0.15	0.02	0.13	0.01	11.31	1.28
1.00	0.45	0.05	0.44	0.04	2.36	0.30	0.55	1.00	1.00	0.45	0.03	0.39	0.04	14.73	1.65
1.00	3.16	0.35	3.18	0.33	-0.75	-0.07	0.87	1.00	1.00	3.45	0.30	2.85	0.25	21.13	2.38
1.00	2.13	0.24	2.13	0.23	-0.37	-0.04	0.93	1.00	1.00	2.26	0.21	1.91	0.19	18.44	1.83
1.00	0.50	0.04	0.50	0.06	0.12	0.01	0.98	1.00	1.00	0.53	0.05	0.46	0.03	16.56	2.69
1.00	4.54	0.38	4.56	0.50	-0.51	-0.05	0.90	1.00	1.00	4.85	0.47	4.29	0.23	13.05	2.40
1.00	5.59	0.52	5.41	0.77	3.46	0.24	0.50	1.00	1.00	5.64	0.57	5.08	0.49	10.87	1.12
1.00	2.55	0.24	2.42	0.29	5.48	0.45	0.24	1.00	1.00	2.73	0.18	2.32	0.19	17.69	2.20
1.00	8.56	0.73	8.44	0.71	1.43	0.17	0.68	1.00	1.00	9.18	0.44	7.95	0.39	15.47	3.18
1.00	1.92	0.21	1.92	0.15	0.22	0.03	0.96	1.00	1.00	2.06	0.09	1.76	0.10	17.14	2.94
1.00	1.75	0.14	1.71	0.13	2.49	0.33	0.45	1.00	1.00	1.89	0.09	1.62	0.10	16.74	2.62
1.00	1.69	0.14	1.69	0.17	0.36	0.03	0.93	1.00	1.00	1.80	0.11	1.60	0.08	12.39	2.54
1.00	2.35	0.21	2.29	0.22	2.75	0.29	0.48	1.00	1.00	2.55	0.15	2.18	0.13	17.28	2.82
1.00	0.84	0.09	0.83	0.11	0.61	0.05	0.90	1.00	1.00	0.88	0.08	0.80	0.05	10.48	1.57
1.00	33.57	2.64	32.57	2.93	3.08	0.34	0.39	1.00	1.00	37.66	0.94	32.11	1.86	17.28	2.99
1.00	8.35	0.67	8.12	0.73	2.78	0.31	0.44	1.00	1.00	9.53	0.21	8.14	0.49	17.06	2.83
1.00	4.02	0.31	3.93	0.31	2.28	0.29	0.49	1.00	1.00	4.53	0.17	3.93	0.23	15.19	2.58
1.00	0.98	0.10	0.94	0.10	4.27	0.39	0.35	1.00	1.00	1.20	0.04	0.99	0.08	22.04	2.70
1.00	0.98	0.10	0.94	0.10	4.27	0.39	0.35	1.00	1.00	1.20	0.04	0.99	0.08	22.04	2.70
1.00	2.34	0.25	2.27	0.26	3.03	0.27	0.51	1.00	1.00	2.66	0.12	2.23	0.16	19.43	2.75
1.00	1.02	0.06	0.99	0.08	2.81	0.35	0.35	1.00	1.00	1.13	0.05	0.99	0.07	14.16	2.15
1.00	1.02	0.06	0.99	0.08	2.81	0.35	0.35	1.00	1.00	1.13	0.05	0.99	0.07	14.16	2.15
1.00	25.22	1.98	24.44	2.20	3.17	0.35	0.38	1.00	1.00	28.14	0.78	23.97	1.38	17.36	3.02
1.00	5.84	0.33	5.82	0.40	0.29	0.04	0.91	1.00	1.00	6.68	0.30	5.68	0.36	17.49	2.79
1.00	0.11	0.01	0.11	0.01	1.65	0.17	0.66	1.00	1.00	0.12	0.01	0.11	0.01	6.15	1.13
0.79	3.05	0.19	3.01	0.28	1.39	0.15	0.68	1.00	1.00	3.40	0.08	3.00	0.17	13.37	2.36
1.00	2.67	0.26	2.70	0.32	-1.00	-0.08	0.83	1.00	1.00	3.16	0.31	2.57	0.31	22.80	1.87
1.00	2.35	0.20	2.24	0.27	5.12	0.42	0.26	1.00	1.00	2.79	0.10	2.24	0.17	24.62	3.28
1.00	16.20	1.54	15.59	1.59	3.95	0.39	0.35	1.00	1.00	17.68	0.76	15.21	0.95	16.25	2.59
1.00	16.20	1.54	15.59	1.59	3.95	0.39	0.35	1.00	1.00	17.68	0.76	15.21	0.95	16.25	2.59
1.00	0.83	0.10	0.80	0.06	3.65	0.46	0.39	1.00	1.00	0.99	0.08	0.84	0.06	17.21	2.60
1.00	0.83	0.10	0.80	0.06	3.65	0.46	0.39	1.00	1.00	0.99	0.08	0.84	0.06	17.21	2.60
1.00	82.95	7.65	82.65	4.83	0.36	0.06	0.91	1.00	1.00	92.41	2.77	79.91	4.60	15.65	2.72
1.00	24.05	2.33	23.77	2.05	1.17	0.14	0.76	1.00	1.00	26.17	0.93	23.38	1.48	11.97	1.89
1.00	10.71	1.06	10.68	0.80	0.31	0.04	0.93	1.00	1.00	11.56	0.45	10.39	0.65	11.30	1.80
1.00	4.29	0.40	4.31	0.37	-0.49	-0.06	0.89	1.00	1.00	4.66	0.14	4.04	0.26	15.45	2.39
1.00	6.42	0.67	6.37	0.67	0.84	0.08	0.85	1.00	1.00	6.90	0.35	6.35	0.42	8.66	1.30
1.00	0.21	0.02	0.21	0.02	-1.55	-0.16	0.69	1.00	1.00	0.24	0.01	0.21	0.02	16.72	2.19
1.00	0.21	0.02	0.21	0.02	-1.55	-0.16	0.69	1.00	1.00	0.24	0.01	0.21	0.02	16.72	2.19
1.00	0.21	0.02	0.21	0.02	-1.55	-0.16	0.69	1.00	1.00	0.24	0.01	0.21	0.02	16.72	2.19
1.00	10.08	0.98	9.93	1.05	1.52	0.14	0.72	1.00	1.00	11.05	0.35	9.88	0.66	11.90	1.78
1.00	3.04	0.29	2.94	0.26	3.32	0.37	0.39	1.00	1.00	3.31	0.14	2.90	0.19	14.27	2.17
1.00	3.04	0.29	2.94	0.26	3.32	0.37	0.39	1.00	1.00	3.31	0.14	2.90	0.19	14.27	2.17
1.00	36.48	3.41	36.99	2.56	-1.37	-0.20	0.68	1.00	1.00	41.65	0.86	35.08	1.98	18.74	3.32
1.00	22.15	2.15	22.78	2.39	-2.79	-0.27	0.50	1.00	1.00	25.45	0.56	21.32	1.26	19.36	3.27
1.00	0.23	0.03	0.23	0.06	-0.33	-0.01	0.97	1.00	1.00	0.27	0.02	0.21	0.03	27.18	2.29
1.00	0.23	0.03	0.23	0.06	-0.33	-0.01	0.97	1.00	1.00	0.27	0.02	0.21	0.03	27.18	2.29
1.00	0.23	0.03	0.23	0.06	-0.33	-0.01	0.97	1.00	1.00	0.27	0.02	0.21	0.03	27.18	2.29
1.00	0.30	0.02	0.27	0.09	9.40	0.29	0.36	1.00	1.00	0.33	0.03	0.30	0.04	10.83	0.89
1.00	0.30	0.02	0.27	0.09	9.40	0.29	0.36	1.00	1.00	0.33	0.03	0.30	0.04	10.83	0.89
1.00	21.62	2.11	22.28	2.47	-2.96	-0.27	0.49	1.00	1.00	24.85	0.53	20.81	1.22	19.41	3.31
1.00	14.33	1.29	14.20	0.83	0.90	0.15	0.77	1.00	1.00	16.20	0.33	13.76	0.76	17.77	3.21
1.00	13.09	1.19	12.97	0.73	0.92	0.16	0.77	1.00	1.00	14.69	0.35	12.60	0.69	16.64	3.03
1.00	0.64	0.08	0.64	0.08	0.59	0.05	0.91	1.00	1.00	0.82	0.07	0.59	0.06	39.66	3.71
1.00	0.64	0.08	0.64	0.08	0.59	0.05	0.91	1.00	1.00	0.82	0.07	0.59	0.06	39.66	3.71
1.00	0.59	0.04	0.59	0.05	0.74	0.08	0.83	1.00	1.00	0.69	0.04	0.57	0.04	20.29	3.07
1.00	0.59	0.04	0.59	0.05	0.74	0.08	0.83	1.00	1.00	0.69	0.04	0.57	0.04	20.29	3.07
1.00	22.42	2.03	21.89	2.32	2.43	0.23	0.56	1.00	1.00	24.58	1.31	21.45	1.32	14.59	2.38
1.00	8.76	0.64	8.40	0.71	4.19	0.50	0.22	1.00	1.00	9.86	0.30	8.37	0.47	17.82	3.14
1.00	8.21	0.59	7.88	0.67	4.19	0.50	0.22	1.00	1.00	9.24	0.25	7.86	0.45	17.50	3.05
1.00	0.54	0.06	0.52	0.05	4.17	0.43	0.35	1.00	1.00	0.62	0.05	0.50	0.04	22.83	3.22
1.00	0.42	0.06	0.40	0.05	4.27	0.37	0.44	1.00	1.00	0.47	0.05	0.37	0.04	24.90	2.29
1.00	0.13	0.01	0.12	0.02	3.85	0.29	0.46	1.00	1.00	0.15	0.01	0.13	0.01	16.74	1.83
1.00	13.67	1.46	13.49	1.69	1.33	0.11	0.79	1.00	1.00	14.72	1.18	13.08	0.92	12.53	1.79
1.00	36.66	3.50	36.47	3.84	0.51	0.05	0.90	1.00	1.00	42.36	2.04	33.58	3.26	26.13	2.70
1.00	35.71	3.42	35.57	3.75	0.39	0.04	0.93	1.00	1.00	41.27	2.04	32.69	3.19	26.26	2.69

1.00	15.47	1.54	15.53	1.57	-0.44	-0.04	0.91	1.00	1.00	17.64	0.67	14.09	1.31	25.19	2.72
1.00	1.56	0.20	1.49	0.15	4.72	0.47	0.34	1.00	1.00	1.70	0.08	1.34	0.09	26.82	3.96
1.00	1.57	0.27	1.65	0.39	-4.95	-0.21	0.57	1.00	1.00	1.67	0.09	1.45	0.15	15.19	1.48
1.00	4.59	0.46	4.64	0.44	-1.13	-0.12	0.78	1.00	1.00	5.26	0.22	4.31	0.36	22.22	2.68
1.00	3.24	0.33	3.33	0.31	-2.50	-0.27	0.53	1.00	1.00	3.71	0.16	3.09	0.27	20.01	2.30
1.00	1.34	0.16	1.31	0.14	2.34	0.22	0.63	1.00	1.00	1.56	0.10	1.22	0.10	27.81	3.43
1.00	2.18	0.27	2.12	0.49	3.11	0.14	0.69	1.00	1.00	2.36	0.13	1.93	0.24	22.60	1.81
1.00	0.79	0.14	0.78	0.25	0.55	0.02	0.96	1.00	1.00	1.00	0.11	0.69	0.10	44.36	3.09
1.00	1.24	0.20	1.22	0.29	1.81	0.08	0.83	1.00	1.00	1.57	0.14	1.09	0.16	43.70	3.00
1.00	2.36	0.29	2.42	0.23	-2.24	-0.24	0.61	1.00	1.00	2.75	0.20	2.20	0.24	25.31	2.29
1.00	1.17	0.10	1.22	0.14	-3.56	-0.31	0.40	1.00	1.00	1.32	0.08	1.08	0.12	21.78	2.03
1.00	20.24	1.90	20.03	2.22	1.05	0.09	0.81	1.00	1.00	23.63	1.44	18.60	1.95	27.07	2.58
1.00	4.12	0.46	4.17	0.46	-1.22	-0.11	0.79	1.00	1.00	4.66	0.25	3.74	0.39	24.54	2.35
1.00	6.84	0.58	6.68	0.91	2.38	0.18	0.62	1.00	1.00	8.09	0.53	6.25	0.73	29.54	2.54
1.00	3.55	0.31	3.48	0.35	2.08	0.21	0.60	1.00	1.00	4.24	0.20	3.21	0.37	32.10	2.77
1.00	3.29	0.29	3.20	0.62	2.70	0.14	0.67	1.00	1.00	3.86	0.35	3.04	0.36	26.84	2.25
1.00	3.50	0.42	3.47	0.52	0.99	0.07	0.86	1.00	1.00	4.05	0.21	3.13	0.40	29.39	2.31
1.00	2.12	0.25	2.00	0.28	6.20	0.45	0.27	1.00	1.00	2.47	0.20	1.84	0.19	34.44	3.35
1.00	0.80	0.09	0.80	0.08	-0.23	-0.02	0.96	1.00	1.00	1.02	0.03	0.75	0.08	34.71	3.19
1.00	2.85	0.33	2.90	0.49	-1.89	-0.11	0.75	1.00	1.00	3.34	0.34	2.88	0.34	15.80	1.34
1.00	0.95	0.10	0.91	0.12	5.10	0.40	0.31	1.00	1.00	1.09	0.03	0.89	0.09	21.47	2.16
1.00	0.27	0.03	0.25	0.04	5.35	0.39	0.31	1.00	1.00	0.31	0.01	0.25	0.02	23.15	2.34
1.00	0.34	0.04	0.32	0.04	4.83	0.36	0.35	1.00	1.00	0.39	0.01	0.32	0.03	21.93	2.17
1.00	0.35	0.04	0.33	0.04	5.18	0.45	0.29	1.00	1.00	0.39	0.02	0.32	0.03	19.72	1.98
1.00	33.96	3.43	33.18	4.27	2.34	0.18	0.63	1.00	1.00	39.90	1.67	32.02	2.43	24.61	3.24
1.00	5.45	0.47	5.28	0.67	3.26	0.26	0.48	1.00	1.00	6.30	0.22	5.27	0.34	19.53	3.00
1.00	2.02	0.16	1.96	0.23	2.98	0.25	0.49	1.00	1.00	2.27	0.13	1.97	0.13	15.19	2.22
1.00	0.81	0.08	0.79	0.11	2.28	0.16	0.66	1.00	1.00	0.93	0.03	0.78	0.06	18.32	2.46
1.00	1.22	0.08	1.17	0.13	3.46	0.32	0.37	1.00	1.00	1.34	0.10	1.19	0.08	13.12	1.91
1.00	0.17	0.02	0.16	0.02	4.37	0.32	0.41	1.00	1.00	0.20	0.01	0.16	0.01	24.69	3.53
1.00	2.02	0.20	1.93	0.32	4.62	0.28	0.43	1.00	1.00	2.34	0.06	1.91	0.13	22.39	3.37
1.00	2.02	0.20	1.93	0.32	4.62	0.28	0.43	1.00	1.00	2.34	0.06	1.91	0.13	22.39	3.37
1.00	2.02	0.20	1.93	0.32	4.62	0.28	0.43	1.00	1.00	2.34	0.06	1.91	0.13	22.39	3.37
1.00	1.14	0.11	1.13	0.11	1.34	0.13	0.74	1.00	1.00	1.37	0.05	1.13	0.09	21.30	2.65
1.00	1.14	0.11	1.13	0.11	1.34	0.13	0.74	1.00	1.00	1.37	0.05	1.13	0.09	21.30	2.65
1.00	0.10	0.01	0.10	0.01	2.47	0.19	0.63	1.00	1.00	0.12	0.01	0.09	0.01	21.77	2.03
1.00	0.10	0.01	0.10	0.01	2.47	0.19	0.63	1.00	1.00	0.12	0.01	0.09	0.01	21.77	2.03
1.00	5.20	0.58	5.05	0.67	3.01	0.23	0.56	1.00	1.00	6.48	0.26	4.92	0.42	31.90	3.74
1.00	4.28	0.50	4.15	0.58	3.14	0.23	0.56	1.00	1.00	5.43	0.22	4.03	0.36	34.55	3.86
1.00	0.30	0.04	0.29	0.04	2.60	0.20	0.62	1.00	1.00	0.37	0.02	0.29	0.03	25.49	2.61
1.00	2.69	0.33	2.61	0.38	3.01	0.21	0.60	1.00	1.00	3.54	0.13	2.53	0.25	39.70	4.01
1.00	2.21	0.28	2.15	0.33	2.83	0.19	0.63	1.00	1.00	2.98	0.11	2.08	0.22	43.35	4.13
1.00	0.48	0.05	0.46	0.06	3.82	0.32	0.45	1.00	1.00	0.56	0.03	0.46	0.04	23.15	2.93
1.00	0.64	0.07	0.62	0.08	3.42	0.28	0.49	1.00	1.00	0.76	0.05	0.61	0.04	25.15	3.87
1.00	0.65	0.07	0.63	0.09	3.69	0.25	0.50	1.00	1.00	0.76	0.06	0.60	0.06	26.73	2.68
1.00	0.92	0.09	0.90	0.10	2.39	0.22	0.58	1.00	1.00	1.06	0.05	0.88	0.06	19.81	2.81
1.00	0.73	0.07	0.71	0.08	2.26	0.21	0.60	1.00	1.00	0.84	0.04	0.70	0.05	20.28	3.00
1.00	0.19	0.02	0.18	0.02	3.44	0.33	0.40	1.00	1.00	0.20	0.01	0.18	0.01	12.64	1.62
1.00	0.02	0.00	0.02	0.00	9.42	0.52	0.19	1.00	1.00	0.03	0.00	0.02	0.00	74.18	4.34
1.00	0.52	0.05	0.51	0.06	1.57	0.14	0.72	1.00	1.00	0.61	0.03	0.50	0.03	21.07	3.16
1.00	0.20	0.02	0.19	0.02	2.86	0.25	0.54	1.00	1.00	0.22	0.01	0.18	0.02	18.02	2.03
1.00	0.20	0.02	0.19	0.02	2.86	0.25	0.54	1.00	1.00	0.22	0.01	0.18	0.02	18.02	2.03
1.00	8.80	0.82	8.59	1.18	2.46	0.18	0.62	1.00	1.00	10.20	0.33	8.09	0.72	26.00	2.91
1.00	2.32	0.21	2.27	0.29	2.27	0.18	0.63	1.00	1.00	2.81	0.07	2.15	0.17	30.64	3.80
1.00	0.62	0.05	0.61	0.09	2.62	0.18	0.60	1.00	1.00	0.75	0.03	0.58	0.05	30.70	3.44
1.00	0.92	0.10	0.90	0.13	2.58	0.18	0.62	1.00	1.00	1.19	0.06	0.83	0.08	43.62	4.36
1.00	0.77	0.08	0.76	0.09	1.63	0.13	0.73	1.00	1.00	0.87	0.02	0.75	0.06	16.14	2.05
1.00	6.48	0.61	6.32	0.90	2.53	0.18	0.62	1.00	1.00	7.38	0.26	5.94	0.56	24.32	2.58
1.00	3.12	0.30	3.07	0.25	1.49	0.18	0.69	1.00	1.00	3.53	0.10	2.88	0.26	22.48	2.49
1.00	0.07	0.01	0.06	0.01	7.47	0.38	0.35	1.00	1.00	0.07	0.01	0.06	0.01	25.32	2.24
1.00	0.13	0.03	0.13	0.03	2.08	0.09	0.84	1.00	1.00	0.15	0.01	0.13	0.02	18.16	1.47
1.00	0.11	0.01	0.10	0.02	4.27	0.25	0.51	1.00	1.00	0.12	0.00	0.10	0.01	21.19	2.42
1.00	0.38	0.05	0.37	0.09	1.98	0.08	0.80	1.00	1.00	0.43	0.02	0.36	0.04	20.37	1.98
1.00	0.54	0.06	0.51	0.16	6.11	0.19	0.55	1.00	1.00	0.57	0.04	0.47	0.05	22.16	1.96
1.00	0.11	0.02	0.11	0.03	-2.18	-0.07	0.83	1.00	1.00	0.13	0.01	0.09	0.03	44.40	1.51
1.00	0.08	0.01	0.08	0.02	-1.43	-0.06	0.86	1.00	1.00	0.09	0.01	0.07	0.01	36.61	2.40
1.00	0.22	0.03	0.22	0.05	0.62	0.03	0.93	1.00	1.00	0.26	0.02	0.20	0.02	29.93	2.61
1.00	0.07	0.01	0.06	0.02	5.94	0.23	0.50	1.00	1.00	0.07	0.00	0.06	0.01	21.34	1.63
1.00	0.07	0.01	0.06	0.02	6.73	0.28	0.43	1.00	1.00	0.08	0.01	0.06	0.01	34.07	3.17
1.00	0.28	0.04	0.27	0.06	3.91	0.17	0.63	1.00	1.00	0.32	0.02	0.25	0.04	27.00	1.86
1.00	0.27	0.04	0.26	0.07	2.65	0.09	0.78	1.00	1.00	0.33	0.02	0.24	0.04	36.88	2.50
1.00	0.13	0.01	0.11	0.03	17.41	0.66	0.05	1.00	1.00	0.12	0.01	0.11	0.02	8.28	0.54
1.00	0.20	0.02	0.20	0.06	-2.82	-0.10	0.77	1.00	1.00	0.24	0.03	0.19	0.03	28.80	1.69
1.00	0.10	0.02	0.11	0.03	-3.42	-0.12	0.73	1.00	1.00	0.13	0.01	0.09	0.02	40.29	1.98
1.00	0.29	0.03	0.26	0.06	10.03	0.45	0.20	1.00	1.00	0.31	0.02	0.25	0.03	23.04	1.68
1.00	0.06	0.01	0.06	0.01	5.70	0.25	0.45	1.00	1.00	0.07	0.01	0.05	0.01	30.26	2.39
1.00	0.23	0.03	0.23	0.06	0.39	0.02	0.96	1.00	1.00	0.29	0.03	0.23	0.03	22.26	1.71
1.00	0.05	0.01	0.05	0.01	2.11	0.13	0.74	1.00	1.00	0.06	0.00	0.04	0.01	40.72	2.25
1.00	14.40	1.59	14.16	1.78	1.70	0.13	0.73	1.00	1.00	16.81	0.96	13.64	1.02	23.20	3.11
1.00	5.28	0.57	5.06	0.69	4.34	0.32	0.41	1.00	1.00	6.13	0.31	4.94	0.35	24.00	3.37
1.00	1.57	0.15	1.52	0.19	2.76	0.23	0.56	1.00	1.00	1.89	0.09	1.48	0.13	27.71	3.27
1.00	1.50	0.18	1.39	0.25	7.31	0.41	0.27	1.00	1.00	1.65	0.09	1.36	0.10	21.19	2.88
1.00	2.22	0.26	2.15	0.28	3.55	0.27	0.50	1.00	1.00	2.59	0.18	2.10	0.14	23.21	3.45
1.00	9.11	1.02	9.09	1.11	0.22	0.02	0.96	1.00	1.00	10.68	0.65	8.70	0.67	22.75	2.94
1.00	0.10	0.01	0.10	0.01	0.67	0.06	0.89	1.00	1.00	0.11	0.01	0.10	0.01	12.29	1.50
1.00	0.10	0.01	0.10	0.01	0.67	0.06	0.89	1.00	1.00	0.11	0.01	0.10	0.01	12.29	1.50
1.00	0.10	0.01	0.10	0.01	0.67	0.06	0.89	1.00	1.00	0.11	0.01	0.10	0.01	12.29	1.50
1.00	4.67	0.80	4.28	0.55	8.88	0.69	0.18	1.00	1.00	7.24	0.77	4.20	0.47	72.40	6.41
1.00	0.42	0.08	0.34	0.05	21.26	1.44	0.01	0.79	0.25	0.48	0.07	0.33	0.03	45.48	4.91
1.00	0.75	0.05	0.72	0.11	4.75	0.30	0.36	1.00	1.00	0.87	0.07	0.65	0.04	33.53	5.14
1.00	2.46	0.59	2.25	0.42	9.40	0.50	0.32	1.00	1.00	4.55	0.69	2.26	0.38	101.78	6.06
1.00	2.41	0.59	2.20	0.41	9.54	0.51	0.32	1.00	1.00	4.51	0.68	2.22	0.38	103.39	6.07
1.00	0.04	0.00	0.04	0.01	2.11	0.14	0.67	1.00	1.00	0.05	0.00	0.04	0.00	13.93	1.54
1.00	1.04	0.12	0.98	0.14	6.38	0.45	0.26	1.00	1.00	1.32	0.06	0.95	0.08	38.91	4.53

				Absolute Volumes Female									
			Relative Volun	ASF		GF							Relative Volumes
P-Value	FDR		FDR	Mean	SD	Mean	SD	%Diff	Effect	P-Value	FDR		FDR
0.00	0.00	**	0.01 **	415.49	15.47	357.61	29.36	16.19	1.97	0.00	0.00	**	0.01 **
0.00	0.00	**	0.00 **	368.41	15.17	320.14	24.71	15.08	1.95	0.00	0.00	**	0.26
0.00	0.00	**	0.05 *	232.86	11.06	201.01	17.19	15.84	1.85	0.00	0.00	**	1.00
0.00	0.00	**	0.21	194.77	9.57	168.44	14.37	15.63	1.83	0.00	0.00	**	1.00
0.00	0.00	**	1.00	12.23	0.46	10.39	0.77	17.79	2.40	0.00	0.00	**	1.00
0.00	0.00	**	0.88	8.92	0.21	7.47	0.55	19.33	2.61	0.00	0.00	**	0.70
0.18	1.00		0.08 -	0.94	0.12	0.87	0.12	7.66	0.58	0.27	1.00		0.42
0.36	1.00		0.01 *	0.29	0.03	0.27	0.04	7.32	0.57	0.24	1.00		0.44
0.56	1.00		0.49	0.19	0.03	0.18	0.03	4.16	0.25	0.63	1.00		0.44
0.08	0.93		0.33	0.45	0.06	0.41	0.05	9.41	0.74	0.17	0.64		0.84
0.00	0.00	**	1.00	2.38	0.18	2.04	0.14	16.48	2.45	0.00	0.00	**	1.00
0.00	0.00	**	1.00	1.86	0.15	1.57	0.12	18.61	2.40	0.00	0.00	**	1.00
0.00	0.00	**	1.00	1.35	0.12	1.13	0.09	19.64	2.34	0.00	0.00	**	1.00
0.00	0.02	*	0.51	0.51	0.04	0.44	0.03	15.97	2.06	0.00	0.00	**	1.00
0.00	0.00	**	1.00	0.52	0.05	0.47	0.04	9.43	1.22	0.05	0.37		1.00
0.00	0.00	**	0.17	182.53	9.23	158.06	13.64	15.48	1.79	0.00	0.00	**	1.00
0.00	0.00	**	1.00	37.02	1.83	32.35	2.54	14.45	1.84	0.00	0.00	**	1.00
0.00	0.00	**	1.00	2.25	0.12	1.99	0.16	12.77	1.62	0.00	0.00	**	1.00
0.00	0.00	**	1.00	1.03	0.06	0.88	0.07	16.46	2.21	0.00	0.00	**	1.00
0.00	0.00	**	1.00	11.02	0.50	9.43	0.66	16.93	2.41	0.00	0.00	**	1.00
0.02	0.00	**	1.00	0.86	0.04	0.70	0.07	22.50	2.42	0.00	0.00	**	1.00
0.00	0.00	**	0.88	10.17	0.49	8.73	0.61	16.49	2.35	0.00	0.00	**	1.00
0.00	0.00	**	1.00	1.13	0.08	1.02	0.09	11.25	1.24	0.02	0.05	*	1.00
0.00	0.00	**	1.00	1.00	0.08	0.90	0.09	10.26	1.00	0.05	0.12		1.00
0.00	0.00	**	1.00	0.14	0.01	0.11	0.01	19.09	2.50	0.00	0.00	**	1.00
0.00	0.00	**	1.00	1.94	0.12	1.67	0.08	16.05	3.35	0.00	0.00	**	1.00
0.00	0.00	**	1.00	1.94	0.12	1.67	0.08	16.05	3.35	0.00	0.00	**	1.00
0.01	0.01	**	1.00	0.86	0.05	0.71	0.05	20.08	3.07	0.00	0.00	**	0.44
0.00	0.00	**	0.69	1.08	0.07	0.96	0.06	13.04	2.19	0.00	0.00	**	1.00
0.00	0.00	**	1.00	0.42	0.03	0.36	0.03	18.88	2.10	0.00	0.00	**	1.00
0.01	0.04	*	0.71	16.44	1.18	14.43	1.63	13.96	1.24	0.01	0.01	**	1.00
0.00	0.00	**	1.00	4.32	0.22	3.63	0.52	19.23	1.35	0.01	0.00	**	1.00
0.02	0.08	-	0.30	6.07	0.48	5.45	0.49	11.46	1.27	0.02	0.02	*	0.66
0.10	0.87		1.00	0.89	0.08	0.77	0.16	14.82	0.71	0.12	0.26		1.00
0.13	1.00		1.00	0.79	0.08	0.69	0.15	14.26	0.65	0.16	0.37		1.00
0.02	0.10	-	0.69	4.37	0.40	3.89	0.41	12.34	1.17	0.03	0.02	*	1.00
0.11	0.59		0.68	0.75	0.06	0.66	0.07	12.11	1.18	0.02	0.03	*	1.00
0.21	1.00		0.49	0.52	0.04	0.47	0.04	10.37	1.09	0.04	0.07	-	1.00
0.03	0.27		1.00	0.23	0.02	0.20	0.03	16.26	1.27	0.01	0.01	*	1.00
0.00	0.01	**	1.00	2.05	0.11	1.92	0.17	6.95	0.79	0.10	0.43		1.00
0.00	0.00	**	0.06 -	38.30	1.26	31.99	2.64	19.72	2.39	0.00	0.00	**	0.01 **
0.00	0.00	**	1.00	17.62	1.16	14.83	0.97	18.83	2.87	0.00	0.00	**	0.28
0.00	0.00	**	1.00	5.37	0.32	4.63	0.47	15.94	1.58	0.00	0.00	**	1.00
0.00	0.00	**	1.00	2.24	0.12	1.95	0.22	15.09	1.34	0.01	0.00	**	1.00
0.00	0.00	**	1.00	3.13	0.25	2.68	0.26	16.56	1.70	0.00	0.00	**	1.00
0.00	0.00	**	0.81	12.26	0.99	10.20	0.59	20.14	3.50	0.00	0.00	**	0.12
0.00	0.00	**	0.06 -	6.08	0.59	5.03	0.33	20.85	3.21	0.00	0.00	**	0.07 -
0.00	0.00	**	1.00	5.49	0.37	4.57	0.38	20.29	2.41	0.00	0.00	**	0.99
0.00	0.00	**	1.00	1.77	0.08	1.47	0.12	20.33	2.47	0.00	0.00	**	1.00
0.00	0.00	**	1.00	2.60	0.19	2.11	0.21	22.90	2.32	0.00	0.00	**	0.44
0.01	0.04	*	0.42	1.13	0.12	0.98	0.07	14.64	2.02	0.00	0.01	**	1.00
0.00	0.00	**	1.00	0.68	0.08	0.61	0.05	13.02	1.47	0.02	0.01	*	1.00
0.00	0.00	**	0.02 *	20.67	0.92	17.16	1.78	20.48	1.97	0.00	0.00	**	0.66
0.00	0.00	**	0.03 *	15.11	0.72	12.44	1.31	21.48	2.04	0.00	0.00	**	0.66
0.00	0.00	**	1.00	7.65	0.56	6.56	0.67	16.64	1.63	0.00	0.00	**	1.00
0.00	0.02	*	0.16	1.98	0.18	1.68	0.22	17.67	1.34	0.01	0.01	*	1.00
0.00	0.00	**	1.00	2.22	0.13	1.93	0.18	14.70	1.59	0.00	0.00	**	1.00
0.00	0.00	**	0.67	2.44	0.18	2.09	0.19	16.97	1.83	0.00	0.00	**	1.00
0.00	0.00	**	1.00	1.01	0.09	0.85	0.09	18.17	1.64	0.00	0.00	**	1.00
0.00	0.00	**	0.00 **	1.20	0.08	0.95	0.10	25.72	2.52	0.00	0.00	**	0.17
0.00	0.00	**	0.01 *	0.21	0.01	0.17	0.02	26.03	2.67	0.00	0.00	**	0.18
0.00	0.00	**	1.00	0.50	0.01	0.41	0.05	21.79	1.84	0.00	0.00	**	1.00
0.00	0.00	**	0.00 **	0.49	0.07	0.38	0.04	29.89	2.97	0.00	0.00	**	0.03 *
0.00	0.00	**	0.00 **	6.26	0.38	4.93	0.55	27.10	2.41	0.00	0.00	**	0.08 -
0.00	0.00	**	0.22	1.04	0.09	0.87	0.10	20.11	1.76	0.00	0.00	**	1.00
0.00	0.00	**	0.00 **	0.14	0.01	0.11	0.01	24.54	2.41	0.00	0.00	**	0.17
0.00	0.00	**	0.61	0.90	0.09	0.75	0.09	19.44	1.63	0.00	0.00	**	1.00
0.00	0.00	**	0.00 **	2.88	0.30	2.08	0.24	38.50	3.33	0.00	0.00	**	0.00 **
0.00	0.00	**	1.00	1.77	0.17	1.47	0.16	20.77	1.96	0.00	0.00	**	1.00
0.03	0.42		0.08 -	0.56	0.10	0.51	0.06	10.52	0.86	0.16	0.44		0.49
0.00	0.00	**	1.00	5.56	0.27	4.72	0.50	17.87	1.67	0.00	0.00	**	1.00
0.00	0.00	**	1.00	3.85	0.17	3.29	0.35	17.00	1.61	0.00	0.00	**	1.00
0.00	0.00	**	0.82	1.72	0.11	1.43	0.16	19.86	1.78	0.00	0.00	**	1.00
0.00	0.00	**	1.00	1.17	0.07	0.98	0.11	19.37	1.74	0.00	0.00	**	1.00
0.00	0.00	**	0.36	0.55	0.03	0.45	0.05	20.92	1.86	0.00	0.00	**	1.00
0.00	0.00	**	0.05 *	107.22	6.83	93.72	8.63	14.40	1.56	0.00	0.00	**	1.00
0.01	0.04	*	1.00	4.51	0.43	4.21	0.45	7.09	0.67	0.19	0.70		1.00
0.01	0.07	-	1.00	2.62	0.21	2.46	0.27	6.43	0.58	0.23	1.00		1.00
0.00	0.03	*	1.00	1.84	0.18	1.72	0.21	7.28	0.59	0.23	1.00		1.00
0.37	1.00		1.00	0.77	0.04	0.74	0.07	4.45	0.48	0.29	1.00		1.00
0.01	0.10		1.00	1.90	0.23	1.75	0.20	8.03	0.70	0.19	0.77		0.77
0.06	0.44		0.98	1.34	0.19	1.24	0.16	8.08	0.64	0.24	1.00		1.00
0.00	0.01	*	1.00	0.56	0.05	0.52	0.06	7.91	0.73	0.15	0.77		0.99
0.00	0.02	*	1.00	0.51	0.05	0.44	0.05	17.28	1.52	0.01	0.01	**	1.00
0.00	0.01	**	1.00	5.87	0.37	5.08	0.52	15.42	1.49	0.00	0.00	**	1.00
0.02	0.08	-	1.00	3.05	0.27	2.69	0.28	13.36	1.29	0.02	0.01	**	1.00
0.01	0.08	-	1.00	0.67	0.07	0.59	0.07	12.97	1.17	0.03	0.03	*	1.00
0.05	0.47		1.00	0.41	0.04	0.35	0.05	16.13	1.18	0.02	0.11		1.00
0.04	0.10		1.00	1.97	0.17	1.74	0.18	12.93	1.26	0.02	0.01	**	1.00
0.00	0.00	**	1.00	2.82	0.22	2.40	0.26	17.73	1.61	0.00	0.00	**	1.00
0.17	1.00		0.45	2.52	0.36	2.30	0.25	9.67	0.89	0.13	0.35		1.00
0.00	0.00	**	0.68	4.78	0.25	4.03	0.40	18.57	1.88	0.00	0.00	**	1.00

0.00	0.00 **	1.00	1.55	0.09	1.30	0.12	19.46	2.04	0.00	0.00 **	1.00
0.00	0.00 **	0.13	1.44	0.05	1.23	0.11	16.72	1.80	0.00	0.00 **	1.00
0.00	0.00 **	1.00	1.79	0.11	1.50	0.17	19.31	1.67	0.00	0.00 **	1.00
0.04	0.04 *	1.00	0.96	0.06	0.91	0.11	5.66	0.49	0.28	1.00	1.00
0.04	0.04 *	1.00	0.96	0.06	0.91	0.11	5.66	0.49	0.28	1.00	1.00
0.00	0.00 **	0.69	10.08	0.98	8.59	1.00	17.33	1.49	0.01	0.01 **	1.00
0.00	0.00 **	1.00	2.61	0.24	2.18	0.32	19.55	1.33	0.01	0.00 **	1.00
0.00	0.01 **	0.83	7.47	0.77	6.41	0.68	16.57	1.55	0.01	0.01 *	1.00
0.00	0.00 **	1.00	14.12	1.00	11.98	1.10	17.90	1.95	0.00	0.00 **	1.00
0.00	0.00 **	1.00	7.96	0.65	6.61	0.57	20.42	2.36	0.00	0.00 **	1.00
0.00	0.00 **	1.00	0.70	0.02	0.58	0.06	20.50	2.07	0.00	0.00 **	1.00
0.00	0.00 **	1.00	7.27	0.64	6.04	0.52	20.41	2.37	0.00	0.00 **	1.00
0.00	0.02 *	1.00	6.16	0.44	5.36	0.56	14.80	1.43	0.01	0.01 *	1.00
0.00	0.04 *	1.00	7.39	0.50	6.76	0.41	9.19	1.50	0.01	0.03 *	1.00
0.01	0.11	0.01 *	6.44	0.49	5.98	0.59	7.78	0.78	0.11	0.28	0.24
0.11	0.93	0.00 **	3.37	0.24	3.12	0.29	8.17	0.89	0.08	0.27	0.44
0.00	0.09 -	0.48	1.67	0.15	1.58	0.16	5.46	0.54	0.28	1.00	0.51
0.00	0.00 **	1.00	1.40	0.10	1.28	0.16	9.69	0.76	0.10	0.12	1.00
0.00	0.01 **	0.41	2.36	0.20	2.01	0.21	17.70	1.68	0.00	0.00 **	1.00
0.01	0.02 *	1.00	0.22	0.02	0.19	0.02	18.95	1.63	0.00	0.00 **	1.00
0.05	0.12	0.33	0.38	0.04	0.32	0.04	19.70	1.70	0.00	0.01 *	1.00
0.02	0.04 *	1.00	0.11	0.01	0.08	0.02	28.71	1.23	0.01	0.00 **	1.00
0.00	0.01 *	1.00	1.65	0.15	1.41	0.14	16.44	1.60	0.00	0.00 **	1.00
0.00	0.00 **	0.61	2.55	0.16	2.06	0.30	23.46	1.60	0.00	0.00 **	1.00
0.00	0.01 *	0.05 -	32.64	2.32	28.52	2.82	14.46	1.46	0.01	0.01 **	1.00
0.00	0.00 **	0.48	26.41	1.91	23.11	2.14	14.26	1.54	0.01	0.01 **	1.00
0.00	0.00 **	1.00	4.35	0.20	3.64	0.37	19.48	1.94	0.00	0.00 **	1.00
0.01	0.06 -	0.28	9.14	0.65	8.23	0.68	11.04	1.34	0.01	0.03 *	1.00
0.01	0.02 *	1.00	1.02	0.08	0.86	0.09	18.27	1.71	0.00	0.00 **	1.00
0.03	0.07 -	1.00	0.33	0.03	0.28	0.04	16.67	1.18	0.02	0.03 *	1.00
0.06	0.26	1.00	0.17	0.02	0.15	0.02	19.21	1.20	0.02	0.01 *	1.00
0.01	0.02 *	1.00	0.52	0.04	0.44	0.04	18.97	2.37	0.00	0.00 **	1.00
0.00	0.00 **	1.00	3.65	0.39	3.18	0.33	14.81	1.41	0.01	0.03 *	1.00
0.00	0.01 *	0.88	2.50	0.25	2.13	0.23	17.09	1.60	0.01	0.02 *	1.00
0.00	0.00 **	1.00	0.58	0.06	0.50	0.06	16.04	1.25	0.02	0.03 *	1.00
0.01	0.06 -	0.06 -	5.16	0.39	4.56	0.50	13.24	1.22	0.02	0.03 *	1.00
0.06	0.55	0.01 **	6.23	0.89	5.41	0.77	15.33	1.08	0.05	0.13	1.00
0.00	0.00 **	0.40	2.85	0.26	2.42	0.29	17.94	1.49	0.01	0.00 **	1.00
0.00	0.01 **	0.31	9.64	0.86	8.44	0.71	14.19	1.69	0.01	0.01 **	1.00
0.00	0.02 *	1.00	2.14	0.18	1.92	0.15	11.61	1.50	0.01	0.09 -	1.00
0.00	0.00 **	1.00	1.93	0.16	1.71	0.13	12.70	1.67	0.01	0.02 *	1.00
0.00	0.07 -	1.00	1.95	0.26	1.69	0.17	15.63	1.53	0.02	0.01 *	1.00
0.00	0.00 **	0.06 -	2.63	0.20	2.29	0.22	15.02	1.59	0.00	0.00 **	1.00
0.02	0.32	0.12	0.98	0.12	0.83	0.11	18.02	1.42	0.01	0.01 **	1.00
0.00	0.00 **	0.38	38.10	2.09	32.57	2.93	16.97	1.89	0.00	0.00 **	1.00
0.00	0.00 **	1.00	9.48	0.45	8.12	0.73	16.72	1.86	0.00	0.00 **	1.00
0.00	0.00 **	1.00	4.47	0.17	3.93	0.31	13.73	1.72	0.00	0.00 **	1.00
0.00	0.00 **	1.00	1.13	0.09	0.94	0.10	20.28	1.86	0.00	0.00 **	1.00
0.00	0.00 **	1.00	1.13	0.09	0.94	0.10	20.28	1.86	0.00	0.00 **	1.00
0.00	0.00 **	1.00	2.74	0.23	2.27	0.26	21.07	1.86	0.00	0.00 **	1.00
0.00	0.00 **	1.00	1.14	0.03	0.99	0.08	15.25	1.91	0.00	0.00 **	1.00
0.00	0.00 **	1.00	1.14	0.03	0.99	0.08	15.25	1.91	0.00	0.00 **	1.00
0.00	0.00 **	0.28	28.61	1.69	24.44	2.20	17.05	1.89	0.00	0.00 **	1.00
0.00	0.00 **	1.00	6.63	0.24	5.82	0.40	13.98	2.01	0.00	0.00 **	1.00
0.04	1.00	0.01 *	0.12	0.01	0.11	0.01	10.88	1.12	0.03	0.15	0.58
0.00	0.00 **	0.05 *	3.41	0.18	3.01	0.28	13.15	1.40	0.01	0.01 **	1.00
0.00	0.00 **	0.69	3.10	0.26	2.70	0.32	15.03	1.27	0.02	0.03 *	1.00
0.00	0.00 **	1.00	2.71	0.14	2.24	0.27	21.27	1.74	0.00	0.00 **	1.00
0.00	0.00 **	0.05 *	18.33	1.53	15.59	1.59	17.58	1.72	0.00	0.00 **	1.00
0.00	0.00 **	0.05 *	18.33	1.53	15.59	1.59	17.58	1.72	0.00	0.00 **	1.00
0.00	0.00 **	1.00	0.94	0.06	0.80	0.06	17.28	2.20	0.00	0.00 **	1.00
0.00	0.00 **	1.00	0.94	0.06	0.80	0.06	17.28	2.20	0.00	0.00 **	1.00
0.00	0.00 **	1.00	92.88	3.93	82.65	4.83	12.38	2.12	0.00	0.00 **	1.00
0.00	0.01 *	0.00 **	26.28	1.52	23.77	2.05	10.56	1.22	0.02	0.06 -	0.12
0.00	0.04 *	0.00 **	11.66	0.64	10.68	0.80	9.19	1.23	0.02	0.11	0.09 -
0.00	0.00 **	0.14	4.75	0.14	4.31	0.37	10.02	1.16	0.01	0.06 -	1.00
0.02	0.31	0.00 **	6.92	0.52	6.37	0.67	8.63	0.82	0.10	0.38	0.02 *
0.00	0.00 **	1.00	0.24	0.01	0.21	0.02	11.45	1.16	0.02	0.04 *	1.00
0.00	0.00 **	1.00	0.24	0.01	0.21	0.02	11.45	1.16	0.02	0.04 *	1.00
0.00	0.00 **	1.00	0.24	0.01	0.21	0.02	11.45	1.16	0.02	0.04 *	1.00
0.00	0.01 *	0.02 *	11.09	0.68	9.93	1.05	11.61	1.10	0.03	0.06 -	0.23
0.00	0.00 **	1.00	3.29	0.21	2.94	0.26	11.93	1.33	0.01	0.02 *	1.00
0.00	0.00 **	1.00	3.29	0.21	2.94	0.26	11.93	1.33	0.01	0.02 *	1.00
0.00	0.00 **	0.33	41.50	1.00	36.99	2.56	12.19	1.76	0.00	0.00 **	1.00
0.00	0.00 **	0.28	25.02	0.64	22.78	2.39	9.81	0.94	0.04	0.06 -	1.00
0.00	0.00 **	0.05 *	0.25	0.02	0.23	0.06	10.61	0.42	0.33	1.00	1.00
0.00	0.00 **	0.05 *	0.25	0.02	0.23	0.06	10.61	0.42	0.33	1.00	1.00
0.00	0.00 **	0.05 *	0.25	0.02	0.23	0.06	10.61	0.42	0.33	1.00	1.00
0.08	0.15	1.00	0.33	0.02	0.27	0.09	20.56	0.64	0.14	0.13	1.00
0.08	0.15	1.00	0.33	0.02	0.27	0.09	20.56	0.64	0.14	0.13	1.00
0.00	0.00 **	0.29	24.44	0.65	22.28	2.47	9.67	0.87	0.05	0.08 -	1.00
0.00	0.00 **	1.00	16.48	0.41	14.20	0.83	16.02	2.76	0.00	0.00 **	1.00
0.00	0.00 **	1.00	14.98	0.44	12.97	0.73	15.46	2.73	0.00	0.00 **	1.00
0.00	0.00 **	0.00 **	0.82	0.03	0.64	0.08	27.48	2.24	0.00	0.00 **	0.44
0.00	0.00 **	0.00 **	0.82	0.03	0.64	0.08	27.48	2.24	0.00	0.00 **	0.44
0.00	0.00 **	1.00	0.68	0.03	0.59	0.05	15.97	1.79	0.00	0.00 **	1.00
0.00	0.00 **	1.00	0.68	0.03	0.59	0.05	15.97	1.79	0.00	0.00 **	1.00
0.00	0.00 **	0.16	25.10	1.66	21.89	2.32	14.66	1.38	0.01	0.00 **	0.99
0.00	0.00 **	1.00	9.74	0.35	8.40	0.71	15.87	1.88	0.00	0.00 **	1.00
0.00	0.00 **	1.00	9.11	0.36	7.88	0.67	15.62	1.85	0.00	0.00 **	1.00
0.00	0.00 **	0.14	0.62	0.04	0.52	0.05	19.62	2.02	0.00	0.00 **	1.00
0.00	0.00 **	0.30	0.49	0.04	0.40	0.05	23.51	2.02	0.00	0.00 **	1.00
0.00	0.00 **	1.00	0.13	0.01	0.12	0.02	7.04	0.53	0.26	1.00	1.00
0.01	0.01 *	0.05 -	15.37	1.33	13.49	1.69	13.91	1.11	0.03	0.03 *	0.58
0.00	0.00 **	0.05 *	42.66	1.28	36.47	3.84	16.97	1.61	0.00	0.00 **	1.00
0.00	0.00 **	0.05 *	41.57	1.25	35.57	3.75	16.87	1.60	0.00	0.00 **	1.00

0.00	0.00 **	0.07 -	17.65	0.66	15.53	1.57	13.63	1.35	0.01	0.01 **	1.00
0.00	0.00 **	1.00	1.57	0.16	1.49	0.15	5.57	0.55	0.29	1.00	1.00
0.01	0.10	1.00	1.80	0.13	1.65	0.39	9.18	0.39	0.37	1.00	1.00
0.00	0.00 **	0.90	5.29	0.28	4.64	0.44	13.94	1.47	0.00	0.00 **	1.00
0.00	0.00 **	1.00	3.76	0.19	3.33	0.31	13.16	1.41	0.01	0.01 *	1.00
0.00	0.00 **	0.48	1.52	0.10	1.31	0.14	15.93	1.47	0.01	0.01 **	1.00
0.00	0.00 **	0.71	2.44	0.08	2.12	0.49	15.08	0.66	0.13	0.16	1.00
0.00	0.00 **	0.02 *	1.00	0.12	0.78	0.25	27.36	0.86	0.06	0.05 -	1.00
0.00	0.00 **	0.01 *	1.57	0.13	1.22	0.29	29.38	1.23	0.01	0.00 **	1.00
0.00	0.00 **	0.27	2.69	0.05	2.42	0.23	11.39	1.20	0.01	0.14	1.00
0.00	0.00 **	0.69	1.29	0.10	1.22	0.14	5.65	0.50	0.29	1.00	1.00
0.00	0.00 **	0.07 -	23.92	1.14	20.03	2.22	19.39	1.75	0.00	0.00 **	1.00
0.00	0.00 **	0.55	4.70	0.35	4.17	0.46	12.49	1.14	0.03	0.06 -	1.00
0.00	0.00 **	0.22	8.26	0.50	6.68	0.91	23.65	1.74	0.00	0.00 **	1.00
0.00	0.00 **	0.02 *	4.31	0.23	3.48	0.35	23.93	2.37	0.00	0.00 **	0.84
0.00	0.00 **	1.00	3.95	0.29	3.20	0.62	23.34	1.21	0.01	0.00 **	1.00
0.00	0.00 **	0.01 **	4.15	0.16	3.47	0.52	19.64	1.32	0.01	0.00 **	1.00
0.00	0.00 **	0.00 **	2.43	0.12	2.00	0.28	21.54	1.55	0.00	0.00 **	1.00
0.00	0.00 **	0.02 *	0.97	0.04	0.80	0.08	20.20	2.07	0.00	0.00 **	1.00
0.02	0.07 -	1.00	3.41	0.31	2.90	0.49	17.49	1.04	0.03	0.04 *	1.00
0.00	0.00 **	1.00	1.10	0.06	0.91	0.12	21.00	1.65	0.00	0.00 **	1.00
0.00	0.00 **	1.00	0.31	0.02	0.25	0.04	21.70	1.57	0.00	0.00 **	1.00
0.00	0.00 **	1.00	0.39	0.02	0.32	0.04	20.55	1.53	0.00	0.00 **	1.00
0.00	0.00 **	1.00	0.40	0.02	0.33	0.04	20.91	1.83	0.00	0.00 **	1.00
0.00	0.00 **	0.08 -	40.48	1.34	33.18	4.27	22.00	1.71	0.00	0.00 **	1.00
0.00	0.00 **	0.71	6.30	0.25	5.28	0.67	19.18	1.51	0.00	0.00 **	1.00
0.00	0.00 **	1.00	2.27	0.14	1.96	0.23	15.46	1.30	0.01	0.00 **	1.00
0.00	0.00 **	1.00	0.92	0.06	0.79	0.11	17.12	1.23	0.01	0.01 **	1.00
0.00	0.01 **	1.00	1.34	0.09	1.17	0.13	14.35	1.34	0.01	0.01 **	1.00
0.00	0.00 **	0.02 *	0.21	0.01	0.16	0.02	28.95	2.09	0.00	0.00 **	0.44
0.00	0.00 **	0.02 *	2.34	0.07	1.93	0.32	21.22	1.27	0.01	0.00 **	1.00
0.00	0.00 **	0.02 *	2.34	0.07	1.93	0.32	21.22	1.27	0.01	0.00 **	1.00
0.00	0.00 **	0.02 *	2.34	0.07	1.93	0.32	21.22	1.27	0.01	0.00 **	1.00
0.00	0.00 **	1.00	1.36	0.07	1.13	0.11	20.74	2.09	0.00	0.00 **	1.00
0.00	0.00 **	1.00	1.36	0.07	1.13	0.11	20.74	2.09	0.00	0.00 **	1.00
0.00	0.00 **	1.00	0.12	0.01	0.10	0.01	19.42	1.47	0.00	0.01 **	1.00
0.00	0.00 **	1.00	0.12	0.01	0.10	0.01	19.42	1.47	0.00	0.01 **	1.00
0.00	0.00 **	0.05 *	6.44	0.28	5.05	0.67	27.50	2.07	0.00	0.00 **	0.70
0.00	0.00 **	0.03 *	5.38	0.23	4.15	0.58	29.59	2.13	0.00	0.00 **	0.44
0.00	0.00 **	0.52	0.37	0.02	0.29	0.04	26.33	2.06	0.00	0.00 **	1.00
0.00	0.00 **	0.02 *	3.48	0.18	2.61	0.38	33.30	2.29	0.00	0.00 **	0.17
0.00	0.00 **	0.01 *	2.91	0.18	2.15	0.33	35.52	2.35	0.00	0.00 **	0.12
0.00	0.00 **	1.00	0.56	0.03	0.46	0.06	22.85	1.89	0.00	0.00 **	1.00
0.00	0.00 **	1.00	0.77	0.04	0.62	0.08	23.99	1.95	0.00	0.00 **	1.00
0.00	0.00 **	1.00	0.76	0.05	0.63	0.09	21.27	1.46	0.00	0.00 **	1.00
0.00	0.00 **	1.00	1.06	0.06	0.90	0.10	17.89	1.65	0.00	0.00 **	1.00
0.00	0.00 **	0.81	0.84	0.04	0.71	0.08	17.90	1.65	0.00	0.00 **	1.00
0.00	0.01 **	1.00	0.21	0.01	0.18	0.02	14.28	1.36	0.01	0.01 *	1.00
0.00	0.00 **	0.00 **	0.03	0.00	0.02	0.00	67.57	3.73	0.00	0.00 **	0.00 **
0.00	0.00 **	0.69	0.60	0.03	0.51	0.06	17.31	1.55	0.00	0.00 **	1.00
0.00	0.00 **	1.00	0.22	0.02	0.19	0.02	17.84	1.58	0.00	0.01 **	1.00
0.00	0.00 **	1.00	0.22	0.02	0.19	0.02	17.84	1.58	0.00	0.01 **	1.00
0.00	0.00 **	0.03 *	10.39	0.26	8.59	1.18	20.87	1.52	0.00	0.00 **	1.00
0.00	0.00 **	0.00 **	2.81	0.04	2.27	0.29	23.95	1.89	0.00	0.00 **	0.99
0.00	0.00 **	0.00 **	0.74	0.01	0.61	0.09	22.15	1.56	0.00	0.00 **	1.00
0.00	0.00 **	0.00 **	1.19	0.03	0.90	0.13	32.51	2.30	0.00	0.00 **	0.09 -
0.00	0.00 **	1.00	0.88	0.06	0.76	0.09	15.26	1.24	0.01	0.01 *	1.00
0.00	0.00 **	0.45	7.57	0.22	6.32	0.90	19.76	1.40	0.00	0.00 **	1.00
0.00	0.00 **	0.68	3.58	0.13	3.07	0.25	16.77	2.02	0.00	0.00 **	1.00
0.00	0.21	1.00	0.07	0.01	0.06	0.01	3.46	0.18	0.70	1.00	0.94
0.01	0.58	1.00	0.17	0.01	0.13	0.03	30.17	1.31	0.01	0.11	1.00
0.00	0.00 **	1.00	0.12	0.01	0.10	0.02	13.37	0.79	0.09	0.23	1.00
0.00	0.00 **	1.00	0.46	0.03	0.37	0.09	23.85	1.02	0.03	0.01 *	1.00
0.00	0.00 **	1.00	0.60	0.03	0.51	0.16	19.11	0.61	0.16	0.16	1.00
0.00	0.00 **	0.26	0.13	0.00	0.11	0.03	22.66	0.75	0.09	0.17	1.00
0.00	0.00 **	0.07 -	0.10	0.01	0.08	0.02	27.11	1.18	0.01	0.00 **	1.00
0.00	0.00 **	0.24	0.27	0.01	0.22	0.05	21.23	1.03	0.02	0.02 *	1.00
0.00	0.03 *	1.00	0.07	0.01	0.06	0.02	13.03	0.50	0.27	0.80	0.25
0.00	0.00 **	1.00	0.08	0.01	0.06	0.02	26.35	1.08	0.02	0.01 *	1.00
0.00	0.00 **	1.00	0.33	0.02	0.27	0.06	23.69	1.06	0.02	0.02 *	1.00
0.00	0.00 **	0.12	0.34	0.01	0.26	0.07	29.12	1.04	0.02	0.01 **	1.00
0.24	0.49	1.00	0.12	0.00	0.11	0.03	15.41	0.59	0.18	0.22	1.00
0.00	0.00 **	1.00	0.26	0.02	0.20	0.06	27.77	0.96	0.04	0.01 *	1.00
0.00	0.00 **	0.05 *	0.14	0.01	0.11	0.03	26.18	0.90	0.05	0.04 *	1.00
0.00	0.00 **	0.70	0.32	0.02	0.26	0.06	22.21	1.00	0.03	0.01 *	1.00
0.00	0.00 **	0.08 -	0.07	0.00	0.06	0.01	18.46	0.81	0.07	0.13	1.00
0.01	0.01 **	1.00	0.29	0.03	0.23	0.06	24.37	0.95	0.04	0.03 *	1.00
0.00	0.00 **	0.09 -	0.06	0.00	0.05	0.01	23.40	1.46	0.00	0.02 *	1.00
0.00	0.00 **	1.00	17.25	0.75	14.16	1.78	21.82	1.73	0.00	0.00 **	1.00
0.00	0.00 **	0.12	6.28	0.31	5.06	0.69	24.06	1.77	0.00	0.00 **	1.00
0.00	0.00 **	0.01 **	1.92	0.07	1.52	0.19	25.88	2.12	0.00	0.00 **	0.17
0.00	0.00 **	1.00	1.67	0.13	1.39	0.25	19.52	1.10	0.02	0.01 **	1.00
0.00	0.00 **	1.00	2.70	0.17	2.15	0.28	25.72	1.99	0.00	0.00 **	1.00
0.00	0.00 **	1.00	10.96	0.49	9.09	1.11	20.57	1.69	0.00	0.00 **	1.00
0.01	0.03 *	1.00	0.11	0.01	0.10	0.01	14.61	1.29	0.01	0.04 *	1.00
0.01	0.03 *	1.00	0.11	0.01	0.10	0.01	14.61	1.29	0.01	0.04 *	1.00
0.01	0.03 *	1.00	0.11	0.01	0.10	0.01	14.61	1.29	0.01	0.04 *	1.00
0.00	0.00 **	0.00 **	6.60	1.25	4.28	0.55	54.09	4.19	0.00	0.00 **	0.01 **
0.00	0.00 **	0.01 *	0.45	0.04	0.34	0.05	31.35	2.12	0.00	0.00 **	1.00
0.00	0.00 **	0.00 **	0.81	0.06	0.72	0.11	13.18	0.84	0.07	0.04 *	1.00
0.00	0.00 **	0.00 **	4.02	1.14	2.25	0.42	79.03	4.23	0.00	0.00 **	0.01 *
0.00	0.00 **	0.00 **	3.98	1.14	2.20	0.41	80.38	4.27	0.00	0.00 **	0.01 *
0.00	0.10	1.00	0.04	0.00	0.04	0.01	7.38	0.49	0.29	1.00	0.52
0.00	0.00 **	0.00 **	1.32	0.10	0.98	0.14	34.86	2.44	0.00	0.00 **	0.12

Chapter 4

Loss of T cells impact behaviour and blood immune phenotypes over postnatal development

Shawna L. Thompson[1], Miranda Green[1], Nima Karimi[1], Dawn Bowdish[2], and Jane A. Foster[1,3]

[1] Psychiatry and Behavioural Neuroscience, McMaster University, Hamilton, ON, Canada

[2] Department of Medicine and McMaster Immunology Research Centre, McMaster University, Hamilton, ON, Canada

[3] Research Institute at St. Joe's Hamilton, Hamilton, ON Canada

CHAPTER LINK – Manuscript #3

In the previous chapter, a significant reduction in total brain volume is described, resulting from the total absence of microbiome in GF mice. To further emphasize the importance of early postnatal development on neuroanatomy, changes were observed in GF mice that were not corrected with recolonization at 5w. Also highlighting the importance of microbiota-immune-brain communication on neurodevelopment, mice with a limited ASF microbiome develop neuroanatomy comparable to control animals. The following study was performed to quantify behaviour in *TCRβ-/-δ-/-* mice from pre-puberty to adulthood in a number of different domains. As part of a new collaboration between Dr. Jane Foster and Dr. Dawn Bowdish, this study also examines how the lack of T cells impacts the innate immune system from pre-puberty to adulthood – at the time of known behavioural phenotypes.

Abstract

Recent studies have revealed that mice with adaptive immune deficiencies perform different from controls on almost all rodent behaviour tasks. Specifically, T cell deficient mice lacking the β and δ chains of the T cell receptor (*TCRβ-/-δ-/-*) showed reduced anxiety-like behaviour in several approach/avoidance behavioural tests. Research from our laboratory also indicates the relevance of early life immune function to later behavioural outcomes, as mice challenged with lipopolysaccharide in the first week of life demonstrated sex-specific alteration in both the temporal emergence and phenotypic expression of anxiety-related and exploratory behaviours. This study examines peripheral immune cells and behaviour in adolescence and adulthood in wild type (WT) and *TCRβ-/-δ-/-* mice. Behaviour was assessed using the elevated plus maze (EPM) at postnatal day 28 (P28, pre-puberty in mice), marble burying at P42, open field at P56, and fear conditioning at week 16. Both male and female *TCRβ-/-δ-/-* mice showed increased exploratory behaviour in the EPM and reduced anxiety-like behaviour. Increased locomotor activity was observed in the open field in *TCRβ-/-δ-/-* mice. Genotype and sex-by-genotype effects were observed in both cued and contextual fear conditioning in *TCRβ-/-δ-/-* mice. The behavioural differences observed in T cell deficient mice pre-puberty mirror previous findings in adult mice, suggesting that T cells influence the central nervous system early in development. Results of immunophenotyping analysis shows decreased neutrophil numbers in both male and female *TCRβ-/-δ-/-* mice at 8 weeks, and atypical developmental trajectories in peripheral immune cell populations. This study indicates that loss of T cells impacts a

broad spectrum of behaviour, including before puberty, and influences populations of innate immune cells in the peripheral blood.

Introduction

Mood disorders and mental health conditions are associated with immune factors in clinical populations, bringing widespread attention to the rapidly growing field of immune-brain communication research. Evidence that the adaptive immune system, and in particular T lymphocytes, affect brain function, neuroanatomy, and behaviour is evident in preclinical and clinical research (Alves de Lima et al., 2020; Pasciuto et al., 2020; Rilett and Foster, 2014). Lack of all functional T cells, due to a double genetic knockout of the T Cell Receptor β and δ chains (*TCRβ-/-δ-/-*) (Mombaerts et al., 1994), impacted brain function and behaviour (Caspani et al., 2021; Rilett et al., 2015; Rilett et al., 2020). Interestingly, *TCRβ-/-δ-/-* mice were found to have decreased anxiety-like behaviour in several approach avoidance tests. In parallel, *ex vivo* structural magnetic resonance imaging (MRI) showed sex-, genotype-, and sex-by-genotype differences in the volume of several brain regions in *TCRβ-/-δ-/-* mice compared to wild type (C57Bl/6, WT) (Rilett et al., 2015). Specifically, the volume of the amygdala was larger, and the hippocampus was smaller in *TCRβ-/-δ-/-* mice compared to WT mice. Female *TCRβ-/-δ-/-* mice had larger periaqueductal grey (PAG) volumes than WT female mice and had larger dorsal raphe (DR) volumes than either male *TCRβ-/-δ-/-* or female WT mice. Voxel wise analysis revealed *TCRβ-/-δ-/-* females had smaller hypothalamus volumes than WT female mice, whereas *TCRβ-/-δ-/-* males had larger volumes than WT male mice (Rilett et al., 2015).

In addition to T cells, evidence suggesting a role for monocytes in conferring messages from the peripheral immune system to the central nervous system (CNS) is building. Ly6C^{hi} monocytes from the bone marrow and spleen have been linked to

anxiety-like behaviour in chronically stressed mice (McKim et al., 2016; Wohleb et al., 2013) and have also been implicated in mechanisms of antibiotic-induced decreases in hippocampal neurogenesis (Mohle et al., 2016). Peripheral monocytes are known to respond to T cell cytokines and chemokines in both homeostatic and inflammatory conditions. The present study investigated circulating myeloid cell populations pre- and post-puberty in T cell deficient mice. In parallel, the behavioural phenotype was measured to determine whether immune and behavioural changes resulting from the absence of T cells are related.

Experimental Procedures

Animals

Mice lacking T cells due to a genetic knockout of the T cell receptor β and δ chains on a C57Bl/6 background (Mombaerts et al., 1994) and C57Bl/6 (WT) mice were bred in-house. Mice were housed in a specific pathogen free environment with a 12-hour light/dark cycle and access to food and water *ad libitum*. All experiments were completed in accordance with the guidelines set out by the Canadian Council on Animal Care and were approved by the McMaster Animal Research Ethics Board.

Behaviour

Animals were handled daily for 2 minutes one week prior to each behaviour task, and weighed weekly. All behaviour experiments were carried out in low light during the active phase of the 12-hour light cycle. Behavioural tests included elevated plus maze (4 w), marble burying (6 w), open field (8 w), and fear conditioning (12 w).

Elevated Plus Maze (EPM)

An automated EPM (Sidor et al., 2010) was used to examine anxiety-like behaviour at 4 weeks of age. This standard approach-avoidance test involves a maze with 4 perpendicular arms (35.5 cm long, 5 cm wide), shaped like a plus sign. The maze surface is elevated 66 cm over the floor, and two of the opposing arms, the closed arms, are surrounded by 15.2 cm high opaque plexiglass walls, while the two open arms have no walls preventing mice from looking over the edge. Mice were transported to the non-colony room and habituated for 30 min in low light. Each mouse was placed in the center of the maze (5 cm x 5 cm area) and behaviour was recorded for 5 min, before returning them to their home cage.

Marble burying

Marble burying was completed at 6 weeks of age. Marble burying measures spontaneous behaviour in rodents and was used to measure repetitive behaviours in mice. A cage was filled with 5 cm deep bedding and 18 glass marbles were evenly distributed on the surface of the bedding approximately 4 cm apart. A test mouse was left in the cage for 30 min. The behaviour was videotaped and the number of marbles buried (to 2/3 depth) was counted by 2 blinded observers.

Open Field Test

Behaviour in the open field was measured at 8 weeks of age using the Kinder Scientific Smart Cage Rack System consisting of a 24 cm wide x 45 cm long x 24 cm high cage system, with 22 infrared beams (7 X & 15 Y) and a rearing option (22 additional beams). Mice were tested in a non-colony behaviour room and were

habituated to the room for 1 hour prior to open field testing. Testing occurred in low light. Behaviours were recorded for 60 min (6 mice in parallel units), using Kinder Scientific Motor Monitor software (Poway, CA).

Fear Conditioning

This 2-day test was conducted at 12 weeks of age and consists of a learning trial (day 1) and 2 testing trials (day 2).

DAY 1 (learning trial) - Animals were placed in the enclosure and given 2 minutes to habituate. At the end of the 2 minutes, recorded movement was started. At 180 seconds mice were presented with an 85dB tone for 30 seconds and then received a 2 second 0.36-0.40mA foot shock. The mouse was removed to its home cage 120 seconds after the foot shock (with food) for 24 hours.

DAY 2 (cued learning test) – 24 hours after the learning phase, animals were placed in an enclosure that has a different context (white wall insert with black floor over grids) from the enclosure that they received the shock in on the previous day. They were presented with the identical 85dB tone from the previous day. Movement was recorded for 5 minutes prior to, during and after the presentation of the tone. This assessed the ability of the animal to remember the tone and pair it with the shock from the previous day.

DAY 2 (context learning test) - Learning and memory fear-conditioning (Context phase) Approximately one hour after the cue phase, inserts were removed and animals were placed back into the identical enclosure that they received the shock in on the previous

day. Movement was recorded for 5 minutes to assess the ability of the animal to remember the context and pair it with the shock from the previous day.

Behavioural data analysis

Behavioural data were analyzed by analysis of variance (ANOVA) with sex, genotype, and time when appropriate followed by Tukey's multiple comparisons test. Statistical analyses were conducted in Prism 9.3.1 for MacOS (GraphPad Software, Inc; La Jolla, CA).

Tissue Collection and Processing

Blood

Blood was collected retro-orbitally under isofluorane anesthetic from female and male WT and *TCR β-/-δ-/-* mice (n=18, 22, 18, and 18 respectively) at 4 w and 8 w of age. 100 µL of blood was collected into a heparinized tube and kept on ice until processed for flow cytometry.

Flow Cytometry

Antibodies were directly applied to 100 µL blood, followed by a 40 min incubation at 4°C. Unstained and isotype controls were prepared by replacing antibody with fluorescence-activated cell sorting (FACS) buffer or isotype antibodies for each fluorophore, respectively. The antibody panel included C - chemokine receptor type – 2 (CCR2) (PE; R&D Systems, Minneapolis, MA, USA), F4/80 (APC), lymphocyte antigen 6 complex (Ly6C) (FITC), lymphocyte common antigen (CD45) (eFluor 450), cluster of differentiation factor 11b (CD11b) (PE-Cy7), and CD3, CD19, NK1.1 (Alexa Fluor 700) from eBioscience (San Diego, CA, USA)). This was followed by a 10 min incubation in

1X Fix/Lyse Buffer (eBioscience), and centrifugation at 2000rpm for 10 minutes at 4°C. Cell pellets were washed in cold phosphate buffered saline (PBS) and re-suspended in isotonic FACS wash buffer (0.5% (w/v) bovine serum albumin (BSA), 5mM EDTA (pH 7.4-7.6), 2mM NaN3). Samples were stored in the dark in FACS buffer overnight at 4°C and run the following day on an LSRII flow cytometer (BD Biosciences, Franklin Lake, NJ, USA), with a target 200000 events recorded.

Analysis of flow cytometry

Analysis was completed with FlowJo 9 software (Treestar, Ashland, OR, USA) as shown in Fig. 4-1. GraphPad Prism 6 (La Jolla, CA) was used for statistical analysis and to create graphs. Data were analyzed by 2-way ANOVA with sex and genotype as factors, and post-hoc analysis using Tukey's Test was completed when appropriate. A p-value of <0.05 was considered significant.

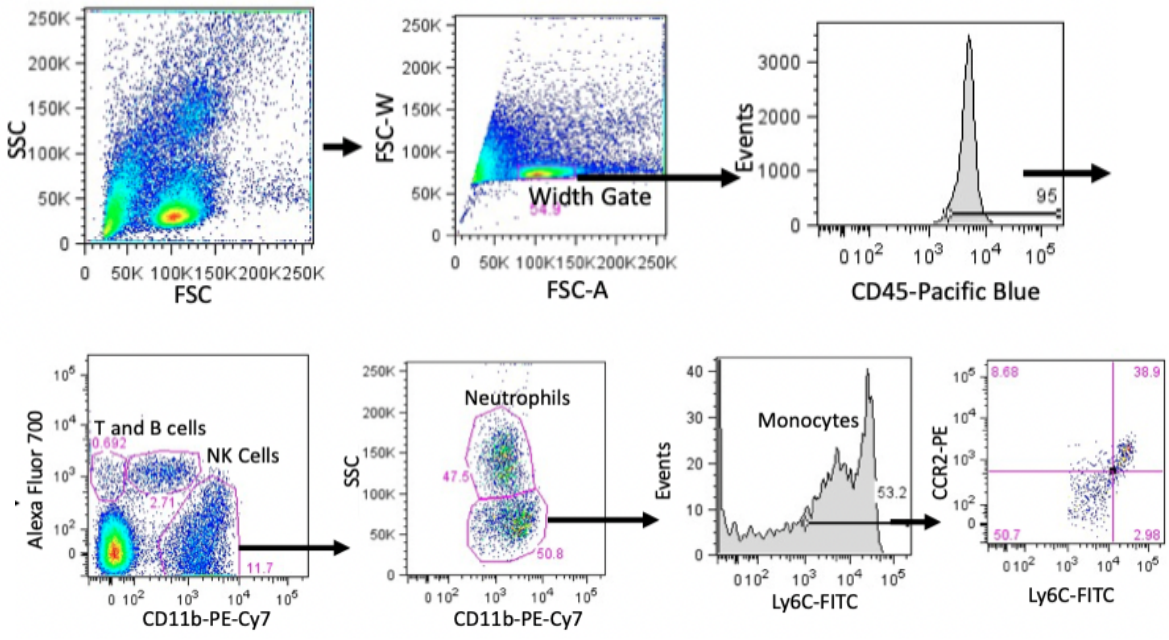

Figure 4-1. Gating strategy for flow cytometry analysis.

Results

Reduced anxiety-like behaviour phenotype was observed in T cell deficient mice pre-puberty

Previous work showed that adult *TCRβ-/-δ-/-* mice and other models of T cell and adaptive immune deficiency demonstrated a consistent behavioural phenotype of reduced anxiety-like behaviour compared to WT controls (Cushman et al., 2003; Rilett et al., 2015). Three-way repeated measures ANOVA showed a significant main effect of EPM zone ($F[2,249]=4311$, $p<0.0001$) and a significant Zone by Genotype interaction ($F[2,249]=26.0$, $p<0.0001$). Both male and female *TCRβ-/-δ-/-* mice spent more time in the intersection compared to WT mice, as well as an increased number of open arm entries (Fig. 2). No difference in closed arm entries were observed.

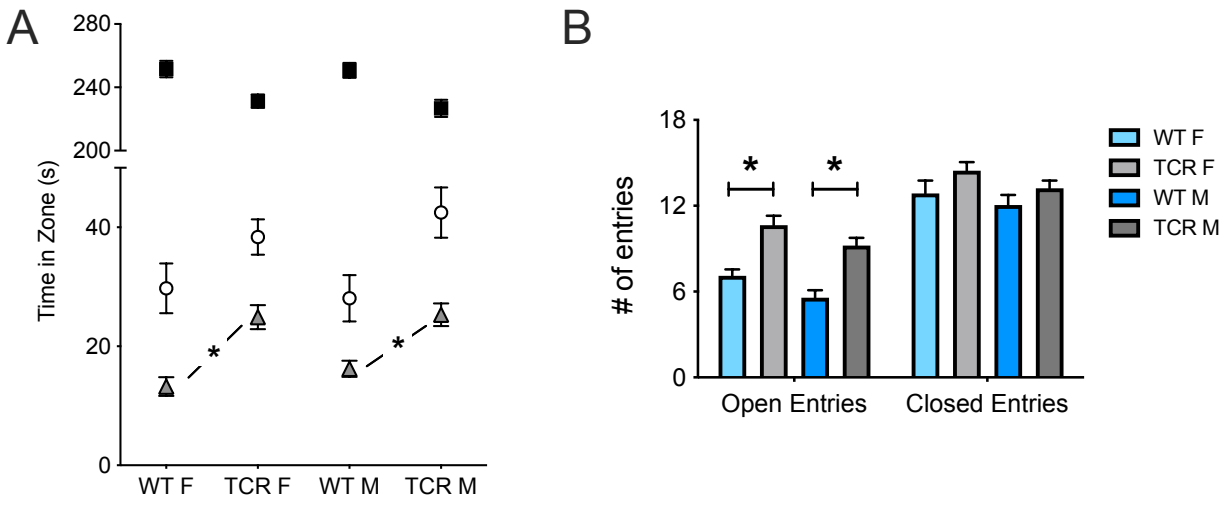

Figure 4-2. Reduced anxiety-like behaviour measured in the elevated plus maze (EPM) in T cell deficient mice. At 4 weeks of age, both male and female *TCRβ-/-δ-/-* mice spent less time in the intersection (grey triangles) of the EPM compared to sex-matched WT mice (A). No difference in closed arm time (black square) or open arm

time (open white circles) was observed. The total number of open arm entries was significantly higher in *TCRβ-/-δ-/-* mice (B).

No genotype differences were observed in marble burying at 6 weeks of age

Three-way repeated measures ANOVA (sex, genotype, time) showed a significant main effect of time ($F[2.97,207.9)=152.3$, $p<0.0001$) and a significant time x sex interaction ($F[4, 280]=3.93$, $p=0.004$), however, posthoc analysis showed no difference by genotype or sex at each time point (Fig. 3).

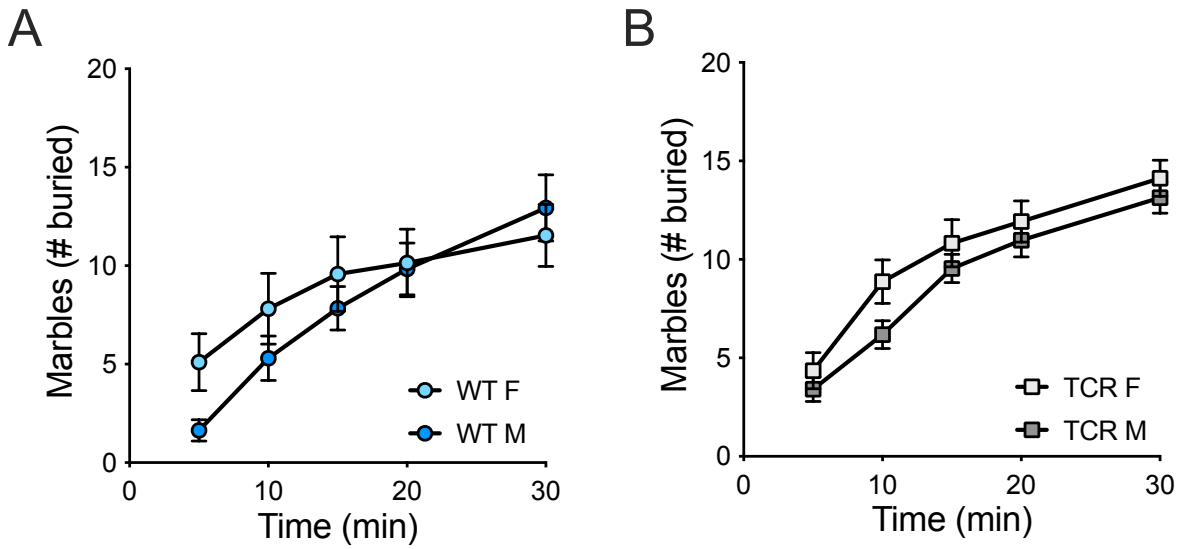

Figure 4-3. Marble burying in WT (A) and *TCRβ-/-δ-/-* (B) mice. No genotype differences were observed in repetitive behaviour measured by number of marbles buried in 30 mins.

Activity in the open field is increased in T cell deficient mice in early adulthood

How a mouse explores the open field can be used to examine many different behaviours. The total distance a mouse travels over the testing period can be used to determine activity levels, and rearing can be used to quantify exploratory behaviour.

During a 30 min testing period, a main effect of genotype was observed for distance travelled in the open field ($F[1,80]=21.1$, $p<0.0001$). T cell deficient mice showed increased locomotor activity in the open field compared to WT. No significant sex and genotype matched differences were observed for rearing in the open field (Fig. 4).

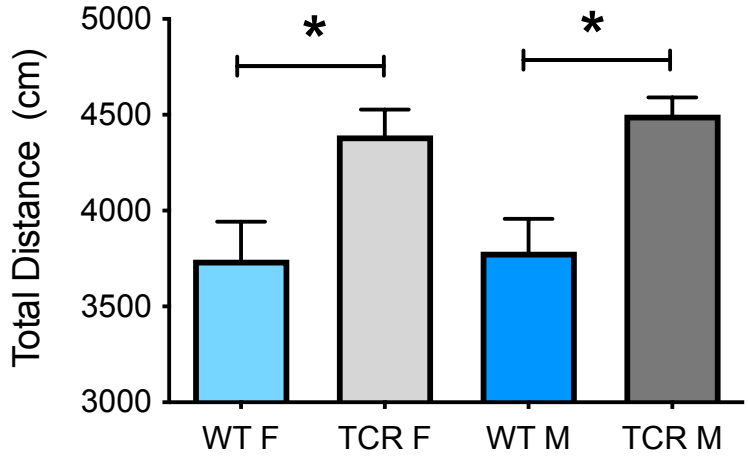

Figure 4-4. T cell deficient mice had increased locomotor activity in the open field. Both male and female *TCRβ-/-δ-/-* mice travelled a greater total distance in the open field. *p<0.05

T cell deficient mice showed sex and genotype differences in fear conditioning

Three-way repeated measures ANOVA revealed a significant main effect of time ($F[9.8, 739]=84.7$, $p<0.0001$) and genotype ($F[1,77]=7.95$, $p=0.006$) on distance travelled during day 1 fear conditioning learning trial, as well as a significant time x genotype interaction ($F[19, 1433]=1.64$, $p=0.04$). Male WT mice were more active prior to and following the cue and shock compared to male *TCRβ-/-δ-/-* mice (Fig. 5). No differences in behaviour were observed on day 1 for female mice.

Three-way repeated measures ANOVA (time, sex, genotype) revealed a significant main effect of time ($F[13.2, 920.4]=18.5$, $p<0.00001$) and genotype ($F[1,70]=33.4$, $p<0.00001$) on distance travelled during the cued learning test on day 2. Significant interactions included time x genotype, time x sex, and time x genotype x sex. Several significant genotype differences were observed in male mice, and less in female mice (Fig. 5). Differences in contextual learning were present as immobility time during the 6 min trial and was also examined at 1 min intervals through the trial (Fig. 5). A significant main effect of sex ($F[1,75]=6.0$, $p=0.017$) and genotype ($F[1,75]=5.92$, $p=0.017$) was observed for immobility time, where female *TCRβ-/-δ-/-* mice had lower immobility time than female WT mice and male *TCRβ-/-δ-/-* mice. A significant main effect of genotype ($F[1, 360]=44.8$, $p<0.00001$) and a significant time x genotype interaction ($F[4,360]=2.55$, $p=0.039$) for distance travelled during the contextual learning trial with WT male mice showed increased activity during the first 2 minutes of the contextual learning trial and no differences between female mice (Fig. 5).

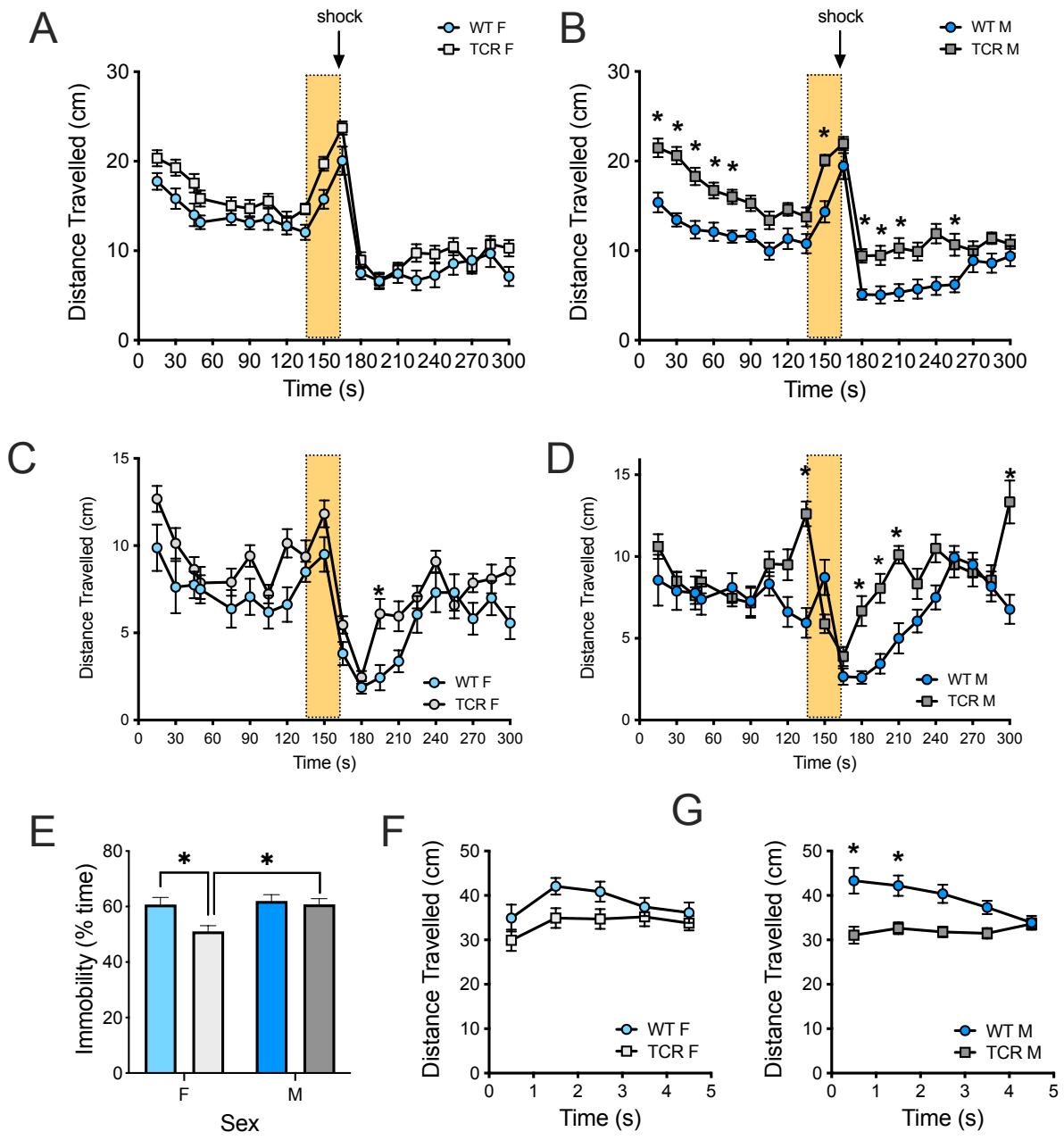

Figure 4-5. Fear conditioning in WT and *TCRβ-/-δ-/-* mice. Distance travelled during day 1 learning trial in female (A) and male (B) mice. Distance travelled during the cued test in female (C) and male (D) mice. Total immobility time during contextual test (E), as well as distance travelled during the contextual text in female (F) and male (G) mice.

T cell deletion impacts numbers of blood myeloid cells

T cells are known to play critical roles in orchestrating immune responses and maintaining immune tone in peripheral tissues. To determine what impact T cell deletion has on peripheral immune phenotypes, myeloid cell numbers were quantified in blood from 4- and 8-week-old mice. When comparing monocyte numbers relative to total myeloid cell number, in *TCRβ-/-δ-/-* and WT mice, a significant main effect of genotype ($F[1,73]=13.4$, $p=0.0005$ and age ($F[1,65]=117.9$, $p<0.0001$) was observed. Posthoc analysis revealed a significant decrease in monocyte numbers from 4 to 8 weeks of age for both sexes and both genotypes (Fig. 6). Density plots for monocytes at 4 weeks and 8 weeks of age (Fig. 6) showed a high level of variability at 4 weeks of age in both WT and *TCRβ-/-δ-/-* mice, that was reduced in 8-week-old WT mice, whereas 8-week-old *TCRβ-/-δ-/-* mice were more variable.

Neutrophils are the predominant cell type in the myeloid cell compartment and are also known to respond to T cell signaling. In order to determine what impact T cells may have on neutrophil numbers over early life, we quantified CD45+CD3-CD19-NK1.1-CD11b+SSC^{hi} cell numbers as a percentage of total myeloid cells in blood collected at 4 and 8 weeks. A significant main effect of genotype ($F[1,77]=21.7$, $p<0.0002$) and age ($F[1,69]=117.2$, $p<0.0001$) was found. Posthoc analysis revealed a significant change in neutrophil numbers from 4 to 8 weeks of age for both sexes and both genotypes (Fig. 6). Density plots for neutrophils at 4 week and 8 weeks of age (Fig. 6) showed a high level of variability at 8 weeks of age in *TCRβ-/-δ-/-* mice compared to WT mice. At 8 weeks of age, male and female *TCRβ-/-δ-/-* mice had significantly more neutrophils than WT mice.

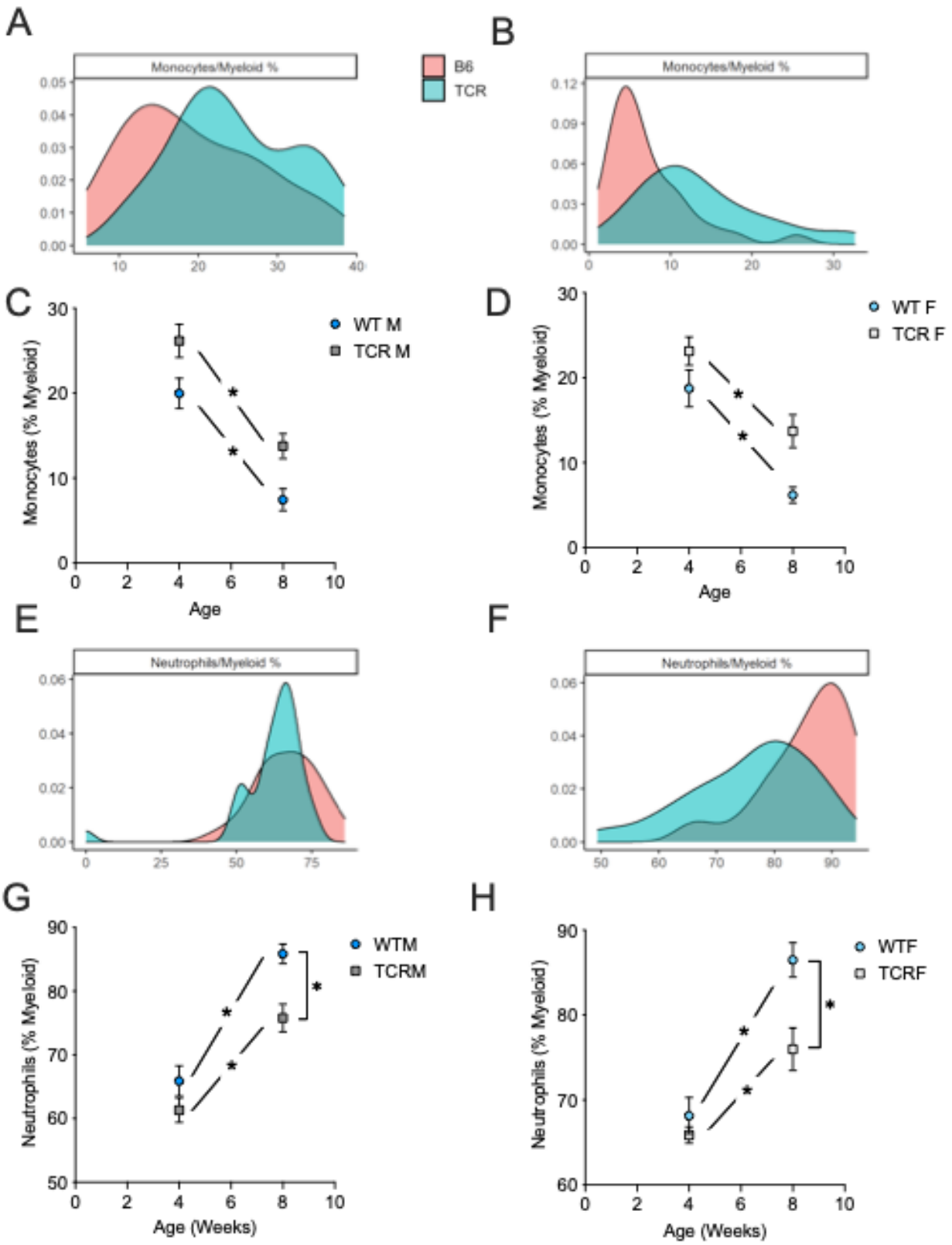
A
Monocytes/Myeloid %
B6
TCR
B
Monocytes/Myeloid %
C
Monocytes (% Myeloid)
WT M
TCR M
Age
D
Monocytes (% Myeloid)
WT F
TCR F
Age
E
Neutrophils/Myeloid %
F
Neutrophils/Myeloid %
G
Neutrophils (% Myeloid)
WTM
TCRM
Age (Weeks)
H
Neutrophils (% Myeloid)
WTF
TCRF
Age (Weeks)

Figure 4-6. Immune phenotype at 4 and 8 weeks of age in WT and *TCRβ-/-δ-/-* mice. Monocyte density plots for WT and *TCRβ-/-δ-/-* mice at 4 weeks (A) and 8 weeks (B) of age. Number of monocytes at 4 weeks and 8 weeks of age in males (C) and females (D). Neutrophil density plots for WT and *TCRβ-/-δ-/-* mice at 4 weeks (E) and 8 weeks (F) of age. Number of monocytes at 4 weeks and 8 weeks of age in males (G) and females (H). *p<0.05

Discussion

The mechanisms for T cell impact on brain development, structure, and behaviour remain unknown. Here, we demonstrate that the low anxiety-like behaviour and high exploratory behaviour and activity levels previously observed in T cell deficient adults are present pre-puberty, and we aim to establish target systems in which mechanisms for these brain changes may occur. To do so, we investigated how loss of T cells affects the immune phenotype, reporting a decrease in neutrophil numbers and increased variability in immune phenotype in *TCRβ-/-δ-/-* mice that was present pre-puberty and persisted to adulthood. We also report no behaviour differences in the marble burying task, and sex- and sex-by-genotype differences in cued and contextual fear conditioning, which indicate impaired fear memory in T cell deficient mice compared to controls.

Importantly, work from our lab demonstrated that mice specifically lacking all mature T cells via a double mutation in T cell receptor genes recapitulated the reduction in anxiety-like behaviour often observed in immunodeficient mice, but *μMT-/-* mice that

were selectively deficient in B cells did not (Rilett et al., 2015). These *TCRβ-/-δ-/-* mice also had neuroanatomical changes in stress circuitry, including genotype- and sex-by-genotype effects, demonstrating that T cells impact brain structure and the resulting behaviour even though they do not appear to reside in the brain parenchyma in significant numbers under homeostatic conditions (Rilett et al., 2015).

TCRβ-/-δ-/- mice have a robust reduced anxiety-like behaviour phenotype that is similar to what we have observed in adults in previous research (Rilett et al., 2015), which we show here to be measurable by week 4 and persist throughout adulthood. These findings agree with past research using a variety of models of adaptive immune deficiency in demonstrating a role for the adaptive immune system, and T cells in particular, in the development of anxiety-like behaviour (Cushman 2003, McGowan 2011, Sankar 2012, Rattazzi 2013, Clark 2014, Brachman 2015, Clark 2015, Desbonnet 2015, Arensten 2018, Nadeen 2019).

A study that focused on restoring cluster of differentiation 4 (CD4+) T cells to recombination activating gene 1 knockout (*RAG1-/-*) mice reverted the observed repetitive and anxiety-like behaviours, but stopped short of identifying the related mechanism, as they found no differences in corticosterone, serum cytokines, or brain structure between groups (Rattazzi et al., 2013). The rescue of repetitive behaviour on the marble burying task is interesting in the context of the present work, as *TCRβ-/-δ-/-* mice do not have any significant difference in marble burying compared to WT (Rattazzi et al., 2013). This suggests that differences in the model of adaptive immunodeficiency may affect behaviour outcomes, either through CNS *RAG1* expression, or the manipulation of both B and T cell populations in *RAG1-/-* mice (Fang et al., 2013;

Mombaerts et al., 1992). It has also been demonstrated that CD8+ T cells are necessary to confer neural and behavioural effects of environmental enrichment, however, no mechanism for T cell-brain communication was determined, as genes controlling T cell function at the choroid plexus were not changed in the experimental group (Zarif et al., 2018).

By measuring the impact of T cell depletion on both behaviour and circulating innate immune cell numbers at pre- and post-puberty time points, we were able to determine whether myeloid cells in the blood are likely to affect approach-avoidance behaviour in mice. While profiles of blood myeloid cells are affected by the absence of T cells, with neutrophil numbers decreased in adult *TCRβ-/-δ-/-* mice, in this study we did not find correlation between immune cell numbers and behaviour outcomes. There is promise for further research investigating $Ly6C^{lo}CCR2^{lo}$ monocytes and EPM poke arounds at pre-puberty time points. Likewise, further investigation into potential roles for $Ly6C^{hi}CCR2^{hi}$ monocytes in affecting distance travelled in the periphery of the open field is merited. Previous work indicates that individual differences in immune outcomes may correspond with relevant behaviour outcomes (Hodes, 2013).

The data presented here suggest that T cells influence behaviour at the earliest stages of postnatal development, as evidenced by behaviour changes on approach-avoidance tasks at P28, before puberty. Recent evidence suggests that behaviour changes in *TCRβ-/-δ-/-* mice can be detected as early as P14, with delays in righting reflex development compared to controls (Francella pers commun, in preparation). Taken together, these findings suggest that changes in innate immune cell numbers in the periphery would be most likely to precede behavioural changes, and future research

investigating circulating innate immune cell levels in the first few weeks of postnatal life is merited.

Alternative mechanisms by which T cells communicate with the CNS through local interactions with innate immune cells and their precursors, may present additional avenues through which immune-brain communication in early life can be detected. Recent work suggests that cdT cells in the meninges affect anxiety-like and exploratory behaviour on the EPM and open field test (Alves de Lima et al., 2020). Delivery of anti-cdT cell antibodies was sufficient to eliminate the behaviour phenotype, and the authors determined that the cdT cell impact on behaviour is dependent on IL-17A (Alves de Lima et al., 2020). The presence of these behaviour changes in early life suggests that the biological changes that occur over puberty are not necessary for the behaviours to manifest.

Because T cells modulate neutrophil generation and release from precursors through interleukin 17-A (IL-17A) and granulocyte monocyte colony stimulating factor (GM-CSF), there remains a possibility that neutrophils may be involved in this immune-brain communication mechanism, at a local rather than systemic level (Lieschke et al., 1994). One way in which this may occur is via a recently described pathway by which motor circuits cause a widespread efflux of neutrophils from the bone marrow to peripheral tissues via chemokine attraction in response to acute stress (Poller et al., 2022). Additionally, in response to corticosterone signaling cues from the paraventricular nucleus of the hypothalamus, monocytes return to the bone marrow from the blood and other immune tissues (Poller et al., 2022).

Mice subjected to stressors have been shown to have peripheral monocytes from the bone marrow or spleen recruited to the brain (Wohleb 2013, McKim 2015). This was found to correlate with the increased levels of anxiety-like behaviour recorded after stress exposure (McKim et al., 2016; Wohleb et al., 2013). Recently, Ly6C^{hi} monocytes have been associated with novel object recognition and have been found to be part of a communication pathway between gut microbes and brain function (Mohle et al., 2016).

Likewise, T cell communication to myeloid precursors and monocytes has recently been determined to play an important role in immune-brain communication at the dural sinuses, additional evidence for immune-brain communication in a highly localized region (Rustenhoven et al., 2021). Under homeostatic conditions, glymphatic processes flush extracellular fluid through the brain parenchyma and into the cerebrospinal fluid (CSF), where antigen presenting cells (APCs) reside. These APCs then present proteins and antigens from the CSF to T cells monitoring the brain perimeters, which reside in higher numbers in the dural sinuses (Rustenhoven et al., 2021). Recently, tiny channels through the skull bone have been discovered, revealing a physical connection for the CSF to access bone marrow in the skull, where myeloid precursors reside, and recruit them directly to the brain meninges via the CSF, where they are likely to interact with T cells (Mazzitelli et al., 2022). Furthermore, research suggests that peripheral T cells responding to chemotactic signals concentrate at the choroid plexus, where they communicate with parenchymal cells and influence microglia activation and adult neurogenesis (Qi et al., 2016). While this is a compelling body of evidence in support of intensive immune-brain communication in the CNS and brain surroundings, immune communication that affects behaviour is likely to also be

localised to the gut mucosal tissue, which is the location of the vast majority of immune cells in both mice and humans. Future research should also identify T cell influence on the innate immune cells and microbiota in the gut as another critical location of immune-brain communication.

References

Alves de Lima, K., Rustenhoven, J., Da Mesquita, S., Wall, M., Salvador, A.F., Smirnov, I., Martelossi Cebinelli, G., Mamuladze, T., Baker, W., Papadopoulos, Z., Lopes, M.B., Cao, W.S., Xie, X.S., Herz, J., and Kipnis, J. (2020). Meningeal gammadelta T cells regulate anxiety-like behavior via IL-17a signaling in neurons. Nat Immunol *21*, 1421-1429.

Caspani, G., Green, M.J., Swann, J.R., and Foster, J.A. (2021). Microbe-immune crosstalk: evidence that T cells influence the brain metabolome. *submitted*.

Cushman, J., Lo, J., Huang, Z., Wasserfall, C., and Petitto, J.M. (2003). Neurobehavioral changes resulting from recombinase activation gene 1 deletion. Clin Diagn Lab Immunol *10*, 13-18.

Fang, M., Yin, Y., Chen, H., Hu, Z., Davies, H., and Ling, S. (2013). Contribution of Rag1 to spatial memory ability in rats. Behav Brain Res *236*, 200-209.

Hodes, G.E. (2013). Sex, stress, and epigenetics: regulation of behavior in animal models of mood disorders. Biology of sex differences *4*, 1.

Lieschke, G.J., Grail, D., Hodgson, G., Metcalf, D., Stanley, E., Cheers, C., Fowler, K.J., Basu, S., Zhan, Y.F., and Dunn, A.R. (1994). Mice lacking granulocyte colony-stimulating factor have chronic neutropenia, granulocyte and macrophage progenitor cell deficiency, and impaired neutrophil mobilization. Blood *84*, 1737-1746.

Mazzitelli, J.A., Smyth, L.C.D., Cross, K.A., Dykstra, T., Sun, J., Du, S., Mamuladze, T., Smirnov, I., Rustenhoven, J., and Kipnis, J. (2022). Cerebrospinal fluid regulates skull bone marrow niches via direct access through dural channels. Nat Neurosci *25*, 555-560.

McKim, D.B., Patterson, J.M., Wohleb, E.S., Jarrett, B.L., Reader, B.F., Godbout, J.P., and Sheridan, J.F. (2016). Sympathetic Release of Splenic Monocytes Promotes Recurring Anxiety Following Repeated Social Defeat. Biol Psychiatry *79*, 803-813.

Mohle, L., Mattei, D., Heimesaat, M.M., Bereswill, S., Fischer, A., Alutis, M., French, T., Hambardzumyan, D., Matzinger, P., Dunay, I.R., and Wolf, S.A. (2016). Ly6C(hi) Monocytes Provide a Link between Antibiotic-Induced Changes in Gut Microbiota and Adult Hippocampal Neurogenesis. Cell Rep *15*, 1945-1956.

Mombaerts, P., Iacomini, J., Johnson, R.S., Herrup, K., Tonegawa, S., and Papaioannou, V.E. (1992). RAG-1-deficient mice have no mature B and T lymphocytes. Cell *68*, 869-877.

Mombaerts, P., Mizoguchi, E., Ljunggren, H.G., Iacomini, J., Ishikawa, H., Wang, L., Grusby, M.J., Glimcher, L.H., Winn, H.J., Bhan, A.K., and Tonegawa, S. (1994). Peripheral lymphoid development and function in TCR mutant mice. Int Immunol *6*, 1061-1070.

Pasciuto, E., Burton, O.T., Roca, C.P., Lagou, V., Rajan, W.D., Theys, T., Mancuso, R., Tito, R.Y., Kouser, L., Callaerts-Vegh, Z., de la Fuente, A.G., Prezzemolo, T., Mascali, L.G., Brajic, A., Whyte, C.E., Yshii, L., Martinez-Muriana, A., Naughton, M., Young, A., Moudra, A., Lemaitre, P., Poovathingal, S., Raes, J., De Strooper, B., Fitzgerald, D.C., Dooley, J., and Liston, A. (2020). Microglia Require CD4 T Cells to Complete the Fetal-to-Adult Transition. Cell *182*, 625-640 e624.

Poller, W.C., Downey, J., Mooslechner, A.A., Khan, N., Li, L., Chan, C.T., McAlpine, C.S., Xu, C., Kahles, F., He, S., Janssen, H., Mindur, J.E., Singh, S., Kiss, M.G., Alonso-Herranz, L., Iwamoto, Y., Kohler, R.H., Wong, L.P., Chetal, K., Russo, S.J.,

Sadreyev, R.I., Weissleder, R., Nahrendorf, M., Frenette, P.S., Divangahi, M., and Swirski, F.K. (2022). Brain motor and fear circuits regulate leukocytes during acute stress. Nature *607*, 578-584.

Qi, F., Yang, J., Xia, Y., Yuan, Q., Guo, K., Zou, J., and Yao, Z. (2016). A(H1N1) vaccination recruits T lymphocytes to the choroid plexus for the promotion of hippocampal neurogenesis and working memory in pregnant mice. Brain Behav Immun *53*, 72-83.

Rattazzi, L., Piras, G., Ono, M., Deacon, R., Pariante, C.M., and D'Acquisto, F. (2013). CD4(+) but not CD8(+) T cells revert the impaired emotional behavior of immunocompromised RAG-1-deficient mice. Transl Psychiatry *3*, e280.

Rilett, K.C., and Foster, J.A. (2014). T lymphocytes and anxiety: A review of clinical and animal studies. Annals of Depression and Anxiety *1*, 1-5.

Rilett, K.C., Friedel, M., Ellegood, J., MacKenzie, R.N., Lerch, J.P., and Foster, J.A. (2015). Loss of T cells influences sex differences in behavior and brain structure. Brain Behav Immun *46*, 249-260.

Rilett, K.C., Luo, O.D., McVey-Neufeld, K.A., MacKenzie, R.N., and Foster, J.A. (2020). Loss of T cells influences sex differences in stress-related gene expression. J Neuroimmunol *343*, 577213.

Rustenhoven, J., Drieu, A., Mamuladze, T., de Lima, K.A., Dykstra, T., Wall, M., Papadopoulos, Z., Kanamori, M., Salvador, A.F., Baker, W., Lemieux, M., Da Mesquita, S., Cugurra, A., Fitzpatrick, J., Sviben, S., Kossina, R., Bayguinov, P., Townsend, R.R., Zhang, Q., Erdmann-Gilmore, P., Smirnov, I., Lopes, M.B., Herz, J., and Kipnis, J.

(2021). Functional characterization of the dural sinuses as a neuroimmune interface. Cell *184*, 1000-1016 e1027.

Wohleb, E.S., Powell, N.D., Godbout, J.P., and Sheridan, J.F. (2013). Stress-induced recruitment of bone marrow-derived monocytes to the brain promotes anxiety-like behavior. J Neurosci *33*, 13820-13833.

Zarif, H., Nicolas, S., Guyot, M., Hosseiny, S., Lazzari, A., Canali, M.M., Cazareth, J., Brau, F., Golzne, V., Dourneau, E., Maillaut, M., Luci, C., Paquet, A., Lebrigand, K., Arguel, M.J., Daoudlarian, D., Heurteaux, C., Glaichenhaus, N., Chabry, J., Guyon, A., and Petit-Paitel, A. (2018). CD8(+) T cells are essential for the effects of enriched environment on hippocampus-dependent behavior, hippocampal neurogenesis and synaptic plasticity. Brain Behav Immun *69*, 235-254.

Chapter 5

General Discussion

Summary of Findings

T cells have long been studied as a principal component of the adaptive immune system, where they communicate with immune and non-immune cells alike. These lymphocytes are able to access the interface of the brain and periphery and to communicate with all cell types. For this reason, a body of research has been rapidly growing, demonstrating that T cells are a key component of the microbiota-immune-brain axis. This thesis addresses gaps in the current literature relating to when T cells affect neurodevelopment, how the loss of T cells affects innate immune cell populations in the CNS and periphery, and how manipulating the microbiome at important times in early life immune-brain communication affects brain structure.

This thesis examined the importance of T cells to brain function using T cell deficient mice. We examined this topic from a number of perspectives, to explore the diverse ways T cells communicate with various cells and systems. These include measuring microglia, brain structure, behaviour, and innate immune cells in the blood. The central hypothesis was that T cells impact brain development and behaviour as well as peripheral and central innate immune cell populations as part of their role in the microbiome-gut-brain axis. To test this hypothesis, two T cell deficient mouse models were used: *TCRβ-/-δ-/-* mice, which lack all mature T cells by genetic knockout of genes encoding the T cell receptor, and GF mice, which have underdeveloped adaptive immune systems due to the absence of microbiota signals during critical times in development.

The first study examined the effect of T cell deficiency on the brain. A loss of T cells led to an increased number of microglia in the BLA of adult mice, and sex-specific

decreases in microglia density in the PFC and HIP. These findings demonstrate that loss of T cells cause lasting changes in microglia in key components of the brain's stress circuitry that persist until adulthood. Associating these specific cellular changes with brain regions known to have volume differences in T cell deficient mice and that are also implicated in the behaviours that are impacted by adaptive immune deficiency is an important first step in determining cellular mechanisms for immune-brain communication. Building on these findings, study two demonstrated that loss of microbiota in GF mice results in widespread impacts on brain volume. Specifically, we found a profound reduction in total brain volume in GF mice that is not corrected by recolonization at 5 weeks. This work also revealed sensitivity of the cortex and hippocampus to microbe manipulation, and sex differences in the number of regions with relative volume changes in GF mice. Combining the findings from study one and two we established the early postnatal window as a critical time for microbiota-immune-brain communication to influence stress circuitry. Lastly, study three addressed the effects of T cell deletion on behaviour and on the developmental trajectory of peripheral myeloid cells. Importantly, we established behavioural phenotypes common to T cell deficient mice are present before puberty, suggesting that T cells affect behaviour in the earliest parts of development. In addition, we report the developmental trajectory of monocyte and neutrophil populations across puberty, describing a maturation in WT mice that is absent or delayed in the absence of T cells.

Combined, the results of these studies provide a multifaceted and thorough examination of the impacts a loss of T cells has on the developing microbiota-immune-brain axis. This work demonstrates that the impacts of T cell deficiency on microglia in

the CNS last until adulthood. These findings reveal adaptive immunodeficiency, and widespread neuroanatomical changes associated with the absence of microbes in GF mice. The neurobiological impacts of microbiota-immune-brain axis inputs and manipulations reveal an early postnatal timeline for their ability to aid brain development. Additionally, this work recapitulates prior findings of reduced anxiety-like behaviour in the *TCRβ-/-δ-/-* mouse before puberty, indicating that T cells affect behaviour early in development. These phenotypes are present long before the maturation of immunological and microbiota systems.

This thesis contributes novel findings addressing gaps in the literature on the role of T cells in microbiota-immune-brain communication at the level of the peripheral immune system the brain behaviour. Ideally, this work will allow for researchers to design future experiments at times where T cells are most likely to be actively influencing neurobiology. Future work translating the understanding of how peripheral immune cells mature should also reduce heterogeneity in clinical trials targeting pathology with known immune-brain components, such as neurodevelopmental and mood disorders. In this chapter, I will broaden the context of these findings to related published literature. Further, I will discuss the location, timing, and mechanisms for T cell communication with the brain. Finally, I will tie key themes of this work to relevant clinical research on immune impacts on mental health.

T cell impacts on CNS development in early postnatal life

Nervous system and gut microbiome development occur in distinct locations but with overlapping time frames. This means that the nervous system is undergoing critical

developmental stages during times of change in the gut microbiome (Borre et al., 2014). Research from our laboratory group reveals that behaviour changes in T cell deficient mice are present from the earliest stages of postnatal life, with detection of delayed righting reflex development from P4. Work from this thesis confirms that reduced anxiety-like behaviour was observed at P28 and persists to adulthood (Rilett *et al.*, 2015). Detecting behaviour changes this early in development suggests that loss of T cells affects neurodevelopment *in utero* or in the earliest stages of postnatal life and is "locked in" after this point.

The findings presented in study 2 of this thesis suggest that microbiota status has its largest impact on brain development in the first few weeks of postnatal life, as the *in utero* environment is largely sterile. The impact of microbiota depletion and manipulation on neuroanatomy is most prominent in the first 5 weeks of postnatal life; the time between when the neonate is born, acquiring its first microbiome, and puberty. This is evidenced by the inability to rescue typical brain structure or total brain volume through recolonization of GF mice with a conventional microbiome at 5 weeks (Thompson et al., submitted). Importantly, while still smaller than control animals, recolonization after 5 weeks increased total brain volume compared to GF in males only, suggesting that susceptibility to developmental effects of microbial signals may be different between the sexes (Thompson *et al.*, submitted).

While studies have examined many aspects of behaviour in GF mice, it is increasingly important to determine changes at the brain level in GF mice. Few studies have done this to date. One key study investigated amygdala and hippocampus volumes and their relation to neuron morphology in GF mice using histological methods

(Luczynski et al., 2016) which may differ from ex vivo MRI, and another MRI study of GF mice compared brain volumes before and after puberty (Lu et al., 2018). These researchers identified increased volume in the basal lateral amygdala, central amygdala, and lateral amygdala in GF mice compared to controls (Luczynski et al., 2016). In study two of this thesis, relative hippocampal volume was decreased in both male and female mice (FDR<0.05), with CA1, CA2, CA3, and dentate gyrus subregions having significantly reduced volumes in GF males, but only the granule layer of the dentate gyrus having significantly decreased volume in GF females. In contrast, past work describes increased hippocampal and CA2/CA3 subregion volume, but no differences were reported in CA1 or the DG (Luczynski et al., 2016). This may partially due to breeding pairs being used and male and female data collapsed, whereas the work presented in this thesis suggests sex differences in hippocampus volume changes resulting from microbiome manipulation (Luczynski et al., 2016). Also, in contrast to our findings, this histological approach identified no difference in total brain volume in GF mice, although whole brain measurements excluded the cerebellum and olfactory bulb (Luczynski et al., 2016). This exclusion may explain the differences in brain volume results, as the cerebellum and olfactory bulb were included in this thesis. Likewise, while this study did not report the age of their animals, using older animals could have had an effect on this finding, as it is possible that GF mice have a delay in brain development that is reduced once the GF mice reach full maturity (Luczynski et al., 2016).

No differences were found in dendrite length in adult BLA neurons between GF and conventionally housed mice, however a reduction in dendrite length in the

hippocampus in GF mice may indicate region-specific delays in maturation of neuron morphology in GF animals compared to controls (Luczynski et al., 2016). Pyramidal neurons in the prefrontal cortex undergo a period of dendrite growth in early postnatal development, between P3 and P21, during which time the length of dendrites increases 13-fold (Ryan et al., 2016). Reconstruction of basolateral amygdala neurons indicated a similar rapid extension of dendrites between P7 and P28 (Ryan *et al.*, 2016). This is supported by transcriptomic evidence demonstrating that GF status impacts differential exon usage in several genes associated with neuron structure, with few differences between GF mice and GF mice recolonized at P21 in this regard (Stilling et al., 2015). Further support for structural changes to neurons in GF mice includes the finding of increased synaptic protein levels of PSD95 and synaptophysin in the striatum, but not PFC or HIP, of male GF mice (Diaz Heijtz et al., 2011). The findings presented in this dissertation, in combination with evidence from the literature, leads to the possibility of neuron morphological changes, specifically in dendritic and axonal arborization, that may be impacted by T cell-microglia signaling in early life. Many of the neuroanatomical changes and behaviours affected by adaptive immune deficiency are related to stress circuitry – which is also where we report changes in microglia number and density. Future research should investigate neuronal morphology in T cell deficient mice in regions associated with microglia differences and stress circuitry to determine whether neuron structure is responsible for the neuroanatomical changes observed in T cell deficient mice (Rilett *et al.*, 2015).

Important work from other research groups lends support to microbe-immune influence on the developing brain being at its peak during the first few weeks of

postnatal life. A study that examined brain development from the day of birth – P0 – to P3 found that neural and neuroimmune factors are drastically affected by microbial status (Castillo-Ruiz et al., 2018). GF mice were found to have considerably decreased pro-inflammatory cytokines compared to conventionally housed controls (Castillo-Ruiz *et al.*, 2018). Neuronal cell death was found to be changed in GF mice compared to controls in sub-regions that are implicated in stress circuitry and metabolism. These changes include increased numbers of dying cells in the PVN and CA1 of the HIP. However, the opposite effect was observed in the arcuate nucleus (ARC), where GF mice had fewer dying neurons than controls (Castillo-Ruiz *et al.*, 2018). Reports of inconsistent impacts of microbiome manipulation between brain regions agrees with the findings presented in study 2 of this thesis, showing microbiome status has varying effects on the development of different brain regions.

Alternatively, some evidence suggests that microbe signaling may affect brain development even earlier, as by embryonic day 18.5, layer V somatosensory cortex thickness was already larger in GF fetuses compared to control, which agrees with our finding of increased relative volume in the cortex of GF mice (Thion *et al.*, 2018a). These findings clearly support an impact of maternal microbiome status on the development of the brain *in utero*, likely through signal transmission across the placenta during gestation. Recent work investigating fetal brain development in dams with microbiome manipulations describes deficiencies in axon growth in the thalamocortical pathway in the absence of a typical maternal microbiome (Vuong et al., 2020). A number of microbiome-specific metabolites were identified that were present in both the maternal serum and fetal brain in the controls, but not GF or antibiotic-treated animals

(Vuong *et al.*, 2020). From there, the researchers discovered that recovering these metabolites in the microbiome-depleted animals corrected the deficiencies in axon development in the fetal brains, supporting the idea that the maternal microbiome plays critical roles in providing the metabolites necessary for typical *in utero* brain development (Vuong *et al.*, 2020).

In relation to microglia, GF mice were found to have more Iba1+ microglia than controls in the PVN, HIP, and ARC, which has also been suggested in other brain regions, including the cortex, corpus callosum, HIP, olfactory bulb, and cerebellum (Castillo-Ruiz *et al.*, 2018; Erny *et al.*, 2015). GF mice were found to have an increase in microglial cell density in the PVN (Castillo-Ruiz *et al.*, 2018), which is in the opposite direction as our findings of decreased microglial density in the PFC and HIP of adult T cell deficient mice in study 1 of this thesis. Also, in agreement with previous research in adult mice, an increase in microglial cell size in the PVN of neonatal GF mice was found in this work (Castillo-Ruiz *et al.*, 2018). Increased microglial size has been suggested, along with increased arborization, to be a sign of delayed maturity in microglial cells of immunodeficient mouse models (Castillo-Ruiz *et al.*, 2018; Erny *et al.*, 2015). Similarly, microglia harvested from early embryos of GF dams were found to have minor transcriptional differences from those harvested from the early embryos of control dams (Thion *et al.*, 2018a). However, embryos harvested at E18.5 – just before birth – had microglia with widespread transcriptional changes in males, but not females, of GF dams (Thion *et al.*, 2018a). These differences in expression were predominantly in genes involved in translation and metabolism. Microglia from adult female GF mice had broad transcriptional changes compared to control mice – mainly decreased expression

of genes involved with adaptive immune responses and increased expression of genes involved with transcription regulation. Microglia from adult GF males had a much smaller number of genes with transcriptional changes (Thion *et al.*, 2018a). Embryos from GF dams also had increased microglia density in the 3 brain regions studied, and at E18.5, male GF embryos had more microglia but not females, whereas at P20, pre-puberty, microglia density was increased in GF females only (Thion *et al.*, 2018a). Examination of adult SPF mice subjected to 1 week of antibiotic treatment revealed minor transcriptomic changes in microglia that differed from those found in GF mice, with no microglia density or morphological differences (Thion *et al.*, 2018a). This suggests a sex-by-GF status interaction in microglia development, both transcriptionally and in cell density, that is no longer susceptible to microbiome manipulation later in adulthood (Thion *et al.*, 2018a).

In study 2 of this thesis, we examine the impacts of the absence of microbiota in the first 5 weeks of postnatal life. Mice with microbiome depletion post-weaning had recognition memory deficits and reduced anxiety-like behaviour, suggesting that some behaviour remains susceptible to the effects of microbiome manipulation post-weaning (Desbonnet et al., 2015). We found that hippocampal structure remains susceptible to the effects of microbial manipulation post-weaning in recolonized GF mice, which was supported by the finding of reduced hippocampal BDNF mRNA expression in mice treated with antibiotics post-weaning (Desbonnet *et al.*, 2015). This may suggest that trophic factor expression may change in response to altered microbial signaling, and lead to differences in cell structure or survival that result in neuroanatomical changes. Evidence that behaviour can be affected by microbiome depletion post-weaning

includes the finding that male mice treated with antibiotics to deplete their gut microbiomes in adulthood had impaired recognition memory on the novel object recognition test, but spatial memory was not impaired (Frohlich et al., 2016). Microbiome depletion in adulthood was associated with decreased expression of tight junction proteins in the hippocampus, but increased expression in the amygdala, and decreased BDNF levels in the HIP, HYP, and PFC (Frohlich *et al.*, 2016). NMDAR2B and SLC6A4 mRNA expression were increased in the amygdala in antibiotic treated animals, but were unchanged in the PFC, HIP, or HYP (Frohlich *et al.*, 2016). These studies demonstrate that some aspects of the developing brain remain susceptible to the influences of microbiome depletion later in life, despite having a more developed adaptive immune system due to presence of a microbiome in early postnatal life.

Additional support for the idea that immune brain communication pre-puberty is a primary driving force influencing brain and behaviour are reports showing that restoring microbe-immune-brain communication in adulthood is insufficient to rescue behaviour and brain outcomes. For example, male rats exposed to antibiotic-mediated microbiome depletion in adulthood had no differences in anxiety-like behaviour compared to controls on the EPM or OF (Hoban et al., 2016). These results indicate that anxiety-like behaviour is not susceptible to the effects of microbiota depletion in adult rats, and that this behaviour is established earlier in postnatal brain development (Hoban *et al.*, 2016). This finding supports the evidence presented in study 2 of this thesis, where we report that the majority of brain changes associated with microbiome status are not rescued by recolonization at weaning.

Seminal work indicating behavioural differences and HPA axis dysregulation in GF animals included an investigation into the effects of recolonization on HPA axis development (Sudo *et al.*, 2004). While recolonization of young adult GF mice partially corrected the HPA axis dysregulation previously observed, it was noted that recolonization of older GF adult mice had no effect on HPA axis responses to stress (Sudo *et al.*, 2004). The results of this study suggest that the developmental timing of recolonization matters to behaviour and brain function, supporting our finding that recolonization at week 5 was insufficient to rescue the majority of neuroanatomical changes caused by GF status (Sudo *et al.*, 2004). Further highlighting the importance of recolonization timing, recolonization of GF mice at P1 corrected behaviours on the EPM (Luk et al., 2018). An interesting sex-by-GF status interaction was noted in the OF, where only female mice recolonized with a complex murine microbiome demonstrated rescue of hyperactive phenotype observed in the OF in GF and T cell deficient mice (Luk *et al.*, 2018).

In study 3 of this thesis, changes to the developmental trajectories of innate immune cells in the peripheral blood in T cell deficient mice compared to controls were considered. Mice without T cells have high between-subject variation that does not decrease over puberty, unlike controls. In the same way, evidence shows that T cell deficient mice have different microbiome maturation trajectories over early postnatal life, including microbiome richness (alpha diversity), which causes *TCRβ-/-δ-/-* mice to cluster separately from controls on measures of microbiome structure and composition (Caspani et al., 2022). Closer examination of T cell deficient mice revealed some taxa to be in increased abundance, while others were decreased compared to controls in both

cecal and fecal samples (Caspani *et al.*, 2022). The microbiomes of control mice at P17 were significantly different than those at P24, P28, and P84, indicating an important maturation step during weaning between P17 and P24 (Caspani *et al.*, 2022). This is important in the context of this dissertation because it supports key developmental processes in the microbiome before P35, and also indicates atypical development in T cell deficient mice. Notably, the evidence suggests that this developmental step is impacted by the loss of T cells, as the microbiomes of *TCRβ-/-δ-/-* mice at P17 are similar to those of older mice at P24, P28, and P84 (Caspani *et al.*, 2022). This effect was mirrored in the cortex and hippocampus metabolomes, where the same differences in maturation trajectory were identified across weaning in control mice but were absent in T cell deficient mice (Caspani *et al.*, 2022). The metabolic profiles of cecal and colon contents of T cell deficient mice also showed marked differences compared to control mice across early life (Caspani *et al.*, 2022). Important differences include decreased abundance of the short chain fatty acid (SCFA) butyrate, and higher levels of 5-aminovalerate, an important metabolite, which have been implicated in gut barrier function and lysine metabolism (Caspani *et al.*, 2022). Among the most important differences in brain metabolite development between T cell deficient and control mice both major inhibitory neurotransmitters and two other metabolites were found to increase drastically over postnatal life in *TCRβ-/-δ-/-* mice, whereas levels were consistent in controls (Caspani *et al.*, 2022). These changes in developmental trajectory of microbes and metabolites mirrors the findings described in circulating innate immune cells in study 3 of this dissertation, with differences between *TCRβ-/-δ-/-* mice and controls appearing after puberty (Caspani *et al.*, 2022). Future work should identify how

metabolites from the gut influence populations of immune cells in the blood, specifically monocytes and neutrophils, in the absence of T cells, considering that there is a substantial body of research describing SCFA modifications to surface receptor expression and chemotaxis of neutrophils and monocytes, so future work should identify how these metabolites affect innate immune cell populations in the blood in the absence of T cells (Vinolo et al., 2011).

Increases in 5HT and 5HIAA levels in the hippocampus of male GF mice are not rescued with colonization at weaning, despite rescue of tryptophan availability in the plasma and kynurenine/tryptophan ratio in recolonized mice (Clarke et al., 2013). MicroRNAs (miRNAs) have been suggested to be a possible mediator of these signals, and evidence supports increased levels in GF mice that are normalized with colonization (Moloney et al., 2017). Together with the changes in brain metabolomic development trajectory over P17 – P24 in control mice, this suggests that the metabolic changes associated with microbiome manipulation and adaptive immune deficiency occur in the first three weeks of postnatal life (Castillo-Ruiz *et al.*, 2018; Clarke *et al.*, 2013).

Conclusions

In this dissertation, I have extended the current body of knowledge related to how loss of T cells impact brain development, and how microbiome manipulation impacts brain development in the early postnatal period. My results show that T cell deficient mice have sex-by-genotype effects in microglial cell density in the PFC and HIP, two regions implicated in stress circuitry, and the behaviour phenotypes reported in mice

with adaptive immune deficiency. I have shown that the absence of microbiome in GF mice impacts brain development and volume by *ex vivo* MRI, and that recolonization at 5 weeks is insufficient to rescue the majority of volume changes observed in GF mice. My results show that ASF mice, which have a limited microbiome that is sufficient for adaptive immune system development, have few changes compared to SPF mice, indicating the importance of adaptive immune signals on neurodevelopment. Finally, I have measured behaviour in T cell deficient mice from pre-puberty to adulthood and determined that T cell deficient mice have an altered developmental trajectory of peripheral blood neutrophils. Altogether, this research suggests the importance of the first few weeks of postnatal life in microbiome-immune-brain signaling for healthy neurodevelopment.

Future Directions

Scientific interest in determining treatment targets for neurodevelopmental disorders has matched growing diagnostic rates. Immune cells and proteins are promising research targets recently identified for mechanisms of neurodevelopmental disorders. Widespread attention underscores the growing interest in, and significance of, the recognized need for mechanistic studies regarding how these immune factors contribute to neurodevelopment. In spite of the now well-documented problem, there is still a critical need to determine exactly when these mechanisms occur, and whether there is a critical window for immune interactions to affect behaviour. Understanding mechanisms for microbiome-immune-brain communication in the first few weeks of postnatal life will allow researchers developing new immune-based biomarkers and

treatments to plan their studies and interventions at times when there is a much greater probability of a positive outcome. Ideally, a better understanding of microbiome-immune-brain communication in early life will lead to the development of assays with greater accuracy for disease prediction or patient stratification in clinical trials. Research following up on the studies described in this dissertation to manipulate myeloid cells in pre-puberty and adult animals is also warranted as it may identify whether there are critical periods for peripheral immune cell communication with the developing nervous system.

References for Introduction and Discussion

Amorosi, S., Vigliano, I., Del Giudice, E., Panico, L., Maruotti, G.M., Fusco, A., Quarantelli, M., Ciccone, C., Ursini, M.V., Martinelli, P., and Pignata, C. (2010). Brain alteration in a Nude/SCID fetus carrying FOXN1 homozygous mutation. J Neurol Sci *298*, 121-123. 10.1016/j.jns.2010.08.066.

Ashwood, P., Corbett, B.A., Kantor, A., Schulman, H., Van de Water, J., and Amaral, D.G. (2011). In search of cellular immunophenotypes in the blood of children with autism. PLoS One *6*, e19299. 10.1371/journal.pone.0019299.

Backhed, F., Roswall, J., Peng, Y., Feng, Q., Jia, H., Kovatcheva-Datchary, P., Li, Y., Xia, Y., Xie, H., Zhong, H., et al. (2015). Dynamics and Stabilization of the Human Gut Microbiome during the First Year of Life. Cell Host Microbe *17*, 690-703. 10.1016/j.chom.2015.04.004.

Bateman, A., Singh, A., Kral, T., and Solomon, S. (1989). The immune-hypothalamic-pituitary-adrenal axis. Endocrine reviews *10*, 92-112. 10.1210/edrv-10-1-92.

Bengmark, S. (2013). Gut microbiota, immune development and function. Pharmacological research *69*, 87-113. 10.1016/j.phrs.2012.09.002.

Berkenbosch, F., van Oers, J., del Rey, A., Tilders, F., and Besedovsky, H. (1987). Corticotropin-releasing factor-producing neurons in the rat activated by interleukin-1. Science *238*, 524-526.

Borre, Y.E., O'Keeffe, G.W., Clarke, G., Stanton, C., Dinan, T.G., and Cryan, J.F. (2014). Microbiota and neurodevelopmental windows: implications for brain disorders. Trends Mol Med *20*, 509-518. 10.1016/j.molmed.2014.05.002.

Caspani, G., Green, M., Swann, J.R., and Foster, J.A. (2022). Microbe-Immune Crosstalk: Evidence That T Cells Influence the Development of the Brain Metabolome. Int J Mol Sci *23*. 10.3390/ijms23063259.

Castillo-Ruiz, A., Mosley, M., George, A.J., Mussaji, L.F., Fullerton, E.F., Ruszkowski, E.M., Jacobs, A.J., Gewirtz, A.T., Chassaing, B., and Forger, N.G. (2018). The microbiota influences cell death and microglial colonization in the perinatal mouse brain. Brain Behav Immun *67*, 218-229. 10.1016/j.bbi.2017.08.027.

Castro-Perez, E., Soto-Soto, E., Perez-Carambot, M., Dionisio-Santos, D., Saied-Santiago, K., Ortiz-Zuazaga, H.G., and Pena de Ortiz, S. (2016). Identification and Characterization of the V(D)J Recombination Activating Gene 1 in Long-Term Memory of Context Fear Conditioning. Neural Plast *2016*, 1752176. 10.1155/2016/1752176.

Clark, S.M., Michael, K.C., Klaus, J., Mert, A., Romano-Verthelyi, A., Sand, J., and Tonelli, L.H. (2015). Dissociation between sickness behavior and emotionality during lipopolysaccharide challenge in lymphocyte deficient Rag2(-/-) mice. Behav Brain Res *278*, 74-82. 10.1016/j.bbr.2014.09.030.

Clark, S.M., Sand, J., Francis, T.C., Nagaraju, A., Michael, K.C., Keegan, A.D., Kusnecov, A., Gould, T.D., and Tonelli, L.H. (2014). Immune status influences fear and anxiety responses in mice after acute stress exposure. Brain Behav Immun *38*, 192-201. 10.1016/j.bbi.2014.02.001.

Clark, S.M., Soroka, J.A., Song, C., Li, X., and Tonelli, L.H. (2016). CD4(+) T cells confer anxiolytic and antidepressant-like effects, but enhance fear memory processes in Rag2(-/-) mice. Stress *19*, 303-311. 10.1080/10253890.2016.1191466.

Clark, S.M., Vaughn, C.N., Soroka, J.A., Li, X., and Tonelli, L.H. (2018). Neonatal adoptive transfer of lymphocytes rescues social behaviour during adolescence in immune-deficient mice. Eur J Neurosci *47*, 968-978. 10.1111/ejn.13860.

Clarke, G., Grenham, S., Scully, P., Fitzgerald, P., Moloney, R.D., Shanahan, F., Dinan, T.G., and Cryan, J.F. (2013). The microbiome-gut-brain axis during early life regulates the hippocampal serotonergic system in a sex-dependent manner. Mol Psychiatry *18*, 666-673. 10.1038/mp.2012.77.

Cronk, J.C., Derecki, N.C., Ji, E., Xu, Y., Lampano, A.E., Smirnov, I., Baker, W., Norris, G.T., Marin, I., Coddington, N., et al. (2015). Methyl-CpG Binding Protein 2 Regulates Microglia and Macrophage Gene Expression in Response to Inflammatory Stimuli. Immunity *42*, 679-691. 10.1016/j.immuni.2015.03.013.

Cryan, J.F., O'Riordan, K.J., Cowan, C.S.M., Sandhu, K.V., Bastiaanssen, T.F.S., Boehme, M., Codagnone, M.G., Cussotto, S., Fulling, C., Golubeva, A.V., et al. (2019). The Microbiota-Gut-Brain Axis. Physiol Rev *99*, 1877-2013. 10.1152/physrev.00018.2018.

Cushman, J., Lo, J., Huang, Z., Wasserfall, C., and Petitto, J.M. (2003). Neurobehavioral changes resulting from recombinase activation gene 1 deletion. Clin Diagn Lab Immunol *10*, 13-18.

Davalos, D., Grutzendler, J., Yang, G., Kim, J.V., Zuo, Y., Jung, S., Littman, D.R., Dustin, M.L., and Gan, W.B. (2005). ATP mediates rapid microglial response to local brain injury in vivo. Nat Neurosci *8*, 752-758. 10.1038/nn1472.

De la Fuente, M., Ferrandez, M.D., Del Rio, M., Sol Burgos, M., and Miquel, J. (1998). Enhancement of leukocyte functions in aged mice supplemented with the antioxidant thioproline. Mech Ageing Dev *104*, 213-225. 10.1016/s0047-6374(98)00071-2.

Desbonnet, L., Clarke, G., Traplin, A., O'Sullivan, O., Crispie, F., Moloney, R.D., Cotter, P.D., Dinan, T.G., and Cryan, J.F. (2015). Gut microbiota depletion from early adolescence in mice: Implications for brain and behaviour. Brain Behav Immun *48*, 165-173. 10.1016/j.bbi.2015.04.004.

Diamond, M.C., Rainbolt, R.D., Guzman, R., Greer, E.R., and Teitelbaum, S. (1986). Regional cerebral cortical deficits in the immune-deficient nude mouse: a preliminary study. Exp Neurol *92*, 311-322. 10.1016/0014-4886(86)90083-x.

Diaz Heijtz, R., Wang, S., Anuar, F., Qian, Y., Bjorkholm, B., Samuelsson, A., Hibberd, M.L., Forssberg, H., and Pettersson, S. (2011). Normal gut microbiota modulates brain development and behavior. Proc Natl Acad Sci U S A *108*, 3047-3052. 10.1073/pnas.1010529108.

Eckburg, P.B., Bik, E.M., Bernstein, C.N., Purdom, E., Dethlefsen, L., Sargent, M., Gill, S.R., Nelson, K.E., and Relman, D.A. (2005). Diversity of the human intestinal microbial flora. Science *308*, 1635-1638. 10.1126/science.1110591.

Erny, D., Hrabe de Angelis, A.L., Jaitin, D., Wieghofer, P., Staszewski, O., David, E., Keren-Shaul, H., Mahlakoiv, T., Jakobshagen, K., Buch, T., et al. (2015). Host microbiota constantly control maturation and function of microglia in the CNS. Nat Neurosci *18*, 965-977. 10.1038/nn.4030.

Estes, M.L., and McAllister, A.K. (2015). Immune mediators in the brain and peripheral tissues in autism spectrum disorder. Nat Rev Neurosci *16*, 469-486. 10.1038/nrn3978.

Filiano, A.J., Gadani, S.P., and Kipnis, J. (2015). Interactions of innate and adaptive immunity in brain development and function. Brain Res *1617*, 18-27. 10.1016/j.brainres.2014.07.050.

Foster, J.A. (2016). Gut Microbiome and Behavior: Focus on Neuroimmune Interactions. Int Rev Neurobiol *131*, 49-65. 10.1016/bs.irn.2016.07.005.

Foster, J.A., and McVey Neufeld, K.A. (2013). Gut-brain axis: how the microbiome influences anxiety and depression. Trends Neurosci *36*, 305-312. 10.1016/j.tins.2013.01.005.

Foster, J.A., Rinaman, L., and Cryan, J.F. (2017). Stress & the gut-brain axis: Regulation by the microbiome. Neurobiol Stress *7*, 124-136. 10.1016/j.ynstr.2017.03.001.

Frohlich, E.E., Farzi, A., Mayerhofer, R., Reichmann, F., Jacan, A., Wagner, B., Zinser, E., Bordag, N., Magnes, C., Frohlich, E., et al. (2016). Cognitive impairment by antibiotic-induced gut dysbiosis: Analysis of gut microbiota-brain communication. Brain Behav Immun *56*, 140-155. 10.1016/j.bbi.2016.02.020.

Gaci, N., Borrel, G., Tottey, W., O'Toole, P.W., and Brugere, J.F. (2014). Archaea and the human gut: new beginning of an old story. World journal of gastroenterology *20*, 16062-16078. 10.3748/wjg.v20.i43.16062.

Gehrmann, J., Matsumoto, Y., and Kreutzberg, G.W. (1995). Microglia: intrinsic immuneffector cell of the brain. Brain Res Brain Res Rev *20*, 269-287.

Genton, L., and Kudsk, K.A. (2003). Interactions between the enteric nervous system and the immune system: role of neuropeptides and nutrition. American journal of surgery *186*, 253-258.

Hoban, A.E., Stilling, R.M., Ryan, F.J., Shanahan, F., Dinan, T.G., Claesson, M.J., Clarke, G., and Cryan, J.F. (2016). Regulation of prefrontal cortex myelination by the microbiota. Transl Psychiatry *6*, e774. 10.1038/tp.2016.42.

Hori, T., Katafuchi, T., Take, S., Shimizu, N., and Niijima, A. (1995). The autonomic nervous system as a communication channel between the brain and the immune system. Neuroimmunomodulation *2*, 203-215.

Ikehara, S., Pahwa, R.N., Fernandes, G., Hansen, C.T., and Good, R.A. (1984). Functional T cells in athymic nude mice. Proc Natl Acad Sci U S A *81*, 886-888. 10.1073/pnas.81.3.886.

Janeway, C.A., Travers, P., Walport, M., and Shlomchik, M.J. (2005). Immunobiology, 6th Edition (Garland Science Publishing).

Kadry, H., Noorani, B., and Cucullo, L. (2020). A blood-brain barrier overview on structure, function, impairment, and biomarkers of integrity. Fluids Barriers CNS *17*, 69. 10.1186/s12987-020-00230-3.

Kipnis, J., Cohen, H., Cardon, M., Ziv, Y., and Schwartz, M. (2004). T cell deficiency leads to cognitive dysfunction: implications for therapeutic vaccination for schizophrenia and other psychiatric conditions. Proc Natl Acad Sci U S A *101*, 8180-8185.

Kreutzberg, G.W. (1995). Microglia, the first line of defence in brain pathologies. Arzneimittelforschung *45*, 357-360.

Lankelma, J.M., Nieuwdorp, M., de Vos, W.M., and Wiersinga, W.J. (2015). The gut microbiota in internal medicine: implications for health and disease. The Netherlands journal of medicine *73*, 61-68.

Lenz, K.M., Nugent, B.M., Haliyur, R., and McCarthy, M.M. (2013). Microglia are essential to masculinization of brain and behavior. J Neurosci *33*, 2761-2772. 10.1523/JNEUROSCI.1268-12.2013.

Leonard, B.E. (2005). The HPA and immune axes in stress: the involvement of the serotonergic system. Eur Psychiatry *20 Suppl 3*, S302-306. S0924-9338(05)80180-4 [pii].

Li, C., Jiang, S., Liu, S.Q., Lykken, E., Zhao, L.T., Sevilla, J., Zhu, B., and Li, Q.J. (2014). MeCP2 enforces Foxp3 expression to promote regulatory T cells' resilience to inflammation. Proc Natl Acad Sci U S A *111*, E2807-2816. 10.1073/pnas.1401505111.

Lorke, D.E., Ip, C.W., and Schumacher, U. (2008). Increased number of microglia in the brain of severe combined immunodeficient (SCID) mice. Histochem Cell Biol *130*, 693-697. 10.1007/s00418-008-0463-2.

Luczynski, P., McVey Neufeld, K.A., Oriach, C.S., Clarke, G., Dinan, T.G., and Cryan, J.F. (2016). Growing up in a Bubble: Using Germ-Free Animals to Assess the Influence of the Gut Microbiota on Brain and Behavior. Int J Neuropsychopharmacol *19*. 10.1093/ijnp/pyw020.

Luk, B., Veeraragavan, S., Engevik, M., Balderas, M., Major, A., Runge, J., Luna, R.A., and Versalovic, J. (2018). Postnatal colonization with human "infant-type" Bifidobacterium species alters behavior of adult gnotobiotic mice. PLoS One *13*, e0196510. 10.1371/journal.pone.0196510.

Mayer, E.A., Savidge, T., and Shulman, R.J. (2014). Brain-gut microbiome interactions and functional bowel disorders. Gastroenterology *146*, 1500-1512. 10.1053/j.gastro.2014.02.037.

Moloney, G.M., O'Leary, O.F., Salvo-Romero, E., Desbonnet, L., Shanahan, F., Dinan, T.G., Clarke, G., and Cryan, J.F. (2017). Microbial regulation of hippocampal miRNA expression: Implications for transcription of kynurenine pathway enzymes. Behav Brain Res *334*, 50-54. 10.1016/j.bbr.2017.07.026.

Mombaerts, P., Iacomini, J., Johnson, R.S., Herrup, K., Tonegawa, S., and Papaioannou, V.E. (1992). RAG-1-deficient mice have no mature B and T lymphocytes. Cell *68*, 869-877.

Murphy, E.F., Cotter, P.D., Healy, S., Marques, T.M., O'Sullivan, O., Fouhy, F., Clarke, S.F., O'Toole, P.W., Quigley, E.M., Stanton, C., et al. (2010). Composition and energy harvesting capacity of the gut microbiota: relationship to diet, obesity and time in mouse models. Gut *59*, 1635-1642. 10.1136/gut.2010.215665.

Nance, D.M., and Sanders, V.M. (2007). Autonomic innervation and regulation of the immune system (1987-2007). Brain, behavior, and immunity *21*, 736-745. 10.1016/j.bbi.2007.03.008.

Neufeld, K.M., Kang, N., Bienenstock, J., and Foster, J.A. (2011). Reduced anxiety-like behavior and central neurochemical change in germ-free mice. Neurogastroenterol Motil *23*, 255-264, e119. 10.1111/j.1365-2982.2010.01620.x.

Nimmerjahn, A., Kirchhoff, F., and Helmchen, F. (2005). Resting microglial cells are highly dynamic surveillants of brain parenchyma in vivo. Science *308*, 1314-1318. 1110647 [pii]
10.1126/science.1110647.

Pan, Y., Xiong, M., Chen, R., Ma, Y., Corman, C., Maricos, M., Kindler, U., Semtner, M., Chen, Y.H., Dahiya, S., and Gutmann, D.H. (2018). Athymic mice reveal a requirement

for T-cell-microglia interactions in establishing a microenvironment supportive of Nf1 low-grade glioma growth. Genes Dev *32*, 491-496. 10.1101/gad.310797.117.

Paolicelli, R.C., Bolasco, G., Pagani, F., Maggi, L., Scianni, M., Panzanelli, P., Giustetto, M., Ferreira, T.A., Guiducci, E., Dumas, L., et al. (2011). Synaptic pruning by microglia is necessary for normal brain development. Science *333*, 1456-1458. science.1202529 [pii]
10.1126/science.1202529.

Petkova, S.B., Yuan, R., Tsaih, S.W., Schott, W., Roopenian, D.C., and Paigen, B. (2008). Genetic influence on immune phenotype revealed strain-specific variations in peripheral blood lineages. Physiol Genomics *34*, 304-314. 10.1152/physiolgenomics.00185.2007.

Prinz, M., and Priller, J. (2014). Microglia and brain macrophages in the molecular age: from origin to neuropsychiatric disease. Nat Rev Neurosci *15*, 300-312. 10.1038/nrn3722.

Pusceddu, M.M., Barboza, M., Keogh, C.E., Schneider, M., Stokes, P., Sladek, J.A., Kim, H.J.D., Torres-Fuentes, C., Goldfild, L.R., Gillis, S.E., et al. (2019). Nod-like receptors are critical for gut-brain axis signalling in mice. J Physiol *597*, 5777-5797. 10.1113/JP278640.

Quan, N., and Banks, W.A. (2007). Brain-immune communication pathways. Brain Behav Immun *21*, 727-735.

Rattazzi, L., Piras, G., Ono, M., Deacon, R., Pariante, C.M., and D'Acquisto, F. (2013). CD4(+) but not CD8(+) T cells revert the impaired emotional behavior of immunocompromised RAG-1-deficient mice. Transl Psychiatry *3*, e280. 10.1038/tp.2013.54.

Rilett, K.C., and Foster, J.A. (2014). T lymphocytes and anxiety: A review of clinical and animal studies. Annals of Depression and Anxiety *1*, 1-5.

Rilett, K.C., Friedel, M., Ellegood, J., MacKenzie, R.N., Lerch, J.P., and Foster, J.A. (2015). Loss of T cells influences sex differences in behavior and brain structure. Brain Behav Immun *46*, 249-260. 10.1016/j.bbi.2015.02.016.

Ryan, S.J., Ehrlich, D.E., and Rainnie, D.G. (2016). Morphology and dendritic maturation of developing principal neurons in the rat basolateral amygdala. Brain Struct Funct *221*, 839-854. 10.1007/s00429-014-0939-x.

Sajja, B.R., Bade, A.N., Zhou, B., Uberti, M.G., Gorantla, S., Gendelman, H.E., Boska, M.D., and Liu, Y. (2016). Generation and Disease Model Relevance of a Manganese Enhanced Magnetic Resonance Imaging-Based NOD/scid-IL-2Rgammac(null) Mouse Brain Atlas. Journal of neuroimmune pharmacology : the official journal of the Society on NeuroImmune Pharmacology *11*, 133-141. 10.1007/s11481-015-9635-8.

Sankar, A., Mackenzie, R.N., and Foster, J.A. (2012). Loss of class I MHC function alters behavior and stress reactivity. J Neuroimmunol *244*, 8-15. S0165-5728(11)00377-8 [pii]
10.1016/j.jneuroim.2011.12.025.

Sapolsky, R., Rivier, C., Yamamoto, G., Plotsky, P., and Vale, W. (1987). Interleukin-1 stimulates the secretion of hypothalamic corticotropin-releasing factor. Science *238*, 522-524.

Scarpellini, E., Ianiro, G., Attili, F., Bassanelli, C., De Santis, A., and Gasbarrini, A. (2015). The human gut microbiota and virome: Potential therapeutic implications. Digestive and liver disease : official journal of the Italian Society of Gastroenterology and the Italian Association for the Study of the Liver *47*, 1007-1012. 10.1016/j.dld.2015.07.008.

Schwarz, J.M., and Bilbo, S.D. (2012). Sex, glia, and development: interactions in health and disease. Horm Behav *62*, 243-253. 10.1016/j.yhbeh.2012.02.018.

Smith, C.J., Emge, J.R., Berzins, K., Lung, L., Khamishon, R., Shah, P., Rodrigues, D.M., Sousa, A.J., Reardon, C., Sherman, P.M., et al. (2014). Probiotics normalize the gut-brain-microbiota axis in immunodeficient mice. Am J Physiol Gastrointest Liver Physiol *307*, G793-802. 10.1152/ajpgi.00238.2014.

Soltys, Z., Ziaja, M., Pawlinski, R., Setkowicz, Z., and Janeczko, K. (2001). Morphology of reactive microglia in the injured cerebral cortex. Fractal analysis and complementary quantitative methods. J Neurosci Res *63*, 90-97. 10.1002/1097-4547(20010101)63:1<90::AID-JNR11>3.0.CO;2-9.

Stilling, R.M., Ryan, F.J., Hoban, A.E., Shanahan, F., Clarke, G., Claesson, M.J., Dinan, T.G., and Cryan, J.F. (2015). Microbes & neurodevelopment--Absence of microbiota during early life increases activity-related transcriptional pathways in the amygdala. Brain Behav Immun *50*, 209-220. 10.1016/j.bbi.2015.07.009.

Sudo, N., Chida, Y., Aiba, Y., Sonoda, J., Oyama, N., Yu, X.N., Kubo, C., and Koga, Y. (2004). Postnatal microbial colonization programs the hypothalamic-pituitary-adrenal system for stress response in mice. J Physiol *558*, 263-275. 10.1113/jphysiol.2004.063388.

Thion, M.S., and Garel, S. (2018). Microglia Under the Spotlight: Activity and Complement-Dependent Engulfment of Synapses. Trends Neurosci *41*, 332-334. 10.1016/j.tins.2018.03.017.

Thion, M.S., Ginhoux, F., and Garel, S. (2018a). Microglia and early brain development: An intimate journey. Science *362*, 185-189. 10.1126/science.aat0474.

Thion, M.S., Low, D., Silvin, A., Chen, J., Grisel, P., Schulte-Schrepping, J., Blecher, R., Ulas, T., Squarzoni, P., Hoeffel, G., et al. (2018b). Microbiome Influences Prenatal and

Adult Microglia in a Sex-Specific Manner. Cell *172*, 500-516 e516. 10.1016/j.cell.2017.11.042.

Thompson, S.L., Ellegood, J., Bowdish, D.M., Lerch, J.P., and Foster, J.A. (submitted). Sex- and brain region-specific alterations in brain volume in germ-free mice.

Tremblay, M.E. (2011). The role of microglia at synapses in the healthy CNS: novel insights from recent imaging studies. Neuron Glia Biol *7*, 67-76. 10.1017/S1740925X12000038.

Tremblay, M.E., Stevens, B., Sierra, A., Wake, H., Bessis, A., and Nimmerjahn, A. (2011). The role of microglia in the healthy brain. J Neurosci *31*, 16064-16069. 10.1523/JNEUROSCI.4158-11.2011.

Turnbaugh, P.J., Ley, R.E., Hamady, M., Fraser-Liggett, C.M., Knight, R., and Gordon, J.I. (2007). The human microbiome project. Nature *449*, 804-810.

Vargas, D.L., Nascimbene, C., Krishnan, C., Zimmerman, A.W., and Pardo, C.A. (2005). Neuroglial activation and neuroinflammation in the brain of patients with autism. Ann Neurol *57*, 67-81. 10.1002/ana.20315.

Vighi, G., Marcucci, F., Sensi, L., Di Cara, G., and Frati, F. (2008). Allergy and the gastrointestinal system. Clinical and experimental immunology *153 Suppl 1*, 3-6. 10.1111/j.1365-2249.2008.03713.x.

Vinolo, M.A., Ferguson, G.J., Kulkarni, S., Damoulakis, G., Anderson, K., Bohlooly, Y.M., Stephens, L., Hawkins, P.T., and Curi, R. (2011). SCFAs induce mouse neutrophil chemotaxis through the GPR43 receptor. PLoS One *6*, e21205. 10.1371/journal.pone.0021205.

Viveros, M.P., Fernandez, B., Guayerbas, N., and De la Fuente, M. (2001). Behavioral characterization of a mouse model of premature immunosenescence. J Neuroimmunol *114*, 80-88. 10.1016/s0165-5728(00)00457-4.

Vuong, H.E., Pronovost, G.N., Williams, D.W., Coley, E.J.L., Siegler, E.L., Qiu, A., Kazantsev, M., Wilson, C.J., Rendon, T., and Hsiao, E.Y. (2020). The maternal microbiome modulates fetal neurodevelopment in mice. Nature *586*, 281-286. 10.1038/s41586-020-2745-3.

Williamson, L.L., McKenney, E.A., Holzknecht, Z.E., Belliveau, C., Rawls, J.F., Poulton, S., Parker, W., and Bilbo, S.D. (2016). Got worms? Perinatal exposure to helminths prevents persistent immune sensitization and cognitive dysfunction induced by early-life infection. Brain, behavior, and immunity *51*, 14-28. 10.1016/j.bbi.2015.07.006.

Wolf, S.A., Steiner, B., Akpinarli, A., Kammertoens, T., Nassenstein, C., Braun, A., Blankenstein, T., and Kempermann, G. (2009). CD4-positive T lymphocytes provide a neuroimmunological link in the control of adult hippocampal neurogenesis. J Immunol *182*, 3979-3984. 182/7/3979 [pii] 10.4049/jimmunol.0801218.

Woodbine, L., Neal, J.A., Sasi, N.K., Shimada, M., Deem, K., Coleman, H., Dobyns, W.B., Ogi, T., Meek, K., Davies, E.G., and Jeggo, P.A. (2013). PRKDC mutations in a SCID patient with profound neurological abnormalities. J Clin Invest *123*, 2969-2980. 10.1172/JCI67349.

Xie, L., Choudhury, G.R., Winters, A., Yang, S.H., and Jin, K. (2015). Cerebral regulatory T cells restrain microglia/macrophage-mediated inflammatory responses via IL-10. Eur J Immunol *45*, 180-191. 10.1002/eji.201444823.

Zhang, X., Shen, D., Fang, Z., Jie, Z., Qiu, X., Zhang, C., Chen, Y., and Ji, L. (2013). Human gut microbiota changes reveal the progression of glucose intolerance. PLoS One *8*, e71108. 10.1371/journal.pone.0071108.

Zhao, Q., and Elson, C.O. (2018). Adaptive immune education by gut microbiota antigens. Immunology *154*, 28-37. 10.1111/imm.12896.

Ziv, Y., Ron, N., Butovsky, O., Landa, G., Sudai, E., Greenberg, N., Cohen, H., Kipnis, J., and Schwartz, M. (2006). Immune cells contribute to the maintenance of neurogenesis and spatial learning abilities in adulthood. Nat Neurosci *9*, 268-275.